Title

Electrochemical Radiofluorination: Carrier and No-Carrier-Added 18F Labelling of Thioethers and Aromatics for use as Positron Emission Tomography Probes

Author

Allison, Nathanael

Publication Date

2018

Peer reviewed|Thesis/dissertation

UNIVERSITY OF CALIFORNIA

Los Angeles

Electrochemical Radiofluorination: Carrier and No-Carrier-Added ^{18}F Labelling of Thioethers and Aromatics for use as Positron Emission Tomography Probes

A dissertation submitted in partial satisfaction

of the requirements for the degree

Doctor of Philosophy in Biomedical Physics

by

Nathanael Allison

2018

ABSTRACT OF THE DISSERTATION

Electrochemical Radiofluorination: Carrier and No-Carrier-Added ^{18}F Labelling of Thioethers and Aromatics for use as Positron Emission Tomography Probes

by

Nathanael Allison

Doctor of Philosophy in Biomedical Physics

University of California, Los Angeles, 2018

Professor Seyed Sam Sadeghi Hosseini, Chair

Abstract: Thioether and aromatic molecules were electrochemically radiolabeled with [^{18}F]Fluoride under carrier-added and no-carrier-added conditions. The addition of excess carrier fluoride (i.e. stable isotope fluoride) in traditional electrochemical fluorination leads to low fluorination yields, which cause low radiochemical yields and molar activity when using [^{18}F]Fluoride. Electrochemical syntheses were extensively investigated herein and optimized to remove the need for the addition of excess carrier fluoride, increasing radiochemical yield and molar activity rendering this electrochemical methodology suitable for the potential use in Positron Emission Tomography radiotracer synthesis. The electrochemical fluorination mechanisms of ECEC, where E is an electrochemical process and C is a chemical reaction, and fluoro-Pummerer rearrangement were explored with the transition to no-carrier-added conditions. New electrochemical fluorination methods and novel reaction conditions were used to perform no-carrier-added ^{18}F-radiolabeling of thioethers and aromatics with improved radiochemical yield and molar activity for use in the synthesis of radiotracers for Positron Emission Tomography.

The dissertation of Nathanael Allison is approved.

Daniel H. Silverman

Robert Michael van Dam

Jennifer M. Murphy

Peter M. Clark

Seyed Sam Sadeghi Hosseini, Committee Chair

University of California, Los Angeles

2018

ACKNOWLEDGEMENT PAGE

With the most respect and admiration, I will like to thank my wife, Diana, for supporting and taking care of me and my two beautiful children, Arabella and Skyla. Through the many days and nights of experiments, reading, and writing, my wife was there to help me along the way.

I will like to thank my research professor, Dr. Sam Sadeghi, for supporting me and the research in his group, which allowed me to learn and experiment in this interesting field. Dr. Sadeghi's expertise and insights helped me make many discoveries. I will like to thank Dr. Mike McNitt-Gray who supported me in the Biomedical Physics Program and throughout my journey from the US Navy to pursue graduate school. I will like to thank Dr. Dan Silverman for his guidance and advise on clinical PET imaging and analysis.

I will also like to thank Dr. Artem Lebedev for teaching me the instrumentation and the basics of this interdisciplinary research area. I will like to thank Dr. Fan Yang who explained organic chemistry and synthesized precursors for my use. I will like to also thank Dr. Mehrdad Balandeh and Dr. Christopher Waldmann, both of which introduced me to the wonders of radiochemistry and electrochemistry and all the possibilities within these research fields. I will like to thank all of my lab-mates and colleagues for supporting me throughout my experiments. I also want to thank the research technicians within the biomedical cyclotron for their support and time with my research.

In addition, I will like to thank the US Navy who provided me with this opportunity to pursue graduate school. I am excited for the next step of my research career at the Uniformed Services University, which is an exciting opportunity presented to me by the US Navy that I am grateful for.

TABLE OF CONTENTS

LIST OF FIGURES

Chapter 1

Chapter 2

Chapter 3

Chapter 4

Chapter 5

Chapter 6

Chapter 7

Chapter 8

Chapter 9

Chapter 10

Chapter 11

Chapter 12

VITA - NATHANAEL ALLISON

EDUCATION

Pennsylvania State University
State College, PA 16801
B.S. Physics, Minor in
Bioengineering and Mathematics
June 2006 – May 2009

Military Training/Education
US Army, Dec 1999 – May 2006
Deployed Iraq, Oct 2003 – Aug 2004
US Navy, Oct 2010 – Present
USS Frank Cable, Dec 2011 – May 2014

PROFESSIONAL EXPERIENCE

Director, Translational Imaging Facility, Uniformed Services University, Bethesda, MD **Present Position**
Responsible for a fully operational small animal imaging core that delivers state of the art small animal imaging using positron emission tomography (PET), single photon emission computed tomography (SPECT), computed tomography (CT), bioluminescence, fluorescence and magnetic resonance imaging (MRI) in support of the University and many Department of Defense Agencies. Manages over one million dollar budget and six highly trained imaging experts in executing research protocols, data analysis and coordinating with principle investigators. Member of the Radiation Safety Committee and Medical Physics Advisory Board.

Radiation Safety Officer, USS Frank Cable, a Submarine Tender Stationed in Guam **Dec 2011 – May 2014**
Responsible for dosimetry and radiation safety requirements of 1500 personnel and environmental monitoring in conjunction with the submarine tender in repair of nuclear submarines on shore or at sea. Lead the anticontamination fast response team, required to respond to any type of radiologic contamination incident in the pacific region. Stood Command Duty Officer (CDO) in charge of the ship at port. Led an emergency response station to rapidly deploy against threats such as enemy combatants, fires, and typhoons.

Health Physicist, Yokota Air Base, Japan **May 2011 – Aug 2011**
Deployed in response to the Fukushima Daiichi Nuclear Reactor Accident, Operation Tomodachi. Performed internal contamination testing on military members thought to be exposed to radioisotopes from the reactor accident. Performed environmental radioisotope air, soil and equipment contamination surveys. Consolidated and analyzed data for 4 star general/admiral briefs.

Junior Medical Physicist, Naval Medical Center Portsmouth, Portsmouth, VA **Dec 2010 – Nov 2011**
Performed duties of assisting in the management of hospital radiation safety. Qualified and conducted annual quality control evaluations of medical imaging equipment to include x-ray, dental x-ray, fluoroscopy, angioscopy, and computed tomography (CT).

Math Tutor/Tutor for Learning Disabled College Students, Rockville, MD and Vienne, VA **June 2009 – Oct 2010**
Tutored college students with a variety of different learning disabilities. Organized and focused students with disabilities such as autism spectral disorders, ADD, ADHD, and various students that have had significant traumatic brain injuries. Tutored math from entry level addition-subtraction all the way through calculus and differential equations. Taught an excelled math curriculum at a private summer school for 4th-5th graders. Tutored students in preparation for SAT, ACT and specific math and science subject tests.

Lab Technician, State College, PA **June 2007 – Apr 2009**
Performed genetic, dietary and longevity experiments on mice in a clean room facility. Handled the upkeep, maintained the barrier, sanitized all incoming and outgoing material and cared for a population of over 600 mice. Observed, tested, collected and analyzed biological data on the mice population to include taking blood and urine samples, weight, and behavioral data.

Soldier, Taji, Iraq – Hanau, Germany **May 2003 – May 2006**
Deployed in Operation Iraqi Freedom. Convoy gunner and driver through hostile areas in Iraq at the begging of the war. Provided security at several different locations, base perimeters and acted as an escort of civilian workers for several rebuilding projects in the Baghdad area. Member of the base fast response force which mobilizes quickly at the first information of a possible threat. In Germany, provided redeployment exercises/training and helped to reallocated equipment due to the force reorganization of the US Army.

Chapter 1: Introduction

The synthesis of Positron Emission Tomography (PET) radiotracers often requires carefully crafted precursors and quick late-stage radiolabelling strategies to avoid the decay of the radioisotope during synthesis. The limitations of PET probe synthesis are primarily due to the short half-life of the positron-emitting isotopes, which, in return, hinders the ability to develop innovative multi-step synthesis with fluorinated building blocks and testing for new radiotracers. Precursors without a positive charge at the site of fluorine labeling are not readily amenable to reactions with negatively charged fluoride causing the radiolabelling of electron rich centers to be challenging. Electrochemistry has often been overlooked but may be the solution to expedite the design and accommodate the late-stage synthesis of PET tracers. By resorting to electrochemical approaches, we can potentially avoid complex precursor construction, as well as overcome many difficulties with developing new PET probe syntheses. These methods may also ease the radiolabeling process for many previously challenging or impossible problems when radiolabeling bio-molecules.

Thus, the goal of this work is to investigate the ability of utilizing electrochemical approaches to overcome current PET probe synthetic challenges, specifically to address late stage fluorination of electron rich centers resulting in fluorinated molecules with increased *in vivo* stability. Particularly herein, we will exclusively focus on [^{18}F]Fluoride radiolabelling since there are currently minimal research contributions and many unknowns in field of Electrochemical Radiofluorination (ECRF). The completion of this work will offer new findings in this scarce research space, increasing the knowledge of ECRF which will bring this technology one step closer towards developing new research tools for radiochemistry.

Since the discovery of [^{18}F]fluorodeoxyglucose ([^{18}F]FDG) within the last several decades [6-8], there is a void in furthering the development of clinically and financially successful Positron

Emission Tomography (PET) probes. FDG is an analog of glucose used in PET as a tracer for metabolic rate. FDG becomes metabolic trapped in the cell making it an excellent metabolic tracer. Once in cells, [^{18}F]FDG undergoes phosphorylation which prevents the molecule from proceeding to glycolysis due to the lack of 2-hydroxyl group. ^{18}F-FDG-6-phosphate formed in the cells are not metabolized and released from the cell until radioactive decay. After decay, the ^{18}F decays into ^{18}O which forms a hydroxy group that can be metabolized similarly as glucose. FDG can offer a high-resolution image to capture metabolic activity in the human body since the ^{18}F is trapped in the cell at the rate of glucose uptake and does not escape the cell until after positron emission. The wide success of FDG and limited success of other PET radiotracers has caused a shift of PET probe research from the commercial sector to academic and government institutions [9].

In contrast to traditional pharmaceutical drug discovery approaches, developing new PET radiotracers requires a vastly different strategy, which introduces additional challenges. For example, one of the biggest challenges is how to synthesize and image the PET probe before significant radioactive decay. These limitations severely prevent the quantity of new PET probes synthesized and experimentally tested each year. Developing new PET tracers is a very time-demanding process that requires a significant amount of money and resources [10]. PET radiotracers benefit greatly from widespread use. This would allow the formation of a database of normal variation in PET imaging for the radiotracer so that abnormalities can be detected and also allow the radiotracer to be profitable encouraging further research. To achieve widespread radiotracer use, synthesis methods should also be easily adaptable with a low barrier of entry. Electrochemistry is a new PET synthesis method that would be easily translatable for wide spread use.

To address these challenges of fluorinating electron rich centers in a short time, electrochemical approaches will be explored as a strategy to improve late-stage radiolabelling for thioether and aromatic precursors in PET probe synthesis. Herein, this work will investigate and discuss: (1) data on carrier added electrochemical fluorination (ECF); (2) electrochemical radiofluorination; (3) provide no-carrier-added (NCA) electrochemical methodology; (4) discussion on the current mechanisms and their agreement with our findings; and, finally (5) additional key insights on NCA electrochemical fluorination (ECF) of molecules with thioether and aromatic moieties.

1.1 Positron Emission Tomography (PET) Introduction

PET is an essential technology in clinical imaging for diagnosis, prognosis and treatment evaluation in medicine, which rapidly grew with the adoption of new technologies in the 1990's and 2000's [11]. Since then, PET has continued to expand with medical imaging techniques along with the innovation of new PET tracers which have allowed for in vivo investigation of specific molecular pathways [7, 12]. For example, PET imaging can (1) provide vital information for many different medical conditions and diseases [13]; (2) play a central role in cancer detection and treatment response [6, 14]; (3) provide key information such as detection and monitoring of coronary artery disease and microvascular health [15, 16]; and, (4) be used for the diagnosis, treatment and monitoring of many inflammatory and infectious diseases [17, 18]. Additionally, many central nervous system (CNS) conditions such as Alzheimer's Disease [19, 20], Parkinson's Disease [21, 22], Huntington's Disease [23, 24], and Epilepsy [25, 26] utilizes PET imaging to offer critical diagnostic, treatment and assessment information. Recent developments have poised PET as an essential tool for drug development [27, 28] to track potential candidates by providing

key molecular information such as visualizing enzyme activity or receptor occupancy [29, 30]. This information can be used to screen out many candidate pharmaceuticals in preclinical trials to narrow down drugs with more favorable pharmacokinetics. To this day, PET technology continues to expand into medical and scientific areas with the advent of new radiotracers.

PET is a unique medical imaging modality used to evaluate *in vivo* molecular interactions of important cellular processes such as metabolism, membrane transport, receptor interactions, enzyme activity, and even gene expression [30-32]. PET probes are designed to specifically tag a targeted biomolecule or structure with a positron-emitting isotope to accurately localize the probe 3-dimensionally with external detectors. The two opposite directing photons are created from the positron annihilation and are detected with a resolution of several millimeter to sub-millimeter range in small animal scanners [33]. This allows the localization of the annihilation site of the positron with the electron. The distance the positron travels before annihilation as well as the slight deviation from 180 degrees of annihilation photons cause the limit in resolution. The deviation from 180 degrees of the annihilation photons is due to momentum conservation of the electron positron pair. PET imaging is sensitive enough to detect localized biochemical concentrations of radioisotopes even down to picomolar level, which enables the visualization of the radioactivity of these molecules in normal bioactive chemistry. Many other molecular imaging techniques can be used *in vitro* or *ex vivo* but often fail to replicate the natural environment, active pathways and binding of live subjects that can be seen with PET.

PET uses positron emitting isotopes which emit a positron during radioactive decay. The positron travels a short distance prior to an annihilating event when it combines with an electron to release two 511 keV photons that travel in opposite directions. These annihilation photons are detected by a ring of detectors around the subject. The time of detection of the photons allows for

the identification of the photon pair and determination of the point of origin based on the trajectory of the photons. PET/CT can co-register the PET probe image with the CT image to better identify anatomical areas of high or low PET probe accumulation.

1.2 [^{18}F]Fluoride, the Isotope of choice for PET

Fluorine-18 is the most widely used isotope for PET imaging due to its ideal half-life (110 mins), low positron energy (0.635 MeV), 97% β+ decay and ability to be produced in high molar activities (A_m). Particularly, its half-life of 110 mins is sufficient to synthesize the probe molecules and transport them to the clinic. It is also long enough for the probe to travel *in vivo* to its intended target while allowing radiolabeled molecules that are not accumulated in the target to leave the area. This minimizes unwanted background noise creating a high signal-to-noise ratio (SNR) to generate high-quality PET images with good resolution. Fluorine-18's half-life, is also short enough to only cause a low dose of radiation to the patient. The lower positron energy of ^{18}F produces higher resolution PET images due to the shorter distance the positron will travel after decay until it annihilates with an electron. The 97% β+ decay shows that ^{18}F produces decays with very little other schemes which can increase the radiation dose and background reducing the SNR. To quantify the amount of the radiolabeled probe to non-radioactive labelled probe; the ratio of ^{18}F labelled probe vs. ^{19}F labelled probe is calculated to determine the molar activity (A_m) often measured in Ci/umol. This calculation is necessary as these isotopes are chemically identical which makes it near impossible to separate isotopes in the 110 min half-life. [^{18}F]fluoride can be produced in a cyclotron with high A_m , which is a significant advantage as lower molar activity can lead to poor contrast in imaging using the PET probe due to *in vivo* competition with the non-radioactive

^{19}F labelled probe which does not generate a detectable gamma pair signal from decay. This is especially important for targets of low abundance (i.e., receptors) that can be easily saturated.

A common design strategy of many PET tracers is to base them on bioactive pharmaceuticals without fluorine. The use of fluorine-18 can minimize bio-activity changes in the PET radiotracer compared to the addition of other radioisotopes. Fluorine replacement of either oxygen, hydrogen or a hydroxyl group typically does not change the shape or conformation of the molecule. This often leads to the desired bioactivity of the fluorinated tracer which will behave similarly to the unfluorinated molecule *in vivo* [34]. Fluorination strategies have also been reported to have a positive effect on biological half-lives, membrane permeability, intrinsic potency, pKa, metabolic stability and pharmacokinetics of bioactive molecules [34-36]. However, since fluorine is rarely found as a constituent of organic molecules in nature, synthetic methods for adding fluorine must be developed.

Two commonly reported radiofluorination approaches in radiochemistry are based on electrophilic and nucleophilic fluorination. The electrophilic method is an effective method to fluorinate organic molecules with high electron density [37]. Electrophilic radiofluorination typically uses fluorine gas or derived fluorinating agents from that gas. However, fluorine gas is highly toxic and reactive which often leads to poor regioselectivity of radiolabelling. Using $[^{18}F]F_2$ requires a significant amount of carrier gas which greatly reduces molar activity. Due to the poor regioselectivity, molar activity and toxicity of fluorine gas using the electrophilic method, radiosynthesis of PET probes that are compatible with this approach are rather limited. The nucleophilic method uses a form of fluoride that reacts to sites of low electron density. This is often achieved by nucleophilic displacement of a leaving group in S_N2 or S_NAr reactions [37]. Many of these nucleophilic substitution reactions often must be performed under harsh conditions

with either high pH and temperatures, require difficult precursor synthesis, or are very regioselective which can prohibit some late stage fluorination. Organic compounds, especially those that possess a high electron density at the fluorination site, present an additional challenge for nucleophilic fluorination due to the disadvantaged interaction between a negatively charged fluoride and an electron rich center. Different strategies have been explored to overcome this disfavored reaction such as utilizing organometallic intermediates [38], aryliodoinum and iodonium ylide groups [39], catalysts [40], and strong oxidizing reagents [41]. An extensive review of ^{18}F fluorination of aromatic molecules has been recently reported [42].

There are two approaches to incorporate [^{18}F]fluoride on a complex biomolecule: the building block approach and the late stage addition. The building block approach enables the radiolabeling of a small starting molecule which is followed by several additional reactions to modify the molecule building it up until the probe is formed. The building block approach is rather unfavorable for PET probe synthesis due to the short life-time of the radioisotope which makes it challenging to attach each sequential building block in a quick manner without decreasing the radioactivity substantially after several steps. Thus, new strategies that can overcome these technical challenges are being sought to minimize the time-extensive process of the building block approach that will complete radiolabeling while minimizing as many steps as possible. This will be critical to decrease synthesis time and improve radiochemical yields (RCY) allowing the method to be able to transition to routine clinical production. Optimizing these processes will also improve the reliability by reducing the steps of automated machine sequences which are necessary in radiochemistry due to the levels of radioactivity [43].

When applicable, radiochemists favor the second option of radiolabelling a complex biomolecule via the late stage approach. This strategy is favorable because it requires fewer steps

and leads to less radioactive decay with potentially high RCY. Electrochemical fluorination (ECF) is a late stage nucleophilic method that takes advantage of the quicker synthesis with fewer steps which can also be regioselective. Through this work, we have effectively demonstrated this possibility of using ECF for synthesizing PET radiotracers with maintaining high molar activity, which is ideal for many PET imaging applications.

1.3 Limitations of PET Probe Synthesis

Despite decades of research and development, clinical translation of PET probes has met significant roadblocks. One of the largest roadblocks is due to the planning and synthesis of new PET probes, which is found to be a highly interdisciplinary undertaking that requires extensive expertise in both chemistry and medicine. In contrast to traditional non-radioactive drug discovery approaches, utilizing PET presents additional difficulties that are unique to radiochemistry. By far the most limiting factor in PET probe creation is the half-life of the radioisotope. For example, in traditional organic chemistry, the chemical intermediates at each stage and the final product can be stored and even maintain its chemical structure for long-extended period of time with a shelf-life spanning over months and even years. Also, in traditional organic chemistry synthesis large masses can be synthesized at one central locations for use all over the world. In stark contrast to traditional organic chemistry synthesis, radiochemistry synthesis must be constantly performed daily at locations close to use and the intermediate stages cannot be stored due to radioactive decay. Due to this limitation, the synthesis of PET probes must be completed in a few hours, which limits the scope of radiolabeled molecules which can be synthesized and tested with PET. For [^{18}F]fluoride, precursors without a positive charge at the targeted labeling site on the molecule are not readily amenable to nucleophilic substitution reactions [44].There are many strategies to

radiolabel electron rich sites such as in thioethers and aromatics and several are mentioned in chapters 3 and 7 respectfully. Each of these methods has synthesis limitations. PET probes synthesized by nucleophilic fluoride would benefit from a convenient late-stage fluorination method with wide applications [43]. Thus, this lack of viable late stage fluorination strategies often hinders the clinical translation of PET probes [45]

Radiochemical PET radiotracer research in the United States is mainly completed by approximately 60 university, government or private companies radiochemistry research facilities which synthesize and test a handful of new PET probes every year [9]. The slow pace of research is due to the large investment of expertise, time and resources to create and test PET probes [46]. The cost of FDA approval for new PET radiotracers can be reduced compared to non-radiopharmaceuticals although the cost can still be signifigant when compared to reimbursement from image acquisition. The reimbursement for this significant investment has not been structured favorably for private PET probe research due the differences of synthesis methods and the approval of PET imaging versus pharmaceutical prescription. Changes in policy and reimbursement strategies could renew commercial PET radiotracers research. Approximately 90% of PET imaging in medical clinics is performed by using 2-deoxy-2-[^{18}F]Fluoro-D-glucose ([^{18}F]FDG) probe [6, 47]. [^{18}F]FDG was first synthesized in 1969 at the Brookhaven National Laboratory [48]. The first PET machines were created in the 1970's which allowed [^{18}F]FDG PET images to be used on humans shortly afterwards [49, 50]. Since [^{18}F]FDG is an analog of glucose and is taken up by cells in a similar rate, cells that utilize more glucose take up more [^{18}F]FDG.

The remaining non-FDG PET probes account for 10% of clinical usage [51]. Due to the slow research progression and inability to identify appropriate applications not already covered by [^{18}F]FDG for new PET radiotracers, has caused many in the commercial sector to halt research.

Although there have been many advances in technology and methodology in radiochemistry synthesis, the field has not seen the growth and investment that many sectors of the pharmaceutical industry have over the same time span the last few decades. The pharmaceutical industry has already gathered a wide variety of biological information that can be applied for the development new PET probes. The majority of PET probes concepts are derived from valuable studies when researching traditional non-radioactive pharmaceutical treatments. In the past, the applications of new research to PET was often overlooked. Research is just beginning to become primarily focused on looking for potential biological processes for new PET radiotracers. The design space for PET probe development has barely been explored. The PET field needs more technologies to increase probe synthesis and validation. Using alternative technologies may lead to more PET tracer discoveries.

1.4 Introduction to Electrochemical Fluorination (ECF)

Selective electrochemical fluorination (ECF) of organic molecules has been used since the 1970's [52-58]. These electrochemical methods have provided accessibility of fluorinated organic compounds to medicinal chemists and biologists, such as fluorinating benzenes [59], [59], for several decades and has a robust history in late-stage fluorination of organic molecules under carrier added conditions. Historically, the main objective of electrochemistry was to produce the highest product yield which led to ECF research using large excess of reactants (fluoride) compared to precursors. This is evident in electrofluorination where the process is often performed using ionic HF as the solvent[54]. ECF was found to be rather effective when using high concentrations of ionic HF sources such as Et_3N*3HF and $Et_4NF*4HF$ [54, 56]. Yet, little research was conducted to explore cases of low concentration of reactants (fluoride), especially when

electrofluorination research is perform with less than 300 (mM) poly HF fluoride concentration [56]. This is rather problematic for developing new PET probes since the ratio of [^{19}F]Fluoride to [^{18}F]Fluoride leads to low molar activity under these conditions. This also limits radiochemical yield which is measured as a function of [^{18}F]Fluoride concentration conversion. The traditional ECF methodologies have to be adapted for low fluoride concentration to be useful in PET probe creation, which is a primary challenge of using this approach. Previous attempts to reduce fluoride concentration for ECF unfortunately led to poor results (low RCY and very low A_m) [4, 5, 60-62].

1.5 Electrochemical Fluorination Mechanisms

Electrochemical nucleophilic fluorination (ECF) relies on reduction of the electron density at the reaction center to activate molecules for a nucleophilic attack by fluoride ions. The ECF mechanism follows the ECEC mechanism which is summarized by four distinct steps (Figure 1): electrochemical oxidation (E) formation of a radical cation; nucleophilic attack of fluoride (C); a secondary oxidation (E); and, finally deprotonation (C). This can be seen in benzene and has previous been fluorinated in high yields through carrier added ECF [52, 59, 63-65]. Fluorobenzene was formed with 39.1% product yields using $Me_4NF*2.8HF$ poly HF fluoride source in acetonitrile [65].

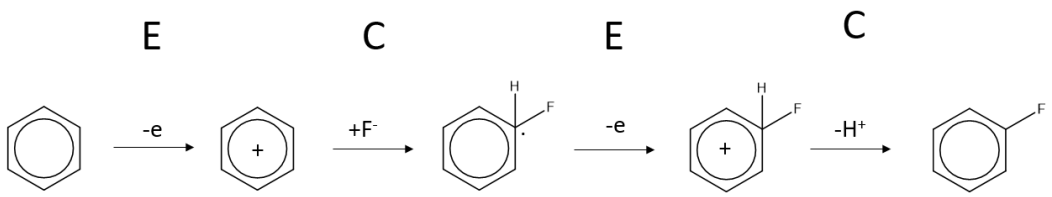

Figure 1: ECEC Mechanism steps of the Electrochemical Fluorination of Benzene.

In some cases, the EC steps are reversed and the deprotonation occurs before the fluoride addition as in the case of benzylic fluorination (Figure 2). Carrier added ECF has been performed on several different molecules at the benzylic position [66, 67]. Benzylic fluorination through electrochemistry produced product yields up to 74% using Et_3N*3HF in acetonitrile [67].

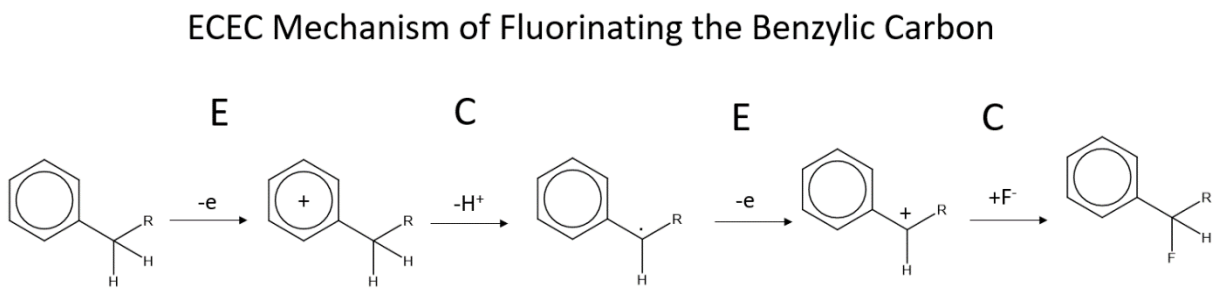

Figure 2: ECEC Mechanism steps of the Electrochemical Fluorination of the Benzylic Carbon.

Carrier added ECF has also been performed successful with naphthalene [68]. The mechanism is similar to benzene (Figure 3). Naphthalene was fluorinated with product yield of 18% using the solvent Et_3N*3HF [68].

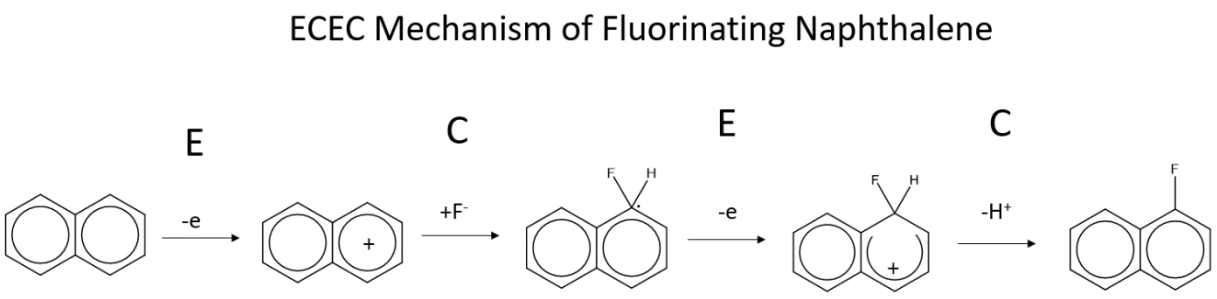

Figure 3: ECEC Mechanism steps of the Electrochemical Fluorination of Naphthalene.

Similarly, carrier added ECF was performed successfully with pyrazole (Figure 4) [69]. Product yield of the pyrazole precursors were obtained up to 47% using 25% by volume pyridine HF (70%) and a ratio of 0.6 of triethylamine to pyridine in acetonitrile [69].

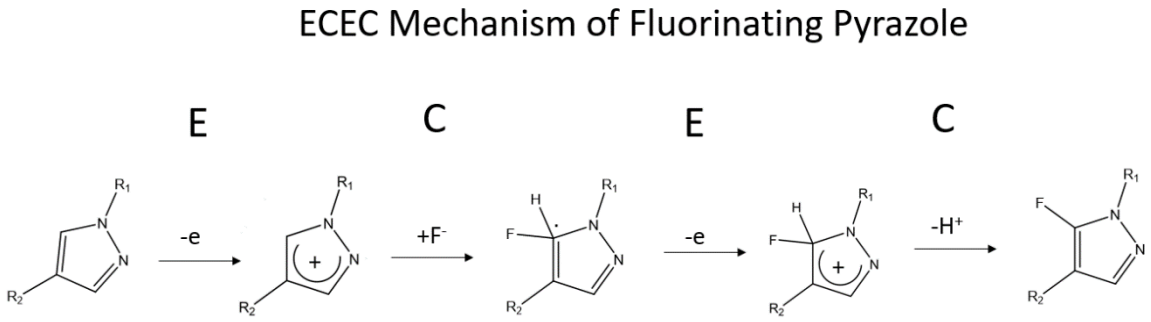

Figure 4: ECEC Mechanism steps of the Electrochemical Fluorination of Pyrazole.

The fluoro-Pummerer rearrangement was proposed for the ECF of thioethers to accommodate fluoride to serve as a stabilizer for oxidized sulfur. (Figure 5) [70]. The mechanism is initiated via oxidation of sulfur stabilized by the binding of fluoride. Next, the hydrogen on the alpha carbon is abstracted to stabilize fluoride as it leaves to form a sulfonium/carbenium ion. This sulfonium/carbenium cation is then attacked by the fluoride anion forming the alpha fluorinated sulfide. This has been proven effective for a number of thioethers- and sulfur-based reactions which have been successfully fluorinated under carrier added conditions [54, 55, 70, 71]. Using

Ethyl (phenylthio) Acetate thioether precursor, Et3*3HF and acetonitrile as solvent the fluorinated product yield was 88% [70].

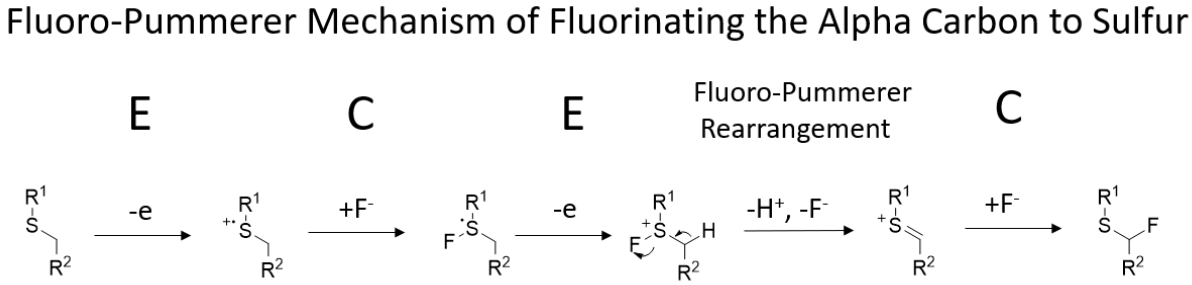

Figure 5: The Fluoro-Pummerer Mechanism steps of the ECF for thioethers.

1.6 Potential Benefits of Electrochemical Fluorination for ^{18}F labelled PET Probe Synthesis

Electrochemical Radiofluorination is an emerging field with promising potential to improve current synthetic approaches for PET probe synthesis. Most electrochemical fluorination reactions are relatively straightforward reactions that proceed rather quickly in order to preserve the radioactivity for short-lived radioisotopes. The precursors often do not need to be pre-modified such as pre-activation with electron-withdrawing groups, positioning a leaving group, post elimination of groups or the need to have complex additions that often limits the scope of these methods due to group hinderance and the synthetic difficulty in preparing precursors [37, 43, 44]. This is true since the charged cation intermediate produced on the anode has a favorable interaction with the fluoride anion. The fluorine source can also be used without extensive modification such as using phase transfer catalysts or organometallic complexes [37].

Electrochemical oxidation reactions can be carried out under mild conditions without the usage of a hazardous chemical oxidant that can limit some radiochemical reactions [55]. Under potentiostatic conditions, the oxidation effect can be precisely controlled making regio-selective

radiofluorination highly amenable [53, 54]. ECF is a late-stage fluorination methodology with great potential to be applicable towards a large scope of different bioactive compounds since this method is based on electron density and oxidation potential in contrast to specific chemical structures. For instance, many chemical methodologies must be tailored to the individual molecular structure and electronic characteristic of the compound. In return, this limits the scope or slows the throughput of identifying potential probes [44, 72]. ECF can be used to fluorinate aromatics [73-76]; an important target due to the stability of fluorinated aromatics *in vivo*, which makes late-stage fluorination strategies for aromatics to be most advantageous for synthesizing PET probes [77]. ECF can also be performed in large scale parallel syntheses using an array of screen printed chips increasing throughput. Finally, ECF of organic compounds provides a means to overcome some current synthetic challenges and approaches in developing PET tracers [76].

1.7 Background on Traditional Electrochemical Fluorination

Traditional ECF requires the use of ^{19}F (stable fluorine) poly HF sources in very high concentrations used as solvent or at concentrations of 1.5M or greater. Electrochemical fluorination was originally used at high oxidation potential (>5V, SHE) on nickel anodes in the Simons process [78, 79], which resulted in Ni-fluoride complexes from oxidizing fluoride above 3.9V (SHE). The Ni-fluoride complexes serve as an electrophilic source of fluoride which is highly reactive and often leads to continual fluorination of the organic molecule precursor. The Simons process is not amenable to regioselective monofluorination and also requires the use of HF as solvent or in high concentrations. The oxidation potential used for the Simons process oxidizes most organic molecules at various sites often causing side reactions of the precursor. The high oxidation potential that the Simons process requires causes many electrochemical side reactions

and significantly limits the number of compatible solvents, electrolytes and precursors. Due to the above reasons, the Simons process of generating Ni-fluoride complexes on the anode is not suited for PET probe creation. However, some of these concepts and thoughts on ECF are still based on the Simons process and are not applicable under the newer lower oxidation potential methods.

Rozhkov first summarizes the ECEC mechanism of electrochemical fluorination under low oxidation potentials [52]. This method oxidizes an organic molecule to form a radical cation which reacts with the fluoride anion (section 1.5.) ECF reactions under these conditions no longer formed the Ni-fluoride complexes at the anode. At these lower oxidation potentials, radical cations are generated which can cause reversible Cyclic Voltammetry (CV) at fast cycling speeds due to the oxidation and reduction reactions occurring in the radical cations chemical life-time. With the addition of fluoride, the CV of the organic precursors will become non-reversible since the radical cations react and incorporate fluoride instead of being reduced to form the original molecule. These CV changes due to the addition of fluoride and the fluorinated product formation which occur at considerably lower oxidation potentials than fluoride (<2V, SHE) rules out the Simons process or oxidation of fluoride as a possible route to fluorination. For example, in the ECEC mechanism using benzene as precursor mono fluorinated fluorobenzene forms in high product yields with little to no formation of di or tri fluorobenzenes [59, 80]. Using the Simons process, the main products are poly fluorinated benzenes with mono fluorination occurring only with low product yields [78]. The ECEC mechanism can be much more selective and can be performed at oxidization potentials that are stable for more complex bio-active organic precursors.

In addition to ECEC, an additional mechanism was proposed to fluorinate molecules through ECF alpha to sulfur, which was found to be rather effective. Fuchigami et al. proposed the fluoro-Pummerer (FP) mechanism via the fluorosulfonium cation (section 1.5) and there is

strong literature evidence for FP to occur in ECF when adding fluoride on the alpha carbon in place of hydrogen. Originally, the proposed mechanism suggested the electron withdrawing groups (EWG) are necessary for FP to occur. However, further investigations showed EWG and electron donating groups (EDG) to be effective on either side of the sulphur or alpha carbon [81, 82]. After electrolysis, alpha methyloxylation in thioethers occurred in methanol with the fluoride source but did not occur without the fluoride source [81]. This strongly suggests that fluoride is critical in the intermediate steps as suggested by the FP mechanism. The addition of chlorine or other halogens did not cause alpha methyloxylation of thioethers suggesting the FP mechanism in ECF is unique to fluoride. Using sulfides and sulphones as precursors did not lead to fluorination, suggesting the first step is oxidation which is followed by the stabilization of the organo-sulfur cation [83]. Methyl phenyl sulphone oxidized added fluoride exclusively to the aromatic ring and not at the alpha carbon to fluoride as in thioethers [84], which also supports the hypothesis that the organo-sulfur cation is stabilized by fluoride. Research into ECF for medical and organic synthesis started to decline in popularity during the late 1990's due to a shift of focus of many of the key ECF researchers. This hindered further discoveries into the ECEC mechanism and FP rearrangement. For instance, there is little to no reporting on the ECF mechanism under low concentration of fluoride applicable to PET probe creation.

In an ideal ECF experiment only the precursor would undergo oxidation at the desired oxidation site. In real ECF, some oxidation of the solvent and electrode will occur as well as precursor at non-desired locations. Also, in an ideal ECF experiment, the reduction process would not infer with the product formation. Poly HF fluoride sources are almost ideal for reduction due to their easy formation of hydrogen gas on the cathode. Shifting to lower poly HF concentration requires another molecule to reduce that does not interfere in ECF. Acids like poly HF fluoride

sources are compatible and favorable in these conditions since they also reduce to hydrogen gas on the cathode.

Since the solvent and electrolyte are required to have a wide electrochemical window for stability in the electrochemical process, the most common solvents used in electrochemistry are MeCN, DME, and Cl_2CH_2. DME oxidizes at a similar potential as some aromatic molecules and can be fluorinated at ~2.9V (SHE)[85]. Cl_2CH_2 has low dielectric constant leading to lower conductivity, low current and oxidation rates. MeCN is the most popular solvent for ECF and has a wide electrochemical window, which his compatible with most organic molecules and high dielectric constant for increased conductivity with added electrolyte. One issue with MeCN is its ability to serve as a nucleophile leading in acetamidation. Due to the oxidation potential of fluoride, organic molecules and the stability of solvents electrolytes, ECEC and FP are the only mechanisms so far to be able to electrochemically perform nucleophilic fluorination of organic molecules for PET radiotracer synthesis. [86].

One of the most complex and theoretically difficult electrochemical processes is the distribution of cation formation sites in larger organic molecules. When the oxidation potential is high enough to oxidize several sites, it is difficult to determine the distribution of oxidation sites. Small-molecular precursors orientate themselves to enable the oxidation of specific sites. However, when organic precursors become large along with higher the oxidation potential, there may be many different potential oxidation sites and radical cations formed.

There are several strategies to overcome these difficulties. For example, different solvents have been investigated to form solvent shells around precursors to direct the formation of the preferred cations. Lower oxidation sites can be protected by protecting groups to increase the oxidation potential of these sites. Molecules with oxidation potentials just above the precursor can

be added to prevent unwanted oxidation. The precursor can be sterically hindered to favor the preferred oxidation or prevent an unwanted oxidation side reaction.

Thioethers oxidation can be controlled easily to only allow for monofluorination due to the large increase in oxidation potential of the alpha fluorinated thioether compared to the thioether precursor [83]. The difference in oxidation potential between mono-fluorinated product and precursor is much lower in benzylic and aromatic compounds. This causes the selectivity in oxidation of the precursor over the products to be less for aromatic and benzylic fluorinations. The benzylic cation is usually much more stable due to aromatic conjugation than the thioether or aromatic intermediate cations. The more stable intermediate cations have been shown in some cases to have the highest fluorination yields. ECF in MeCN with $Et_4NF*4HF$, the more stable benzylic cations generally were shown to have the highest yields [87]. In this case, fluoride reacts preferably to more stable benzylic cations and acetamidation occurred more preferentially in less stable benzylic cations.

Precursors with different potential fluorination sites have been successfully electrochemically fluorinated in some cases at one site while other cases fluorination was split between sites. For instance, fluorination almost always preferentially occurs alpha to sulfur in thioethers rather than on aromatic carbons in compounds containing both groups even at high oxidation potentials. With O-methyl S-aralkyl thiocarbonate precursors are oxidized exclusively at the alpha carbon of sulfur and not the benzene ring [88]. Both single fluorinated and difluorinated thioethers have oxidization potentials lower than benzene, making sulfur the more likely cation formation site. Aromatic and benzylic fluorination sites on the same precursor usually favor benzylic fluorination but can occur together or even with aromatic fluorination exceeding benzylic fluorination in traditional carrier added ECF [56]. When using N-alkylphenylacetamides

both aromatic and benzylic fluorinations were major products in MeCN using poly HF fluoride sources [89].

There are several troublesome specific cases in electrochemical fluorination for common organic precursors. When oxygen is unprotected and attached to aromatics rings such as phenols, di or trimethoxybenzenes, the oxidation of oxygen results in a double bond, which causes the loss of aromaticity leading to side product formation [90]. The cyclohexadienyl cations formed via this mechanism are likely to react with each other and the original precursor, leading to dimerization. Another troublesome group are amines which may act as nucleophiles after oxidation attacking aromatics or other electron-dense sites, leading to dimerization and side product formation. In past traditional carrier added ECF, the amine group is often protected by a single methyl or other protecting group which keep the amine group from interfering and reducing product yields [89]. Unprotected amine groups tend to be reactive and reduce or inhibit ECF product yields. Alkenes are a third group that can be easily oxidized at low potentials but are avoided in precursors where oxidation is preferable at other sites.

Past ECF methods have shown to be powerful methods of fluorination under high fluoride concentration which is evident in fluorinated organic molecules such as amino acids. Amino acid derived oxazolidines from L-serine and L-threonine were both successfully fluorinated with ECF. Both fluorinated alpha N with product yield past 70% using MeCN as the solvent [91]. Pulsing the electrode every 5 seconds and using a temperature of 0° C was found to generate improved yields rather than conducting the reaction under warmer or colder temperatures. This pulsing prevents adsorbed molecules from forming on the anode which interferes with ECF. Negative pulses can send adsorbed molecules from the anode to prevent build up. In the case of these amino acid

precursors, a protective group for the nitrogen was unnecessary since it is already sterically hindered and unable to act as a nucleophile.

In the ECEC mechanism, it is important for the radical cation to have a long enough lifetime to react with fluoride. In successful ECF fluoride react quickly with the cation intermediate before any other chemical process occurs to the radical cation. There are several different processes that occur after oxidation to the radical cation which decreases fluorination yields. There are several alternative reaction of the radical cation besides reacting with fluoride that reduce fluorination yields which are reactions with the solvent, precursor, another radical cation, a nucleophile, or degradation termed disproportiation [92]. When disproportiation occurs, it is often a bond at the alpha or beta carbon that is broken [82].

The reaction of radical cations with nucleophilic solvents can produce side product formation such as acetoxylation, cyanation, and methoxylation. The solvent plays a key role in the oxidation process and stabilization of the cation. Solvent molecules form a solvent shell around the organic precursor. The solvent shell reorients itself upon oxidation to incorporate a positive charge on the radical cation. Depending on the shape, conformation, and reactivity of the solvent, this radical cation can react almost immediately with the solvent [88]. For aromatics, successful ECF has been performed in electrochemically stable solvents, such as MeCN and DME. The solvent shell also can direct or encourage the other potential processes after oxidation such as dimerization, nucleophile addition or other side product formation. This is quite noticeable from our experiments when performing ECF in a mixture of two solvents where certain side product formation occurs in the mixture and not in either solvent alone.

Nucleophilic addition to radical cations produced in ECF has been studied under a variety of conditions. Competing nucleophiles placed in the solution or produced from the electrodes can

hinder ECF yields. Fluoride can replace hydrogen atoms which is most common or replace chlorine, bromine, methoxyl, isopropyl, and t-butyl via ipso attack in the ECEC mechanism as seen in mono substituted benzenes. The nucleophilic attack by a fluoride anion is determined by the density distribution of positive charge in the radical cation which confirms the ECEC mechanism as the most likely explanation of electrochemical fluorination. However, the orientation of the produced radical cation on the anode as well as the geometry of the solvation shell around the radical cation also have significant effects.

Dimerization or reactivity of a radical cation, precursor molecules or other produced side products, is a current obstacle in ECF reactions, specifically, for most aromatic precursors. There are two main methods of electro-dimerization in aromatics. First, the arene cation produced on the anode nucleophilically attacks the starting aromatic molecule. Second, these two arene radical cations react with each other [86]. Dimerization or the bonding of precursor components after electrolysis is the main cause of passivation, which leads to build-up on the electrode that occur very quickly covering the anode often completely preventing product formation.

Preventing unwanted secondary electrochemical reactions remain to be a challenge in ECF, especially when performing reaction under low fluoride concentration. Without an abundance of fluoride, produced cation intermediates will react with another molecule in the vicinity such as solvent, precursor, another cation. This can lead to a buildup of side products which can undergo oxidation and further reactions. With an abundance of fluoride, most the radical cations that are produced will react with fluoride which significantly lowers side product formation and secondary electrochemical reactions.

Additionally, there are several other electrochemical processes that can negatively affect ECF. For some precursors, fluorination significantly increases the oxidation potential to protect

from additional oxidation of the mono fluorinated product preventing further fluorination. However, for benzyl and aromatic fluorinations, fluorine does not greatly increase oxidation potential. The product oxidation potential is still quite similar to the oxidation potential of the precursor. This lead to a second oxidation which further fluorination or more often side product formation in the case of low fluoride concentration [65]. Benzylic positions onset oxidation potential can change from fluorination in some cases by only about ~0.1V [80]. To achieve sufficient current and amount of oxidation an oxidation potential of at least ~ 0.3V above the onset oxidation potential is usually necessary. This can lead to multiple oxidation and side product formation for benzylic precursors.

Reduction of the precursor can also lead to precursor changes that affect oxidation and side product formation. Reduction can lead to the loss of aromaticity lowering the oxidation potential of the newly formed alkene electrons compared to aromatic electrons. Additionally, these reduced molecules may have favorable reactions with the radical cations decreasing ECF yields. For instance, oligomers are more stable than dimers which have a lower oxidation and tend to undergo preferential oxidation over the oligomer precursors. Once enough dimerization or polymerization occurs, oxidation of the precursor will be excluded due to undesired buildup of these alkenes, dimers or polymers.

To overcomes these challenges, some researchers resorted to utilizing modeling approaches to predict electrochemical reactions. Yet these initiatives were found to be rather difficult in low fluoride concentration due to side product build up effects and the unpredictable reaction conditions that are continually changing over time. For instance, the reaction solution can contain different concentration of constituents at different times during the reaction. There may be significant concentrations of 20 or 30 different side product during electrochemical synthesis in

no-carrier-added conditions. The product and side product formation are not a constant rate through the reaction and may not even occur throughout the duration of electrolysis, which can result in a very dynamic environment with constantly changing parameters. As a result, the combination of these challenges makes theoretical modeling of the entire reaction process to include all electrochemical and chemical reactions unfeasible for complex precursors and low fluoride concentrations. There are also additional experimental variations and errors within these dynamic processes even under similar conditions.

A key step for ECEC mechanism is the proton abstraction step, which is often known to be the rate determining step [56, 87, 91]. This is especially true if the deprotonation step occurs after the first oxidation, which requires a base or anion to abstract the proton shortly after oxidation on the anode. In traditional ECF, the anionic fluoride species are favored to perform these activities due to its availability in high concentration. Without high concentration of fluoride, proton abstraction may be difficult since the pH can change over time due to electrolysis and tends to be more acidic. High concentration of poly HF fluoride sources can help buffer anodic production of protons and cations creating acidity whereas lower fluoride concentration cannot buffer the ionic flux near the electrodes. Weak bases present can become strong acids near the anode due to the availability of protons, which in return may react with intermediates, precursor, or product lowering yields.

There are many strategies used in this work to overcome challenges associated with ECF transitioning to NCA-ECF. Protection of lower oxidation groups hinders oxidation so that cation formation occurs at the preferred site. The tert-butyloxycarbonyl protecting group (BOC) is used in this work but methyl groups can also be used depending on the oxidation potential. Using different solvents can address these problems which can help stabilize the radical cation to increase

their lifetime to react with fluoride. Additionally, the solvent can undergo reduction to prevent precursor or other unfavorable reduction. The solvent can help ECF directly or deter side reactions in many different ways. The solvent can undergo oxidation above the onset oxidation of the precursor to prevent unwanted further oxidation of the product. The solvent in reduction may become a base and help with proton abstraction. The solvent or other additive can help prevent and interfere with dimerization or polymerization. The solvent or other additive can also help prevent passivation or help control pH during electrolysis.

1.8 Electrochemistry Physics

The chemical steps in electrochemistry and normal chemistry are vastly different where the electrode creates a physical environmental that is not reproducible thorough only chemical means. The electrical potential can orientate solvents, electrolyte, and precursor molecules, which can change the chemical behavior. The potential also changes the electron density of the molecule as it approaches the electrode which can alter its chemical reactivity. The formation of a sheet of ions being produced and diffusing away from the electrodes also differs from chemistry. For example, biphenyls can form from aromatic precursors as the radical cation diffuse and electrophilically attack unreacted aromatic rings of the precursor. Anions such as fluoride are attracted and move quickly to the positive potential of the anode. Fluoride adjacent to the anode is attracted to the anode surface and moves toward the anode continually building up concentration. One of the possible explanations of the efficiency of using poly HF fluoride sources is the availability of H_nF_{n+1} species adjacent to the anode. This creates an exceptional different environment than in non-electrical chemistry where a positive anode with a layer of anions next to it where cations are produced and quickly move away. The inner layer near the electrode was

historically called the Inner Helmholtz Layer (IHL), which is composed of a layer of molecules next to the electrode surface that excludes molecules with a similar charge as the electrode due to repulsion. The next layer is historically called the Outer Helmholtz Layer (OHL), which is composed of molecules attracted to the electrode by electrostatic potential. This has many more opposite charge molecules but also a few liked charge molecules as the electrode. Outside the Double Layer (DL), consisting of the IHL and OHL, is the bulk solution where there are minimal electrostatic forces present. The DL theory has evolved since the Helmholtz era and has been refined to include more continuous approximations. These layers, ions, and forces are important when considering ECF mechanism under different conditions. Currently, there is a large difference of many orders of magnitude in the concentration of fluoride and precursor in traditional carrier added ECF compared to the NCA-ECF experiments presented herein. In most traditional ECF experiments, the precursor is 1 mM concentration and fluoride are at least in 1.2M concentration, a factor of 1:1200 – (precursor:fluoride) ratio. This small precursor concentration prevents accumulation of side products and dimerization. In NCA-ECF, a greater concentration of precursor is used to produce more radical cations to interact with the scare availability of fluoride. In the NCA-ECF experiments herein, 50 (mM) of precursor is used for most the experiments and approximately 1 (uM) of fluoride is used due to normal fluoride contamination found in chemicals and from cyclotron production and transfer, a ratio of 50,000:1 – (precursor: fluoride) ratio under NCA conditions which is much less compared to the original 1:1200 in carrier added traditional ECF. The change from precursor:fluoride ratio is over 7 orders of magnitude. This dramatically shift in ratio discouraged many researchers to continue pursuing research in the NCA-ECF space in the past.

Additionally, in non-radioactive ECF, these syntheses can occur over hours or days at potentials very close to the onset oxidation potential to avoid side product formation and reduce the production rate of radical cations which decreases dimerization or passivation. In the radioactive case, this is not possible and higher oxidation potential must be used to achieve detectable yields in a short time.

1.9 Form of the Anionic Fluorine Source

Besides, poly HF fluoride, other fluoride sources such as KF, CsF, TBAF and pyridine fluoride (non-HF) were reported to perform poorly since the lack of hydrogen fluoride (HF) in these sources led to no or little product formation. The effectiveness of poly HF fluoride sources led to research into the form of the fluoride species, which in traditional ECF is known to be the anionic nucleophilic H_nF_{n+1} species form [93-96]. The anionic fluorine species react with oxidized precursors to form the fluorinated product and also participates in hydrogen abstraction. Many electrochemical experiments were previously performed with pyridine fluoride sources without HF but resulted in no success when testing thioether precursor previously fluorinated with Et_3N*3HF [82, 97, 98]. These non-HF fluoride sources did not work.

Several studies have been performed to determine the form of fluoride in poly HF sources in ECF. Molecular dynamics studies showed hydrogen fluoride in ionic liquids formed poly fluoride species [99] such as $F(HF)^-$, $F(HF)_2^-$, and $F(HF)_3^-$, At equilibrium, these anions exist in proportions of approximately 10%, 40% and 50%. A study of the anion fraction of EMIM $(HF)_nF$- reported the ratio of HF to EMIM effected the ratios of the $(HF)_nF$- anion complexes [94] where greater concentrations of HF led to a larger n-value. Particularly, at high concentration of HF, the average n was 2.6 which is comparable to the previous reported molecular dynamic studies. The

structure of the $(HF)_nF^-$ was also investigated by NMR, Raman spectroscopy, IR and x-ray diffraction [100] with three types of $(HF)_nF^-$ anions of n = 1, 2, and 3.

Under high concentration of poly HF sources, the form of fluoride was determined to be $(HF)_nF^-$ anion complexes that participate in fluorination and proton abstraction in the ECEC mechanism. Yet, there is little information to uncover the form of fluoride under NCA conditions or low fluoride concentrations since it is difficult to determine the reactive fluoride species in NCA-ECF experiments. It is hypothesized another molecule is serving as the HF and responsible to form the anionic species of fluoride with similar reactivity. However, this may not be likely since the nucleophilicity of fluoride near the anode is challenging to determine even when using high concentration of poly HF. Determining the nucleophilicity of fluoride under NCA condition in ECF is more difficult to determine. The presence of protons or trace amounts of water could affect nucleophilicity or the form of fluoride in NCA conditions.

Several studies have attempted to use other halogens as mediators in ECF. Adding bromine or iodide into the reaction with fluoride as a potential mediator which can lead to BrF^- and IF^- complexes that serves as nucleophilic sources of fluoride. However, electrophilic species of the Br and I also form, as well as electrophilic complexes with fluoride leading to the non-selective addition of fluoride and halogens to the precursor. This is due to the low oxidation of the other halogens and the neutral and positive species formed on the anode of these other halogens.

One unexpected finding from exploring reaction results under different forms of poly HF fluoride sources is that they lead to different product yields. It is reasoned that the amount and type of the H_nF_{n+1} form may have different fluorination and proton abstraction capabilities where the acidity of the solution with different poly HF fluoride sources can have a role in these electrochemical processes. This is evident in studies with oxidation of 1,3-Oxathiol-5-ones

fluorinated in high yields using $Et_4NF*4HF$ but not with Et_3N*3HF in MeCN[57]. Additionally, there are many reports where higher concentration of poly HF fluoride sources reduced or stopped fluorination yields [55].

Several different groups have attempted to stabilize cations or make fluoride more reactive to increase product yields in traditional ECF. For example, the triflate anion was hypothesized to stabilize cation intermediates and increase fluorination yields. 1-ethyl-3-methylimidazolium trifluoromethanesulfonate [EMIM][OTf] increased the fluorination yields of phthalide using poly HF fluoride source in MeCN [54]. The use of [EMIM][HF] without -OTf had poor yields. In the difluorodesulfurization of O-ethyl benzothioate, Polyethylene glycol (PEG) can increased fluorination yields, it was hypothesized the PEG's anodic stability can coordinate counter cations to the fluoride ions. Not much has been investigated with sulfoxide difluorination beyond the initial publication and its suitability under low fluoride concentration is still unknown [71].

Kryptofix chelator (K222) with potassium bicarbonate is widely used in radiochemistry to ^{18}F label organic molecules. The Kryptofix chelator contains a potassium ion so that fluoride is weakly bound to the shell instead of tightly bound to potassium. It is useful for substitution reactions with good leaving groups such as triflate. K222 is electrochemical unstable and does not produce product yields during ECF. K222 undergoes redox and degrades in the electrochemical cell. The complex of K222+potassium+fluoride tends to disassociate in an electrochemical solution with the added electrolyte in solution for conductivity. Potassium also undergoes redox, as well as carbonate or bicarbonate under the normal potentials used in ECF. For all of these reasons Kryptofix does not work well in an electrochemical cell for ECF.

1.10 From Published ECF to PET Application

There are several important milestones that were achieved to be able to use ECF for PET applications. The first milestone was reducing poly HF concentration in ECF while maintaining fluorination yields. To do this an easy to fluorinate thioether was used. The second milestone was to test many different parameters and thioether functional groups to better understand the ECF process under low fluoride concentration. The third milestone was to use the lesson learned from the first and second milestone to perform ECF on simple aromatics under the same low fluoride concentration. Naphthalene and an F-DOPA intermediary was used for this. The fourth milestone using the knowledge from milestone 3 was to perform ECF on and form a complex aromatic PET tracer. The COX-2 Inhibitor tracer was used for this milestone. Additionally, this work contains the first no-carrier-added electrochemical fluorination using fluorine-18 on thioethers and aromatics.

Chapter 2: Experimental

2.1 ^{18}F-Fluoride and Crude Product Preprocessing

[^{18}F]Fluoride is produced from proton bombardment of [^{18}O]water by a cyclotron. Fluoride is highly solvated by water making the ion unreactive in the presence of water. Water is removed from the reaction before transferring the [^{18}F]Fluoride into an organic solvent in order for it to be reactive in the electrochemical cell. To perform this, the [^{18}F]Fluoride was trapped on an MP-1 (Bio-Rad) anion exchange resin. Water on the resin was removed by drying with N_2 or Ar gas for 5-10 mins, washing the resin with pure solvent (the same solvent used in the electrochemical cell), and drying for 5-10 mins under N_2 or Ar gas. [^{18}F]Fluoride was then eluted from the resin with tetrabutylammonium perchlorate (TBAP) under no-carrier-added condition or by $Et_4NF*4HF$ under carrier-added conditions in organic solvent. This process is controlled with the automated electroradiochemistry platform (ERCP) described in section 2.2 due to the high levels of radioactivity. P_2O_5 was used to help remove trace amounts of water and the exchange resin was heated for better trap and release (Figure 6).

After the electrolysis, the reaction will consist of the crude product, precursor, unreacted [^{18}F]Fluoride, and side products which need to be removed for various analytical testing. Thin layer chromatography (TLC) with gamma detector was performed immediately on the crude product sample to determine radiochemical conversion (RCC). High pressure liquid chromatography (HPLC) with gamma detector was used to determine radiochemical purity (RCP). For carrier added experiments, gas chromatography (GC) was used to identify the products. To remove unreacted fluoride, the crude sample was added to 20 times the volume of water and passed through a Sep-Pak C18 classic cartridge and eluded with methanol or ethanol. Samples were chosen for HPLC separation and isolated for proton or fluoride nuclear magnetic resonance (NMR)

by the automated platform in section 2.2. The details and specifics of the synthesis conditions, analytical testing and processing will be described in the following sections of this chapter.

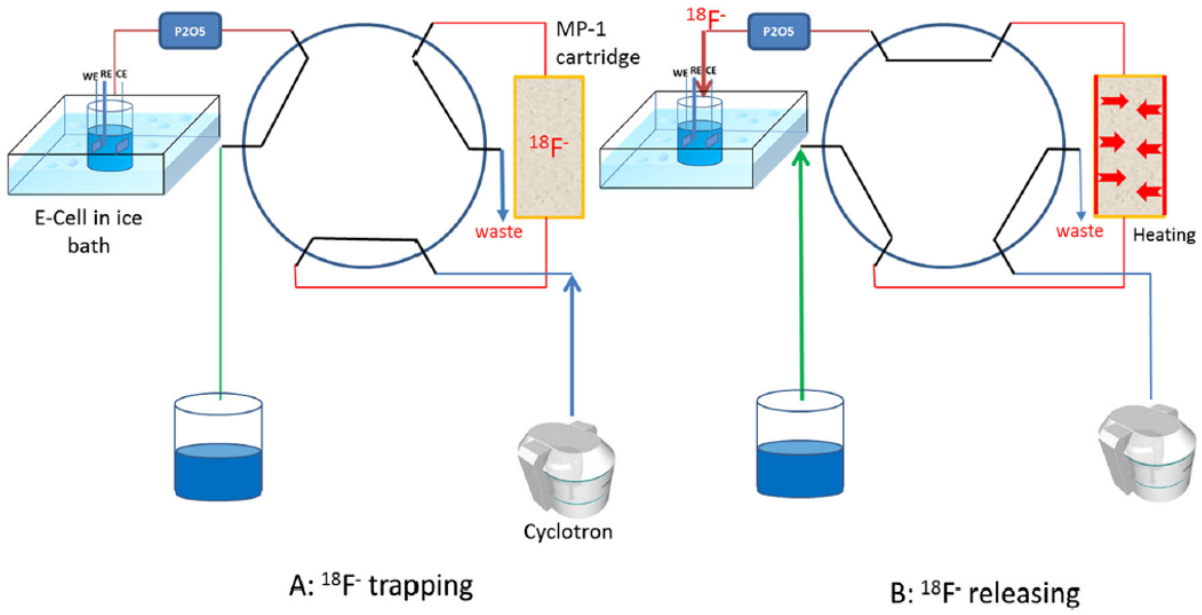

Figure 6: An Example of [18F]Fluoride Exchange Using MP-1 Resin.

2.2 Experimental Electrochemical Cells

Single chamber electrochemical cells were used here which contain one compartment with platinum (Pt) anode and cathode with a silver (Ag) wire used as a pseudo reference electrode. A stirring bar is added at the bottom of the cell for improved convection. The electrochemical cell was placed in a heated oil or ice bath for temperature control. Additionally, inert gas is used to purge the solution of air and to cover the liquid during electrolysis.

Several other types of electrochemical cells besides single chamber cells were also used. Screen printed electrochemical cells (DropSense) have all the electrodes on a single chip. This chip contains all electrodes on a single surface which was used for static or flow cells. The advantages of this approach allow solutions to flow through them creating a shorter time for the

molecules to be oxidized. This prevents over oxidation or unwanted oxidation of product or precursor. Another type of electrochemical cell used was the two-chamber electrochemical cell which was separated by a membrane to divide the oxidation and reduction. The anode and reference electrode in one chamber and cathode in the other chamber. An anion or cation exchange membrane is used to allow one or the other to travel through the membrane to the opposite chamber. By allowing only anions or cations to pass between the chambers, it limits unwanted reduction in the anodic chamber. An additional proton sink was also used with the two-chamber cell to reduce acidity since the addition of base is not compatible with the ECF due too low oxidation potential of the base and also due to the nucleophilicity of the base which competes with fluoride.

Electrolysis was conducted in a three-electrode system under a constant – potential mode controlled by an Autolab128 potentiostat-galvanostat (Metrohm USA). A pulsing technique, switching the potential from a high level to a low level periodically, was often used to minimize anode passivation, surface polymerization, and poisoning issues. The Pt electrode used was selected from either 0.1 mm wire in a mesh formation or Pt mesh. A leakless Ag/AgCl electrode (EDAQ Inc, USA) was also used instead of an Ag wire. Tetrabutylammonium perchlorate was used as electrolyte for conductivity. $Et_3NF*4HF$ was used as the fluoride source under carrier added conditions. Carrier added ECF of thioethers was performed at an oxidation potential of 1.9V (Ag/Ag+), Modafinil Precursor at 2.0 V (Ag/Ag+), Naphthalene at 2.0 V (Ag/Ag+), F-DOPA Intermediate Molecule at 2.6V and COX-2 Inhibitor Precursor at 2.7V (Ag/Ag+) unless otherwise noted.

2.2.1 Single Chamber Electrochemical Cells

2.2.1.1 Single Chamber Electrochemical 20 ml Cell

The 20 ml single chamber electrochemical cell was used for carrier added synthesis. This cell was used to make the fluorinated reference samples for analytical verification with MeCN as solvent and 100 (mM) $Et_4NF*4HF$ as the fluoride source and 50 (mM) of TBAP. The polarity of the electrode was switched every 60s with the chosen oxidation potential for 60 seconds and -0.6V for 5 seconds.

2.2.1.2 Single Chamber Electrochemical 6 ml Cell

The 6 (ml) single chamber electrochemical cell was used for the optimization work with carrier added ($Et_4NF*4HF$) and No-Carrier-Added (NCA) ECF of methyl (phenylthio) acetate precursor (Figure 7).

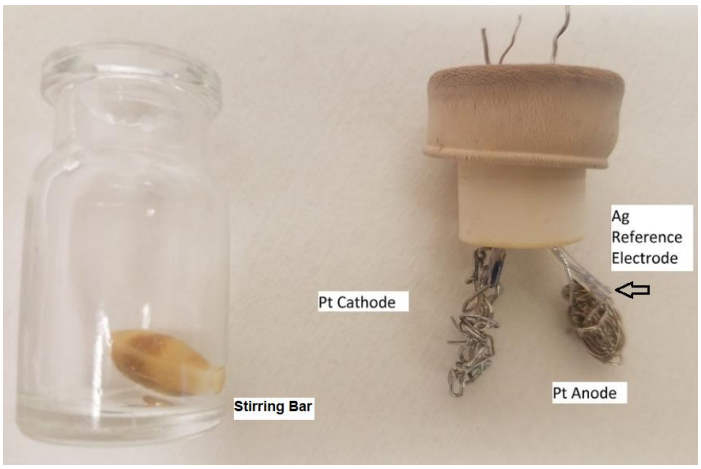

Figure 7: The 6 (ml) Single Chamber Electrochemical Cell. Contains Pt Anode and Cathode and Ag pseudo reference electrode.

2.2.1.3 Single Chamber Electrochemical 1.5 ml Cell

The 1.5 ml single chamber electrochemical cell was used for NCA-ECF of thioethers and aromatics (Figure 8). The smaller size is advantageous to reduce costs and to concentrate the fluoride in a smaller volume. This is especially beneficial in a small volume as the positive charge

of the anode brings the negatively charged fluoride ions in close proximity to the formed cation intermediates. The 1.5 ml electrochemical cell (Figure 8) was made from a glass 12X32 mm HPLC vial with a standard 4.6mm opening. The vial was replaced with a new one after each experiment. An 8 mm long 1.7 mm wide PTFE stirring bar was placed in the cell for stirring during electrolysis. A 11.5 mm wide PTFE HPLC vial cap was with rubber septum was used to seal the cell. Three small holes were punched in the cap septum to accommodate the 3-electrode cell. The anode and cathode were made from platinum wire with surface area approximately 600 mm^2, wrapped around a 1 mm diameter platinum wire. A 0.5 mm diameter silver wire was used as a pseudo reference electrode. PEEK tubing was placed around the platinum wire for the anode and cathode to form a seal with the rubber septum. PEEK tubing 18 mm long was placed around the silver pseudo reference wire only exposing the last 2 mm of the wire to solution. The PEEK tubing for the anode, cathode, and reference further ensured electrical isolation and consistent placement geometry of the reference electrode with respect to the working electrode in the cell. Additional PEEK tubing was used to hold the anode and reference together and as a separator for the cathode, ensuring a rigid geometry during the synthesis. The electrochemical cell was placed in a heated oil bath or ice bath for temperature control.

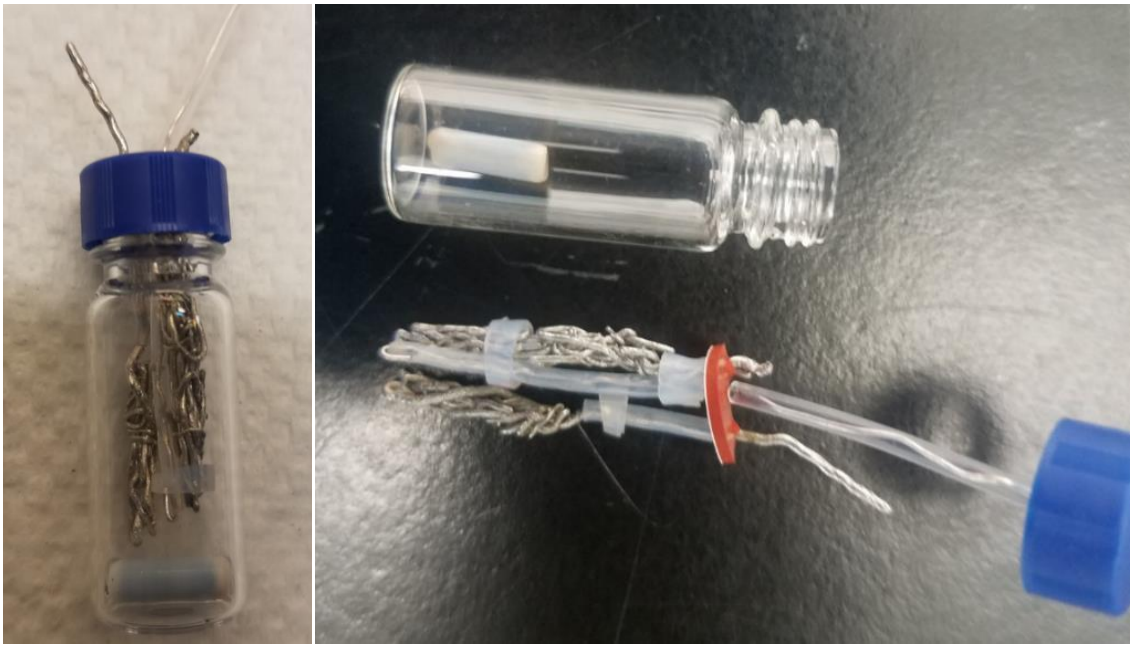

Figure 8: The 1.5 (ml) Single Chamber Electrochemical Cell. Contains Pt Anode and Cathode and Ag pseudo reference electrode. Made from HPLC vial for easy cleaning and vial exchange.

2.2.1.4 Single Chamber Electrochemical Screen-Printed Chip Cells

Screen-printed electrochemical cells contain three electrodes on a signal disposable and low-costing chip and were filled with 500 uL solution (Figure 9). This high throughput assay is beneficial since many experiments can be completed in parallel which is important especially for the limited timely nature of radiochemical synthesis. Additionally, it is not necessary to perform cleaning on the electrodes as the chips are meant to be disposable. The experiments in the static chip electrochemical cell were conducted in a three-electrode system under a constant – potential mode controlled by an uStat 8000 Potentiostat (DropSens). The chip contains 8 sets of electrodes allowing 8 experiments to be performed at once.

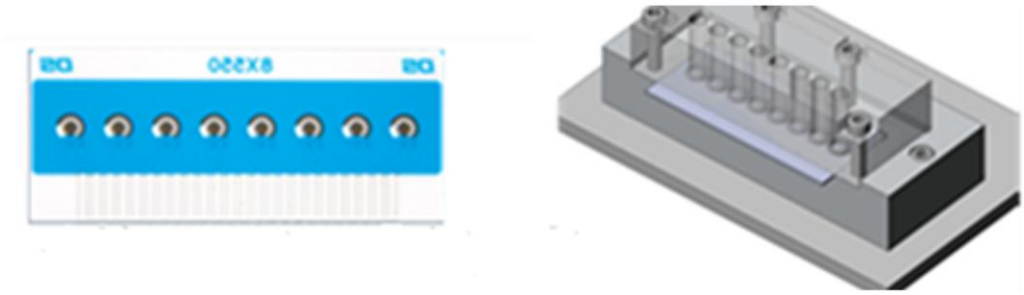

Figure 9: Static Screen-Printed Electrochemical Cells. There are 8 separate cells that can be used at the same time.

2.2.2 Single Chamber Electrochemical Flow cells

Electrochemical flow cells have constant flow of solution that pass over the electrodes to create a short dwell time for solvent molecules. This reduces unwanted oxidation and decomposition of the product increasing radioyields. Flow cells have a high surface-to-volume ratio, which is beneficial to increase efficiency in electrochemistry as the reaction happens on the electrode surface. Two different flow cells were used the Pt foil and screen-printed electrochemical flow cells where both cells had Pt working and counter electrodes and Ag pseudo reference electrode. The flow cells volume used was 250uL at 16.6uL/min flow rate for 15 mins and also repeated 5 times through with the same solution for 75 mins electrolysis time. The flow cells used an oxidation potential pulse of 2.0 V (Ag/Ag+) for 2 seconds and a cleaning potential pulse of -1.0 V (Ag/Ag+) for 1 second unless otherwise noted.

2.2.2.1 Single Chamber Electrochemical Platinum Foil Flow Cell

The first flow cell used screen printed chip electrodes and the cell design had similar dimensions to DRP-FLWCL flow cell (DropSens) (Figure 10). The static chip cell wells were 4 mm diameter and used the uStat 8000 Potentiostat (DropSens).

Figure 10: Screen Printed Chip Flow Electrochemical Cell

2.2.2.2 Single Chamber Electrochemical Screen-Printed Chip Flow Cell

Pt foil flow cell used the cross-flow A-012798 cell (Bio Logic) with Pt foil was placed overtop the working and counter electrodes with silver paste (Figure 11). This flow cell used the Autolab128 potentiostat-galvanostat (Metrohm USA). The flow path can be seen in Figure 10 on the bottom right.

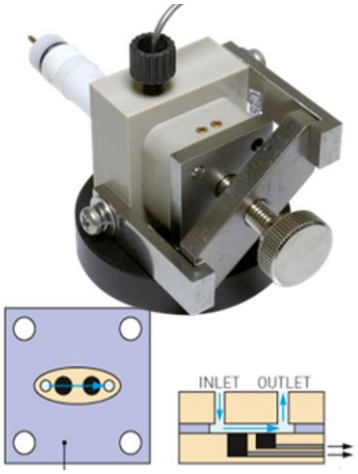

Figure 11: Pt Foil Flow Electrochemical Cell. Pt Foil was placed over the Anode and Cathode with Ag paste.

2.2.3 Two Chamber Electrochemical Cells

Two chamber electrochemical cells (Autolab128 potentiostat-galvanostat; Metrohm USA). divide the cathode and anode into two separate chambers by a permeable membrane that allows for selected control to permeate cations or anions between the two chambers. This setup removes

reduction from the ECF process in the anodic chamber. Reduction on the cathode can interfere by causing unwanted reactions of the precursor or product while producing other nucleophiles that may compete with fluoride. There were 2 different two-compartment cells used, a 15 ml and a 6 ml compartment H cell. The two compartments cells used 12 ml solution for the 15-ml compartment and 5 ml solution for the 6-ml compartment cell. Lower oxidation potential chemicals that would cause problems in the anodic chamber can be added to the counter chamber which may reduce reduction bottlenecks and help control pH.

2.2.3.1 Two Chamber Electrochemical Cell with Cation Exchange Membrane

The cation exchange membrane (CEM) used was a nafion membrane NR211 (Ion Power) between the compartment s (Figure 12).

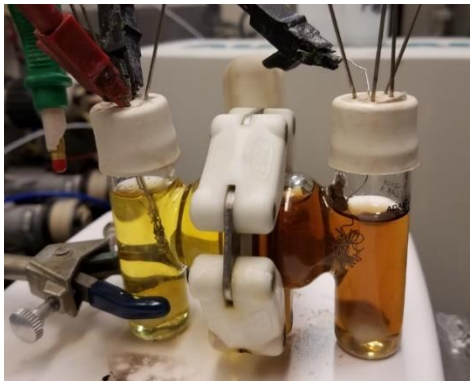

Figure 12: Two Chamber Electrochemical Cell with Cation Exchange Membrane (CEM).

2.2.3.2 Two Chamber Electrochemical Cell with Anion Exchange Membrane

The anion exchange membrane used was a Fumasep (fab pk 130) between the two compartments (Figure 13).

Figure 13: Two Chamber Electrochemical Cell with Anion Exchange Membrane (AEM).

2.2.4 Two Chamber Electrochemical Cell with Additional Proton Sink Chamber

The additional chamber which served as a proton sink chamber was added to the anodic chamber of the two-chamber cell to increase pH (Figure 14). This is necessary since bases cannot be directly added to the anodic chamber when performing ECF with a high oxidation precursor. If so, the base will oxidize which interferes with precursor fluorination and the base can act as a nucleophile that competes with fluoride.

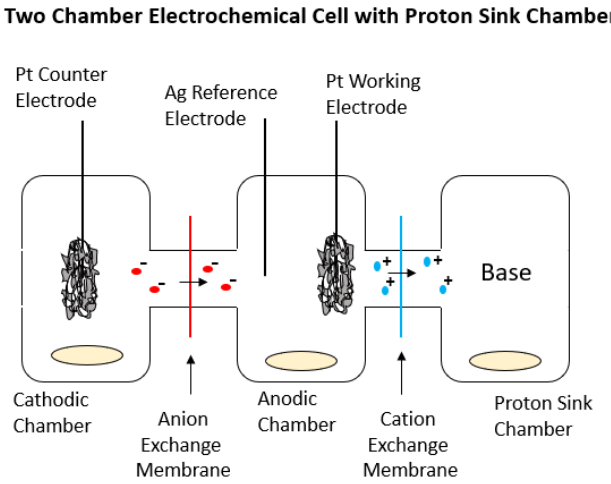

Figure 14: Two Chamber Electrochemical Cell with additional Proton Sink Chamber. Reduces the Acidity in the Anodic Chamber.

2.3 ElectroRadioChemistry Platform (ERCP)

Our lab developed the first automated synthesizer for [^{18}F]Fluoride radiolabelling using electrochemistry where its set-up and testing can be found in our previous work (Figure 15) [61]. The synthesizer performs the drying and phase transfer of the [18F]Fluoride from the cyclotron, electrochemical incorporation of the [^{18}F]Fluoride into the precursor molecule, removal of protecting groups, HPLC purification, and final formulation of the tracer.

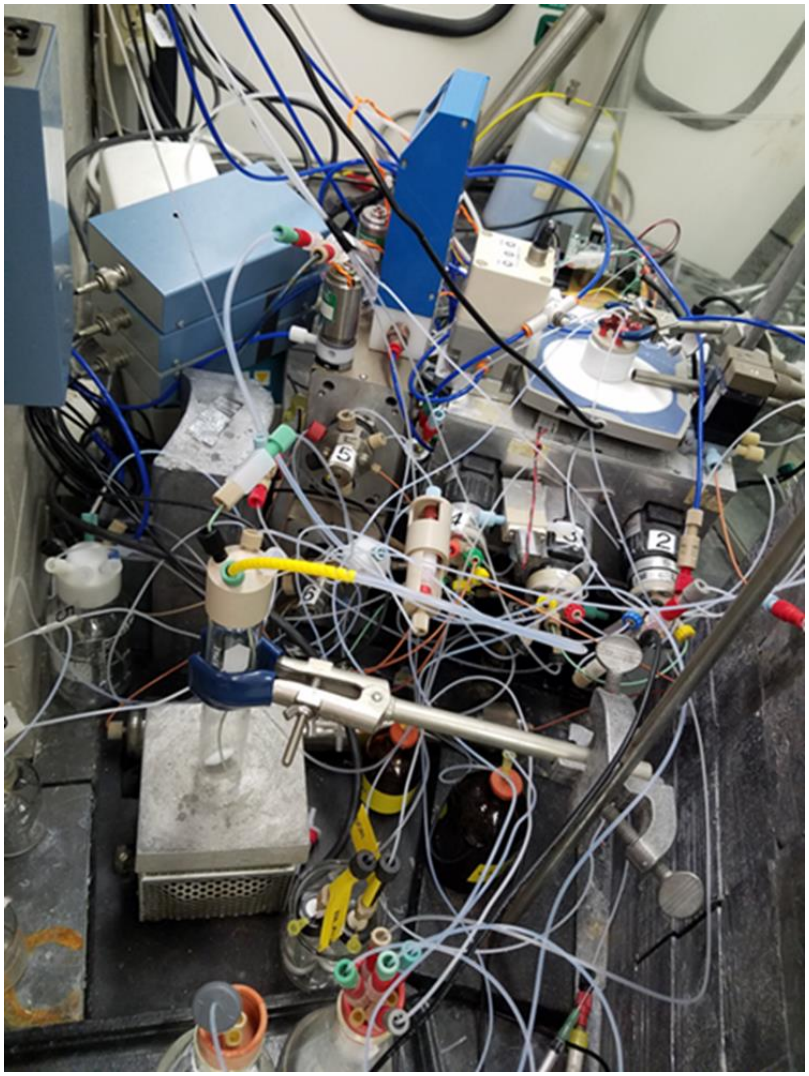

Figure 15: A Photo of the ElectroRadioChemistry Platform (ERCP)

The platform setup is composed of 4 major subsystems (Figure 16): the fluoride processing, electrochemistry, post processing, and purification. The radiochemical processing components of the instrument are fully shielded and remotely controlled to handle high activity. The purification module was developed to address current challenges of electrochemistry with high concentrations of electrolyte and side product formation. Additionally, our system can perform multiple experimental runs in the same day with different precursors and electrochemical conditions.

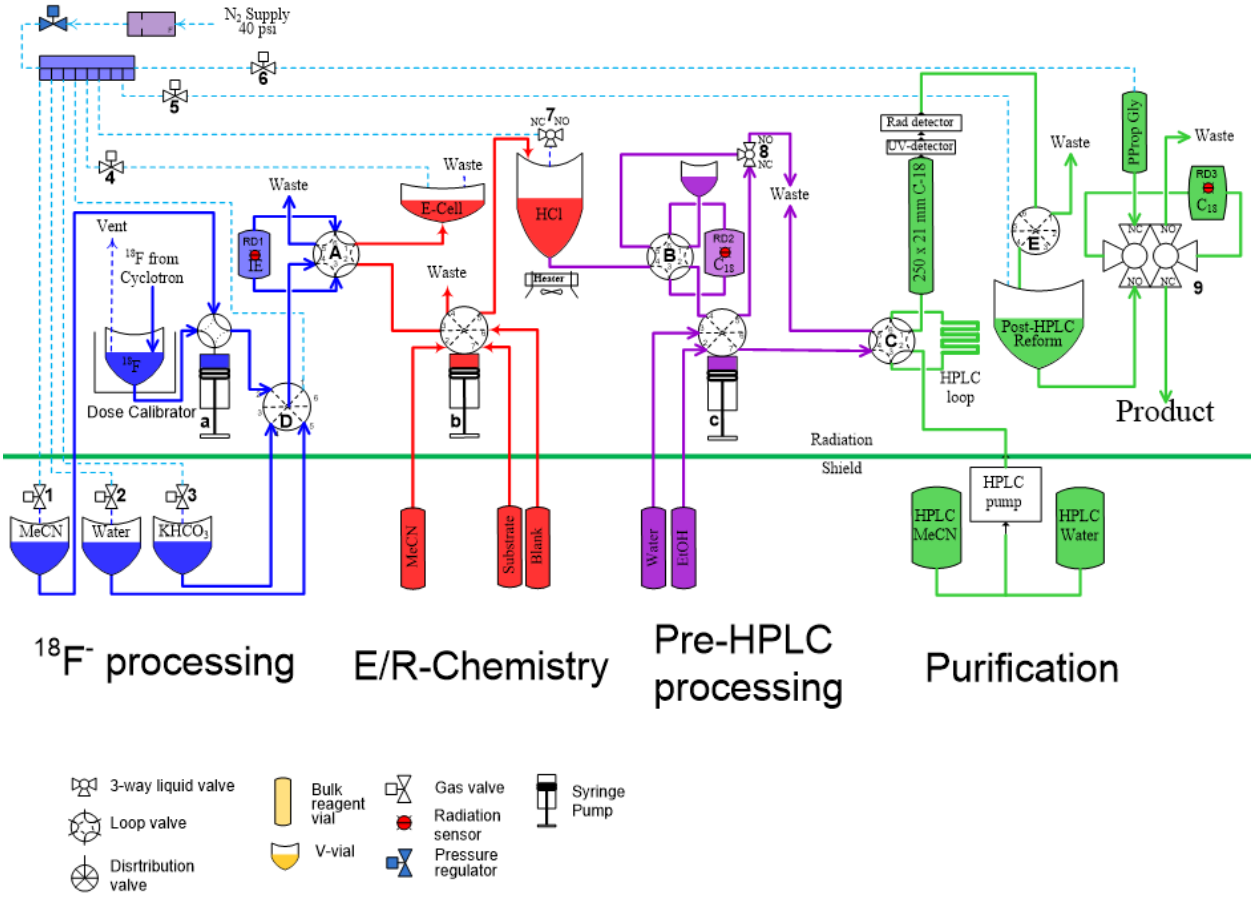

Figure 16: A Schematic of the ERCP with each of the 4 Modules.

The electrochemical cell in the ERCP used Pt wire electrodes with approximate surface area of the working electrode at 800 mm^2 and counter electrode at 1300 mm^2 and 1.5 mm^2. Ag wire as a pseudo reference electrode. The electrolysis was performed in a 6 ml Teflon cell (Figure

17) using an Autolab PGSTAT204 driven by Nova 1.9 software (Metrohm USA). A dry stream of nitrogen was used to remove hydrogen gas formed on the counter electrode.

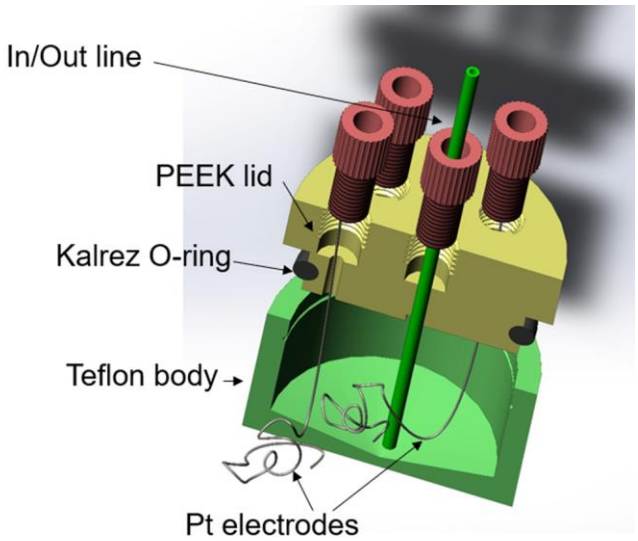

Figure 17: The Electrochemical Cell Design of the ERCP.

Water was added to the crude reaction mixture after electrolysis which was processed using a reversed phase C-18 SPE cartridge (Waters Sep-Pak Classic Short) to remove salts and polar reagents which makes HPLC separation much easier due to the overall mass of these compounds. The product was eluted with 1 ml of ethanol and 1 ml water was added before purification. 2 ml of ethanol/water containing the crude product was then transferred into the loading loop of the HPLC purification module using a Phenomenex Gemini column (21x250 mm). The product fractions were collected and passed through a C-18 SPE cartridge (Waters Sep-Pak Light) and washed off with approximately 400uL of ethanol to concentrate the product.

A smaller automated system was setup to run electrochemical synthesis more quickly without the pre-processing and purification modules (Figure 18).

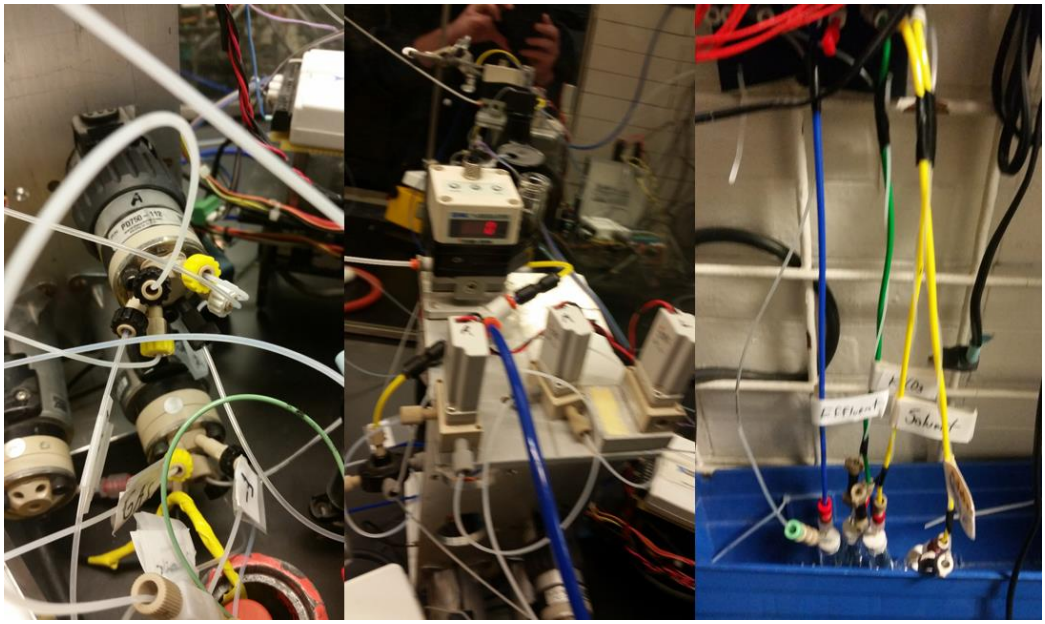

Figure 18: Photos of the Smaller Automated Setup just for Electrochemical Synthesis.

2.3 Thin Layer Chromatography with Gamma Detector (rTLC)

Radiochemical conversion (RCC) was determined using radio-thinlayer chromatography (radio-TLC) on silica plates (TLC Silica gel 60 W F254s, Merck) using a glass capillary and MeCN mobile phase. A radio-TLC scanner (miniGita Star, Raytest) or an AR-2000 TLC Imaging Scanner (Bioscan, Washington DC, USA) was used to obtain the chromatograms. The RCC refers to the amount of incorporated fluoride into organic molecules whereas any unreacted fluoride is not mobile in MeCN while reacted fluoride with organics will be mobile on the TLC plate. RCC was measured by dividing the area under the curve (AUC) for the desired product by the sum of AUC for all peaks.

2.4 High Performance Liquid Chromatography with Gamma Detector (rHPLC)

The radiochemical purity (RCP) was determined by HPLC. RCP is the amount of activity in the product compared to other organic radio side products. The HPLC used was a 1200 Series

Analytical High-Performance Liquid Chromatography (HPLC) system (Agilent Technologies). The HPLC is equipped with a GabiStar flow-through gamma detector (Raytest) and Knauer K-501 HPLC pump, coupled with a Knauer K-2500 UV detector (254 nm) and a NaI (Tl) scintillation detector (Carroll & Ramsey Associates, USA). RCP was measured by dividing the area under the curve (AUC) for the desired product by the sum of AUC for all organic peaks. To remove unreacted fluoride, water was added to the reaction mixture following electrolysis and the solution was passed through a Sep-Pak® C18 Classic Cartridge and subsequently eluded with ethanol.

To improve the reproducibility and to make comparisons analysis between batches, the analytical HPLC methods included here will all be from the same method. The column used was a Phenomenex Luna 5u C18 (2) 100 A, 250 × 4.6 mm, 5-micron column. The gradient was A = ACN; B = water; flow rate = 1.8 mL/min; 0–12 min 80% B to 40% B, 10–12 min 5% B, 13–20 min 5% B to 80% B. Past Analytical HPLC methods are described in our previous papers and supporting materials [60, 61, 73, 74, 76].

2.5 Gas Chromatography (GC)

Gas Chromatography (GC) was performed on the carrier added experiments. The crude product samples were filtered with a silica or alumina SPE (Waters) to remove unbound fluoride before GC. Mass spectra and chromatograms were obtained with an Agilent 5975C TAD inert MSD mass spectrometer coupled with an Agilent 7890A gas chromatograph. Additional details regarding the GC specification and results of past experiments is found in our previous work [60, 61].

2.6 Nuclear Magnetic Resonance (^{19}F-NMR)

The chromatography peaks have been isolated and the product further identified by proton and fluorine NMR obtained on a Bruker AV400. Additional details regarding the NMR specification and results is found in our previous work [60, 61, 76, 101].

2.7 Cyclic Voltammetry (CV)

Cyclic voltammetry (CV) and electrosynthesis experiments were performed with the appropriate electrochemical workstation for the electrochemical cell. All CVs were performed at room temperature using a 200 mV/s scan rate unless otherwise noted. The electrodes were cleaned before each experiment using potential cycling between 2V and -1V in 1M sulfuric acid solution in water.

2.7 Materials and Reagents

Trifluoromethanesulfonic acid (triflic acid) (99%) and methyl(phenylthio)acetate (99%) were purchased from Oakwood Chemical. Acetonitrile (anhydrous, 98%), Triethylamine (Et_3N), acetic acid (99.7 %), tetrabutylammonium perchlorate (TBAP) (99.9%), and anhydrous phosphorus pentaoxide (99%), tetrabutylammonium fluoride solution 1.0 M in THF (TBAF solution, ~5 wt% water) and platinum wire (99.9%) were purchased from Sigma-Aldrich. Tetrabutylammonium perchlorate (TBAP) (>99%, for electrochemical analysis) was purchased from Fluka. Tetraethylammonium fluoride tetrahydrofluoride ($Et_4NF{\cdot}4$ HF, >97%) and propylene carbonate (>98%) were purchased from TCI. Methyl (phenylthio) acetate (99%) and hydrocloric acid (99.9%) were purchased from Alfa Aesar. Acetonitrile (MeCN, anhydrous, >99.8%) dicloromethane (>99.9%), tetrabutyl ammonium hydroxide (40% wt in water), 1-Fluoronaphthalene (>99.9%), nitromethane (>99%) and pToluenesulphonic Acid (99%) were purchased from Agros Organics. Fomamide (>99.5%), (Phenylthiol) Acetonitrile (98%),

Diethyl phenylthiomethylphosphonate (96%), Dimethoxyethane (DME) (>99%), Trifluoroethanol (TFE) (>99%) and acetone (>99.5%) were purchased from Fisher. Ethanol (200 proof, anhydrous) was purchased from Decon. (Phenylthiol) Acetamide (97%) was purchased from Synthonix. Hexafluoroisopropanol (HFIP) (99%) was purchased from VWR International. The water used was purified to 18MΩ with a 0.1 mm filtration system. No-carrier-added [^{18}F]fluoride was produced by the (p,n) nuclear reaction. The production of [^{18}F]fluoride uses [^{18}O]H_2O (84% isotopic purity, Medical Isotopes) in a RDS-112 cyclotron (Siemens) bombarded with protons at 11 MeV with a 1 mL tantalum target with havar foil.

2.8 Terminology

Radiochemical fluorination efficiency (RCFE) was determined by the equation: RCFE = RCC X RCP. Where radiochemical conversion (RCC) was determined by radio-TLC and radiochemical purity was determined by radio-HPLC. RCP and RCC were measured by using the area under the curve (AUC) of the desired product compared to the sum of all AUC peaks. The TLC RCC accounts for all unreacted [^{18}F]Fluoride and HPLC RCP accounts for radiochemical side-products. For carrier added experiments, the product yield is based on the conversion of starting precursor. In carrier added or in NCA experiments, RCFE is based on fluorination conversion. RCFE was used specifically to avoid using radiochemical yield (RCY). RCY is defined by the isolated product radioyield whereas RCFE the product was not isolated.

Chapter 3: Carrier Added Methyl (phenylthio) Acetate ^{18}F ECF

3.1 Introduction to Electrochemical Fluorination of Thioethers

Thioethers and similar sulfur containing molecules have been electrochemically fluorinated with high concentrations of fluoride over the last 20 years primarily by the Fuchigami group [54, 82, 102]. The majority of electrochemical methods have used HF containing fluoride sources, with the most common being triethylamine trihydrofluoride (Et_3N*3HF) as either the solvent or in excess of 300 (mM) concentrations [56]. Several anode materials were also tested with platinum yielding the highest yield to date [83]. Various solvents were used in fluorination with MeCN being most common [102-105]. However, radiochemical yield is based on fluoride conversion, which has been negligible in previous ECF studies due to the low product yields formed in low concentrations of poly HF fluoride sources. The ECF methodology requires reduced fluoride concentrations to be applicable to PET probe synthesis which requires improved radioyield and molar activity. To date, there has not been an easily available method to ^{18}F radiolabel thioethers for PET probe development [106]. Current chemical methods for fluorinating thioethers utilizes agents such as XeF_2, CsFOF, and DAST, most of which are derived from F_2 gas and are not easily translatable to the production of PET probes with high molar activity [66, 107, 108].

3.2 ^{18}F Electrochemical Fluorination of Methyl (phenylthio) Acetate using Et_4NF*4HF

Thioethers were specifically selected for this study due to their history of successful electrochemical fluorination (ECF) and biological significance [54, 102, 109]. Thioethers are important chemical compounds in biology with two essential amino acids being thioethers; methionine and cysteine. [^{11}C]methionine is an important PET probe which is frequently used in

detecting brain tumor volumes and for planning treatments [110]. Additionally, many high grossing pharmaceutical products contain both sulfur and fluorine including thioethers [111]. It may be advantageous to develop PET radiotracers based on these target molecules. Finding a reliable no-carrier-added method for late stage fluorination of these molecules could lead to new thioether PET probes for imaging or drug discovery.

Sulfur containing molecules, similar to Methyl (phenylthiol) Acetate, have been electrochemically fluorinated since the 1990's primarily by the Fuchigami group [54, 82, 102] using mainly triethylamine trihydrofluoride (Et_3N*3HF). The best carrier added fluorination yields reported to date of thioethers was Ethyl (phenylthiol) acetate which was mono-fluorinated up to 88% using 5 mM substrate and 370 mM of Et_3N*3HF in MeCN [70]. Methyl (phenylthio) Acetate was optimized in the single compartment electrochemical cell under different parameters and 100 (mM) Et_4NF*4HF as the fluoride source. This concentration of fluoride was chosen to form a moderate amount of product to determine the effects of different parameters of optimization that were thought may increase fluorination yields. A detailed optimization of these different parameters follows in an attempt to understand the full scope and mechanism of this process. It is important that a detailed optimization is performed because it has not been previously completed in low fluoride and NCA conditions.

3.2.1 Optimization Parameter: Time

Figure 19 depicts the effect of the electrolysis time on the precursor consumption and product formation for a single ECF experiment using Methyl (phenylthio) Acetate. It was reported that 30 minutes electrolysis led to the highest product formation yield of 60.9%. Performing electrolysis for longer oxidization times for the product led to lowers product yields. It is important to note that under carrier added conditions, high concentrations of poly HF fluoride source could

shield the precursor and product from reduction in the single compartment cell. However, in contrast, the decrease in the product after 30 mins is quite drastic. This is due to the oxidation of almost all the precursor leaving only the product left as the next lowest oxidation molecule to be oxidized.

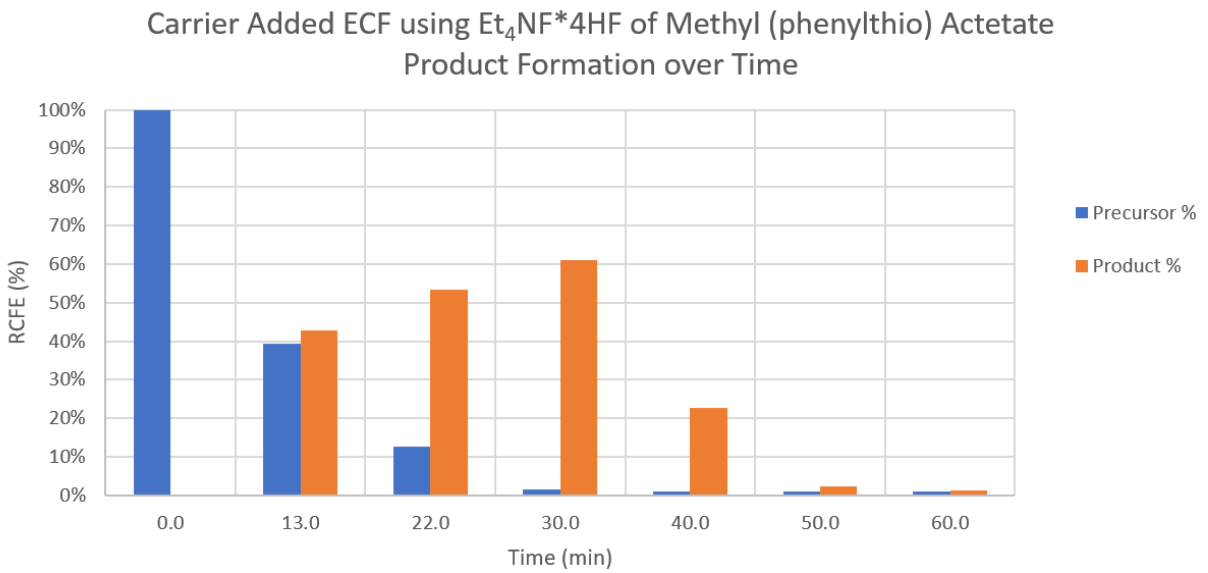

Figure 19: Carrier Added ECF using $Et_4NF*4HF$ of Methyl (phenylthio) Acetate. Product formation over Time. The product formation of the fluorinated product peaks at 30 mins. After that time, the precursor is consumed from oxidation and the product then becomes oxidized reducing product concentration.

3.2.2 Optimization Parameter: Temperature

Temperature increases towards 70 °C was observed to improve the fluorinated product yields (Methyl 2-fluoro-2-(phenylthio) Acetate) from 42.3%±3.7% (n=3) at 20 °C to 63.4%±4.6% (n=3) at 70 °C (Figure 20). Product concentration was determined by HPLC and GC. Product yield is defined as a percent of the starting precursor concentration. Increasing temperature above 70 °C caused excessive evaporation and was not feasible in this setup.

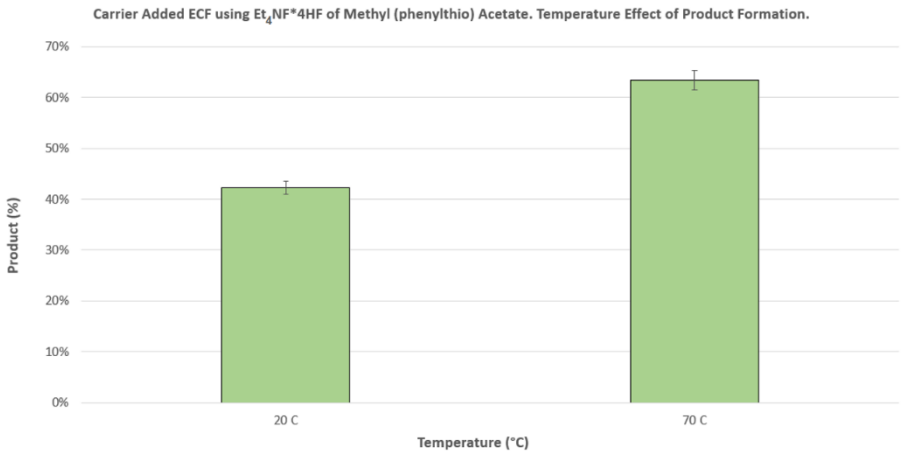

Figure 20: Carrier Added ECF using $Et_4NF*4HF$ of Methyl (phenylthio) Acetate. Temperature Effect of Product Formation. Increasing temperature also increased product formation.

3.2.3 Optimization Parameter: Convection

Increasing the stirring rate increased the product yield (Figure 21) up to 62.7% at 10 rev/sec. Further convection rates above 10 rev/sec resulted in air bubble formation and decreased stability of the setup due to excessive vibration. We found increasing stirring rates led to increased product yield whereas low product yields resulted with no stirring.

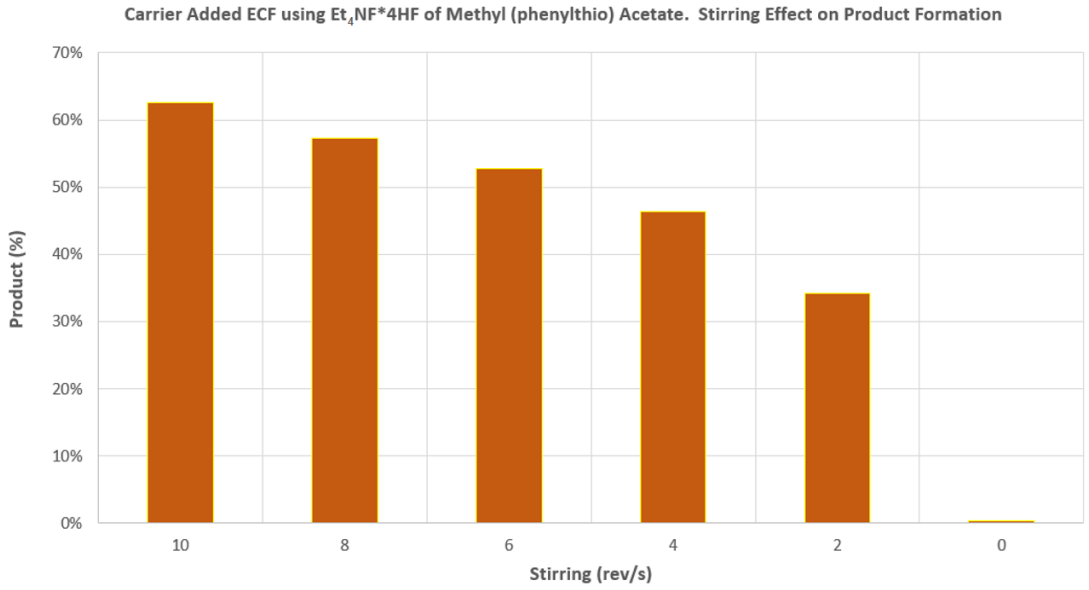

Figure 21: Carrier Added ECF using $Et_4NF*4HF$ of Methyl (phenylthio) Acetate. Stirring Effect on Product Formation. Increased stirring rate increased product formation. With no stirring very little product formation.

Previous reports on fluorination of ethyl (phenylthiol) acetate using sonication resulted in 85% yields using $Et_3NF*3HF$ as solvent [54]. In our results, sonication provided a similar increase yields as with stirring likely due to increase mixing at the anode surface. The product yield was 30.6%±1.5% (n=3) (Figure 22). Heating at 70 °C in combination with sonication also improved the product yield to 40.1%±1.6% (n=3) (Figure 17).

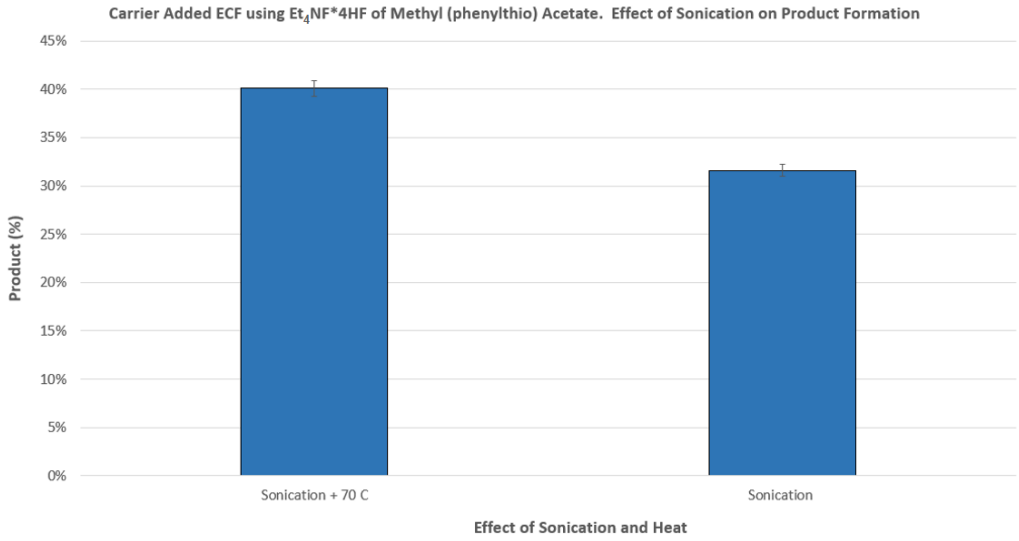

Figure 22: Carrier Added ECF using $Et_4NF*4HF$ of Methyl (phenylthio) Acetate. Effect of Sonication on Product Formation. Sonication increased result compared to no convection. Heat with sonication was better than just sonication.

3.2.4 Optimization Parameter: Oxidation Voltage

Increasing the oxidation potential to 2.2V (Ag/Ag+) led to improved product yields (Figure 23). Further increase of the electrolysis potential led to decreased yields, which was attributed to product breakdown at higher potentials due to increase in radio side product formation on HPLC. A potential of 2.2V (Ag/Ag+) was chosen as the optimum electrolysis potential.

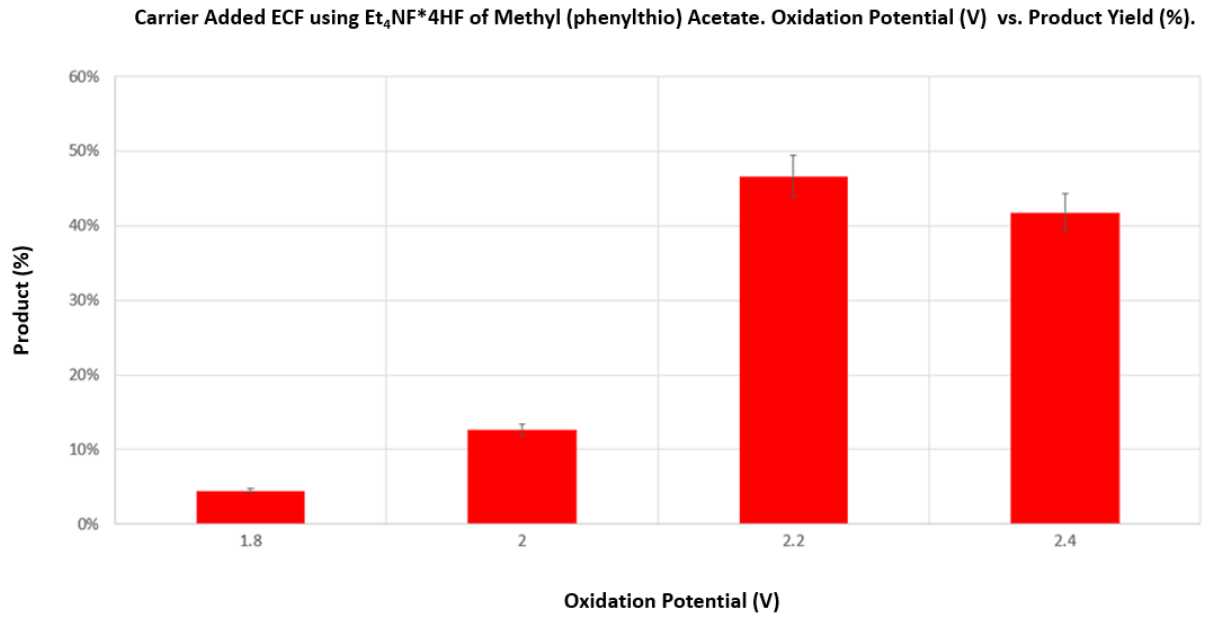

Figure 23: Carrier Added ECF using $Et_4NF*4HF$ of Methyl (phenylthio) Acetate. Oxidation Potential vs. Product Formation. Product formation increased up to 2.2V and then decreased at 2.4V.

3.2.5 Optimization Parameter: Pulsing

Pulsing the electrode was found to reduce anode passivation; the formation of adsorbed molecules or films on the anode surface. When pulsing a negative potential for a short time, can help to remove adsorbed molecules and films on the anode. Alternatively, pulsing short positive pulses can help remove adsorption on the cathode. The negative pulse can be considered a "cleaning" pulse and was further investigated the cleaning pulse time and potential was investigated to determine the optimum time required to reduce passivation. Product yields were observed to be consistent with changes in the cleaning potential in the range of 0 to -0.6V and started to decrease at -0.8V. When adjusting the cleaning pulse time while controlling the total oxidation and reduction, we noticed this did not significantly impact the resulting product yield. For this investigation, -0.6V was chosen for the cleaning pulse potential under 60 sec oxidation pulse time with 6 sec cleaning pulse time for pulse cycling (Figure 24). The drop off in product

yield at 10 milliseconds was suspected to be due to the time it takes the Potentiostat to charge the anode.

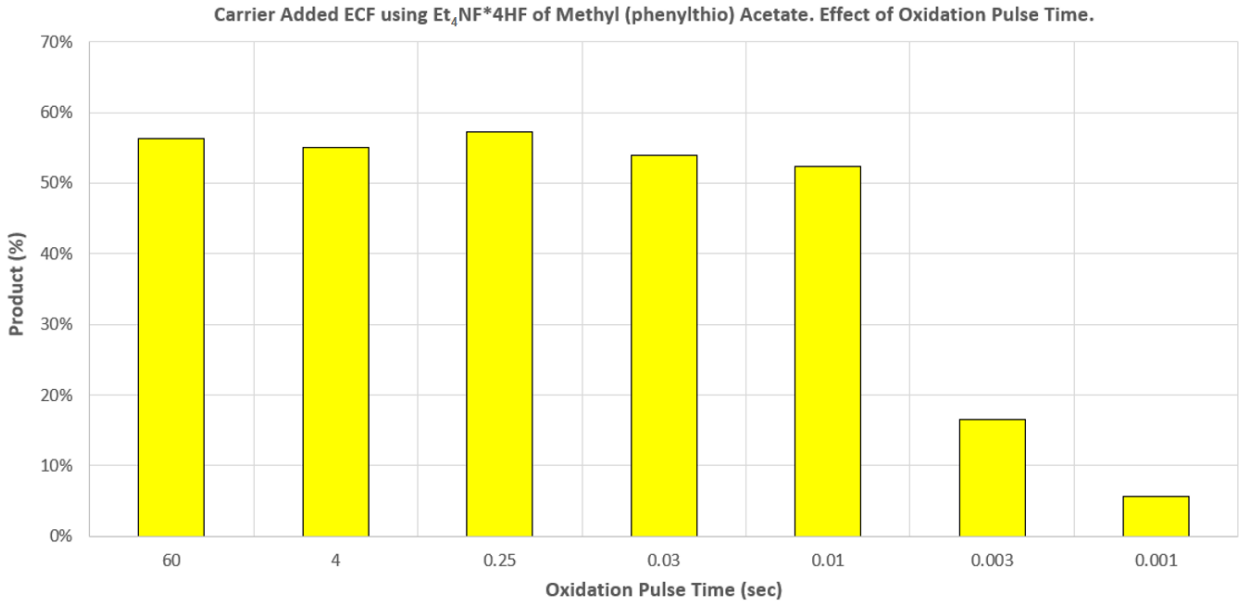

Figure 24: Carrier Added ECF using $Et_4NF*4HF$ of Methyl (phenylthio) Acetate. Effect of Oxidation Pulse Time. Production Formation remained relatively the same until the oxidation pulse was lower than 10 msec.

3.2.6 Optimization Parameter: Anode Material

Several anode materials have successfully been used to fluorinate organic molecules with the most common being platinum, carbon, and nickel [112, 113]. Platinum had the highest product yields with carbon felt having almost as much product yield as platinum (Figure 25). Precursor % in Figure 25 is the concentration of precursor remain as a percent of starting precursor concentration. Carbon felt also did not oxidize as much precursor. The conversion of precursor to product was rather similar with carbon felt as with platinum. Using nickel, the majority of current generated is likely a result of oxidation from the nickel and performed poorly and did not efficiently oxidize the precursor.

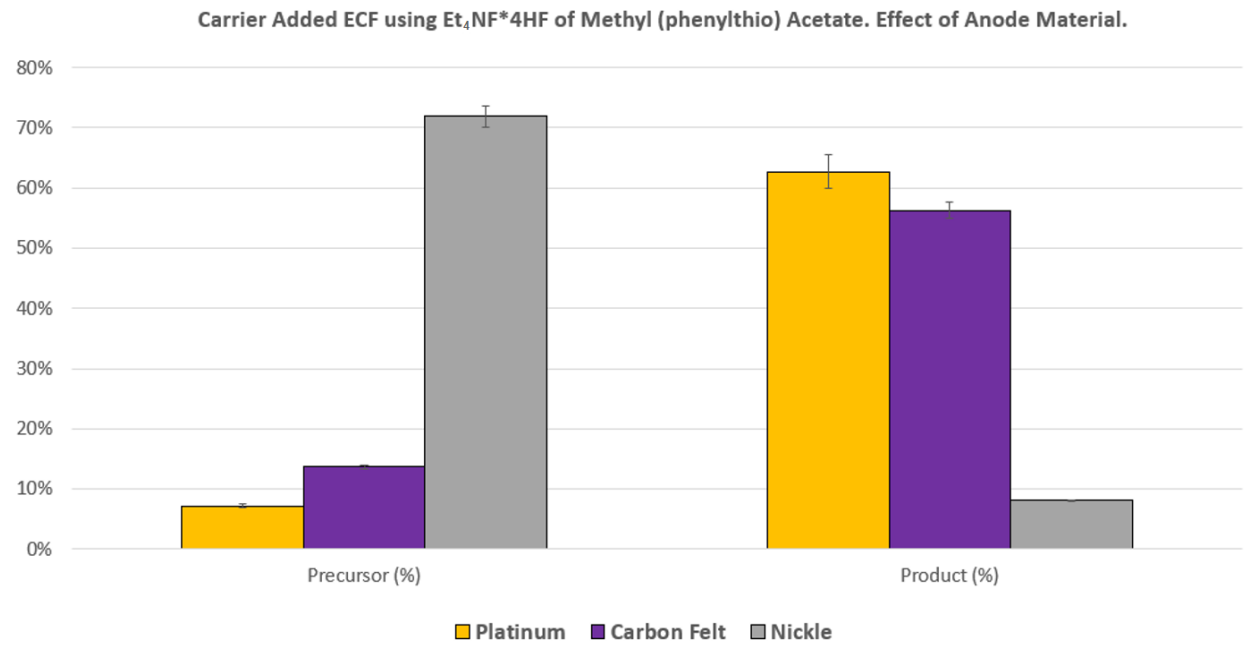

Figure 25: Carrier Added ECF using $Et_4NF*4HF$ of Methyl (phenylthio) Acetate. Effect of Anode Material. Platinum performed the best followed closely by Carbon Felt. Nickle performed poorly.

3.2.7 Optimization Parameter: Solvent

The ECF of 50 mM Methyl (phenylthio) Acetate using the platinum anode in different solvents was performed with 100 mM $Et_4NF*4HF$. Electrolysis in acetonitrile (MeCN) had the highest product yield (Figure 26) which agreed with past results reporting MeCN to be an effective to electrofluorinate molecules using poly-HF fluoride sources [54, 55, 103]. We found using formamide and propylene carbonate as solvents with higher dielectric constants led to lower product yields. Acetone performed moderately well despite having a similar oxidation potential as the precursor. Upon investigation of these different solvents, it was noticed those resulted in good product yields showed low polarizability [52, 114]. For example, nitromethane is a moderately good candidate for these reactions behind MeCN, followed by propylene carbonate, formamide and acetone. Dichloromethane performed the worst and had low conductivity. Many other solvents

were used but did not produce product yields likely due to the solvents' low oxidation potential or high polarizability destabilizing the intermediates.

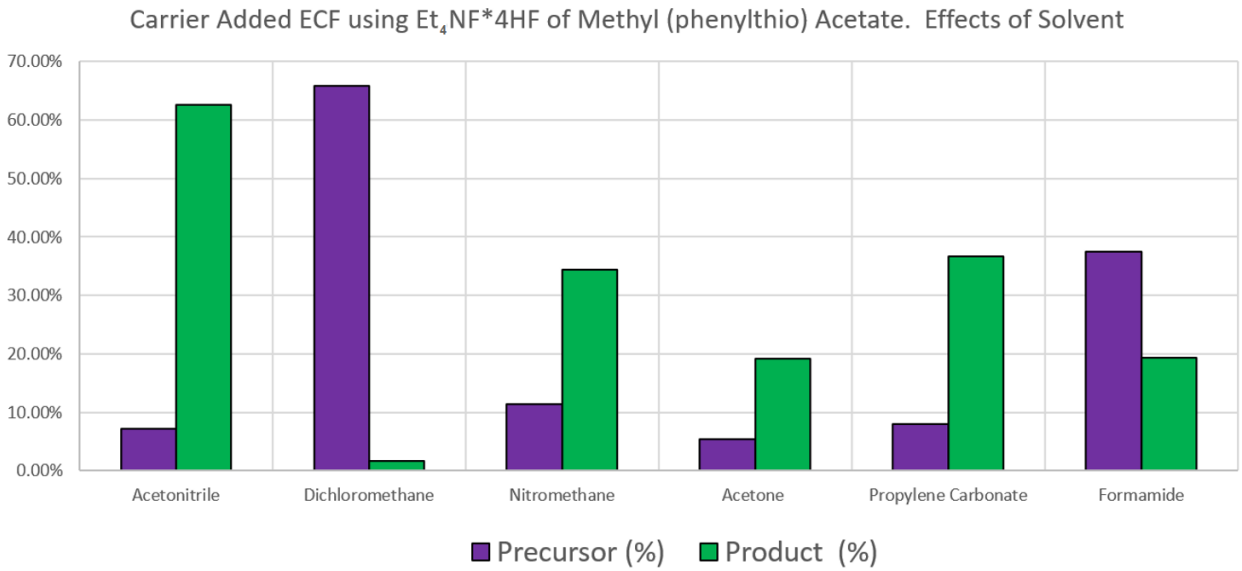

Figure 26: Carrier Added ECF using $Et_4NF*4HF$ of Methyl (phenylthio) Acetate. Effects of Solvent. Acetonitrile was still the best solvent using this $Et_3NF*4HF$ fluoride source.

3.2.8 Optimization Parameter: Acid

Hydrochloric acid (HCL) dramatically reduced yields even when added at low 5 mM concentrations (Figure 27). Chlorination was not seen on GC results suggesting acidity is responsible for the low fluorination yields.

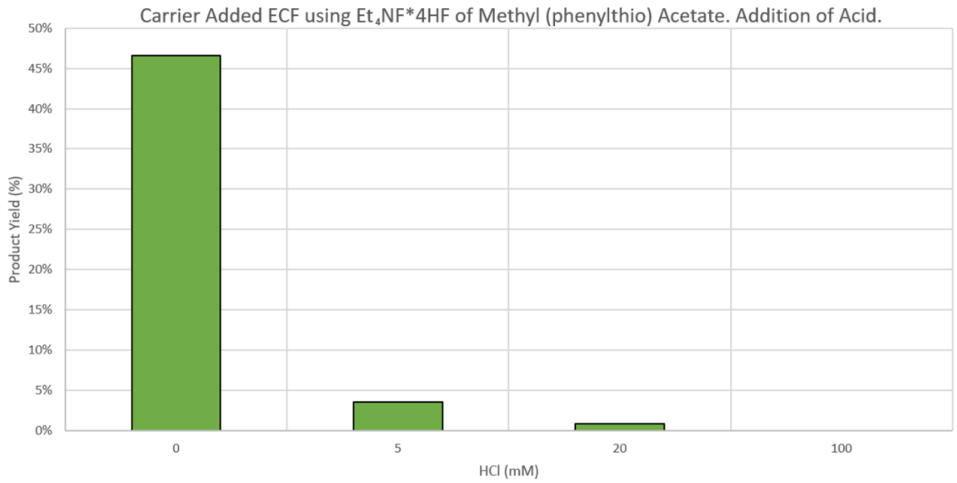

Figure 27: Carrier Added ECF using $Et_4NF*4HF$ of Methyl (phenylthio) Acetate. Addition of Acid. Adding HCL significantly reduced product yields.

3.2.9 Optimization Parameter: Base

The addition of tetrabutylammonium hydroxide (TBAOH) 60% in H_2O dramatically reduced yields even at low concentrations of 5 mM (Figure 28). Hydroxyl groups are known to have low oxidization potentials which interferes with precursor oxidation. Additionally, water also solvates fluoride which makes fluoride unreactive. Even with these additional factors, the base had less of a reduction on product yields than the acid at similar concentrations Hydroxide may also compete with fluoride as a nucleophile. Yet base/water substantially reduce product yields even at 5 mM compared with 500 mM fluoride. We reasoned the negative effect is primarily due to the presence of water which is known to undergo redox at these potentials as well and to solvate fluoride.

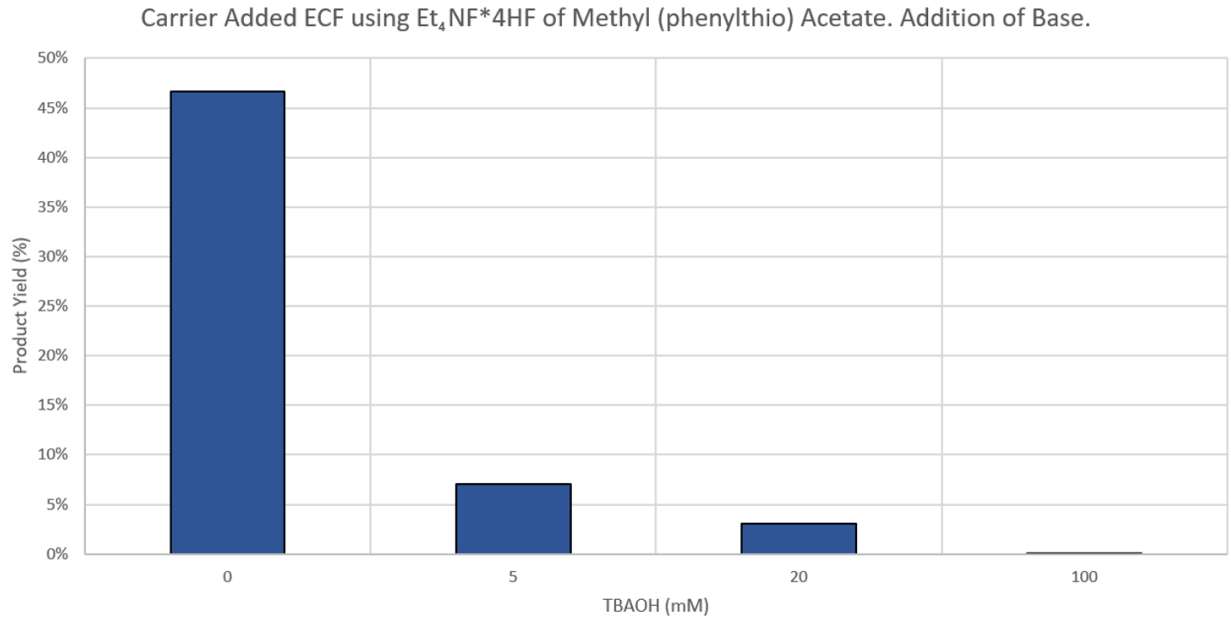

Figure 28: Carrier Added ECF using $Et_4NF*4HF$ of Methyl (phenylthio) Acetate. Addition of Base. The addition of base also reduced product yields but to less extend as the acid which may also be due from the 40% water content of the base solution.

3.2.10 Optimization Parameter: Electrolyte

Electrolytes are commonly used in electrochemistry to increase conductivity [115]. Small concentrations of tetrabutylammonium perchlorate (TBAP) increased product yield (Figure 29), whereas higher concentration of TBAP contrastingly reduced product yields. Although TBAP is not necessary for conductivity due to the presence of 100 mM of the ionic fluoride source. TBAP also noticeable reduces some common reduction side products of the precursor as seen on HPLC. This gain in product yield is likely due to either presence of stable anion near the anode or by decrease in reduction of the precursor where the optimal product yield was obtained using 10 mM TBAP. At higher concentration of TBAP the product yields decreased likely due to the electrolyte destabilizing the cation intermediate or interfering with the reactive form of fluoride.

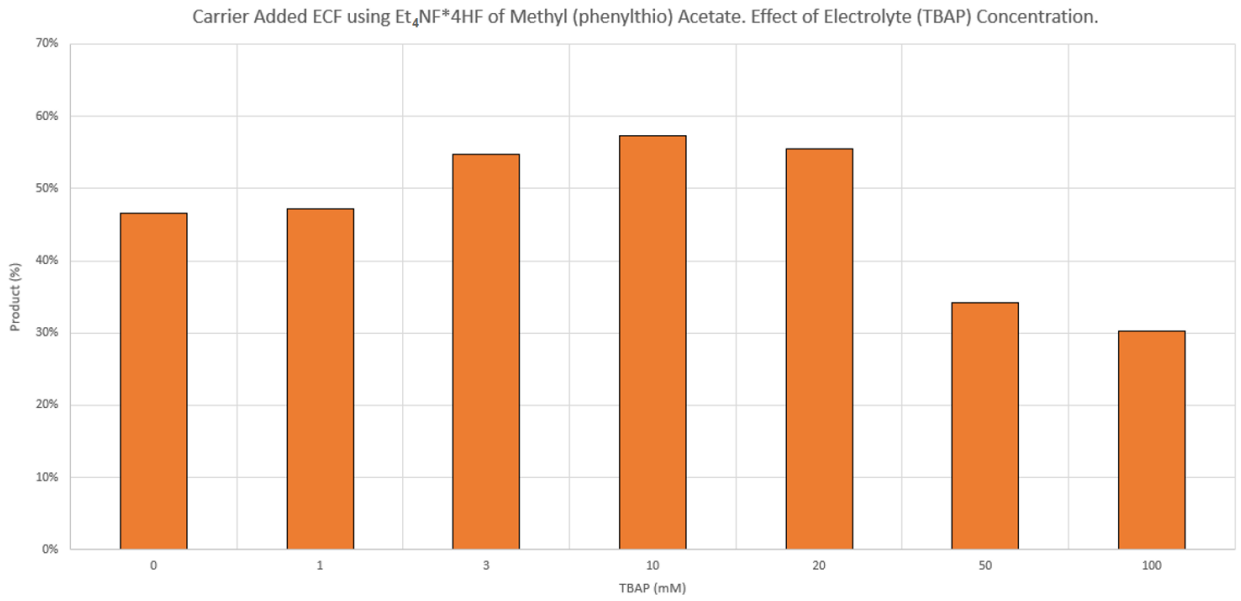

Figure 29: Carrier Added ECF using $Et_4NF*4HF$ of Methyl (phenylthio) Acetate. Effect of Electrolyte (TBAP) Concentration. Under this carrier added condition the fluoride source provides excellent conductivity. The addition of a stable electrolyte still increases product yield.

3.2.11 Best Conditions for the Single Chamber Electrochemical Cell

The optimized condition for electrochemical fluorination in a single compartment cell utilized the following conditions: a Pt anode material, MeCN solvent, 10 rev/s stirring rate, 70 °C, 10 mM TBAP electrolyte, 60 sec oxidation pulses at a potential of 2.2V and 6 sec cleaning pulses at a potential of -0.6V for a total duration of 30 minutes with 100 (mM) $Et_4NF*4HF$ and 50 mM Methyl (phenylthio) Acetate. Under these optimized conditions, the product yield was 79.4±7.7% (n=3). The 10/1 fluoride/Methyl (phenylthio) Acetate concentration ratio in these parameters limited the maximum fluoride conversion to 10%. Although a further increase in fluoride concentration provided higher chemical conversion yields of Methyl (phenylthio) Acetate, the increase fluoride concentration would limit the yield based on fluoride conversion, used in calculation of radiochemical yields. To compare the optimized conditions under high fluoride concentrations with published results a 300 (mM) $Et_4NF*4HF$ concentration sample was performed a single time with a resulting product yield of 93.4% (Figure 30).

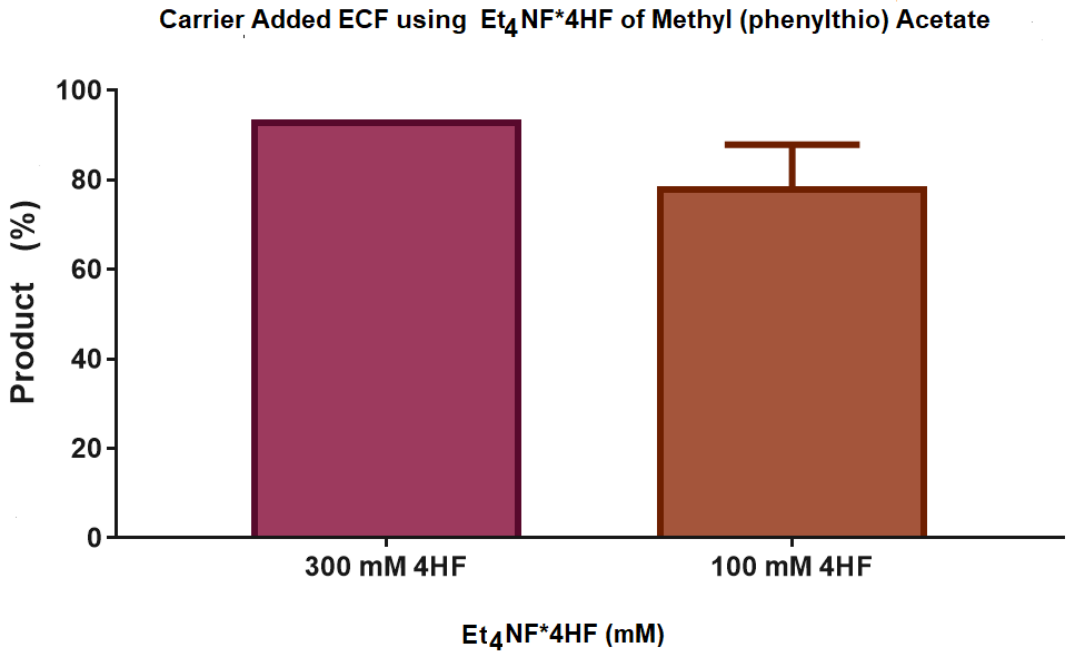

Figure 30: Best Single Chamber Results. Carrier Added ECF using $Et_4NF*4HF$ of Methyl (phenylthio) Acetate.

3.2.12 Static Chip Electrochemical Cell

Screen printed electrochemical cells are convenient tools to perform high throughput screening studies. Herein, an 8-chamber cell setup was used which was manufactured out of PEEK pictured in chapter 2 and used with an 8-cell screen printed electrode chips manufactured by DropSens. In our experiments, we found longer oxidation pulses produced only trace product yields. Shortening the pulse rate while increasing the reduction pulse potential led to increased product yields. We reported the optimal pulsing method using an oxidation potential to be 2.0V (Ag/Ag+) for 2 seconds and cleaning potential of -1.0V (Ag/Ag+) for 0.5 seconds (Figure 26). Rapid cycling from positive to negative potential was critical to form product in static cells, which suggests the positive species produced near the anode without convection or strong migratory forces inhibited fluorination. The maximum product yield of Methyl 2-fluoro-2(phenylthio)

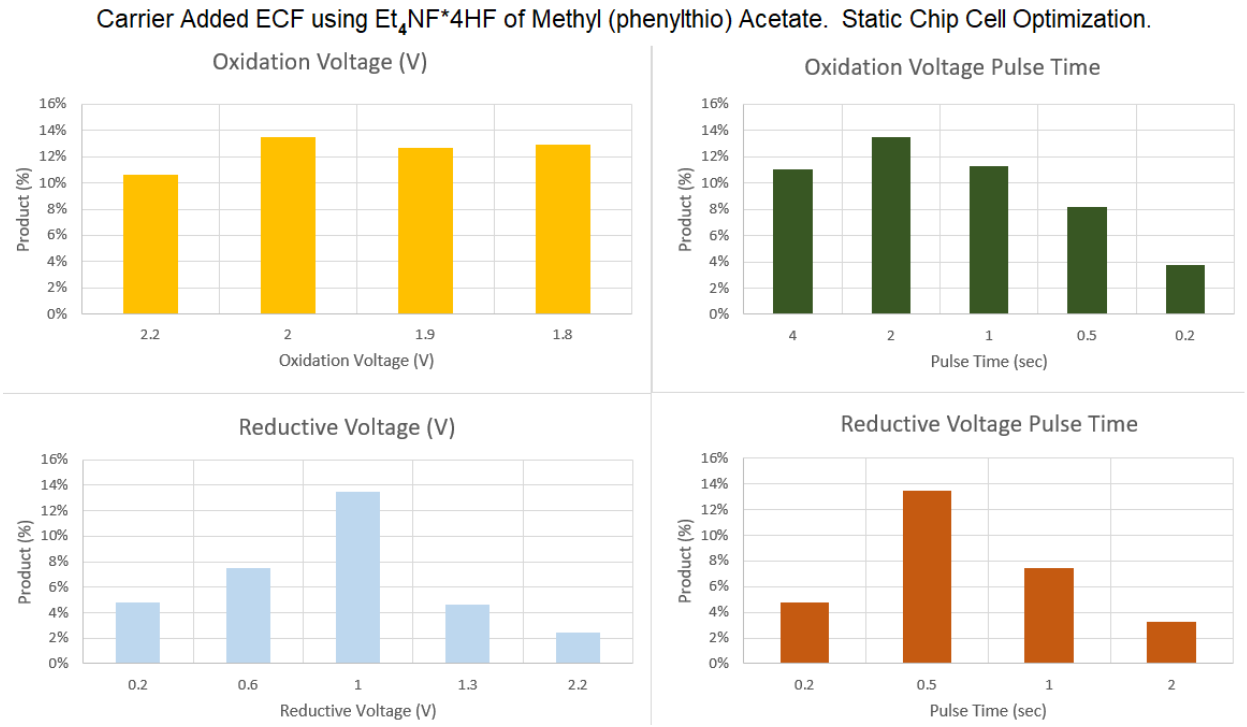

Figure 31: Carrier Added ECF using $Et_4NF*4HF$ of Methyl (phenylthio) Acetate. Static Chip Cell Optimization. The optimal oxidation voltage was 2.0 V with pulse time of 2 secs. The optimal reductive voltage was 1.0 V for 0.5 secs.

Acetate for the static screen-printed electrode cell was 13.7% using MeCN as solvent and 50 mM precursor, 50 mM TBAP and 100 mM $Et_4NF*4HF$ poly HF fluoride source (Figure 31).

3.2.13 Chip Electrochemical Flow Cell

Microfluidics has many distinct advantages for performing electrochemistry. Microfluidic reactors are characterized by high surface-to-volume ratio where increasing the electrode surface-to-volume ratio accelerates electrochemical reactions because electrochemistry is a surface-controlled reaction. Microfluidic flow cells have a short distance between electrodes, which increases electrolysis efficiency by reducing electrical resistance of the solution. Microfluidics also has the advantage of reducing unwanted reductive or oxidative exposure on products by controlling the flow rate to increase yield while avoiding degradation. The two different flow cells shown in chapter 2 were used herein: (1) a cross flow cell (manufactured by Biologic) with platinum foil placed over the anode and cathode with silver paste (Pt foil flow cell, PtFC); and, (2) a chip flow cell used with the 3-electrode chip (manufactured by DropSens; chip flow cell, CFC). Both flow cells used Pt for the working electrode (WE) and counter electrode (CE) with a silver wire serving as the quasi-reference electrode. The same material was used in the single chamber electrochemical cell. The PtFC flow path travels in between the WE and CE, which is followed towards a small chamber nearby containing an Ag wire which serves as the reference electrode (RE). The chip flow cell is comparable to that found in the static chip cell containing 3 electrodes printed except the solutions flows over the chip's surface as the only difference. The flow rate used here was recorded to be 16.6 μL/min where 250μL was passed through both flow cells one time in 15 min for the single runs. The electrochemical solution was also collected and passed though the flow cell 5 times in 75 mins (15 mins each time) at the same flow rate to produce a larger fluorination yield for radiochemical TLC measurements which the CFC was 2.4%$\pm$0.1% (n=3) for

a single run through and 12.3% for 5 times through (Figure 27). The current and oxidation per time was observed to be less in the flow cell than in the single chamber cell due to less surface area of the electrodes and less convection of the solution.

3.2.14 Pt Foil Electrochemical Flow Cell

The product yield for the platinum foil flow cell (PtFC) was 2.6±0.2% (n=3) for a single run through and for 5 times through the product yield was 16.7% (Figure 32).

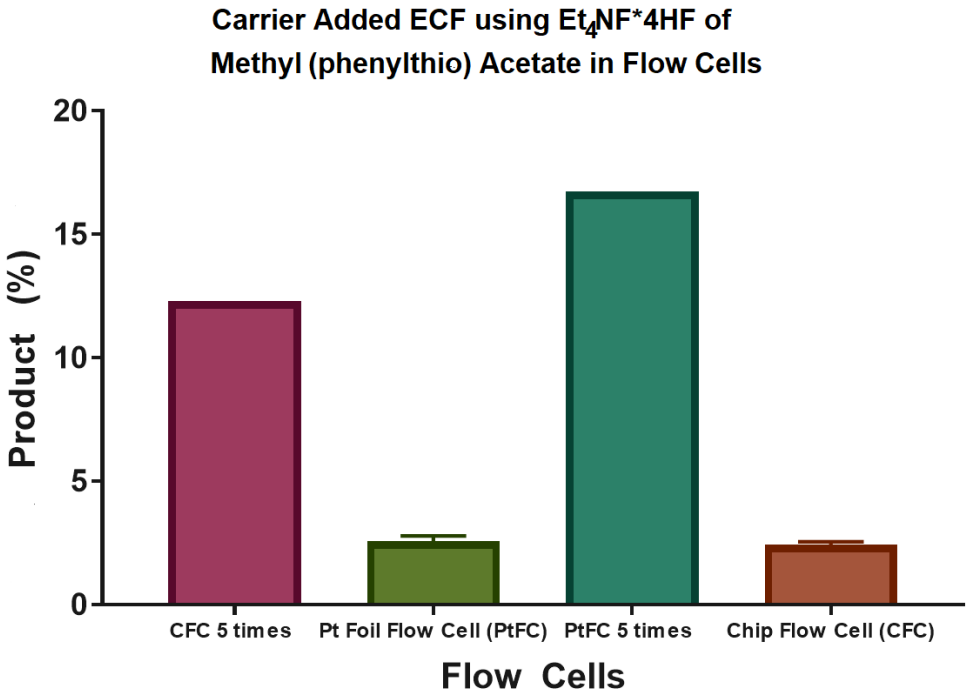

Figure 32: Carrier Added ECF using $Et_4NF*4HF$ of Methyl (phenylthio) Acetate in Flow Cells.
The solutions were passed through the flows cells 5 times to see appreciable radiochemical yields.

3.2.15 Two Chamber Nafion Membrane Electrochemical Cell

The two-chamber electrochemical cell separates the anode and cathode into two compartments by a membrane. The nafion membrane allows the transfer of protons (H^+) between these two chambers which prevents reduction in the anodic chamber where the product is produced. This set-up enables the two-chamber cell to increase fluorination yields which may

benefit from the ability to add strong acidic media to the cathodic chamber. Although this addition is not compatible with nucleophilic fluorination in the anodic chamber, it can be added to the cathodic chamber for rapid reduction, it could remove redox reaction bottlenecks formed in the counter electrode half-cell. A solution of trifluoromethanesulfonic acid in MeCN was used in the cathodic chamber with a resulting maximum product yield of 16.4% when using a 25mM concentration of the acid. Increasing the acid concentration in the two-chamber cell reduced these results (Figure 33). Lower concentration of acid didn't provide enough conductivity and reduced product yields. One of the biggest challenges when using this two-chamber nafion cell set-up is preventing acidity buildup which rapidly accumulates in the anodic chamber due to the production of cations and protons generated on the anode. This production outpaces the diffusion of protons through the nafion membrane. We found poly HF fluoride sources in high concentration could buffer some of the acidity but it does not significantly delay reaching low pH (2-3) in the anodic chamber in the first few minutes.

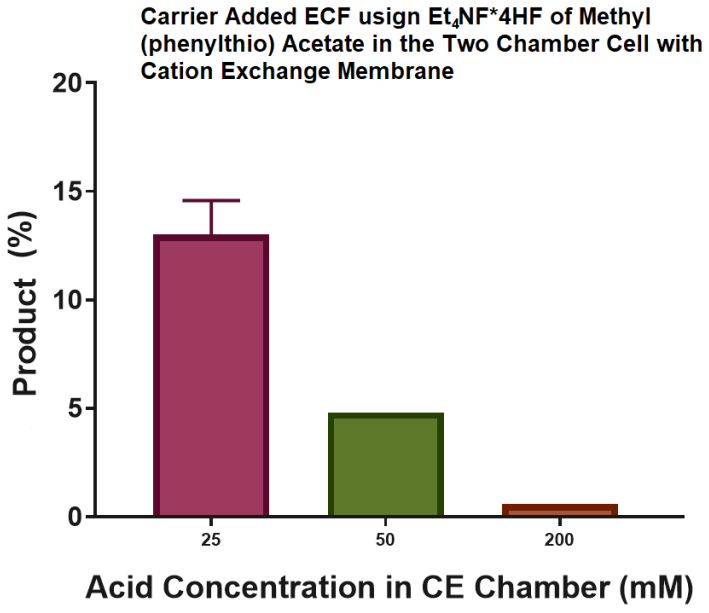

Figure 33: Carrier Added ECF using $Et_4NF*4HF$ of Methyl (phenylthio) Acetate in the Two Chamber Cell. Increasing acid concentration in the counter chamber greatly reduced product yields.

3.2.16 Electrochemical Radiofluorination with different Electrochemical Cells

[^{18}F]Fluoride synthesis using methyl (phenylthio) acetate with $Et_4NF*4HF$ fluoride source was performed under the optimal condition for all the electrochemical cells using the anion exchange method to transfer the [^{18}F]fluoride to organic solvent (Figure 34). The TLC RCC obtained in the optimized single compartment electrochemical cell was measured to be 9.2%±0.1% (n=3). The radiopurity of the methyl-2-[18F]fluoro-2-(phenylthiol) acetate was determined by HPLC to be 88.1%±5.1% (n=3). The RCFE was determined to be 8.1±0.5% (n=3) which was in close agreement with the GCMS quantification of the product yield of 79.4±7.7% (n=3) considering this was performed with 10 times more fluoride than precursor so the maximum RCFE would be 10% when there is 100% product yield. The static chip cell TLC RCC was 2.2%±0.7% (n=3) and RCFE was 1.4%±0.8% (n=3). The two-chamber cell TLC RCC was 2.1%±0.6% (n=3) and RCFE was 1.3±0.7 (n=3). Running the solution through flow cells 5 times produced the highest flow cell yields with CFC RCC measurements to be 1.8%, RCFE to be 1.4%, PtFC RCC to be 2.1%, and RCFE to be 1.7%.

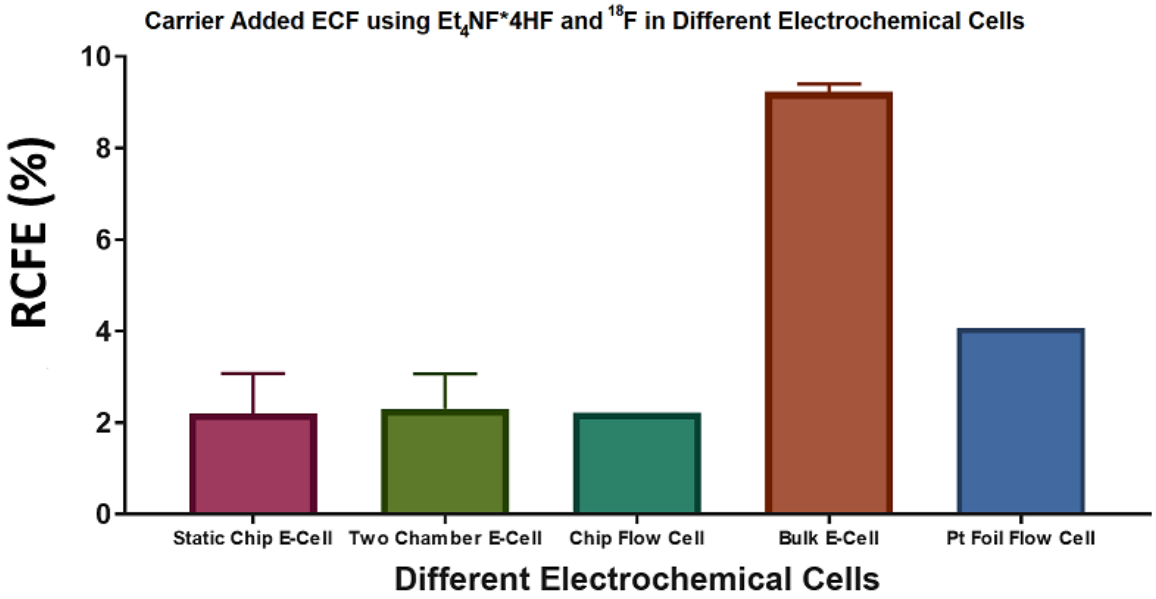

Figure 34: Carrier Added ECF using $Et_4NF*4HF$ and [^{18}F]fluoride in different electrochemical cells. The single chamber cell worked the best.

3.2.17 Effect of Lowering Carrier Fluoride Concentration

A primary obstacle for translating reported studies from the ECF literature to produce PET probes is performing those methodologies under lower concentrations of fluoride. Lowering fluoride concentration leads to low RCY and $A_{m.}$ due to low or 0 fluorination yields. ECF experiments performed under the conditions using MeCN as solvent, 50 mM TBAP, 50 mM Methyl (phenylthio) Acetate as precursor generates low product yields when dropping poly HF fluoride concentration (Figure 35). This was evident when comparing 50 (mM) and 5 (mM) $Et_4NF*4HF$ where product yield dropped from 46.8% to 1.6%. We reasoned fluoride served multiple roles within the FP mechanism which led to the significant drop in product yields in presence of lower fluoride concentrations. Another explanation could relate to the low presence of HF in solution which is required for the formation of anionic species of fluoride to react with the cation intermediate or to abstract protons.

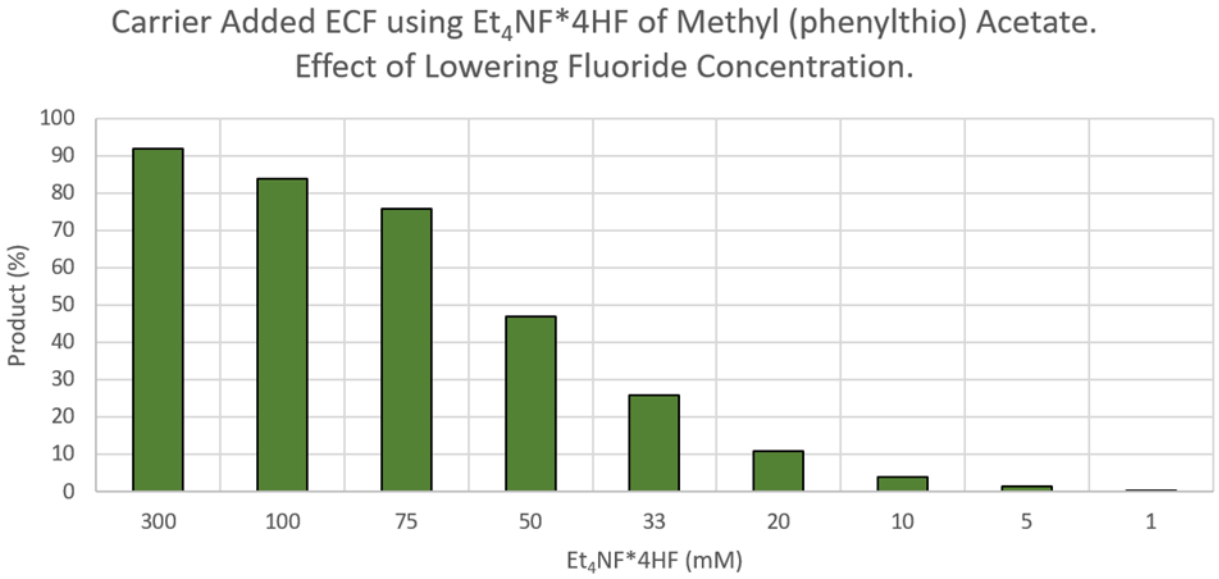

Figure 35: Carrier Added ECF using $Et_4NF*4HF$ of Methyl (phenylthio) Acetate in the Single Chamber Electrochemical Cell. Effect of Lowering Fluoride Concentration. The product yield drops of substantially at lower concentrations of fluoride.

3.2.18 Data Summary of Methyl (phenylthio) Acetate using 100 (mM) $Et_4NF*4HF$

Carrier Added Electrochemical Fluorination Optimization and ^{18}F Radiolabelling of Methyl (phenylthio) Acetate (PTA) using 100 (mM) $Et_4NF*4HF$											
	Oxidation Potential	Anode Material	Solvent	TBAP (mM)	Temp (°C)	Stirring Rate (rev/sec)	Electrochemical Cell	Product Yield % (GC)	TLC RCC %	HPLC RCP %	RCFE %
1	1.8	Pt	MeCN	-	20	4	Single Chamber Cell	3.7±0.7 (n=3)	-	-	-
2	2	Pt	MeCN	-	20	4	Single Chamber Cell	10.7±1.6 (n=3)	-	-	-
3	2.2	Pt	MeCN	-	20	4	Single Chamber Cell	42.3±3.7 (n=3)	-	-	-
4	2.4	Pt	MeCN	-	20	4	Single Chamber Cell	36.9+4.1 (n=3)	-	-	-
5	2.2	Pt	MeCN	1	20	4	Single Chamber Cell	47.2	-	-	-
6	2.2	Pt	MeCN	3	20	4	Single Chamber Cell	54.7	-	-	-
7	2.2	Pt	MeCN	10	20	4	Single Chamber Cell	57.3	-	-	-
8	2.2	Pt	MeCN	20	20	4	Single Chamber Cell	55.5	-	-	-
9	2.2	Pt	MeCN	50	20	4	Single Chamber Cell	34.2	-	-	-
10	2.2	Pt	MeCN	100	20	4	Single Chamber Cell	30.3	-	-	-
11	2.2	Pt	MeCN	-	45	4	Single Chamber Cell	55.2	-	-	-
12	2.2	Pt	MeCN	-	70	4	Single Chamber Cell	63.4±0.6 (n=3)	-	-	-
13	2.2	Pt	MeCN	-	20	0	Single Chamber Cell	0.4+0.1 (n=3)	-	-	-
14	2.2	Pt	MeCN	-	20	2	Single Chamber Cell	38.2	-	-	-
15	2.2	Pt	MeCN	-	20	6	Single Chamber Cell	52.8	-	-	-
16	2.2	Pt	MeCN	-	20	8	Single Chamber Cell	57.4	-	-	-
17	2.2	Pt	MeCN	-	20	10	Single Chamber Cell	62.4±1.6 (n=3)	-	-	-
18	2.2	Pt	MeCN	-	20	-	Single Chamber Cell	23.4+1.5 (n=3)[1]	-	-	-
19	2.2	Pt	MeCN	-	70	-	Single Chamber Cell	40.3+1.6 (n=3)[1]	-	-	-
20	2.2	Carbon Felt	MeCN	-	20	10	Single Chamber Cell	56.3±2.5 (n=3)	-	-	-
21	2.2	Nickle	MeCN	-	20	10	Single Chamber Cell	8.1±0.5 (n=3)	-	-	-
22	2.2	Pt	Dicloromethane	-	20	10	Single Chamber Cell	1.8±0.2 (n=3)	-	-	-
23	2.2	Pt	Nitromethane	-	20	10	Single Chamber Cell	34.5±2.3 (n=3)	-	-	-
24	2.2	Pt	Acetone	-	20	10	Single Chamber Cell	19.1±0.4 (n=3)	-	-	-
25	2.2	Pt	Propylene Carbonate	-	20	10	Single Chamber Cell	36.6±0.9 (n=3)	-	-	-
26	2.2	Pt	Formamide	-	20	10	Single Chamber Cell	19.3+1.3 (n=3)	-	-	-
27	2.2	Pt	MeCN	10	70	10	Single Chamber Cell	78.5±7.7 (n=3)	9.2±0.1 (n=3)	88.1±5.1 (n=3)	8.1±0.5 (n=3)
28	2.2	Pt	MeCN	10	70	10	Single Chamber Cell	93.4*	-	-	-
29	2.2	Pt	MeCN	10	20	-	Static Chip Cell	13.5±1.7 (n=3)	2.2±0.7 (n=3)	64.5±3.2 (n=3)	1.4±0.8 (n=3)
30	2.2	Pt	MeCN	10	20	-	Two Chamber Cell	13.1±1.3 (n=3)[2]	2.1±0.6 (n=3)	61.9±4.4 (n=3)	1.3±0.7 (n=3)
31	2.2	Pt	MeCN	10	20	-	Chip Flow Cell	2.4±0.1 (n=3)	-	-	-
32	2.2	Pt	MeCN	10	20	-	Chip Flow Cell	12.3**	1.8	77.8	1.4
33	2.2	Pt	MeCN	10	20	-	Pt Foil Flow Cell	2.6±0.2 (n=3)	-	-	-
34	2.2	Pt	MeCN	10	20	-	Pt Foil Flow Cell	16.7**	2.1	80.9	1.7
1. Under Sonication,*Used 300mM Et3NF*4HF, 2. Cathodic Chamber had 25mM Triflic Acid in MeCN, **Solution passed 5 times through Flow Cell											

Figure 36: Data Summary of Methyl (phenylthio) Acetate using 100 (mM) Et4NF*4HF

3.2.19 Effect of Lowering Fluoride on RCY with the Electroradiochemistry Platform

The Electro Radiochemical Platform (ERCP) was used when lowering $Et_4NF*4HF$ concentration which incorporated [^{18}F]Fluoride with Methyl (phenylthio) Acetate (Figure 37). The RCFE measurement was also observed to drop substantially at lower fluoride concentration with the maximum RCFE measurement at25 (mM) $Et_4NF*4HF$.

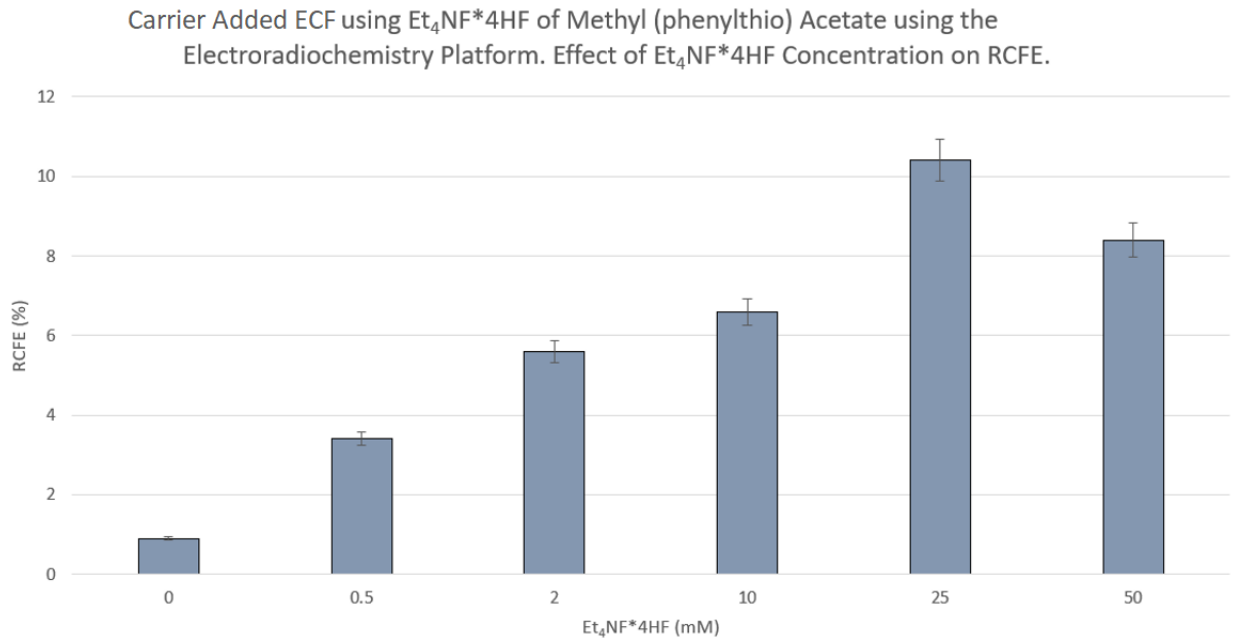

Figure 37: Carrier Added ECF using Et4NF*4HF of Methyl (phenylthio) Acetate using the ERCP. Effect of lowering fluoride concentration on RCFE. The maximum RCFE was at 25 (mM) of the fluoride source.

3.2.20 Effect of Lowering Fluoride on Molar Activity using the ERCP

Molar Activity (A_m) was also determined using the ERCP while lowering fluoride concentration with Methyl (phenylthio) Acetate (Figure 38). The A_m measurement was determined by HPLC integration area based on precursor concentration curve. The A_m gradually increased from 2 MBq/umol to 11 MBq/umol under these conditions along with a decrease in $Et_4NF*4HF$ concentration from 25 (mM) to 0.5 (mM). The low molar activity resulted due to the added fluoride source. Although the fluoride source was reduced by a factor of 50, the A_m measurement only

increased by a factor of 5.5 due to the decreasing fluorination yields with lower fluoride concentration.

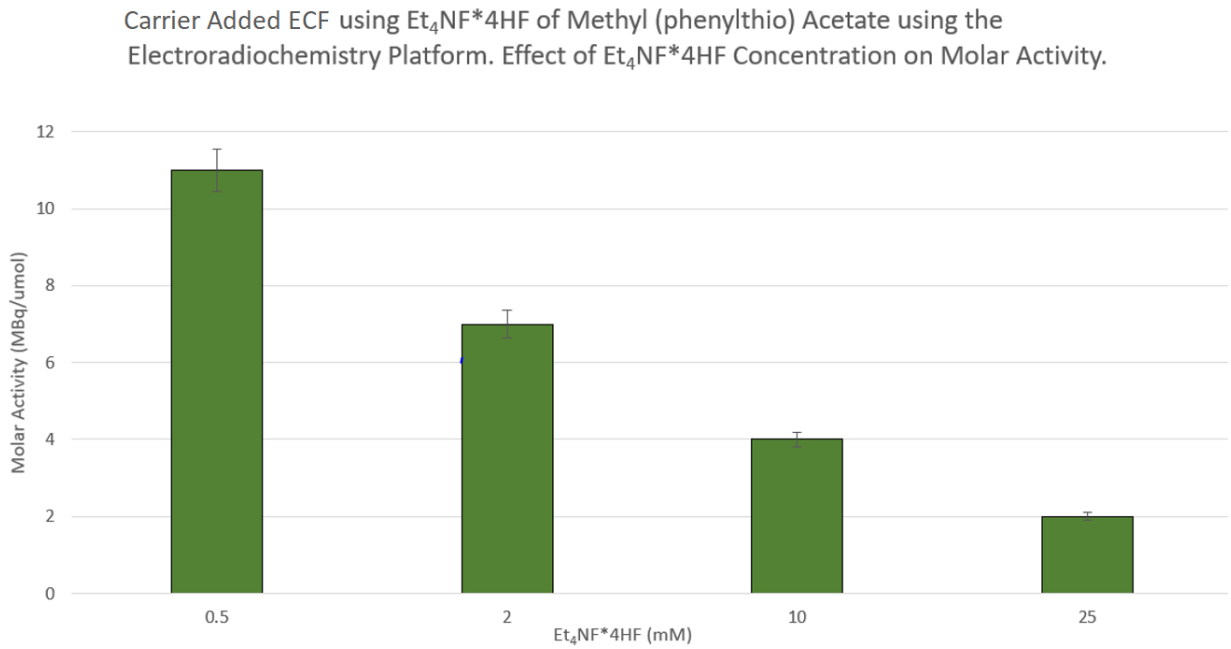

Figure 38: Carrier Added ECF using Et4NF*4HF of Methyl (phenylthio) Acetate using the ERCP. Effect of lowering fluoride concentration on molar activity (A_m). A_m increased with decreasing fluoride concentration.

3.3 ^{18}F Electrochemical Fluorination of Methyl (phenylthio) Acetate using TBAF

Tetrabutylammonium fluoride (TBAF) was investigated to learn its effectiveness to serve as a fluoride source with the precursor Methyl(phenylthio)acetate in an attempt to replace poly HF fluoride sources. However, TBAF did not work well without the addition of triflic acid to form HF even after several optimization attempts to vary the oxidation potential, time, temperature, sonication, TBAF concentration and triflic acid concentration in the reaction. Methyl(phenylthio)acetate was electrochemically fluorinated in a single compartments cell using MeCN in a similar manner as when using $Et_4NF*4HF$, except with TBAF/triflic acid as the poly HF source. The triflic acid to TBAF concentration ratio had a critical role for fluorination. Triflic acid's conjugate base is a weak nucleophile. Here we found this reagent does not compete with

fluoride. Upon further investigation, the addition of TBAF and triflic acid further complicates ECF with concentrations of TBAF, TBA+, F-, HF, H_nF_{n+1}- species, triflic acid and triflate. Triflate has also been found to increase product yield in some ECF conditions. The full results can be found in our previous work [60].

3.3.1 Optimization Parameter: Electrolysis Time

The optimal electrolysis reaction time was determined to be 30 mins (Figure 39). The product yield under these conditions was measured to be 29%. Here we noted the addition of triflic acid, TBAF which includes THF and water, does not significantly reduce product formation compared to using $Et_4NF*4HF$.

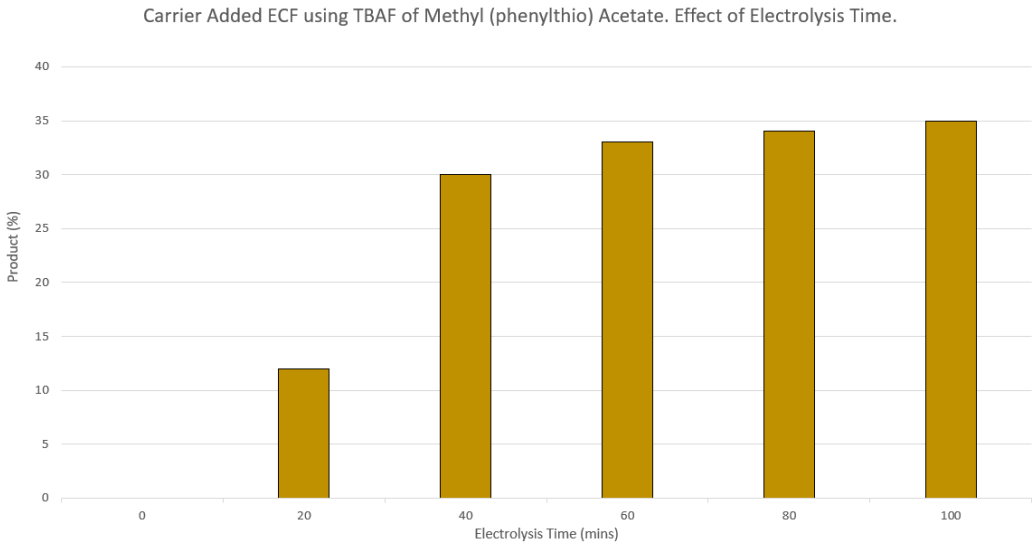

Figure 39: Carrier added ECF using TBAF of Methyl (phenylthio) Acetate. The optimal time was chosen to be 60 mins.

3.3.2 Optimization Parameter: Oxidation Potential

The optimal oxidation potential was found to be 1.4V using the isolated (Ag/Ag+) reference electrode which is lower than using the pseudo Ag reference electrode where the optimal potential was 2.2V (Ag/Ag+). This is likely to be due to the low oxidation of triflic acid. (Figure

40). Higher potential had slightly lower product yields whereas lower potentials led to a slow fluorination process, which is not acceptable for radiofluorination yields due to decay.

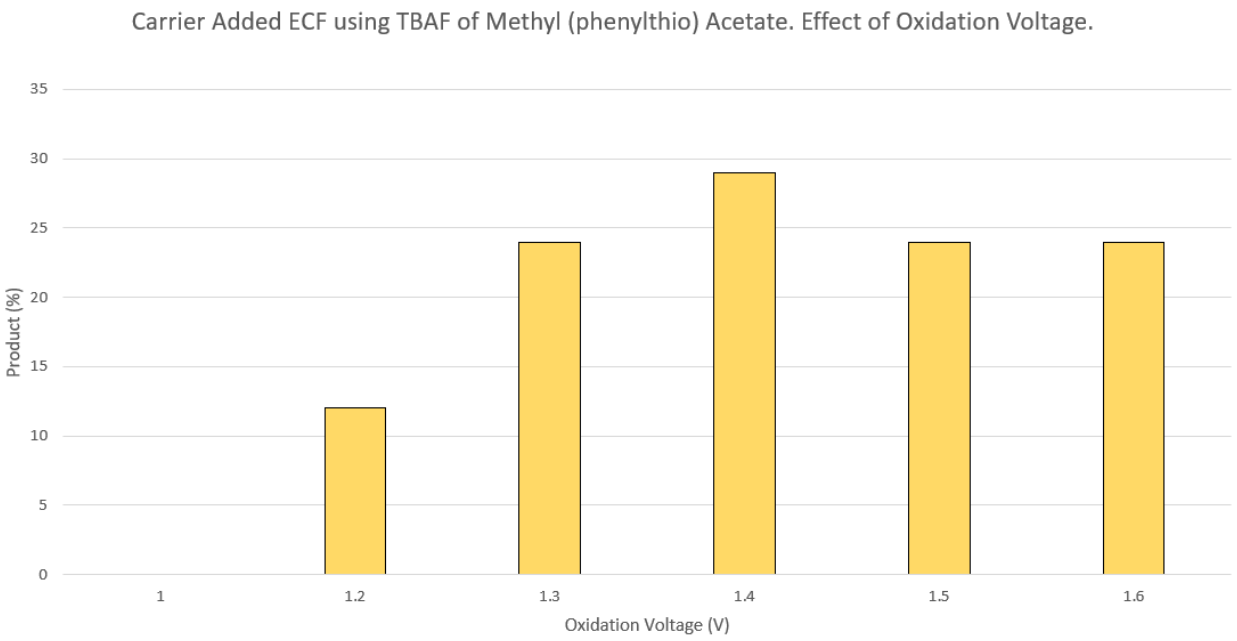

Figure 40: Carrier Added ECF using TBAF of Methyl (phenylthio) Acetate. Effect of Oxidation Voltage. The optimal oxidation voltage was 1.4V.

3.3.3 Optimization Parameter: Triflic Acid Concentration

The effect of adding different concentrations of triflic acid was investigated while holding the TBAF concentration constant (Figure 41). The product yield increases with greater triflic acid concentration of 104.6 mM. Triflic acid concentrations higher than 104.6 mM reduced product yields. We found product yields decreased under conditions with equivalent triflic acid to TBAF concentrations with a notable decrease upon increasing triflic acid exceeding TBAF concentration.

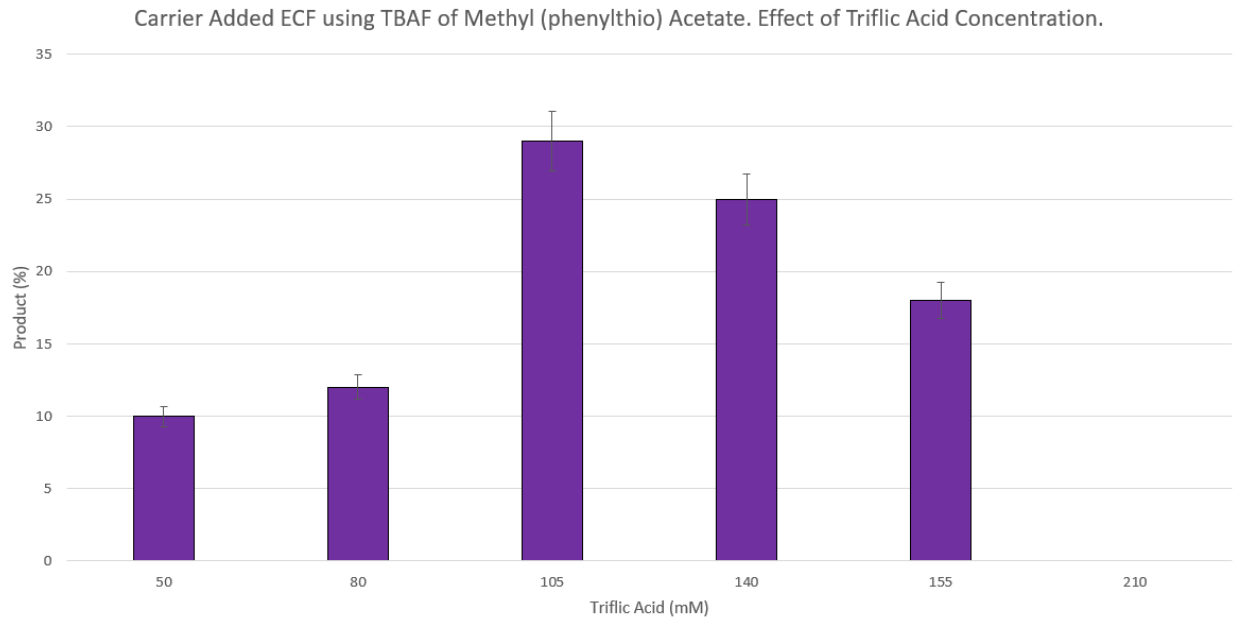

Figure 41: Carrier Added ECF using TBAF of Methyl (phenylthio) Acetate. Effect of Triflic Acid Concentration. The optimal triflic acid concentration was found to be 104.6 (mM).

3.3.4 Optimization Parameter: Type of Acid

Acetic and sulfuric acid were investigated and compared to triflic acid (Figure 42) in these electrochemical reactions which resulted in triflic acid producing the greatest product yield. We reasoned this outcome resulted in the low oxidation potential of acetic and sulfuric which can interfere with oxidation of the precursor and the nucleophilicity of the conjugate bases of these acids competing with fluoride.

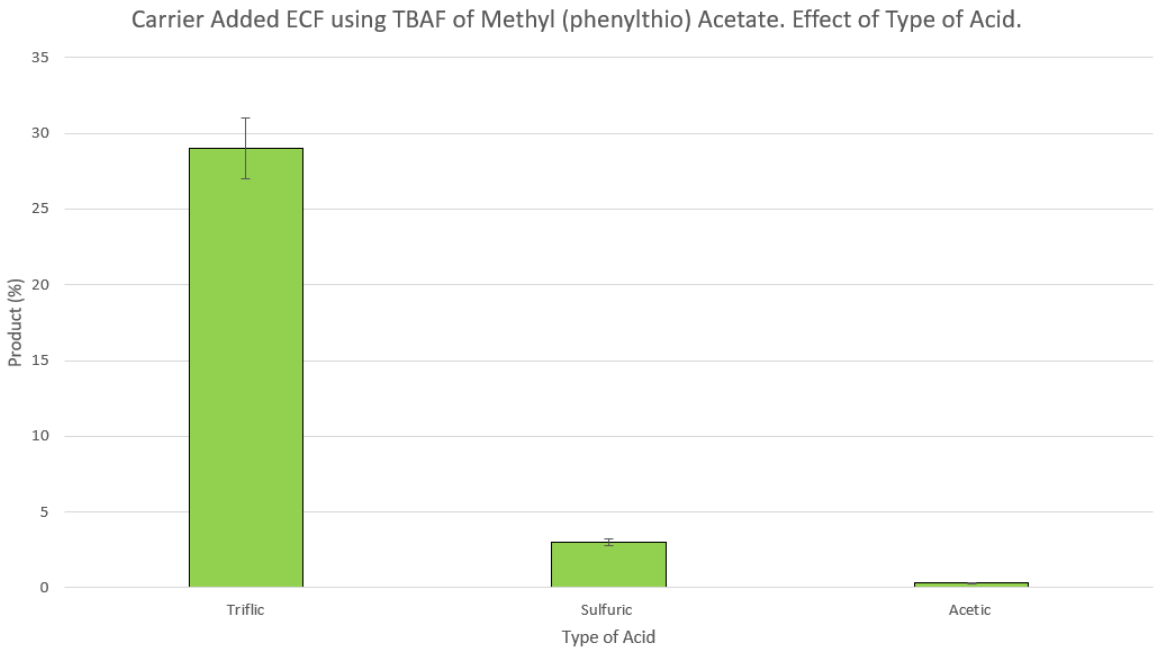

Figure 42: Carrier Added ECF using TBAF of Methyl (phenylthio) Acetate. Effect of Type of Acid. Triflic acid was the best acid.

3.3.5 Optimization Parameter: Temperature

Increasing temperature from 0 °C to 60 °C increased the product yield from 8% to 44%. The optimal temperature was noted to be 60 °C seen in Figure 43 which agreed to previously reported ECF data of thioethers.

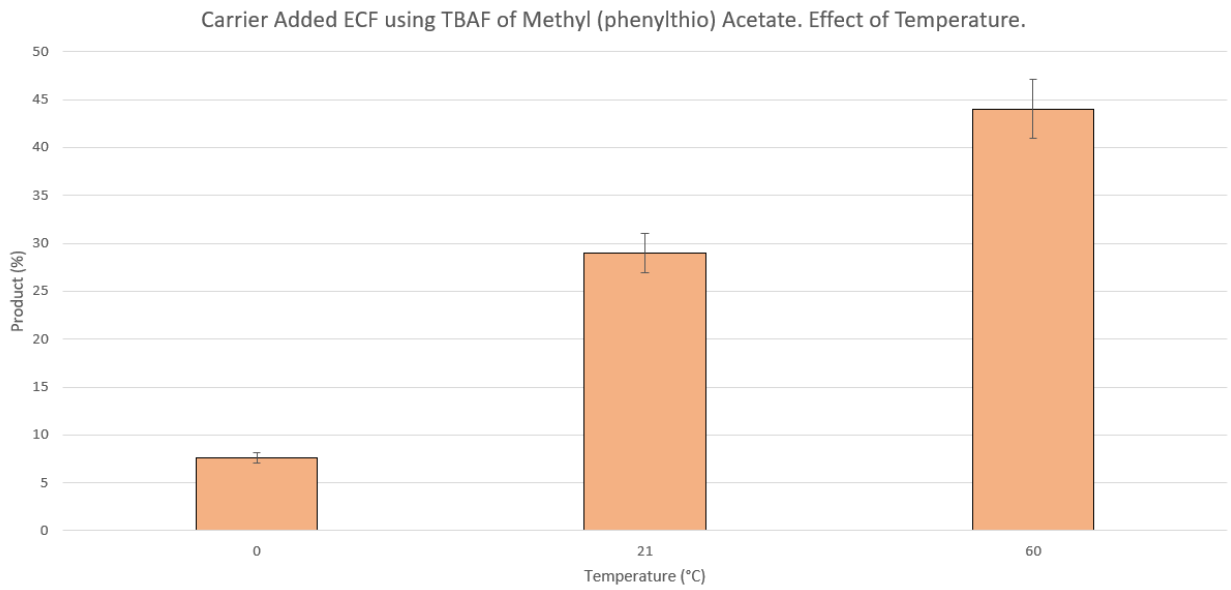

Figure 43: Carrier Added ECF using TBAF of Methyl (phenylthio) Acetate. Effect of Temperature. The optimal temperature was 60 °C.

3.3.6 Optimization Parameter: TBAF Concentration

The effects of varying TBAF concentration was tested under the same triflic acid concentration with the optimal TBAF concentration to be 154 (mM) (Figure 44). Lower TBAF concentrations produced lower product yields which supported our previous findings that increasing the acidity reduces product yields.

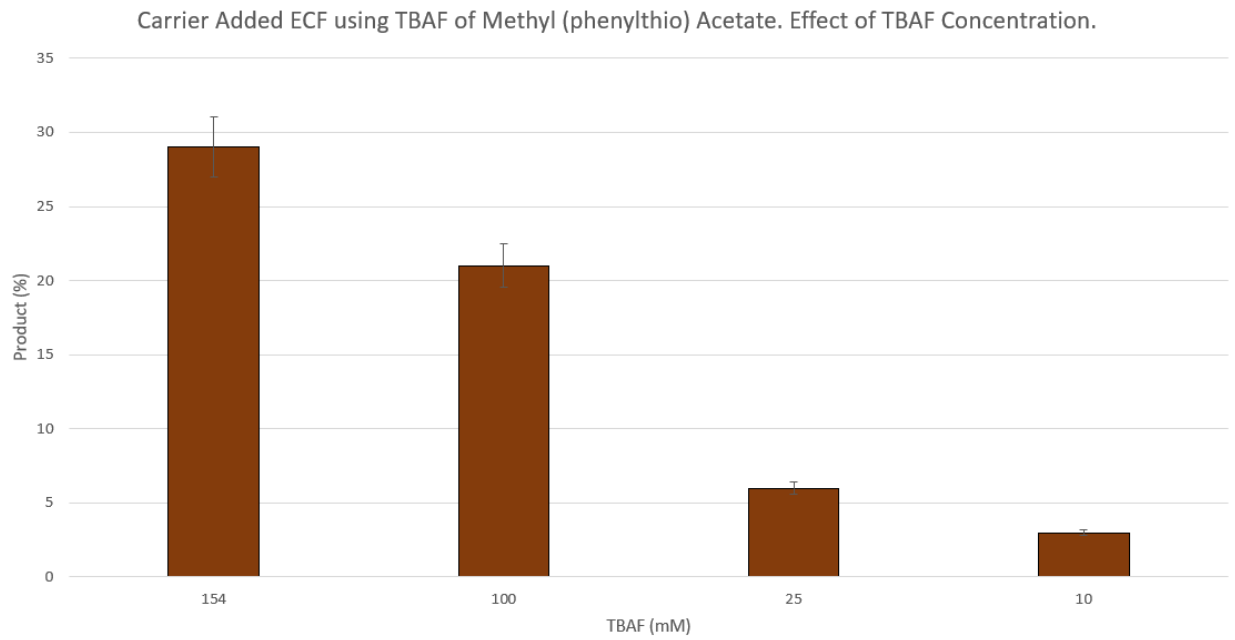

Figure 44: Carrier Added ECF using TBAF of Methyl (phenylthio) Acetate. Effect of TBAF Concentration. The optimal amount of TBAF was found to be 154 (mM).

3.3.7 Optimization Parameter: Ratio Acid/TBAF

Understanding the critical role of the triflic acid/TBAF ratio played in the reaction, we investigated optimizing these concentrations. We reported the optimal ratio was 0.68 triflic acid/TBAF with the optimal concentrations to be 154 mM of TBAF and 104.6 mM of triflic acid (Figure 45). Increasing the concentration reproducibility produced the same product yield and decreasing the concentration reduced product yield all while maintaining the ratio constant. Under these conditions, the product yields dropped rapidly when lowering fluoride concentrations which was also seen with $Et_4NF*4HF$.

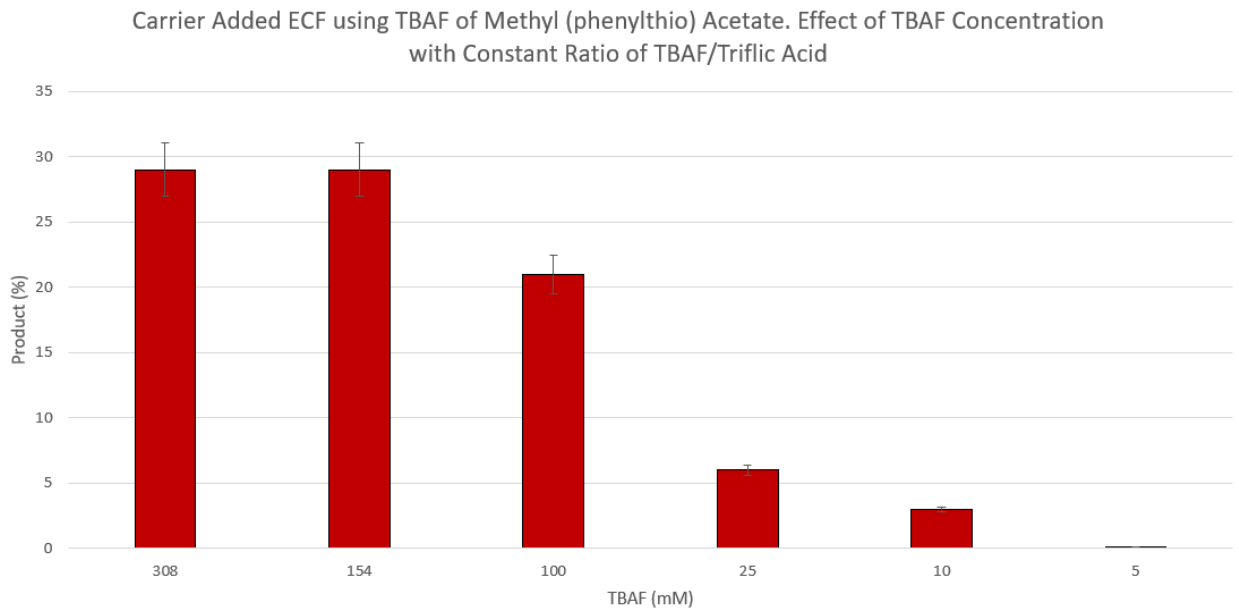

Figure 45: Carrier Added ECF using TBAF of Methyl (phenylthio) Acetate. Effect of triflic acid/TBAF ratio and concentration. The optimal concentration of TBAF was 154 (mM) with a ratio of 0.68 triflic acid/TBAF.

3.3.8 Radiochemical Fluorination Efficiency using TBAF

Using the optimal conditions with the single chamber electrochemical cell, the RCFE was measured to be 7 ± 1% (n = 3) with the product yield to be 43% ± 3% (n = 3). These findings were aligned with previously predicted fluorination yields. The optimal condition is as followed: 30 min of electrolysis; 1.4 V, MeCN solvent, 154 (mM) of TBAF, and 104.6 (mM) of triflic acid at 60 °C. The RCFE of 7 ± 1% (n = 3) is very similar to result with the use of $E^t_4NF*4HF$ fluoride source that had a product yield of 8.1+.05% (n=3). This measurement is in good agreement when one factors in fluoride concentration. The triflic acid/TBAF syntheses achieved similar results with 3 times less fluoride, thus suggesting a beneficial role of triflate.

Chapter 4: No-Carrier-Added (NCA) Methyl (phenylthio) Acetate ^{18}F ECF

We hypothesized that the requirement of having multiple fluoride ions participating in the fluoro-Pummerer rearrangement is the cause of the low product yield when decreasing fluoride concentration in ECF reactions of thioethers using $Et_4NF*4HF$ or Triflic acid/TBAF. Figure 46 shows the fluoro-Pummerer (FP) mechanism with the carrier added poly HF fluoride sources. Fluoride is necessary to stabilize sulfur after the first oxidation and is also responsible to abstract protons, causing the rearrangement for the last fluoride to be added onto the alpha carbon. Additionally, multiple fluorides may be necessary to form anionic species of fluoride that react with the cation intermediates and abstract the protons. Figure 47 shows the fluoro-Pummerer (FP) mechanism replacing poly HF fluoride species with an auxiliary molecule. In this mechanism the auxiliary performs all the roles of the poly HF species except in the last step where fluoride attacks the cation intermediate before bonding onto the alpha carbon. By adding the auxiliary, it was no longer necessary to add in a high concentration of additional stable fluoride to perform ECF. This approach enabled us to perform NCA-ECF with higher RCY and A_m. After screening several different potential auxiliary molecules, trifluoroethanol (TFE) and hexafluoroisopropanol (HFIP) were identified to be the optimal solvent choices for this reaction. These solvents are weak acids which form strong conjugate bases from reduction on the cathode. The conjugate bases of TFE and HFIP may participate as auxiliary molecules stabilizing the cation intermediate and abstraction of the proton in the FP rearrangement.

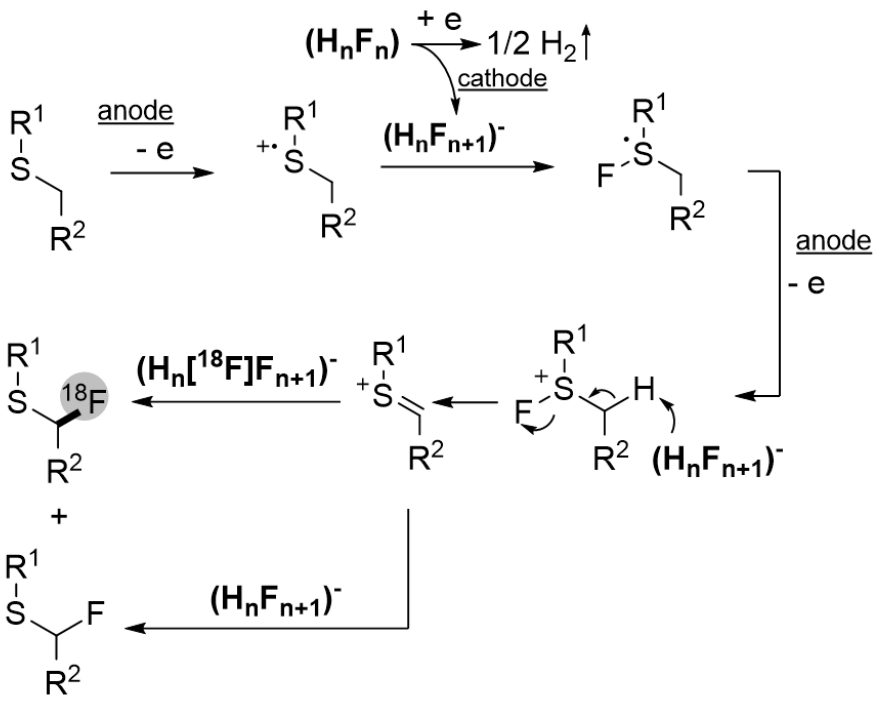

Figure 46: Fluoro-Pummerer Mechanism using high concentration of Poly HF sources for ECF of Thioethers.

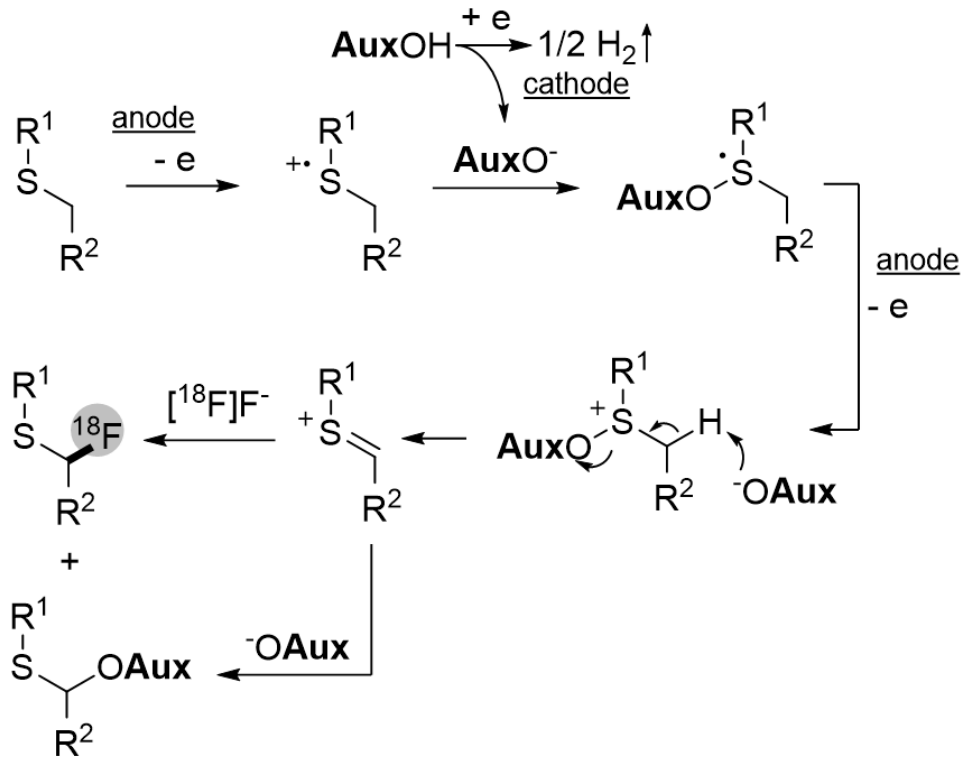

Figure 47: Fluoro-Pummerer Mechanism using an Auxiliary to facilitate No-Carrier-Added ECF of Thioethers.

Trifluoroethanol (TFE) and hexafluoroisopropanol (HFIP) are very interesting solvents for electrochemical syntheses. The high dielectric constants provide good conductivity ow polarizability which helps with the stability of intermediates. Both TFE and HFIP have good solubility for organic molecules and the propensity to solvate competing anions which increases the lifetime of cation intermediates. This finding is critical in the ECEC mechanism to prevent competing processes of the cation intermediate, such as reaction with precursor, solvent, or another competing nucleophile or disproportiation. In return, we can have a greater yield of fluorination for the resulting product. TFE and HFIP also have low nucleophilicity, which limits the competition of the solvent with fluoride [116-118]. In addition, TFE and HFIP, are hydrogen bond donating solvents which can often form complexes with themselves. It is likely that their hydrogen donating ability helps to form anionic forms of fluoride, similar to those found with poly HF fluoride species which increases fluoride reactivity.

4.1 NCA ^{18}F Electrochemical Fluorination Methyl (phenylthio) Acetate (6ml Cell)

We proceeded to conduct a series of NCA experiments using TFE instead of MeCN for NCA-ECF of Methyl (phenylthio) Acetate that were performed in a 6 (ml) single chamber electrochemical cell using TFE solvent. The similar cell was also prepared with $Et_4NF*4HF$ in parallel of these studies for accurate comparison. All experiments used 50 (mM) of TBAP added for conductivity unless otherwise noted. This is necessary due to the NCA experiments do not contain poly HF fluoride salts for conductivity.

4.1.1 Optimization Parameter: Oxidation Potential

Similar to our previous optimization attempts, we investigated performing another series of reactions using TFE as solvent under no-carrier-added conditions instead. We found the optimal oxidation potential to be at 3.5V (Ag/Ag+) where the RCFE increased from an oxidation potential of 2.0V (Ag/Ag+) up to 3.5V (Ag/Ag+) and then decreased at 4.0V (Ag/Ag+) (Figure 48). At an oxidation potential of 4.0V (Ag/Ag+) the electrolyte (TBAP) begins to oxidize which is seen by decreasing RCP measurements on HPLC along with side product formation. We were surprised these reactions generated higher RCFE at a greater oxidation potential than in the carrier added experiments. Under NCA conditions less than 0.06% of the precursor has to follow the mechanism to achieve high RCFE due to large excess of precursor and low fluoride concentration present in solution. This often leads to a large mass and many different side products formed in NCA-ECF experiments. One important thing to note was when using TFE as solvent reduction of the TFE causes build up on counter electrode (CE) but did not interfere with product formation. TFE may help shield the precursor, product and even side products from this reduction and it may be the reason why the optimal potential may be higher when using this solvent. The working electrode remains clean during electrolysis.

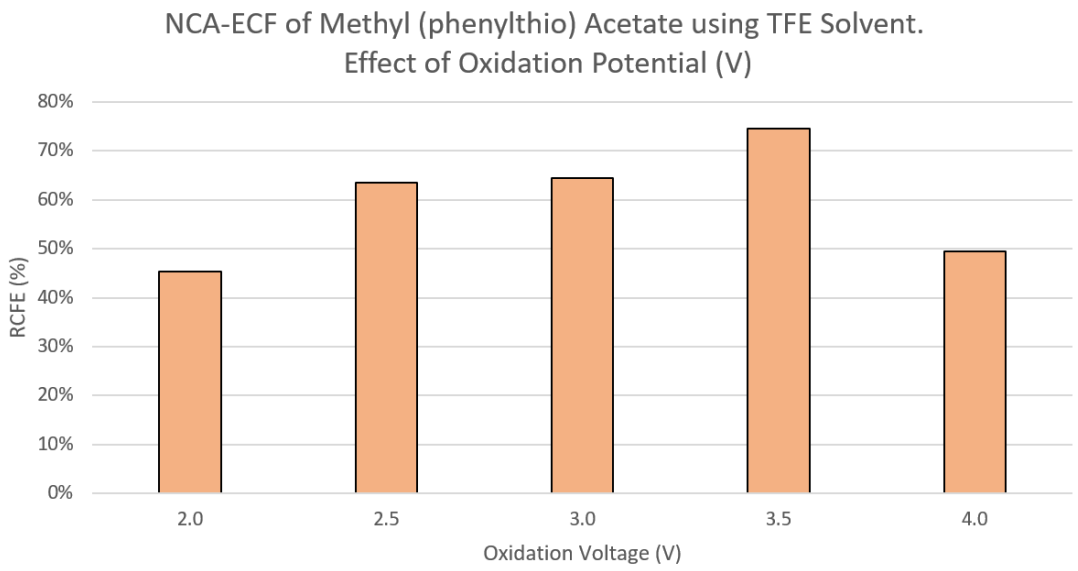

Figure 48: NCA-ECF of Methyl (phenylthio) Acetate using TFE Solvent. Effect of Oxidation Potential. The optimal oxidation potential was at 3.5V.

4.1.2 Optimization Parameter: Temperature

We noticed increasing the temperature led to greater RFCE measurements. Here we found the optimal temperature to conduct these reactions was 70 °C. Our initial setup was not configured for higher temperatures which would cause TFE to boil unless under pressure. The same temperature trend of increasing temperature with increasing RCFE was seen in all carrier added synthesis with thioethers (Figure 49).

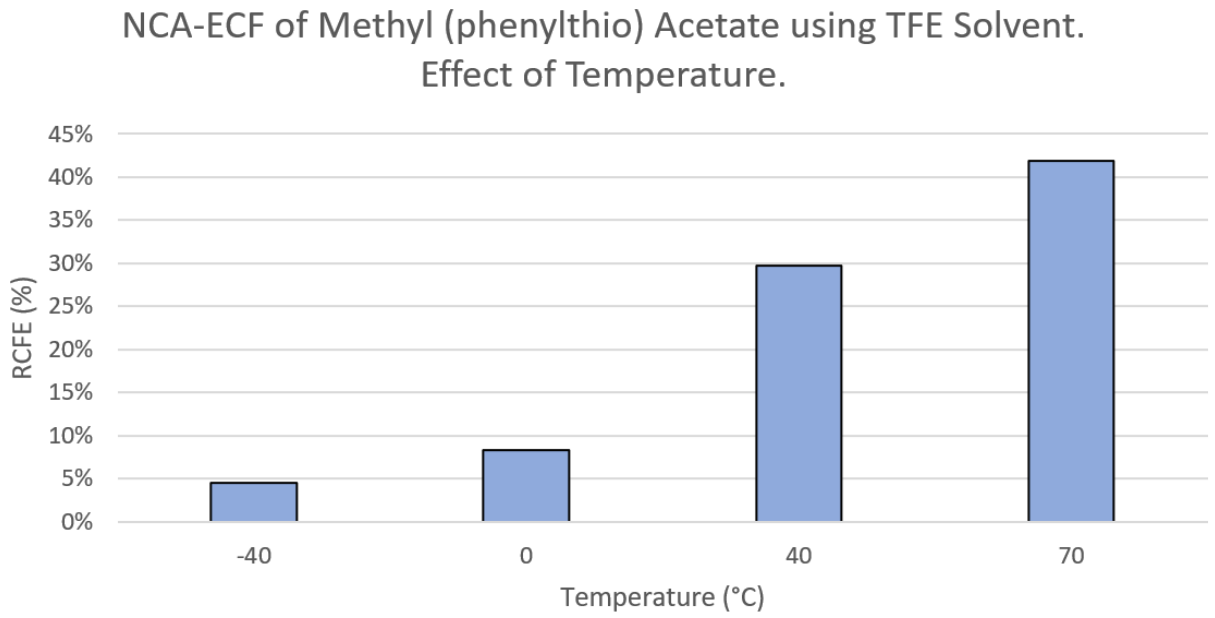

Figure 49: NCA-ECF of Methyl (phenylthio) Acetate using TFE Solvent. Effect of Temperature. The optimal temperature was 70 °C.

4.1.3 Optimization Parameter: Electrolyte Concentration

The optimal TBAP concentration was also investigated for NCA-ECF of Methyl (phenylthio) Acetate since this provides conductivity of the solution. We noticed that lower TBAP concentrations resulted in lower currents and less oxidized precursor. The optimal amount of TBAP was found to 25 mM for 50 mM of precursor (Figure 50). The of optimal TBAP concentration depended on the oxidation current where increased oxidation current required increased precursor concentration. This suggests TBAP to have a beneficial role at the anode.

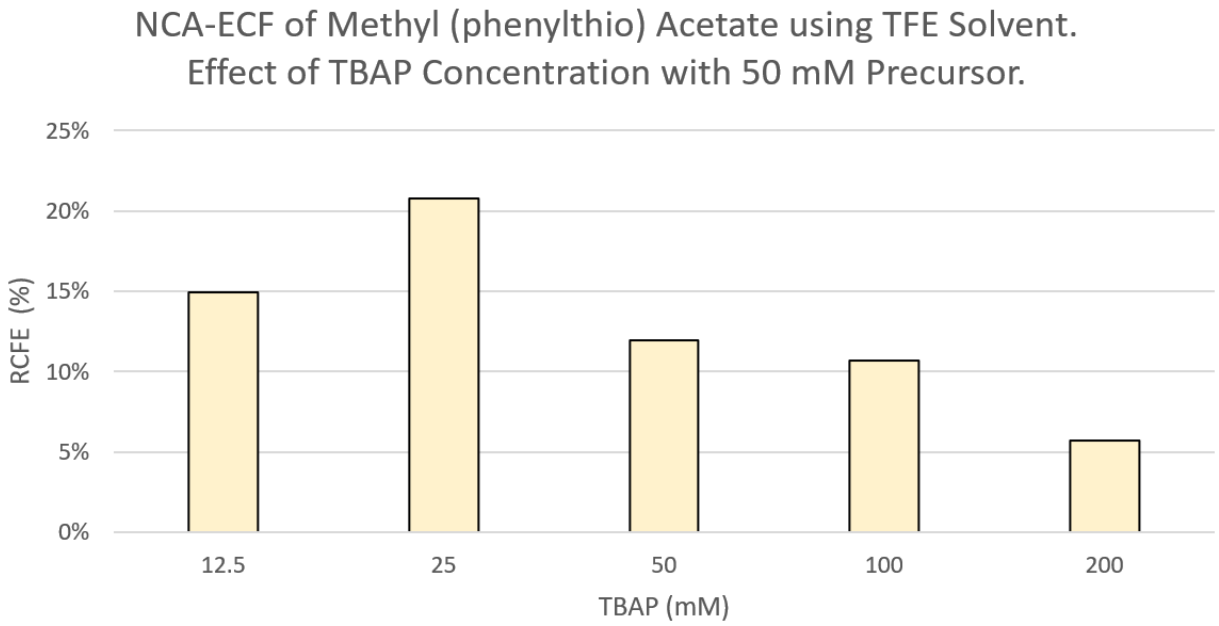

Figure 50: NCA-ECF of Methyl (phenylthio) Acetate using TFE Solvent. Effect of TBAP concentration. The optimal amount of TBAP was 25 (mM) with 50 (mM) Precursor.

4.1.4 Optimization Parameter: Precursor Concentration

Precursor concentration was also optimized with 25 mM TBAP as the optimal precursor concentration and Methyl (Phenylthio) Acetate at 50 mM (Figure 51). We found great concentrations of precursor led to a decrease in RCFE. We investigated maintaining the same TBAP and precursor concentration ratio (Figure 52) with 100 mM of both TBAP and Precursor. Greater product yields were generated under these conditions than using a precursor concentration with 25 mM TBAP. Following this reaction, we also explored using 150 mM and 200 mM of both reagents, respectively, which also performed well with slightly less RCFE for each increase in concentration. Thus, we concluded the optimal precursor concentration was dependent on the TBAP concentration where increasing the precursor concentration led to an increased in current. Similarly, lower precursor concentration (lower current), led to lower optimal TBAP

concentration.

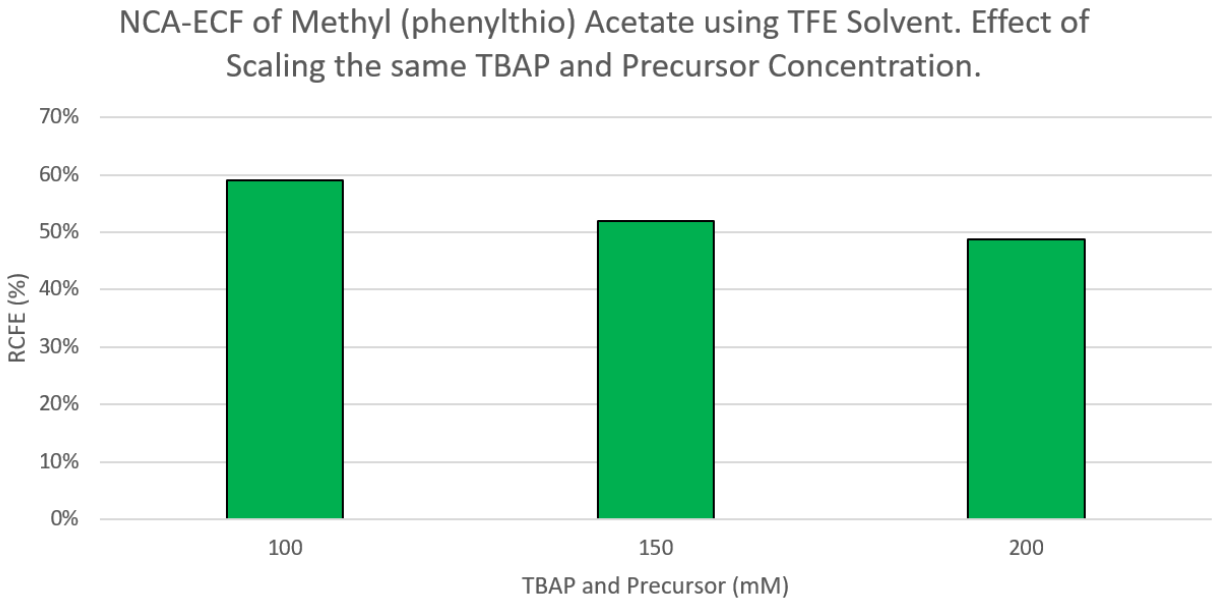

Figure 51: NCA-ECF of Methyl (phenylthio) Acetate using TFE Solvent. Effect of Precursor Concentration at 25 (mM) TBAP. The optimal precursor concentration was 50 (mM).

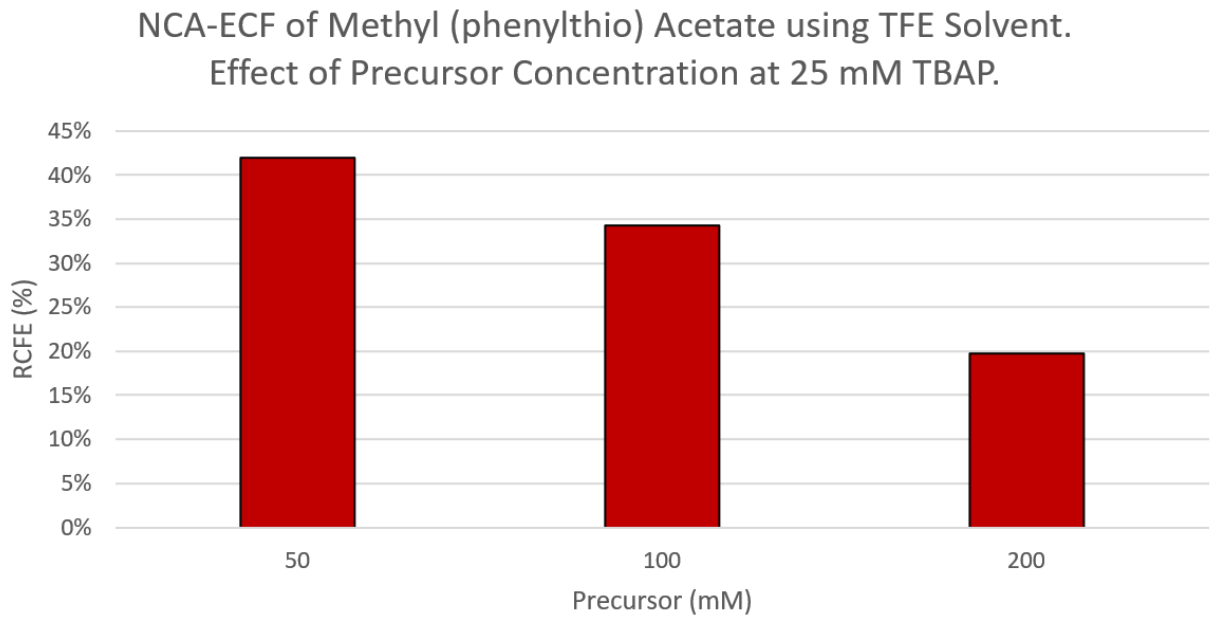

Figure 52: NCA-ECF of Methyl (phenylthio) Acetate using TFE Solvent. Effect of Scaling TBAP and Precursor Concentration. The optimal concentration of both was found to be 100 (mM).

4.1.5 Data Summary of NCA-ECF Methyl (phenylthio) Acetate (6ml cell)

NCA-ECF Optimization of Methyl (phenylthio) Acetate (PTA) in the Single Chamber 6ml Electrochemical Cell										
#	Precursor (mM)	Electrolyte (mM)	Temperature (°C)	Oxidation Voltage	Duration (min)	Oxidation Pulse (min)	Starting Activity (mCi)	RCC (%)	RCP (%)	RCFE (%)
Best 3	PTA 150 mM	100	70	3.50	60	60	1.64±0.31	85.6±1.6%	84.2±1.2%	72.1±1.9%
1	PTA 50 mM	12.5	20	2.25	60	60	0.63	18.1%	82.4%	14.9%
2	PTA 50 mM	25	20	2.25	60	60	0.38	28.6%	72.6%	20.8%
3	PTA 50 mM	50	20	2.25	60	60	0.26	15.7%	76.3%	12.0%
4	PTA 50 mM	100	20	2.25	60	60	0.17	13.9%	76.9%	10.7%
5	PTA 50 mM	200	20	2.25	60	60	2.08	11.7%	48.6%	5.7%
6	PTA 50 mM	25	-40	2.25	60	60	1.47	4.7%	97.3%	4.5%
7	PTA 50 mM	25	0	2.25	60	60	0.89	9.3%	89.4%	8.3%
8	PTA 50 mM	25	40	2.25	60	60	0.48	37.4%	79.5%	29.7%
9	PTA 50 mM	25	70	2.25	60	60	0.31	47.9%	87.5%	41.9%
10	PTA 100 mM	50	70	2.25	60	60	0.16	43.8%	85.9%	37.6%
11	PTA 100 mM	100	70	2.25	60	60	0.55	68.5%	86.2%	59.0%
12	PTA 150 mM	150	70	2.25	60	60	0.53	63.8%	81.5%	52.0%
13	PTA 200 mM	200	70	2.25	60	60	1.43	63.5%	76.8%	48.8%
14	PTA 100 mM	25	70	2.25	60	60	0.81	41.5%	82.7%	34.3%
15	PTA 200 mM	25	70	2.25	60	60	0.63	26.5%	74.5%	19.7%
16	PTA 100 mM	100	70	2.25	60	6	2.47	65.1%	87.8%	57.2%
17	PTA 100 mM	100	70	2.25	60	0.12	1.16	56.6%	74.5%	42.2%
18	PTA 100 mM	100	70	1.50	30	60	3.28	26.1%	83.9%	21.9%
19	PTA 100 mM	100	70	1.50	60	60	3.28	52.3%	85.4%	44.7%
20	PTA 100 mM	100	70	1.50	90	60	3.28	61.2%	84.7%	51.8%
21	PTA 100 mM	100	70	1.50	120	60	3.28	71.8%	82.7%	59.4%
22	PTA 100 mM	100	70	1.75	30	60	2.71	25.1%	82.8%	20.8%
23	PTA 100 mM	100	70	1.75	60	60	2.71	59.2%	81.7%	48.4%
24	PTA 100 mM	100	70	1.75	90	60	2.71	76.0%	83.8%	63.7%
25	PTA 100 mM	100	70	1.75	120	60	2.71	75.2%	78.2%	58.8%
26	PTA 100 mM	100	70	2.00	30	60	2.39	29.0%	80.7%	23.4%
27	PTA 100 mM	100	70	2.00	60	60	2.39	59.6%	81.3%	48.5%
28	PTA 100 mM	100	70	2.00	90	60	2.39	70.0%	80.6%	56.4%
29	PTA 100 mM	100	70	2.00	120	60	2.39	63.9%	61.9%	39.6%
30	PTA 100 mM	100	70	2.25	30	60	3.05	49.3%	75.9%	37.4%
31	PTA 100 mM	100	70	2.25	60	60	3.05	69.2%	83.4%	57.7%
32	PTA 100 mM	100	70	2.25	90	60	3.05	58.7%	24.1%	14.1%
33	PTA 100 mM	100	70	2.25	120	60	3.05	53.5%	3.1%	1.7%
34	PTA 100 mM	100	70	2.50	30	60	2.88	55.3%	79.5%	44.0%
35	PTA 100 mM	100	70	2.50	60	60	2.88	73.5%	80.1%	58.9%
36	PTA 100 mM	100	70	2.50	90	60	2.88	68.5%	48.1%	32.9%
37	PTA 100 mM	100	70	2.50	120	60	2.88	58.9%	18.5%	10.9%
38	PTA 150 mM	100	70	2.00	60	60	1.35	56.4%	80.3%	45.3%
39	PTA 150 mM	100	70	2.50	60	60	0.92	76.8%	82.7%	63.5%
40	PTA 150 mM	100	70	3.00	60	60	0.74	79.1%	81.4%	64.4%
41	PTA 150 mM	100	70	3.50	60	60	2.02	87.8%	84.9%	74.5%
42	PTA 150 mM	100	70	3.50	60	60	1.63	84.3%	85.2%	71.8%
43	PTA 150 mM	100	70	3.50	60	60	1.27	84.7%	82.5%	69.9%
44	PTA 150 mM	100	70	4.00	60	60	0.97	72.4%	68.3%	49.4%

Figure 53: Data Summary Table of the NCA-ECF Preliminary Experiments using Methyl (phenylthio) Acetate (PTA).

4.2 NCA ^{18}F Electrochemical Fluorination Methyl (phenylthio) Acetate (1.5ml Cell)

Several other additive molecules and solvents were also tested as potential auxiliary molecules in the FP mechanism for NCA-ECF of thioethers. These experiments were performed in a 1.5 ml electrochemical cell built out an HPLC vial to decrease the experiment duration which enabled us to perform and screen multiple experiments in quick succession. Due to minimizing the reaction volume, we proceeded to optimize the reaction conditions, such as mass of chemicals changes in surface area, and electrode distance, to ensure similar results were attainable when repeating these experiments on a larger-scale. Products were isolated with HPLC separation and the molar activity (A_m) was found to be 0.47+0.03 Ci/uM (n=2) (Figure 66).

4.2.1 Optimization Parameter: Time

The optimal electrolysis time was 30 mins (Figure 54) where reactions running longer than 30 mins resulted in more oxidation and decreased product concentration. At 10 mins, 50% of the product was of synthesized compared to the optimal 30 min synthesis.

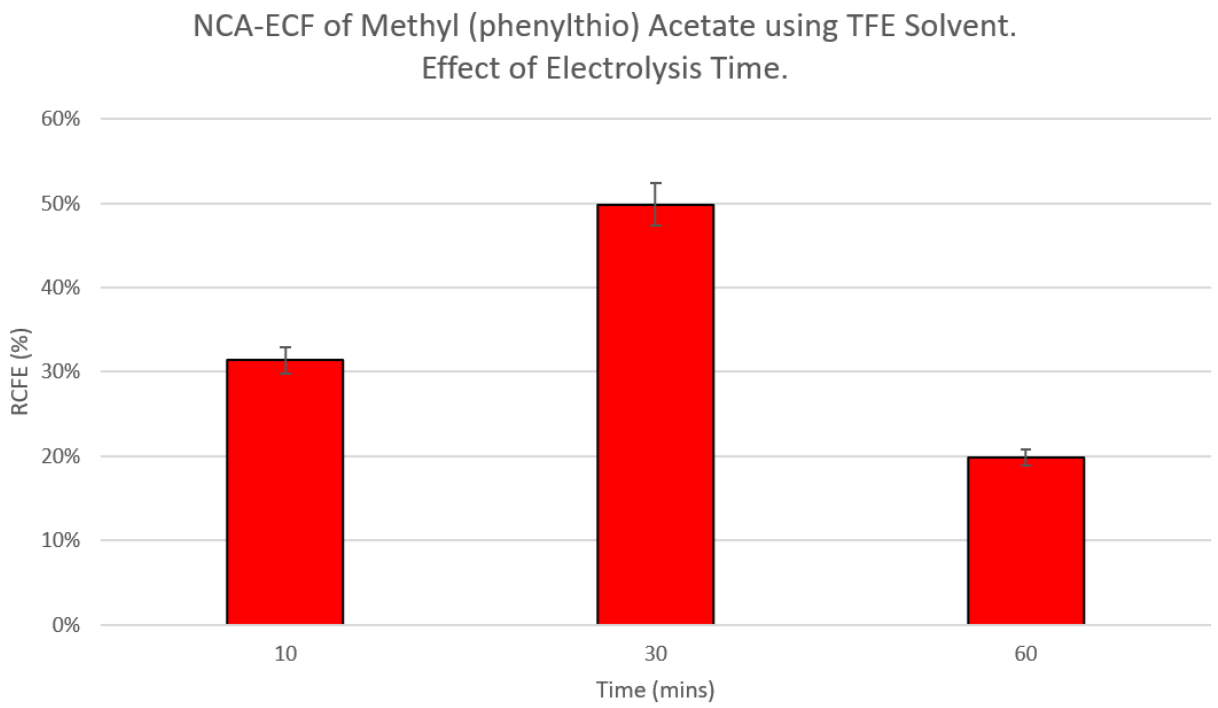

Figure 54: NCA-ECF of Methyl (phenylthio) Acetate using TFE Solvent. Effect of Electrolysis Time. The optimal time was 30 mins.

4.2.2 Optimization Parameter: Temperature

Based on our previous observations where RCFE increased with increasing temperatures (Figure 55), we found that performing reactions at 70 °C resulted in an RCFE of 49.8±0.5% (n=2), which was more than double the originally measured 19.2±0.2% (n=2) at 25 °C. When downsizing the reaction in the 1.5 ml cell compared to the 6 ml cell, we found a greater impact when increasing the temperature. This caused a much larger gain in RCFE with temperature using the smaller cell. We reasoned the closer distance of the electrodes may have affected these outcomes, which led to more anions produced on the cathode to reach the anode, as well as cations produced on the anode to reach the cathode. In return, this could prevent the buildup of ions at either electrode which could interfere with ECF. This would be beneficial to single chamber cells since this effect would help control anodic acidity.

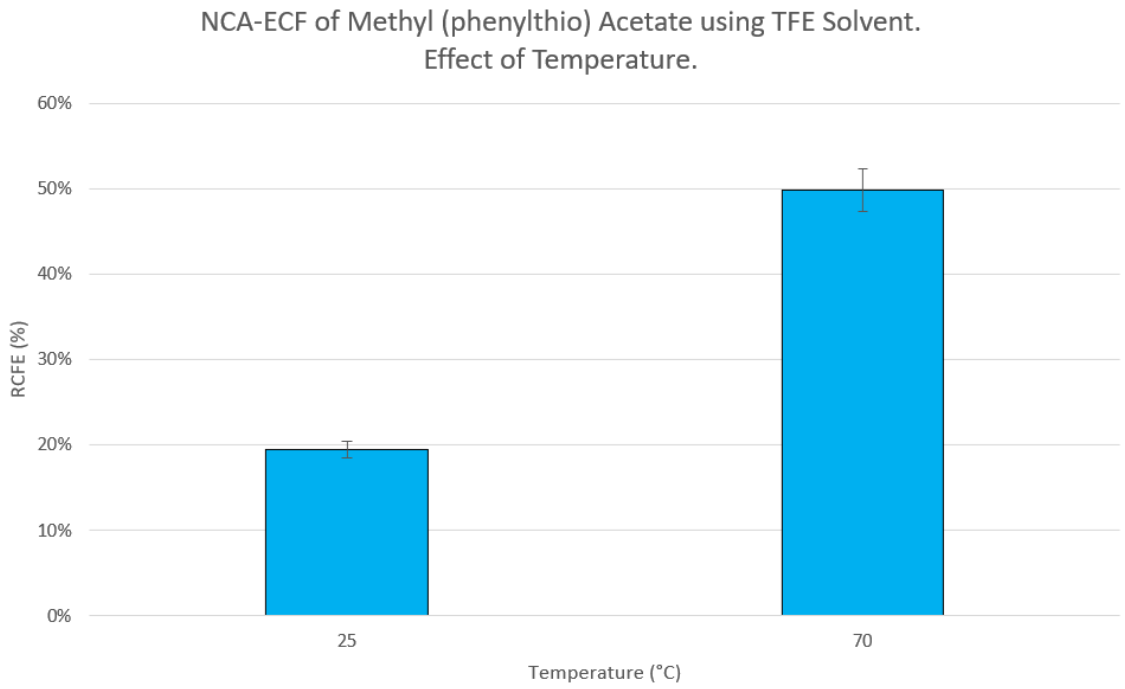

Figure 55: NCA-ECF of Methyl (phenylthio) Acetate using TFE Solvent. Effect of Temperature. The optimal temperature was 70°C.

4.2.3 Optimization Parameter: Aqueous Conditions

Water is usually present in trace amounts in radiochemical reactions since it is produced in $[^{18}O]H_2O$ in a cyclotron. However, water solvates fluoride which makes ions unreactive as a nucleophile due to hydrogen bonding. Although, it is not clear how much trace water remains after electrolysis due to water's low redox potentials. Additionally, it is not well understood the solvation effect of water on fluorination efficiency of the final product or when fluoride complexes are near an applied potential. To investigate the resilience of NCA-ECF when using TFE as solvent, different volume percent of cyclotron water containing [18F]Fluoride was added. Using 1.9V oxidation potential, the RCFE dropped from 49.8±0.5% (n=2) without water to 17.2±1.3% (n=2) at 1% water. This decreasing trend continued when repeating experiments at 3% and 5% water (Figure 56). Yet, with increasing water content, the drop in RCFE may be due to solvation

or from side product formation of water which interferes in ECF. The greater amount of hydroxyl group present in solution can also hydrolyze products and even be compete as nucleophiles.

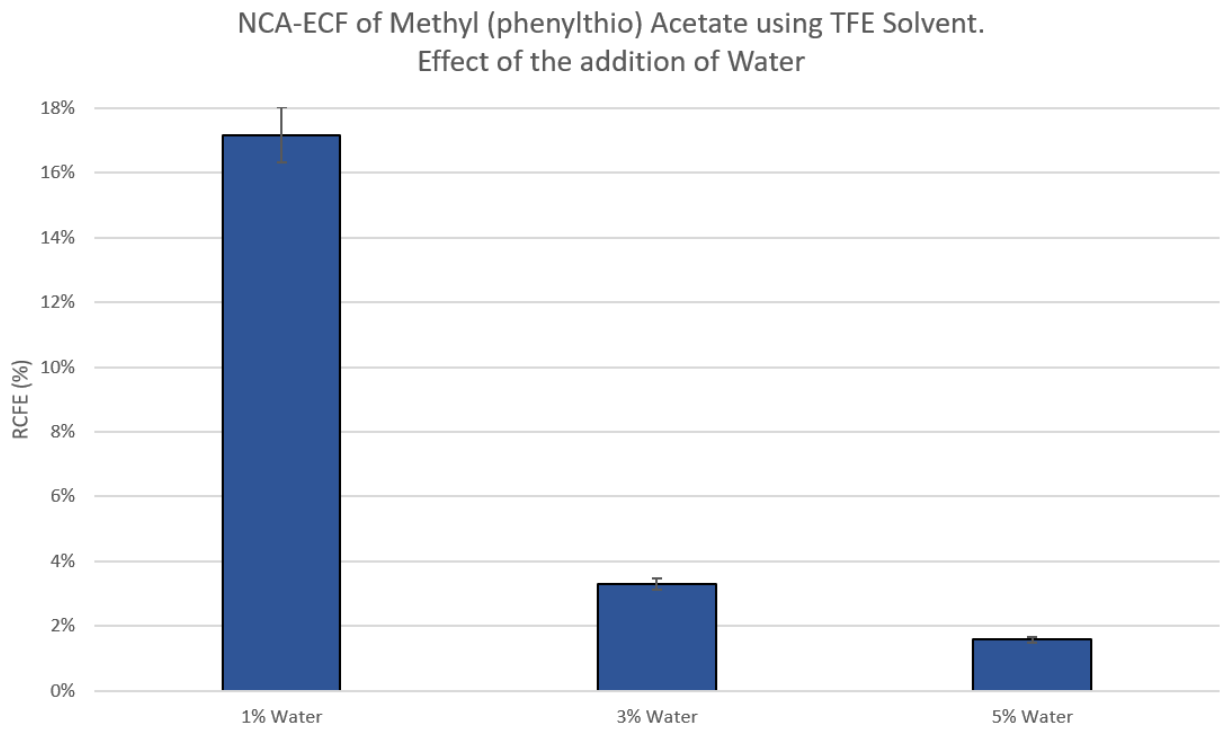

Figure 56: NCA-ECF of Methyl (phenylthio) Acetate using TFE Solvent. Effect of the addition of Water. Water reduced the RCFE but did not stop the fluorination process.

4.2.4 Optimization Parameter: Solvents

Different solvents can affect fluorination yield since they can form different solvation shells leading to varying orientations and stabilizations of the precursor during oxidation. In return, these solvents can result in different oxidation percentage of the product on varying sites of the precursor. Most importantly, the solvent can stabilize or destabilize the radical cation intermediate. Solvents with low polarizability work well in ECF because they tend to not destabilize these intermediates. The different solvation can also shield or make available the positively charged site available for fluoride attachments since, the solvent can facilitate or block cation intermediate

stability and fluorination. Additionally, the solvent may also affect the reactivity of fluoride depending on hydrogen bonding.

We investigated different solvents for NCA-ECF of Methyl (phenylthio) Acetate reaction (Figure 57). MeCN is commonly used for ECF but is not favorable when lowering fluoride concentration from the results with $Et_4NF*4HF$ (chapter 3). DME is also a favorable solvent since it was reported to solvate cationic counter ions which can increase the availability of fluoride. DME can also facilitate anode passivation, overoxidation and stabilizing the radical cationic intermediates [119]. HFIP is similar to TFE with favorable propertied listed as summarized in section 4.0. No RCC or RCP peaks were observed for DME under NCA conditions. MeCN had a low RCFE of 0.5% under NCA conditions which agreed to our past findings in chapter 3. HFIP under NCA conditions had similar RCC as TFE but less RCP due to a substantial radio side product formation. Trichloroethanol was also investigated as a solvent due to its similarity to TFE which resulted in a significant RCC due to producing a radio side product but did not produce product. MeCN was also used with several different electrolytes, acids and bases as additives (Figure 52). These will be explained in more detail in the next section.

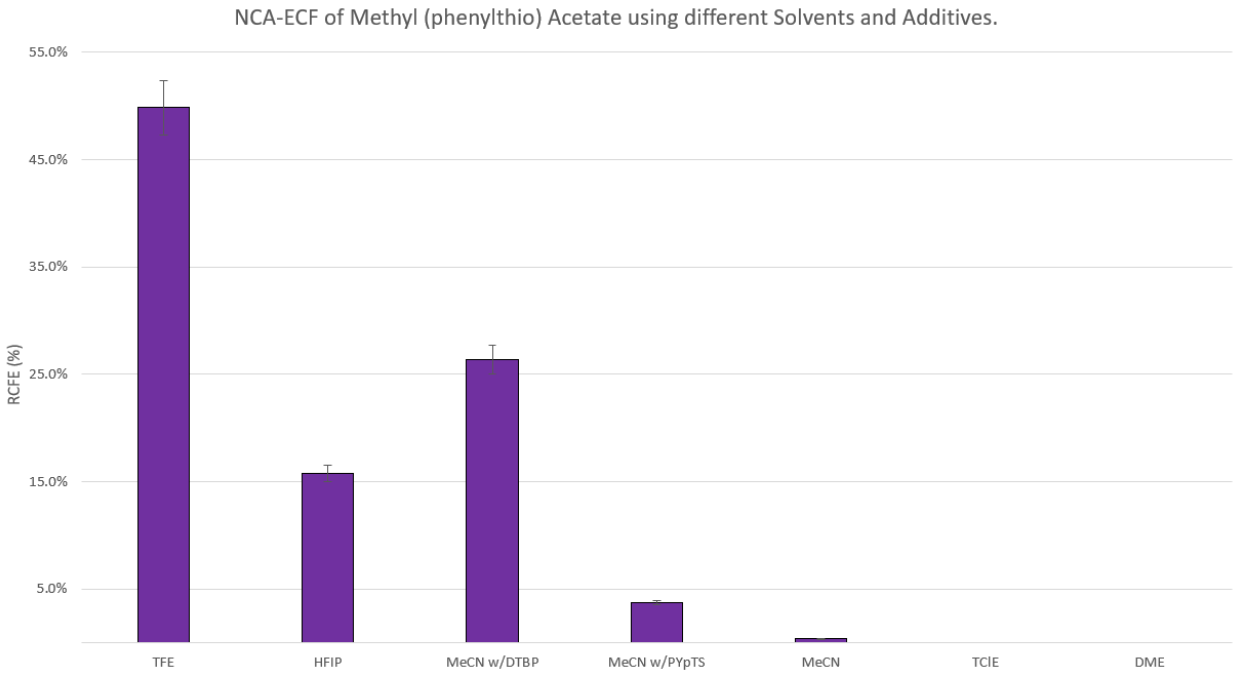

Figure 57: NCA-ECF of Methyl (phenylthio) Acetate using different Solvents and Additives. TFE was still optimal condition. MeCN with added DTBP base also performed well.

4.2.5 Optimization Parameter: Acids

Triflate and tosylate are common leaving groups used in radiochemistry substitutions reaction with [^{18}F]Fluoride. Triflate has been shown to increase the product yield in ECF under carrier addition conditions [120]. Thus, we tested triflate and tosylate bases to serve as auxiliary molecules in the FP mechanism by using Triflic (TA) and pToluenesulphonic acids (pTSA). These acids in MeCN had 0% RCFE. Using TFE without TBAP electrolyte had RCFE of >1% when using TA or pTSA. The addition of 50 mM TBAP in TFE resulted in the reduction of acids which raised the RCFE compared to without TBAP but was still lower when compared to using TFE without acid by ~50% (Figure 58). Both of these acids hinder NCA-ECF in MeCN and in TFE, which is similar to the unwanted acidity effects in the carrier added experiments.

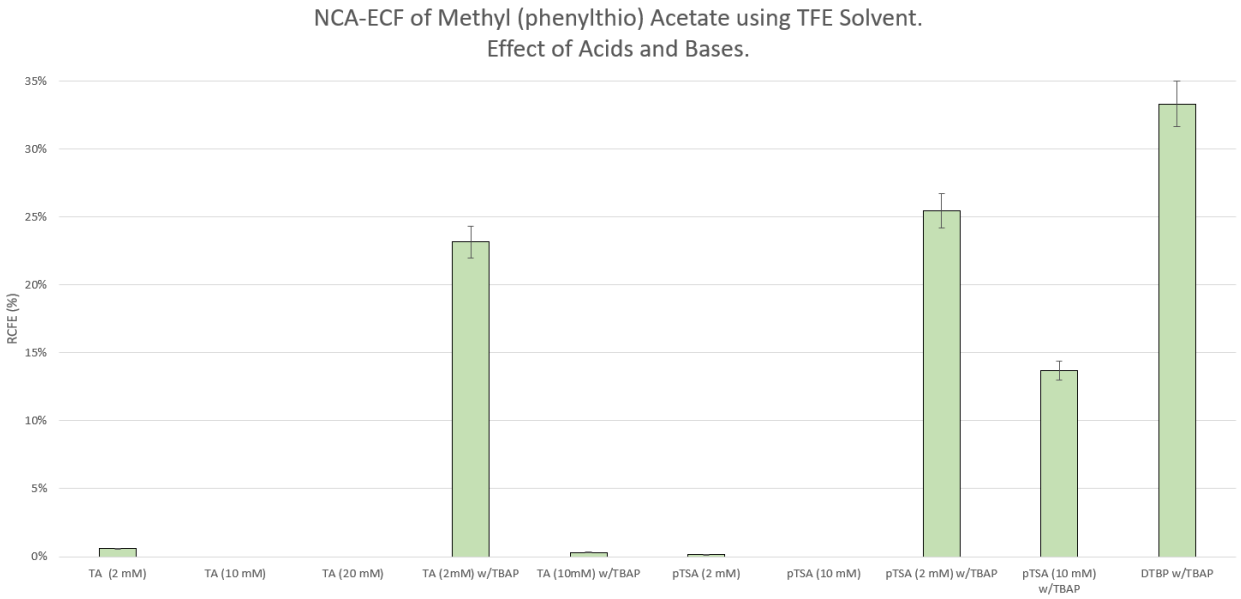

Figure 58*:* NCA-ECF of Methyl (phenylthio) Acetate using TFE Solvent. Effect of Acids and Bases. Acids greatly reduced results in TFE (at 70 °C). The Base slightly increased yields in TFE (at 25 °C).

4.2.6 Optimization Parameter: Electrolytes

Pyridinium pToluenesulfonate (PpTS) and tetrabutylammonium trifluoromethanesulfonate (TBATF) were used as electrolyte in MeCN. No product was observed when using TBATF. PpTS increased the RCY in MeCN from 0.5% with TBAP up to 5.1% with PpTS. These solvents were also tested in TFE where TBAP had better performance than PpTS and TBATF (Figure 59). Both PpTS and TBATF reduced RCFE in TFE compared to using TBAP as an electrolyte. The increase in RCFE of PpTS in MeCN suggest a beneficial use of this electrolyte in MeCN even though it was lowered RCFE in TFE. One explanation is that the pyridinium, or formed pyridine through electrolysis, acts similarly as the conjugate base of TFE.

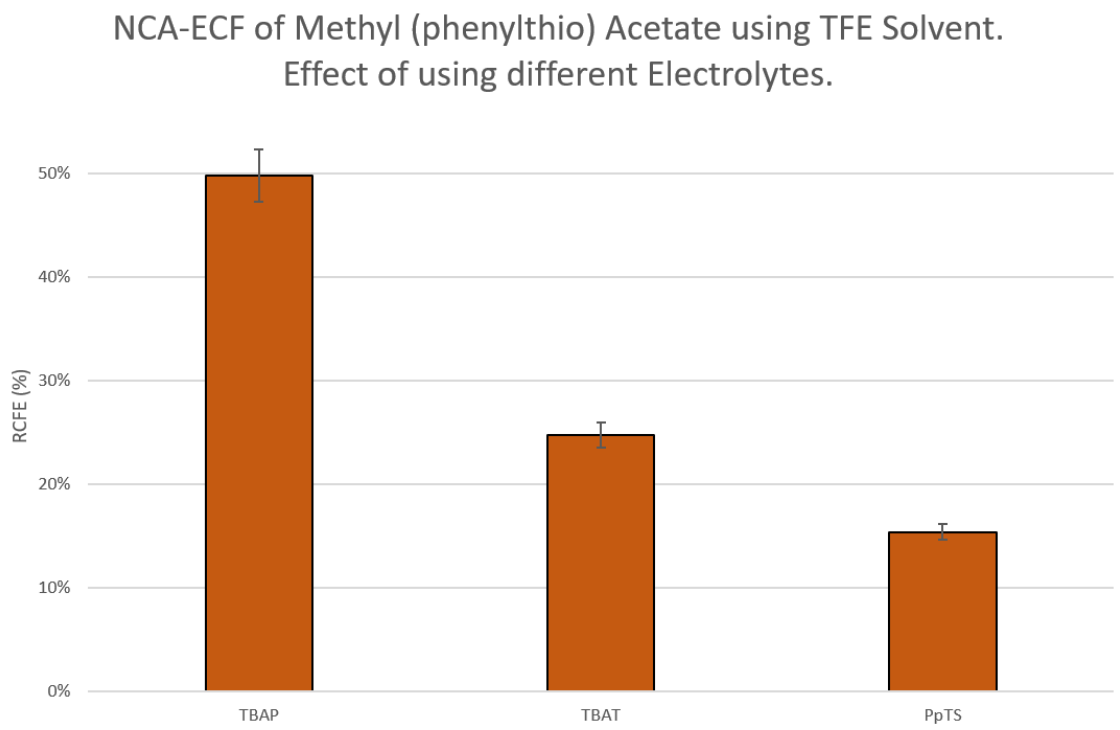

Figure 59: NCA-ECF of Methyl (phenylthio) Acetate using TFE Solvent. Effect of using different Electrolytes. TBAP performed the best in TFE.

4.2.7 Optimization Parameter: Base

We encountered an unexpected result through the addition of a non-nucleophilic base in MeCN, which increased the RCFE in MeCN. In these studies, 50 mM of 2,6-Ditertbutylpyridine (DTBP) was tested in MeCN at 25 °C. However, when increasing the temperature at 70 °C, this resulted in a precipitate forming and a low RCFE. Thus, experiments with DTBP were performed at 25 °C instead. Here DTBP increased the NCA-ECF from 0.5% up to 26.4±1.4% (n=2), which is comparable to using TFE at 25 °C which produced 19.4±2.2% (n=2). The combination of TFE and 50 (mM) DTBP at 25 °C had an RCFE of 33.3±0.9% (n=2) (Figure 58). This higher result in comparison to TFE without DTBP at 25 °C, suggested that TFE is be advantageous to be used as a conjugate base of the solvent to increase hydrogen abstraction.

4.2.8 Data Summary Methyl (phenylthio) Acetate (1.5ml Cell)

Optmization of Methyl (phenylthio) Acetate (PTA) in the 1.5ml Electrochemical Cell												
#	Precursor (mM)	Electrolyte (mM)	Other Additive (mM)	Solvent	Temperature (°C)	Oxidation Voltage	Duration (min)	Starting Activity (mCi)	Volume (ml)	RCC (%)	RCP (%)	RCFE (%)
Best 3	PTA (50 mM)	TBAP (50mM)	-	TFE	70	1.90	30	13.9±17.5	1.5	59.3±1.0%	84.1±2.1%	49.8±0.5%
1	PTA (50 mM)	TBAP (50mM)	-	TFE	70	1.90	10	3.60	1.5	39.7%	94.0%	37.3%
2	PTA (50 mM)	TBAP (50mM)	-	TFE	70	1.90	10	2.07	1.5	29.3%	86.9%	25.5%
3	PTA (50 mM)	TBAP (50mM)	-	TFE	70	1.90	30	1.74	1.5	58.0%	86.8%	50.3%
4	PTA (50 mM)	TBAP (50mM)	-	TFE	70	1.90	30	44.10	1.5	60.3%	81.6%	49.2%
5	PTA (50 mM)	TBAP (50mM)	-	TFE	70	1.90	30	38.70	1.5	59.6%	83.8%	49.9%
6	PTA (50 mM)	TBAP (50mM)	-	TFE	70	1.90	60	0.81	1.5	58.9%	29.8%	17.6%
7	PTA (50 mM)	TBAP (50mM)	-	TFE	70	1.90	60	0.51	1.5	56.1%	39.5%	22.2%
8	PTA (50 mM)	TBAP (50mM)	-	TFE	25	1.90	30	0.61	1.5	23.7%	91.3%	21.6%
9	PTA (50 mM)	TBAP (50mM)	-	TFE	25	1.90	30	0.36	1.5	18.6%	92.6%	17.2%
10	PTA (150 mM)	TBAP (100 mM)	-	TFE	70	3.50	30	2.97	1.5	64.9%	77.4%	50.2%
11	PTA (150 mM)	TBAP (100 mM)	-	TFE	70	3.50	30	2.31	1.5	67.1%	79.3%	53.2%
12	PTA (300 mM)	TBAP (100 mM)	-	TFE	70	3.50	30	1.68	1.5	73.5%	72.7%	53.4%
13	PTA (300 mM)	TBAP (100 mM)	-	TFE	70	3.50	30	1.33	1.5	76.7%	75.9%	58.2%
Water Tolerance												
#	Precursor (mM)	Electrolyte (mM)	Other Additive (mM)	Solvent	Temperature (°C)	Oxidation Voltage	Duration (min)	Starting Activity (mCi)	Volume (ml)	RCC (%)	RCP (%)	RCFE (%)
1	PTA (50 mM)	TBAP (50mM)	1% H2O	TFE	70	1.90	30	1.25	1.5	27.2%	68.1%	18.5%
2	PTA (50 mM)	TBAP (50mM)	1% H2O	TFE	70	1.90	30	0.38	1.5	21.5%	73.5%	15.8%
3	PTA (50 mM)	TBAP (50mM)	3% H2O	TFE	70	1.90	30	0.81	1.5	5.5%	62.3%	3.4%
4	PTA (50 mM)	TBAP (50mM)	3% H2O	TFE	70	1.90	30	1.13	1.5	4.9%	64.9%	3.2%
5	PTA (50 mM)	TBAP (50mM)	5% H2O	TFE	70	1.90	30	0.29	1.5	6.2%	26.3%	1.6%
6	PTA (50 mM)	TBAP (50mM)	5% H2O	TFE	70	1.90	30	1.31	1.5	5.9%	25.9%	1.5%

NCA-ECF of Methyl (phenylthio) Acetate in different Solvents												
#	Precursor (mM)	Electrolyte (mM)	Other Additive (mM)	Solvent	Temperature (°C)	Oxidation Voltage	Duration (min)	Starting Activity (mCi)	Volume (ml)	RCC (%)	RCP (%)	RCFE (%)
1	PTA (50 mM)	TBAP (50mM)	-	MeCN	70	1.90	30	0.29	1.5	19.7%	2.3%	0.5%
2	PTA (50 mM)	TBAP (50mM)	-	MeCN	70	1.90	30	0.21	1.5	18.1%	2.1%	0.4%
3	PTA (50 mM)	TBAP (50mM)	-	HFIP	50	1.90	30	1.28	1.5	62.5%	27.5%	17.2%
4	PTA (50 mM)	TBAP (50mM)	-	HFIP	50	1.90	30	0.98	1.5	53.7%	26.8%	14.4%
5	PTA (50 mM)	TBAP (50mM)	-	TCIE	70	1.90	30	0.17	1.5	16.7%	0.0%	0.0%
6	PTA (50 mM)	TBAP (50mM)	-	TCIE	70	1.90	30	0.37	1.5	16.3%	0.0%	0.0%
7	PTA (50 mM)	TBAP (200mM)	-	TCIE	95	3.00	30	0.29	1.5	21.8%	0.0%	0.0%
8	PTA (50 mM)	TBAP (200mM)	-	TCIE	95	3.00	30	0.13	1.5	20.5%	0.0%	0.0%
9	PTA (50 mM)	TBAP (50mM)	-	5% TCIE 95% MeCN	70	1.90	30	0.35	1.5	3.4%	0.0%	0.0%
10	PTA (50 mM)	TBAP (50mM)	-	5% TCIE 95% MeCN	70	1.90	30	0.29	1.5	2.9%	0.0%	0.0%
11	PTA (50 mM)	TBAP (50mM)	-	DME	70	1.90	30	0.15	1.5	0.0%	0.0%	0.0%
12	PTA (50 mM)	TBAP (50mM)	-	DME	70	1.90	30	0.14	1.5	0.0%	0.0%	0.0%
13	PTA (50 mM)	TBAP (200mM)	-	DME	70	3.00	30	0.38	1.5	0.0%	0.0%	0.0%
14	PTA (50 mM)	TBAP (200mM)	-	DME	70	3.00	30	0.27	1.5	0.0%	0.0%	0.0%

NCA-ECF of Methyl (phenylthio) Acetate (PTA) with the Addition of Base						
#	Other Additive (mM)	Solvent	Starting Activity (mCi)	RCC (%)	RCP (%)	RCFE (%)
1	2,6 Ditertbutylpyridine (50 mM)	TFE	1.73	40.1%	80.8%	32.4%
2	2,6 Ditertbutylpyridine (50 mM)	TFE	1.29	43.7%	78.4%	34.3%
3	2,6 Ditertbutylpyridine (50 mM)	MeCN	2.47	25.5%	62.8%	16.0%
4	2,6 Ditertbutylpyridine (50 mM)	MeCN	1.88	28.7%	41.9%	12.0%
5	2,6 Ditertbutylpyridine (50 mM)	MeCN	1.52	45.1%	61.6%	27.8%
6	2,6 Ditertbutylpyridine (50 mM)	MeCN	0.94	42.9%	58.3%	25.0%

All experiments used 50 mM of precursor and TBAP at 25C with oxidation voltage of 1.9V with electrolysis for 30 mins in the 1.5 ml electrochemical cell

Figure 60: Data Summary of NCA-ECF of Methyl (phenylthio) Acetate in the single chamber electrochemical cell (1.5ml)

NCA-ECF of Methyl (phenylthio) Acetate (PTA) with the addition of Acids and Salts							
#	Electrolyte (mM)	Other Additive (mM)	Solvent	Starting Activity (mCi)	RCC (%)	RCP (%)	RCFE (%)
1	-	Triflic acid (2 mM)	TFE	0.84	5.1%	18.3%	0.9%
2	-	Triflic acid (2 mM)	TFE	0.77	1.2%	21.9%	0.3%
3	-	Triflic acid (10 mM)	TFE	0.63	0.0%	0.0%	0.0%
4	-	Triflic acid (10 mM)	TFE	0.54	0.0%	0.0%	0.0%
5	-	Triflic acid (20 mM)	TFE	0.60	0.0%	0.0%	0.0%
6	-	Triflic acid (20 mM)	TFE	0.42	0.0%	0.0%	0.0%
7	TBAP (50 mM)	Triflic acid (2mM)	TFE	0.36	28.6%	88.3%	25.3%
8	TBAP (50 mM)	Triflic acid (2mM)	TFE	0.49	26.3%	80.1%	21.1%
9	TBAP (50 mM)	Triflic acid (10mM)	TFE	0.28	2.4%	12.7%	0.3%
10	TBAP (50 mM)	Triflic acid (10mM)	TFE	0.37	2.3%	14.2%	0.3%
11	-	Triflic acid (50 mM)	MeCN	1.36	0.0%	0.0%	0.0%
12	-	pToluene Sulfonic acid (2 mM)	TFE	0.27	1.9%	9.6%	0.2%
13	-	pToluene Sulfonic acid (2 mM)	TFE	0.24	1.7%	10.3%	0.2%
14	-	pToluene Sulfonic acid (10 mM)	TFE	0.36	0.0%	0.0%	0.0%
15	-	pToluene Sulfonic acid (10 mM)	TFE	0.29	0.0%	0.0%	0.0%
16	TBAP (50 mM)	pToluene Sulfonic acid (2 mM)	TFE	0.59	35.4%	72.8%	25.8%
17	TBAP (50 mM)	pToluene Sulfonic acid (2 mM)	TFE	0.47	36.2%	69.4%	25.1%
18	TBAP (50 mM)	pToluene Sulfonic acid (10 mM)	TFE	0.42	15.5%	83.2%	12.9%
19	TBAP (50 mM)	pToluene Sulfonic acid (10 mM)	TFE	0.33	16.4%	88.3%	14.5%
20	-	pToluene Sulfonic acid (50 mM)	MeCN	1.21	0.7%	0.0%	0.0%
21	Pyridinium pToluenesulfonate (50 mM)	-	TFE	2.76	23.7%	24.5%	5.8%
22	Pyridinium pToluenesulfonate (50 mM)	-	TFE	1.83	48.4%	21.9%	10.6%
23	Pyridinium pToluenesulfonate (50 mM)	-	TFE	1.22	71.9%	22.5%	16.2%
24	Pyridinium pToluenesulfonate (50 mM)	-	TFE	0.84	68.2%	21.4%	14.6%
25	Pyridinium pToluenesulfonate (25 mM)	-	MeCN	2.85	9.1%	36.8%	3.3%
26	Pyridinium pToluenesulfonate (50 mM)	-	MeCN	2.02	54.9%	4.9%	2.7%
27	Pyridinium pToluenesulfonate (50 mM)	-	MeCN	1.63	70.3%	7.3%	5.1%
28	TBA trifluoromethanesulfonate (50 mM)	-	TFE	2.84	32.7%	81.3%	26.6%
29	TBA trifluoromethanesulfonate (50 mM)	-	TFE	1.97	29.1%	78.6%	22.9%
30	TBA trifluoromethanesulfonate (50 mM)	-	MeCN	3.19	0.0%	0.0%	0.0%
31	TBA trifluoromethanesulfonate (50 mM)	-	MeCN	2.26	0.0%	0.0%	0.0%
All experiments used 50 mM Precursor, at 70C and 1.9V oxidation potential with 30 mins electrolysis in 1.5 ml electrochemical cell							

Figure 60: Data Summary of NCA-ECF of Methyl (phenylthio) Acetate in the single chamber electrochemical cell (1.5ml)

4.3 NCA ^{18}F ECF Methyl (phenylthio) Acetate Using Two Chamber Cell

NCA-ECF was used in the two-chamber electrochemical cell. The separation of reduction was hypothesized to increase RCFE. One major concern in this set-up was to minimize the amount of acid formation in the anodic chamber which hinders fluorination. Here, several different solvents were used along with both Anion Exchange (AEM) and Cation Exchange Membranes (CEM). Triethylamine (TEA) was used in the cathodic chamber (CC) while DTBP was used in both CC and anodic chambers (AC). The results are summarized in Figure 61. Using only MeCN or TFE with the CEM led to a high acidic environment in the first 2 minutes of pH 2-3, which resulted in a low RCFE. Using TEA in the CC increased results using CEM in TFE, whereas using AEM results improved over using CEM in the two-chamber cell. Anions are known to move faster

through the membranes which can more rapidly counter changes in pH to minimize acidity in the anodic chamber. The buildup of acidity was much slower using the AEM than CEM. Combining AEM and DTPB in the AC further increased results, where the two-chamber using the NCA-ECF resulted in an RCFE of 13.3±0.4% which was less than that was reported when using a single chamber electrochemical cell. We reasoned this outcome was a likely result of anodic acidity and the rapid lowering of pH in the first few minutes of electrolysis. Additionally, there is no flux of anions from the cathode to reduce acidity like there is in the single chamber electrochemical cell due to the membrane separation.

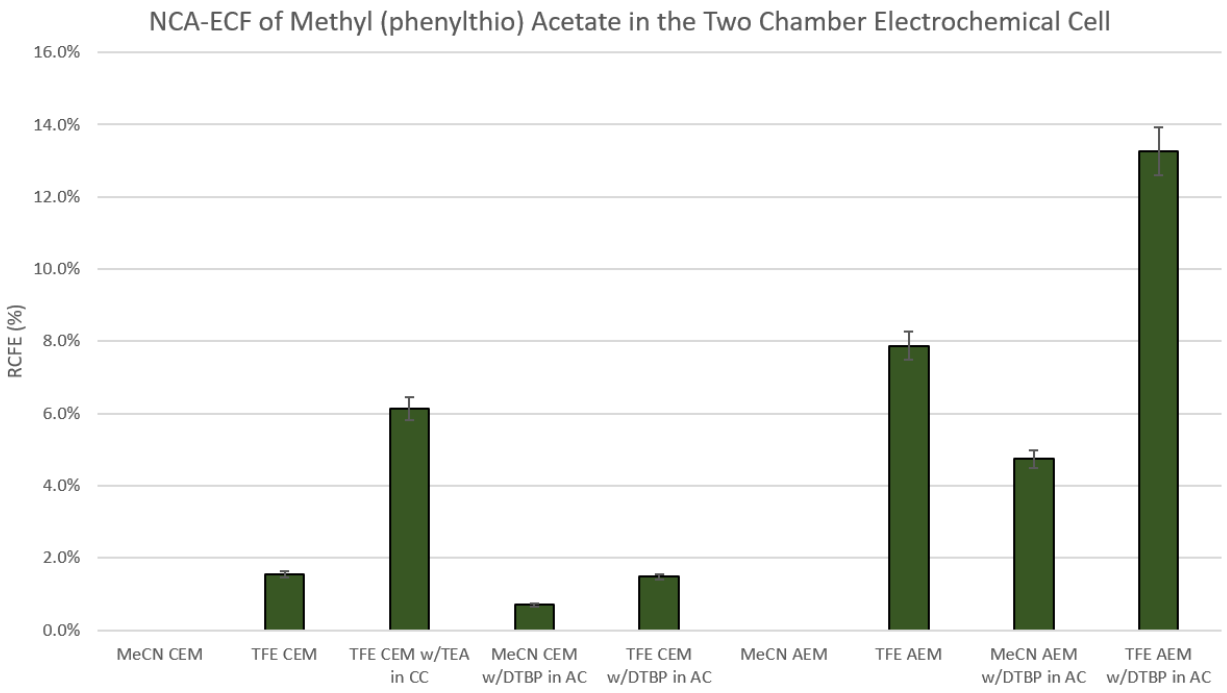

Figure 61: NCA-ECF of Methyl (phenylthio) Acetate using the Two Chamber Electrochemical Cell. Using the anion exchange membrane (AEM) with base (DTBP) in the anodic chamber (AC) had the highest RCFE.

4.3.1 Data Summary Methyl (phenylthio) Acetate in Two Chamber Cell

NCA-ECF in Two Chamber Cell with Methyl (phenylthio) Acetate									
#	AC Additive (mM)	AC Solvent	Membrane	CC Solvent	CC Additive (mM)	Starting Activity (mCi)	RCC (%)	RCP(%)	RCFE (%)
Best 3	Ditertbutylpyridine 50 mM	TFE	Anion	TFE	-	17.8±1.5	16.5±0.5%	80.5±1.8%	13.3±0.4%
1	-	MeCN	Cation	MeCN	-	17.3	0.0%	0.0%	0.0%
2	-	MeCN	Cation	MeCN	-	15.8	0.0%	0.0%	0.0%
3	-	TFE	Cation	TFE	-	20.2	2.3%	72.8%	1.7%
4	-	TFE	Cation	TFE	-	15.6	1.9%	74.4%	1.4%
5	-	TFE	Cation	TFE	Triethylamine 100 mM	23.6	8.4%	79.1%	6.6%
6	-	TFE	Cation	TFE	Triethylamine 100 mM	18.8	7.3%	77.2%	5.6%
7	Ditertbutylpyridine 50 mM	MeCN	Cation	MeCN	-	19.4	1.8%	43.8%	0.8%
8	Ditertbutylpyridine 50 mM	MeCN	Cation	MeCN	-	15.1	1.6%	38.5%	0.6%
9	Ditertbutylpyridine 50 mM	TFE	Cation	TFE	-	26.9	2.3%	62.9%	1.4%
10	Ditertbutylpyridine 50 mM	TFE	Cation	TFE	-	21.2	2.6%	58.1%	1.5%
11	-	MeCN	Anion	MeCN	-	19.7	0.0%	0.0%	0.0%
12	-	MeCN	Anion	MeCN	-	16.5	0.0%	0.0%	0.0%
13	-	TFE	Anion	TFE	-	18.1	9.9%	82.8%	8.2%
14	-	TFE	Anion	TFE	-	14.7	9.4%	80.3%	7.5%
15	Ditertbutylpyridine 50 mM	MeCN	Anion	MeCN	-	20.8	6.2%	72.0%	4.5%
16	Ditertbutylpyridine 50 mM	MeCN	Anion	MeCN	-	16.2	6.5%	77.1%	5.0%
17	Ditertbutylpyridine 50 mM	TFE	Anion	TFE	-	17.1	15.9%	82.6%	13.1%
18	Ditertbutylpyridine 50 mM	TFE	Anion	TFE	-	19.9	17.1%	80.7%	13.8%
19	Ditertbutylpyridine 50 mM	TFE	Anion	TFE	-	16.5	16.4%	78.3%	12.8%

All experiments used 12 ml solution each chamber, 50 mM Precursor and TBAP, 1.9V oxidation potential, room temperature, stirring 600 RPM and electrolysis 60 mins

Figure 62: Data Summary of NCA-ECF of Methyl (phenylthio) Acetate in the Two Chamber Electrochemical Cell.

4.4 HPLC, 19F-NMR, TLC and A_m of NCA-ECF using Methyl (phenylthio) Acetate

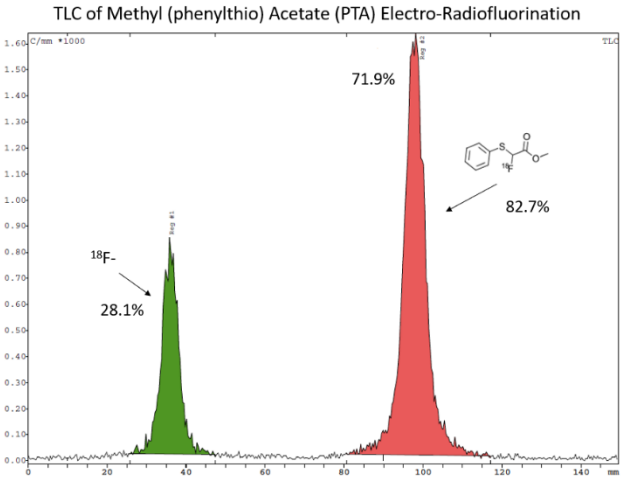

Figure 63: TLC after NCA-ECF of Methyl (phenylthio) Acetate.

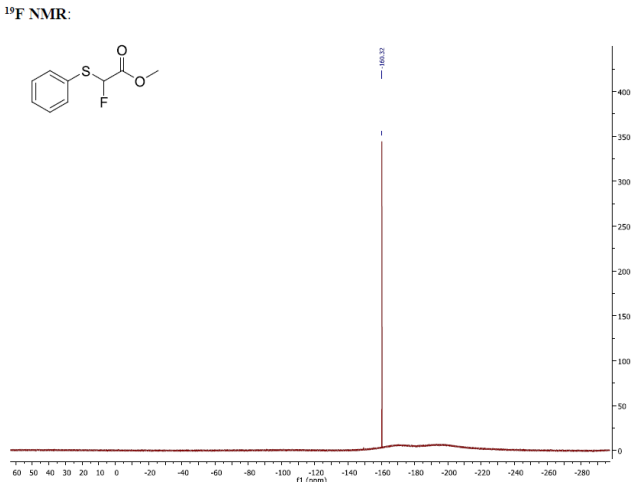

Figure 64: 19F-NMR after CA-ECF of Methyl (phenylthio) Acetate.

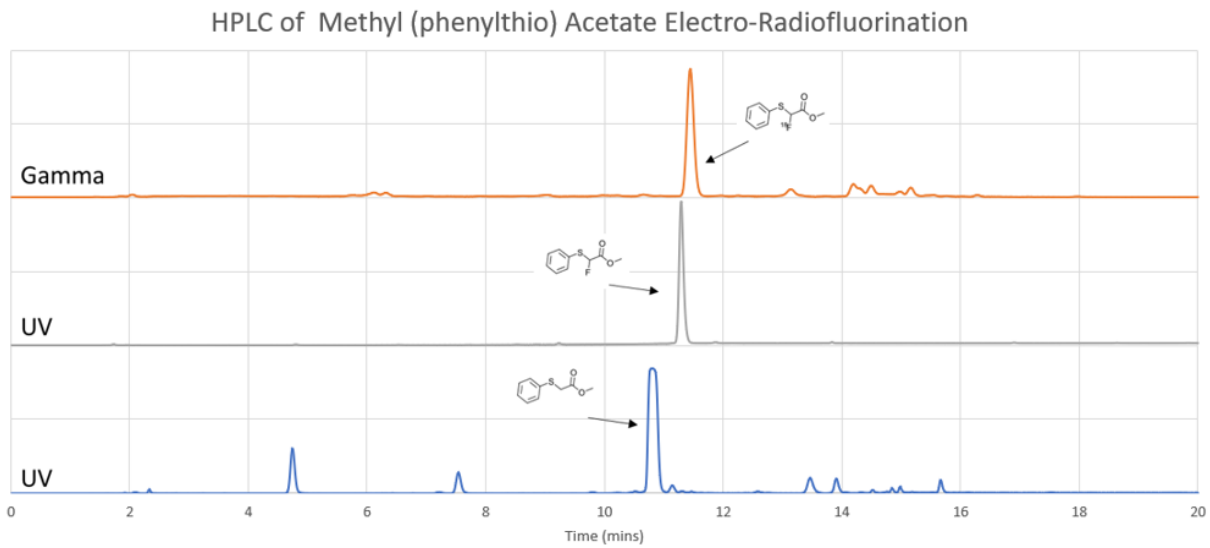

Figure 65: HPLC after NCA-ECF of Methyl (phenylthio) Acetate. (Bottom) UV after electrolysis. (Middle) UV of isolated product with a carrier added synthesis. (Top) NCA-ECF Gamma signal of the product.

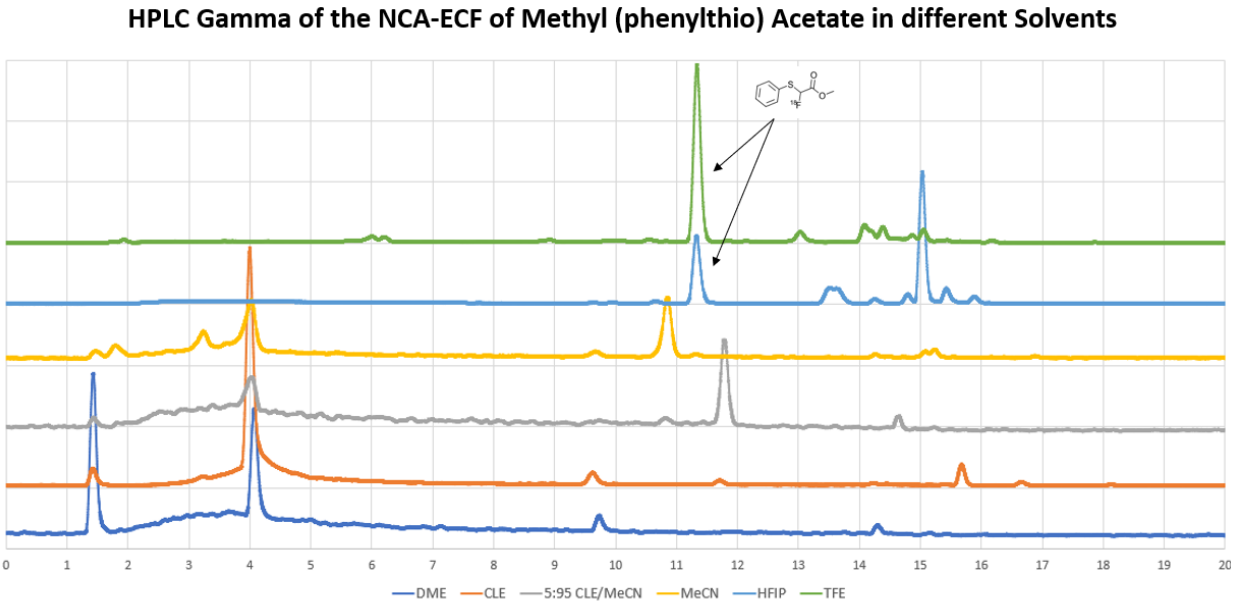

Figure 66: HPLC Gamma of the NCA-ECF of Methyl (phenylthio) Acetate in different Solvents. TFE performed the best followed by HFIP. There are many different radio side products using these solvents under NCA-ECF conditions. Additionally, some radio side products can be formed from a solvent mixture that are not firmed in either solvent alone.

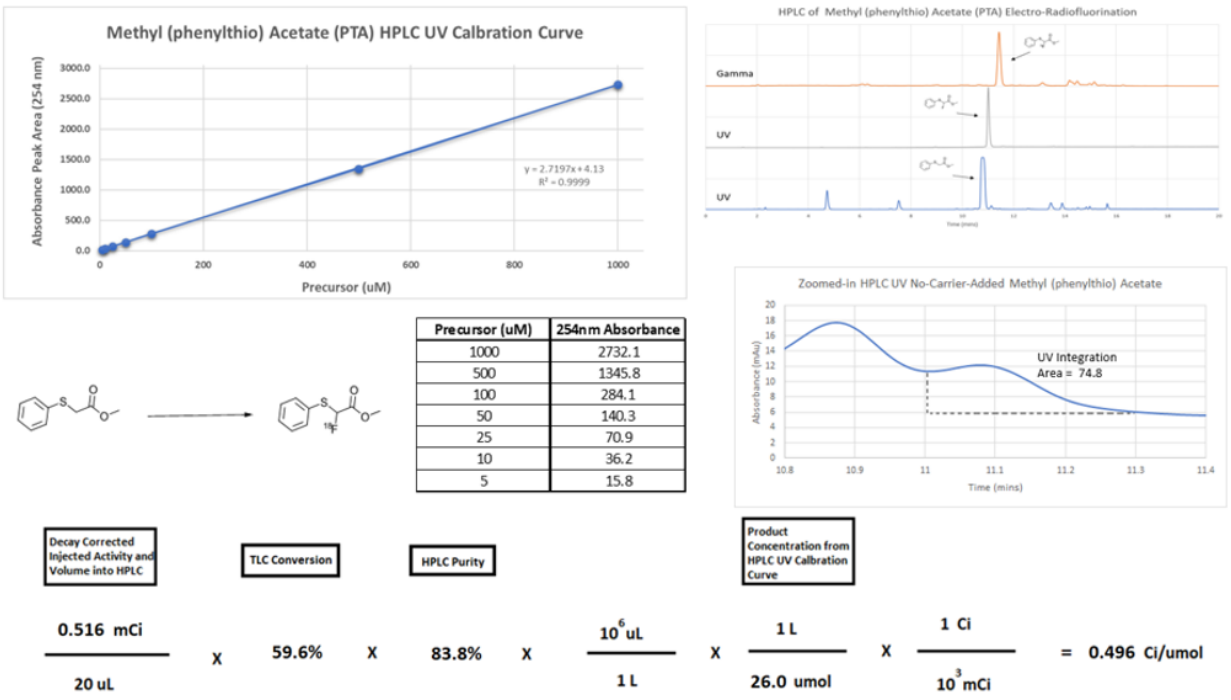

Figure 67: Molar Activity Calculation of Methyl (phenylthio) Acetate.

4.5 Radio Side Product Formation

Solvent effect had a large determination on radio side product formation. We proceeded to characterize and identify these side products formations that can occur during the fluorination in PET probe synthesis. The HPLC (Figure 66) of the NCA-ECF of Methyl (phenylthio) Acetate using different solvents shows several different species of side-product formation where the fluorinated product can be seen at 11.3 mins (see arrows). Using MeCN in the reaction led to a large radio side product about 1 min before the fluorinated product peak. This HPLC side product peak was not seen in the carrier added synthesis. Under NCA conditions ECF can produce different side products of radiolabeled organic molecules than under carrier added conditions. This can be problematic as there may not an easy solution to obtain mass for GC or NMR analysis to identify the fluorinated molecules. When performing reactions using a ratio of CLE and MeCN as solvent, a large radio side product occurs 0.5 mins after the main product. Using pure CLE as solvent, this

radio side product is produced in only trace amounts and in pure MeCN will eliminate this side product formation. An interesting finding is that the carrier added ECF ratios of different solvents mixtures can produce side products that neither solvent produce independently. Both TFE and HFIP solvents produced small radio side products in the 13-16 min range with HFIP solvent producing a large radio side product at 15 mins. This range is consistent with dimerization, molecules that contain 2 aromatic rings, a similar mass and lipophilicity elude from HPLC at this time range for the method used.

Several of these NCA fluorination side products may be interesting for further applications. However, further investigations are needed to determine their structure which is a challenging undertaking since adding a carrier to produce substantial mass may change the radio side products produced.

Chapter 5: No-Carrier-Added ^{18}F Electrochemical Fluorination of Thioethers

5.1 Introduction to Thioethers in Biology and Pharmacology

Sulfur containing molecules serve a variety of different important functions in biology. Two of the 21 amino acids contain sulfur which are methionine and cysteine. Many organosulfur molecules have a large number of metabolites which can have different biological activities [121]. Sulfur containing compounds continue to become more important in many different pharmaceutical applications [122]. Additionally, many of the bestselling drugs in the US are organosulfur compounds [123]. Therefore, developing a straightforward strategy to fluorinate sulfur containing molecules may lead to new innovative discoveries of applying PET probes in medicine and drug discovery.

5.2 NCA ^{18}F Electrochemical Fluorination of Thioethers

To provide scope of the NCA-ECF method for thioethers several different thioether compounds with different functional groups were used in NCA-ECF synthesis. The best condition with Methyl (phenylthio) Acetate was used and individual optimization for each thioether was not done. Based on previous results with Methyl (phenylthio) Acetate the optimal conditions to perform these experiments to be at 70 °C in TFE with 50 mM TBAP and an oxidation potential of 1.9V (Ag/Ag+) with electrolysis for 30 mins. Our findings are summarized in Figure 68-70 with a more detailed explanation of the conditioned performed with each thioether noted in subsections of 5.2.

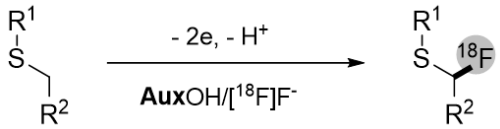

Figure 68: Scheme of using an Auxiliary in the FP mechanism for NCA-ECF of Thioethers.

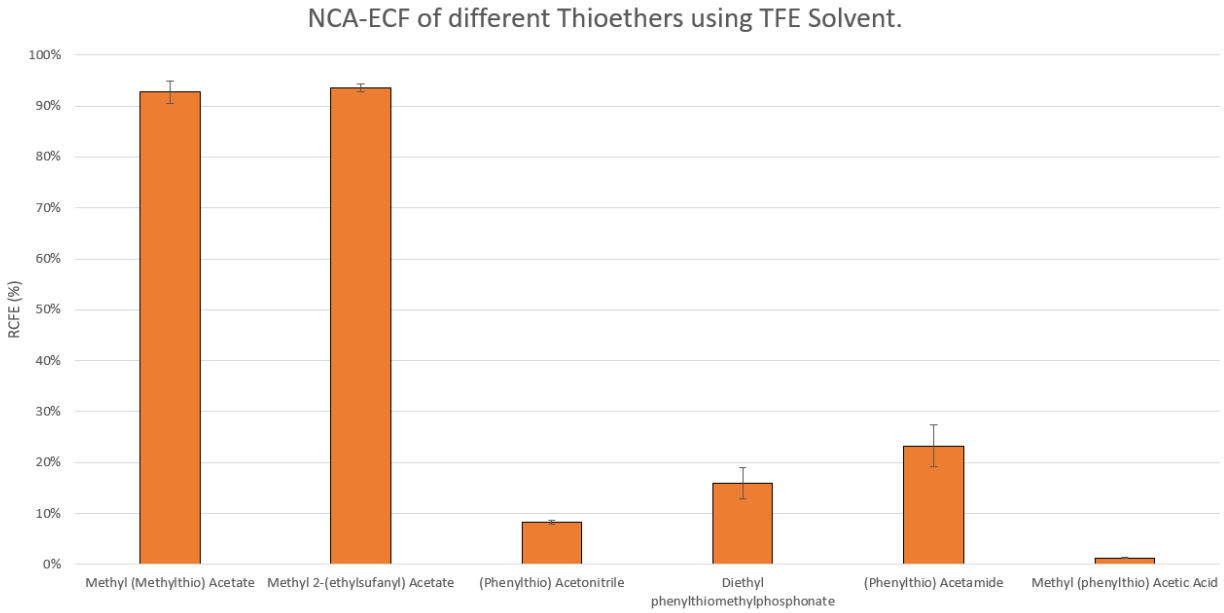

Figure 69: NCA-ECF using TFE with different Thioether Precursors.

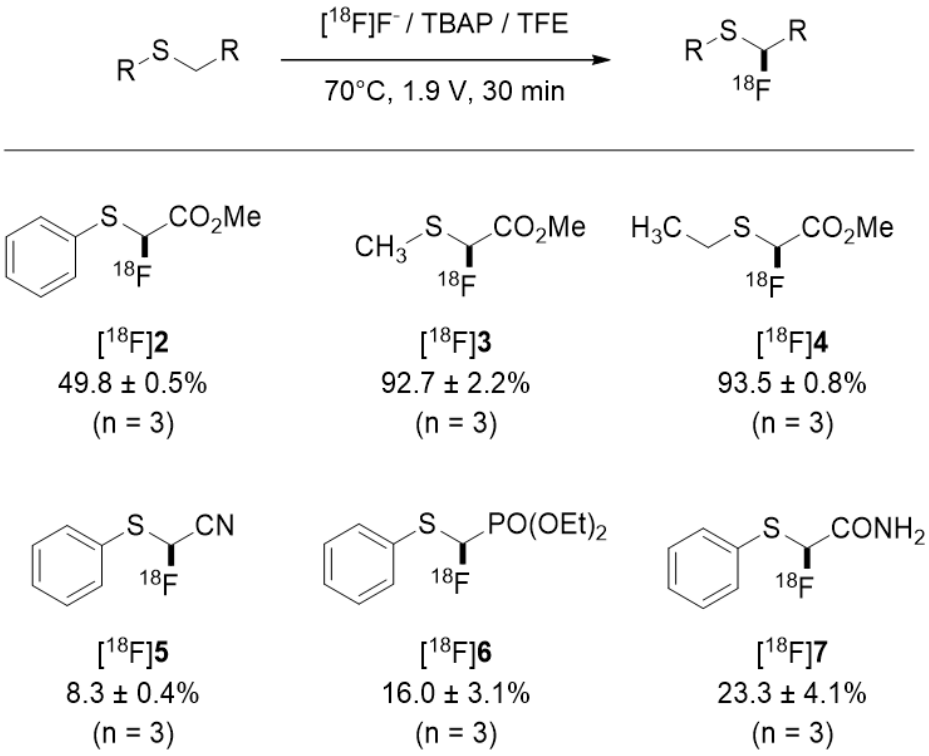

Figure 70: NCA-ECF using TFE with different Thioether Precursors with R groups.

5.2.1 Methyl (methylthiol) Acetate

NCA-ECF of Methyl (methylthiol) Acetate in TFE had an RCFE of 92.7±2.2% (n=3). A carrier added synthesis was performed with $Et_4NF*4HF$ for the product standard and verified by ^{19}F-NMR and used to verify the product formed under NCA conditions. The results can be seen in Figures 71-74. The product was isolated by HPLC separation and the molar activity (A_m) was 0.52±0.02 Ci/uM (n=2) (Figure 69).

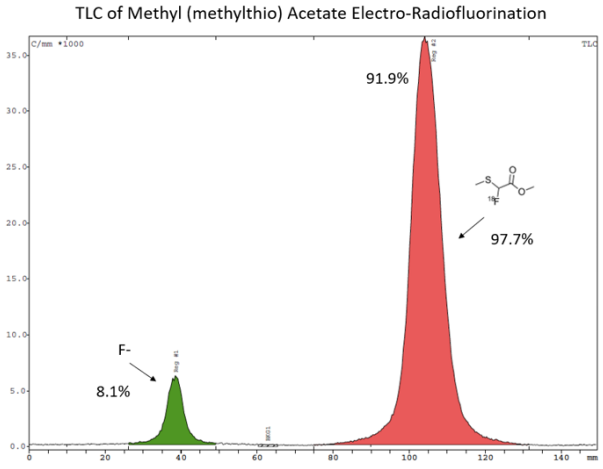

Figure 71: TLC after NCA-ECF of Methyl (methylthio) Acetate.

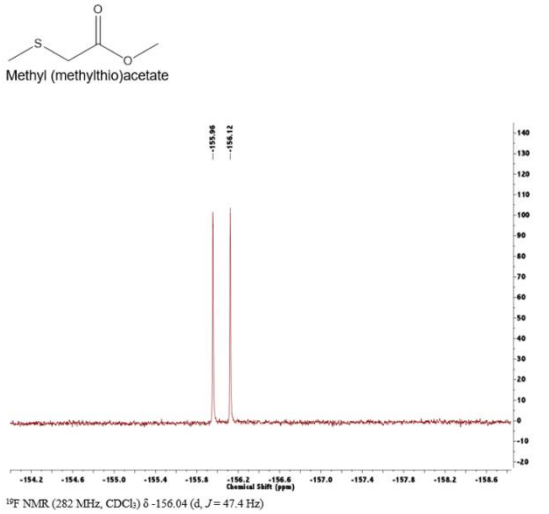

Figure 72: 19F-NMR of CA ECF of Methyl (methylthio) Acetate.

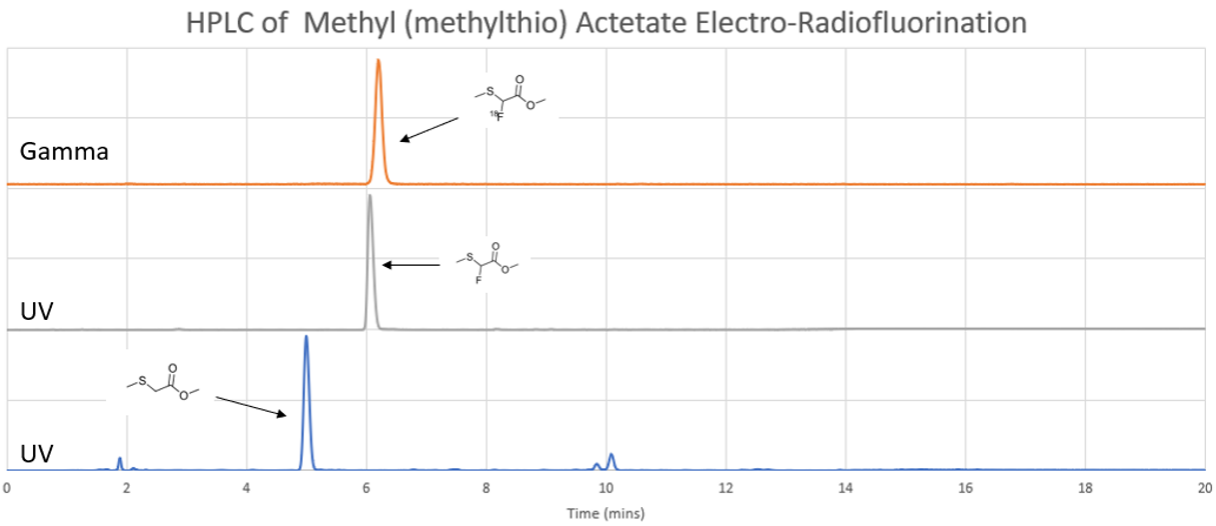

Figure 73*:* HPLC after NCA-ECF of Methyl (methylthio) Acetate. (Bottom) UV after electrolysis. (Middle) UV of isolated product with a carrier added synthesis. (Top) NCA-ECF Gamma signal of the product.

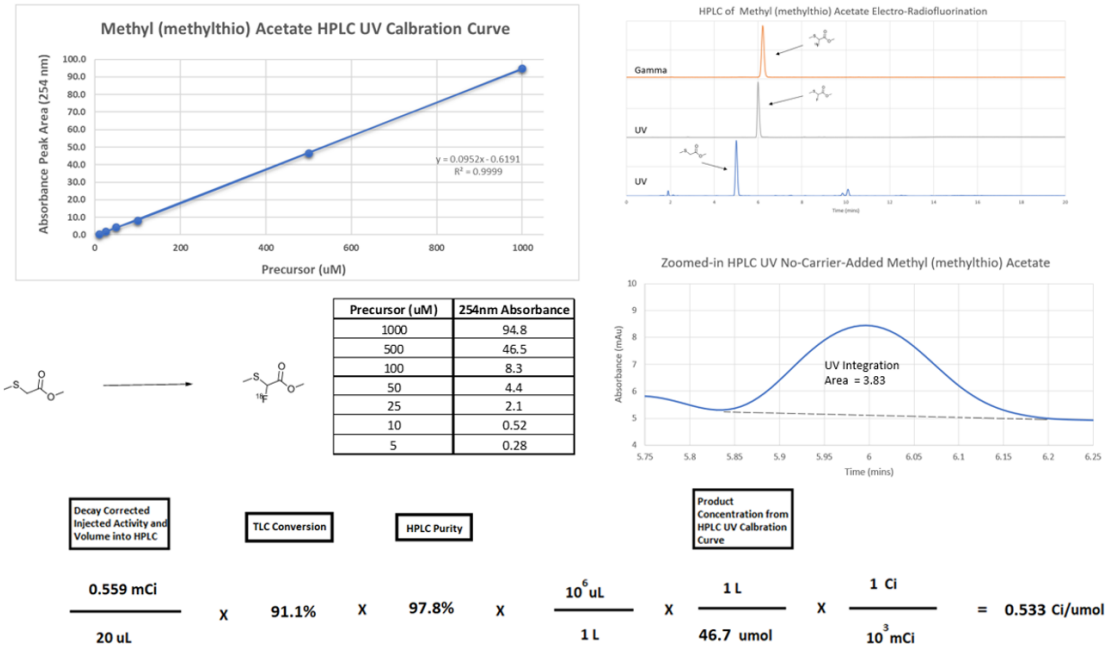

Figure 74: Molar Activity Calculation for Methyl (methylthio) Acetate

5.2.2 Methyl 2-(ethylsulfanyl) Acetate

NCA-ECF of Methyl 2-(ethylsulfanyl) Acetate in TFE had an RCFE of 93.5±0.8% (n=3). A carrier added synthesis was performed with $Et_4NF*4HF$ for the product standard and verified by ^{19}F-NMR and used to verify the product formed under NCA conditions. The results are summarized in Figures 75-77.

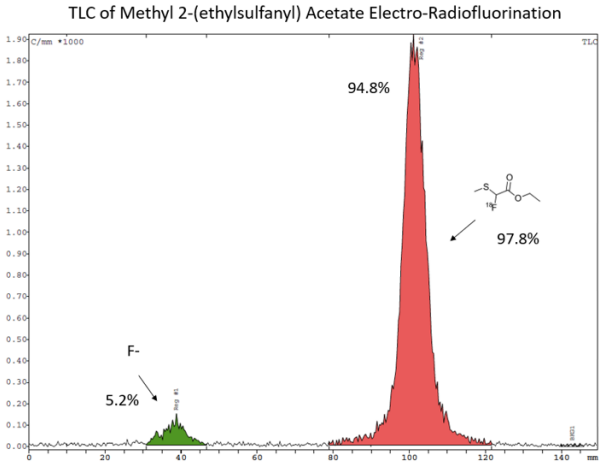

Figure 75: TLC after NCA-ECF of Methyl 2-(ethylsulfanyl) Acetate.

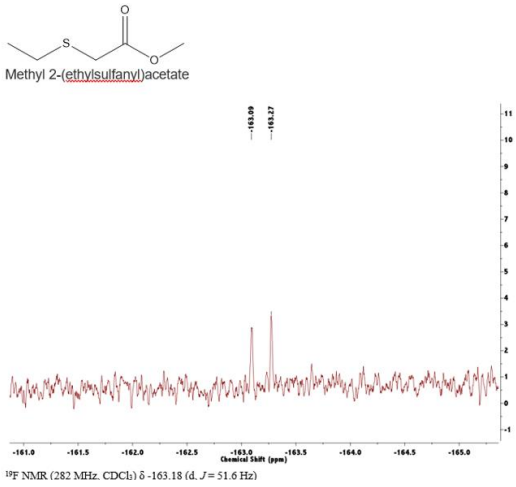

Figure 76: 19F-NMR of CA ECF of Methyl 2-(ethylsulfanyl) Acetate.

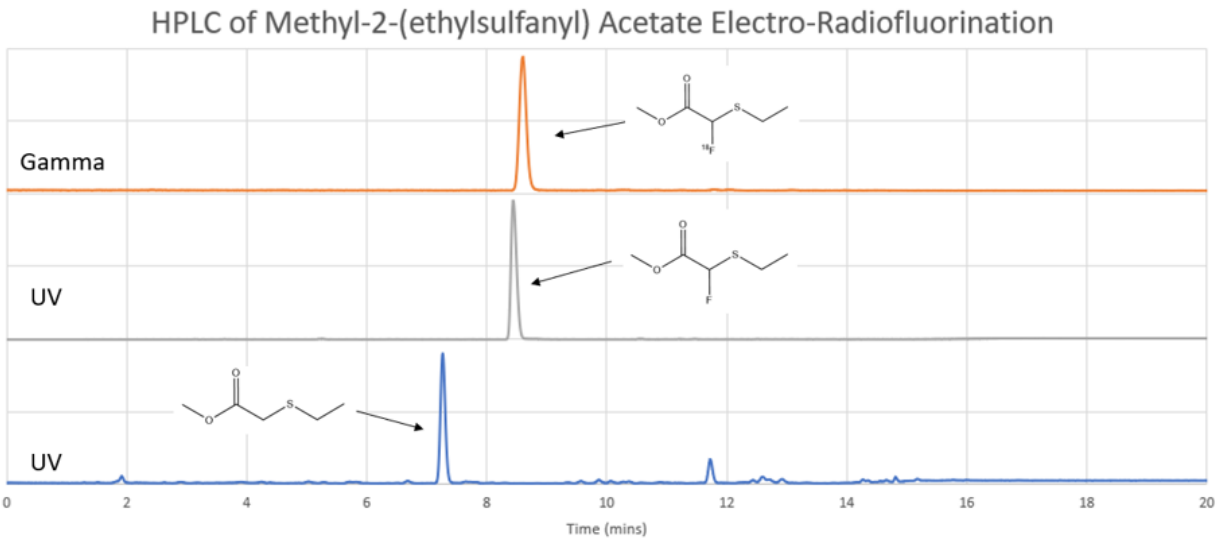

Figure 77: HPLC after NCA-ECF of Methyl 2-(ethylsulfanyl) Acetate. (Bottom) UV after electrolysis. (Middle) UV of isolated product with a carrier added synthesis. (Top) NCA-ECF Gamma signal of the product.

5.2.3 (Phenylthiol) Acetonitrile

NCA-ECF of (Phenylthiol) Acetonitrile in TFE had an RCFE of 8.3±0.4 (n=3). A carrier added synthesis was performed with Et4NF*4HF for the product standard and verified by ^{19}F-NMR and used to verify the product formed under NCA conditions. The results can be seen in Figures 78-80.

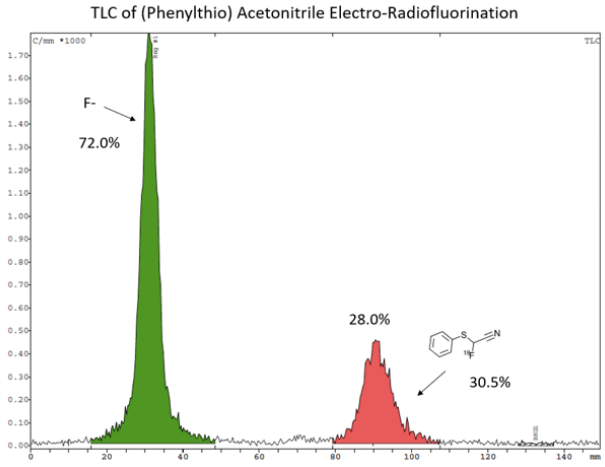

Figure 78: TLC after NCA-ECF of (Phenylthiol) Acetonitrile.

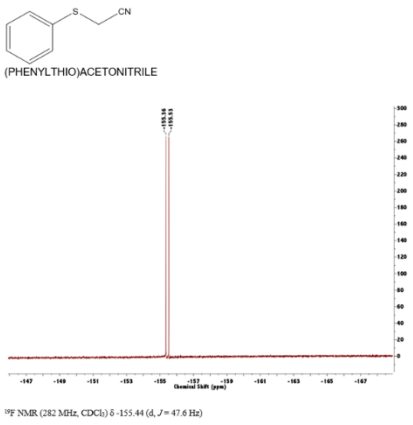

Figure 79: ^{19}F-NMR of CA ECF of (Phenylthiol) Acetonitrile.

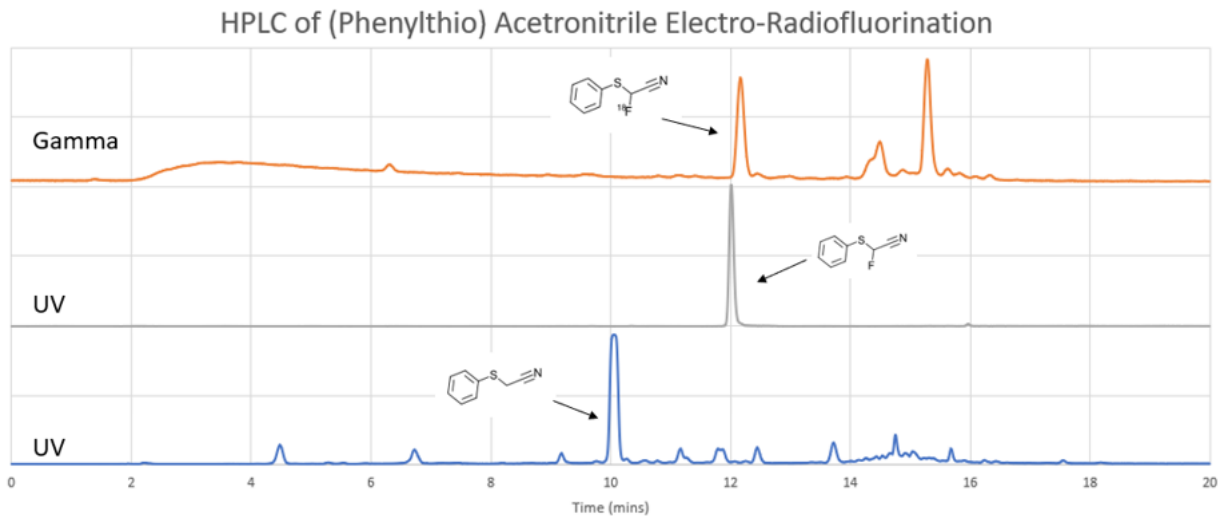

Figure 80: HPLC after NCA-ECF of (Phenylthiol) Acetonitrile. (Bottom) UV after electrolysis. (Middle) UV of isolated product with a carrier added synthesis. (Top) NCA-ECF Gamma signal of the product.

5.2.4 Diethyl phenylthiomethylphosphonate

NCA-ECF of Diethyl phenylthiomethylphosphonate in TFE had an RCFE of 16.0±3.1% (n=3). A carrier added synthesis was performed with $Et_4NF*4HF$ for the product standard and verified by ^{19}F-NMR and used to verify the product formed under NCA conditions. The results can be seen in Figures 81-83.

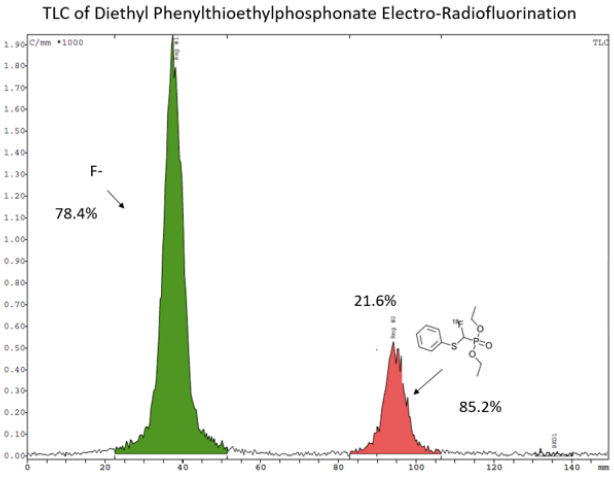

Figure 81*:* TLC after NCA-ECF of Diethyl phenylthiomethylphosphonate.

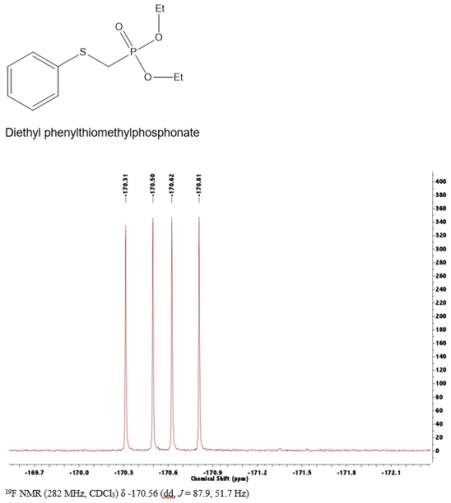

Figure 82: ^{19}F-NMR of CA ECF of Diethyl phenylthiomethylphosphonate.

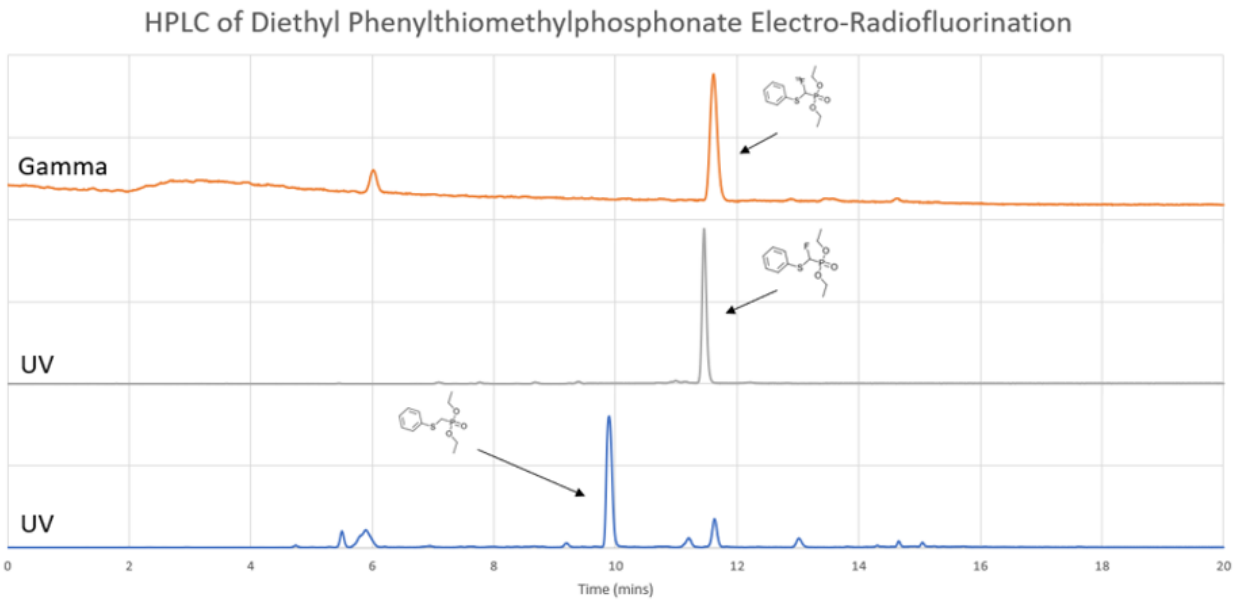

Figure 83: HPLC after NCA-ECF of Diethyl phenylthiomethylphosphonate. (Bottom) UV after electrolysis. (Middle) UV of isolated product with a carrier added synthesis. (Top) NCA-ECF Gamma signal of the product.

5.2.5 (Phenylthiol) Acetamide

NCA-ECF of (Phenylthiol) Acetamide in TFE had an RCFE of 23.3±4.1% (n=3). A carrier added synthesis was performed with $Et_4NF*4HF$ for the product standard and verified by ^{19}F-NMR and used to verify the product formed under NCA conditions. The results can be seen in Figures 84-86.

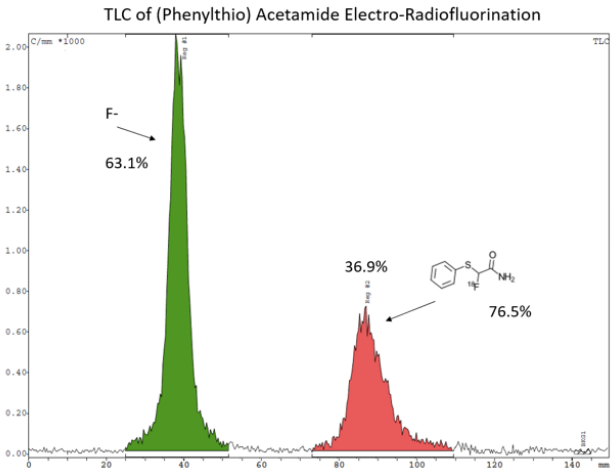

Figure 84: TLC after NCA-ECF of (Phenylthiol) Acetamide.

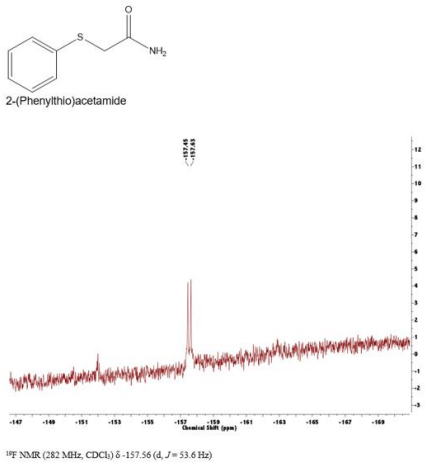

Figure 85: ^{19}F-NMR of CA ECF of (Phenylthiol) Acetamide.

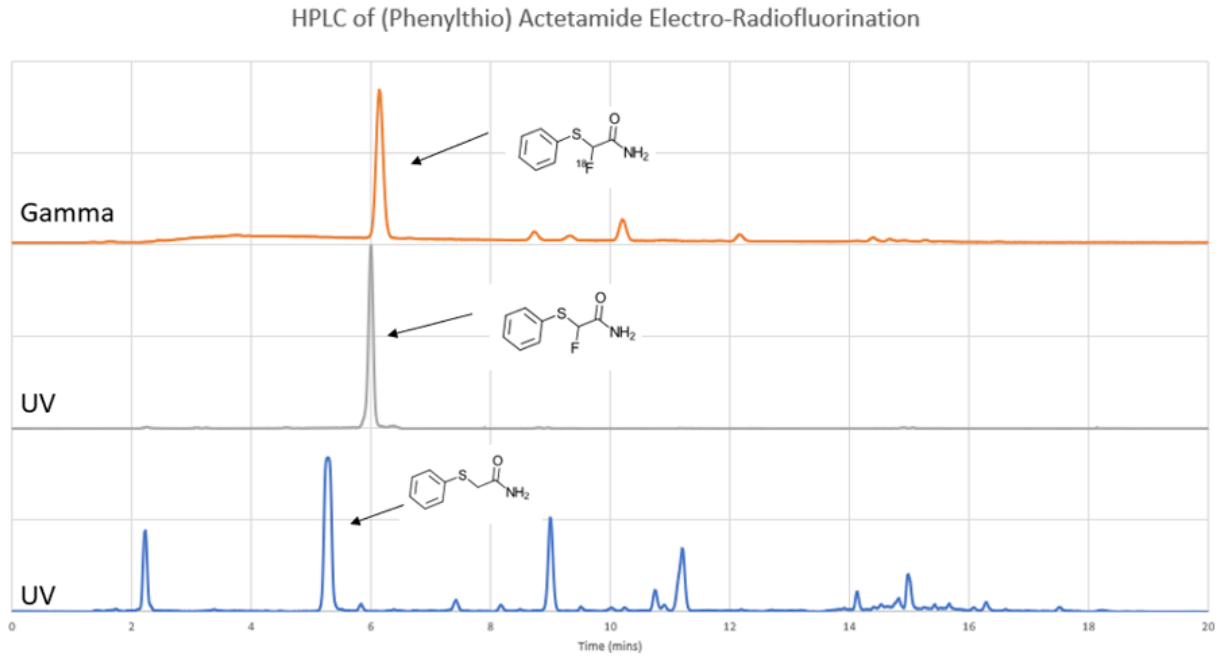

Figure 86*:* HPLC after NCA-ECF of (Phenylthiol) Acetamide. (Bottom) UV after electrolysis. (Middle) UV of isolated product with a carrier added synthesis. (Top) NCA-ECF Gamma signal of the product.

5.2.6 (Phenylthio) Acetic Acid

NCA-ECF of (Phenylthio) Acetic Acid in TFE had an RCFE of 1.3±0.1% (n=3). Due to the low RCC of 1.5±0.1% (n=2) and RCFE of this precursor, the synthesis for the product standard was not performed. The low RCFE is likely due to the increased acidity caused by the precursor being an acid. Decreasing precursor concentration did not increase RCFE. The HPLC and TLC are seen in Figure 87 and 88.

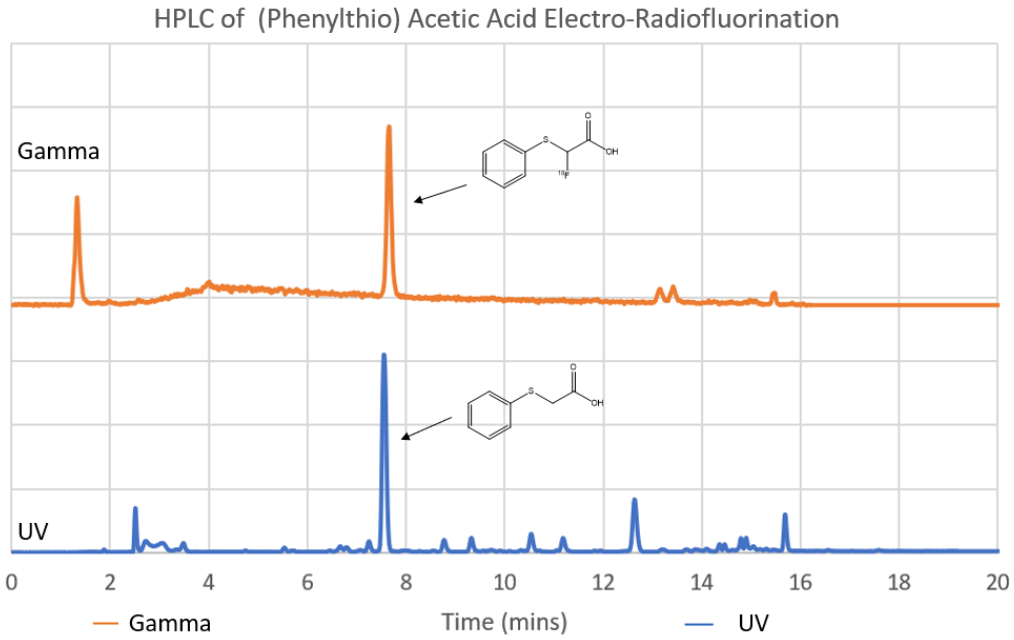

Figure 87: HPLC after NCA-ECF of (Phenylthio) Acetic Acid. (Bottom) UV after electrolysis. (Top) NCA-ECF Gamma signal of the product.

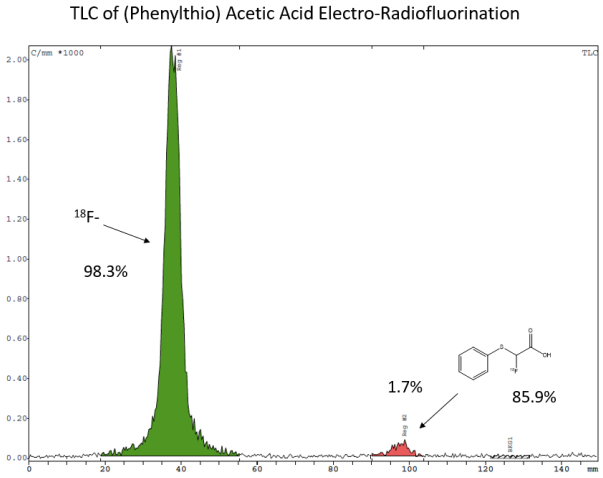

Figure 88: TLC after NCA-ECF of (Phenylthio) Acetic Acid.

5.2.7 NCA ^{18}F Electrochemical Fluorination of Thioethers in MeCN

The thioethers precursors were also fluorinated in the single chamber electrochemical cell with MeCN and 50 mM DTBP. It was successful up to 5.2% RCFE for these other 5 thioethers. However, Methyl (phenylthio) Acetate resulted in the most efficient product yield with RCFE up

to 27.8%. More optimization work is underway to determine the feasibility of this solvent and base system for applicability for a wider range of thioethers. The results are found in 5.2.8.

5.2.8 Data Summary of NCA-ECF of different Thioethers

NCA-ECF of Methyl (Methylthio) Acetate									
#	Other Additive (mM)	Solvent	Temperature (°C)	Oxidation Voltage	Duration (min)	Starting Activity (mCi)	RCC (%)	RCP (%)	RCFE (%)
Best 3	-	TFE	70	1.90	30	14.8±19.2	93.7±1.5%	98.9+0.9%	92.7±2.2%
1	-	TFE	70	1.90	30	41.9	91.9%	97.7%	89.8%
2	-	TFE	70	1.90	30	37.2	95.5%	99.6%	95.1%
3	-	TFE	70	1.90	30	1.54	93.7%	99.4%	93.1%
4	Ditertbutylpyridine 50 mM	MeCN	RT	1.90	30	1.31	5.5%	93.3%	5.1%
NCA-ECF of Methyl 2-(ethylsufanyl) Acetate									
#	Other Additive (mM)	Solvent	Temperature (°C)	Oxidation Voltage	Duration (min)	Starting Activity (mCi)	RCC (%)	RCP (%)	RCFE (%)
Best 3	-	TFE	70	1.90	30	2.26+0.34	95.5+0.5%	97.9+0.4%	93.5+0.8%
1	-	TFE	70	1.90	30	2.73	96.0%	98.5%	94.6%
2	-	TFE	70	1.90	30	2.11	94.8%	97.8%	92.7%
3	-	TFE	70	1.90	30	1.95	95.6%	97.5%	93.2%
4	Ditertbutylpyridine 50 mM	MeCN	70	1.90	30	1.38	5.7%	91.8%	5.2%
NCA-ECF of (Phenylthio) Acetonitrile									
#	Other Additive (mM)	Solvent	Temperature (°C)	Oxidation Voltage	Duration (min)	Starting Activity (mCi)	RCC (%)	RCP (%)	RCFE (%)
Best 3	-	TFE	70	1.90	30	1.27±0.32	24.7±3.0%	34.0±2.6%	8.3±0.4%
1	-	TFE	70	1.90	30	1.38	20.8%	36.8%	7.7%
2	-	TFE	70	1.90	30	0.84	28.0%	30.5%	8.5%
3	-	TFE	70	1.90	30	1.59	25.3%	34.7%	8.8%
4	Ditertbutylpyridine 50 mM	MeCN	RT	1.90	30	0.93	13.7%	28.3%	3.9%
NCA-ECF of Diethyl phenylthiomethylphosphonate									
#	Other Additive (mM)	Solvent	Temperature (°C)	Oxidation Voltage	Duration (min)	Starting Activity (mCi)	RCC (%)	RCP (%)	RCFE (%)
Best 3	-	TFE	70	1.90	30	2.22+0.42	26.0+3.5%	64.1+19.2%	16.0+3.1%
1	-	TFE	70	1.90	30	2.74	30.1%	38.7%	11.6%
2	-	TFE	70	1.90	30	2.20	21.6%	85.2%	18.4%
3	-	TFE	70	1.90	30	1.71	26.2%	68.3%	17.9%
4	Ditertbutylpyridine 50 mM	MeCN	RT	1.90	30	1.38	54.0%	8.7%	4.7%
NCA-ECF of (Phenylthio) Acetamide									
#	Other Additive (mM)	Solvent	Temperature (°C)	Oxidation Voltage	Duration (min)	Starting Activity (mCi)	RCC (%)	RCP (%)	RCFE (%)
Best 3	-	TFE	70	1.90	30	1.67±0.55	33.0±3.3%	70.2±5.5%	23.3±4.1%
1	-	TFE	70	1.90	30	2.27	28.9%	63.2%	18.3%
2	-	TFE	70	1.90	30	1.79	36.9%	76.5%	28.2%
3	-	TFE	70	1.90	30	0.94	33.1%	70.9%	23.5%
4	Ditertbutylpyridine 50 mM	MeCN	RT	1.90	30	1.19	16.4%	20.7%	3.4%
NCA-ECF of Methyl (phenylthio) Acetic Acid									
#	Other Additive (mM)	Solvent	Temperature (°C)	Oxidation Voltage	Duration (min)	Starting Activity (mCi)	RCC (%)	RCP (%)	RCFE (%)
Best 3	-	TFE	70	1.90	30	1.46±0.29	1.5±0.1%	87.2±1.0%	1.3±0.1%
1	-	TFE	70	1.90	5	0.62	0.4%	64.2%	0.3%
2	-	TFE	70	1.90	30	1.74	1.4%	88.3%	1.3%
3	-	TFE	70	1.90	30	1.58	1.7%	85.9%	1.4%
4	-	TFE	70	1.90	30	1.06	1.4%	87.4%	1.2%
5	Ditertbutylpyridine 50 mM	MeCN	RT	1.90	30	0.83	0.6%	trace	trace

All experiments used 50 mM of precursor and TBAP with 1.9V oxidation voltage in the 1.5 ml electrochemical cell

Figure 89: Data Summary of NCA-ECF of different Thioether Precursors.

Chapter 6: No-Carrier-Added ^{18}F ECF of Modafinil Precursor

6.1 Introduction to Modafinil

Modafinil is a recent pharmaceutical popularized by mainstream media in the movie and TV series, Limitless. In practical medicine, modafinil has been used as a wakefulness-promoting agent. It currently is prescribed for treatment of disorders such as narcolepsy, and sleeping disorders [124, 125]. Modafinil is currently being researched as a treatment for cocaine addiction and as a potential cognitive enhancement agent [126, 127].

Additionally, modafinil has known to be an effective dopamine transporter (DAT) with the ability to act as a dopamine uptake inhibitor (DRI) [128]. Studies have demonstrated modafinil can very selectively raises dopamine levels in several different areas of the brain [129] Contrasting to addictive drugs (i.e., cocaine), modafinil has potential to serve as an effective DAT blocker without its addictive side-effects which can be advantageous to minimize drug abuse [129, 130]. Modafinil is thought to have several other molecular effects in the brain that cannot be explained by DRI behavior. It is hypothesized that modafinil may have other stimulant inducing effects, with one being the release of histamine in the brain [128]. There have been many other proposed alternate effects of modafinil which may have additional mechanisms of action besides the effects of DAT [131].

Literature precedence suggests modafinil may serve as an interesting PET image for several reasons. First, modafinil would be useful as a PET probe to understand the brain regions and pathways it is involved in. This would help understanding sleeping disorders and the potential effects of a treatment for cocaine addiction or as a cognitive enhancer. In this way, a modafinil PET probe may be advantageous for the diagnosis of different types of sleep disorders or for evaluating treatment of cocaine addiction. Additionally, a modafinil PET probe may help elucidate

the cognitive enhancement affects. However, further research is required in order to validate whether modafinil can be used in further drug design and potential treatments.

6.2 Electrochemical Fluorination of Modafinil Precursor

Modafinil is a thioether similar to the thioethers that have been previously fluorinated in our NCA-ECF reactions. The sulfur would need an additional chemical step to form sulfoxide after the ECF process. The amine group is also BOC protected and would need to be removed deprotected after ECF as well. The general proposed modafinil precursor scheme is seen in Figure 89. Due to the product instability, NMR could not be completed to identify the chemical structure of the product. Fluorination is suspected to occur on the benzylic position due to the cation intermediate being the most stable, instability of the product and loss of fluorination of the product due to instability.

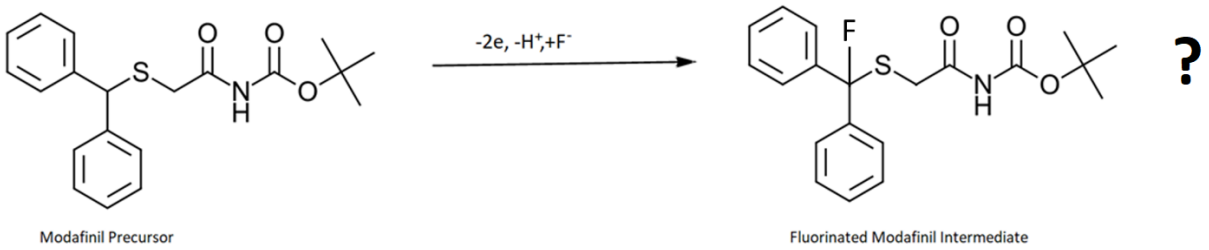

Figure 89: General ECF Scheme of the Modafinil Precursor.

Performing NCA-ECF with TFE solvent in a similar manner as the previous thioethers did not generate any product as noted via HPLC under BOC protected or unprotected precursor conditions. Switching to MeCN with DTBP base resulted in low RCFE with the unprotected modafinil precursor without BOC. After BOC protecting the amine, NCA-ECF was performed in MeCN with 50 mM DTBP which resulted in a RCFE of 9.7±0.6% (n=3). There are several

possibilities for why the modafinil thioether did not produce product using TFE solvent unlike the other thioethers. It is likely that the intermediates are not stable in TFE due to the benzylic group or that fluorination or proton abstraction is hindered by the solvent shell in TFE for the modafinil precursor likely due to the two adjacent aromatic rings.

6.2.1 Optimization Parameter: Oxidation Potential

Using MeCN and 50 mM DTBP several different oxidation potentials were tested. An oxidation potential of 2.0V (Ag/Ag+) was the most optimal (Figure 90). It important to note that DTBP onset oxidation potential starts at approximately 2.1V (Ag/Ag+). Oxidizing at higher potentials than 2.0V greatly reduced RCFE due to oxidation of the DTBP base which interferes in ECF and also fluorine adding to the DTBP at higher potentials than 2.0V (Ag/Ag+).

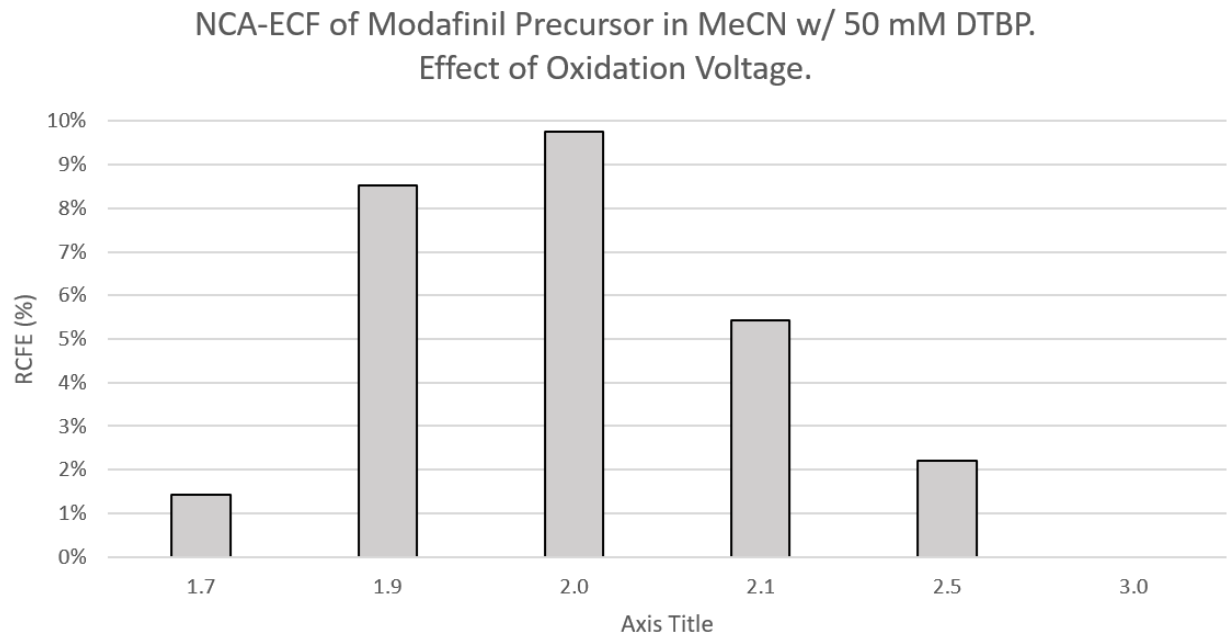

Figure 90: NCA-ECF of the Modafinil Precursor in MeCN with 50 (mM) DTBP. Effect of Oxidation Potential. The optimal oxidation potential was found to be 2.0V.

6.2.2 Optimization Parameter: DTBP Concentration

The concentration of DTBP was optimized in MeCN using the Modafinil Precursor at the 50 mM optimal concentration (Figure 91). It is evident that the presence of excess base inhibits NCA-ECF This may be due to destabilizing the cation intermediate or a change in fluoride reactivity under more basic conditions.

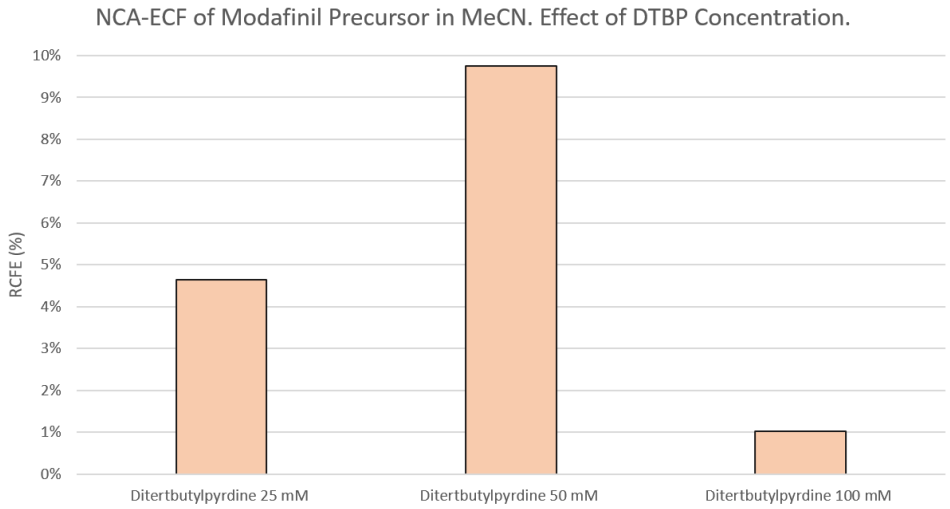

Figure 91: NCA-ECF of the Modafinil Precursor in MeCN. Effect of DTBP Concentration. The optimal DTBP concentration was found to be 50 (mM).

6.2.3 HPLC and TLC of Modafinil Precursor

HPLC, TLC and A_m of the modafinil precursor are shown in Figures 92-94. The A_m was calculated to be 0.18±0.01 Ci/uM (n=2). The individual experiments are recorded in Figure 95.

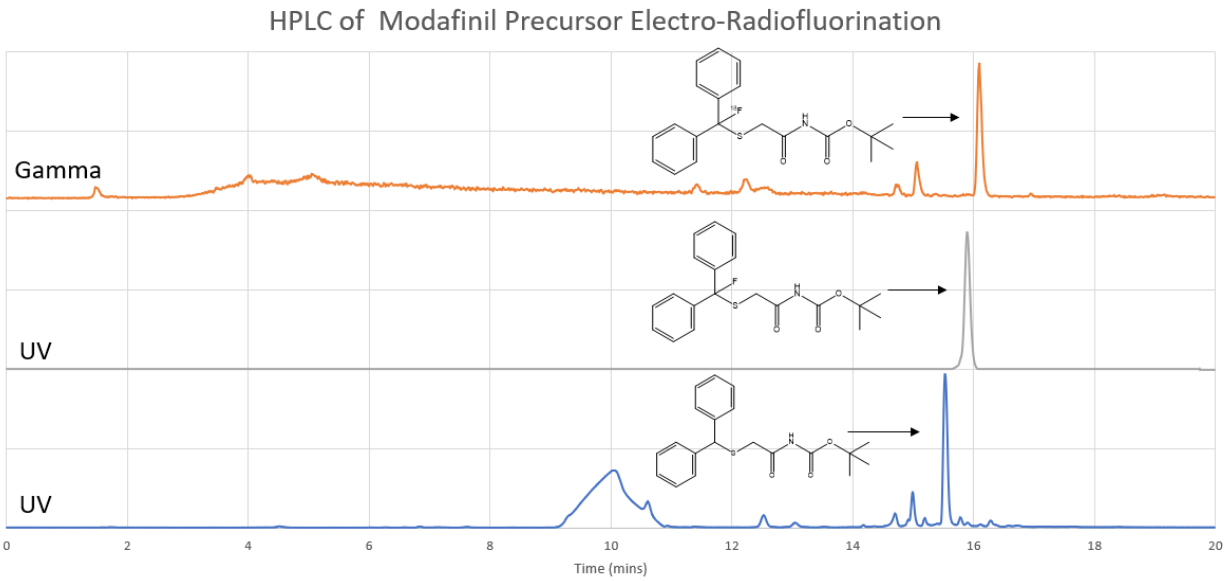

Figure 92: HPLC after NCA-ECF of the Modafinil Precursor. (Bottom) UV after electrolysis. (Middle) UV of isolated product with a carrier added synthesis. (Top) NCA-ECF Gamma signal of the product.

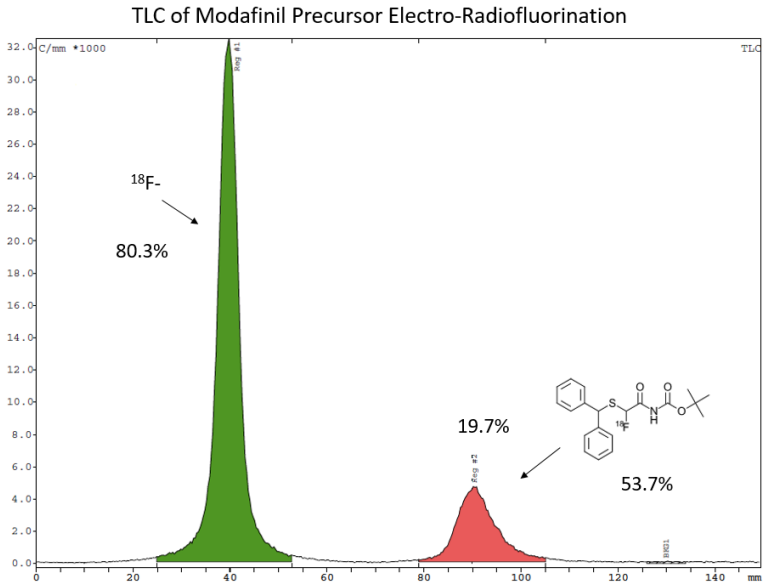

Figure 93: TLC after NCA-ECF of the Modafinil Precursor.

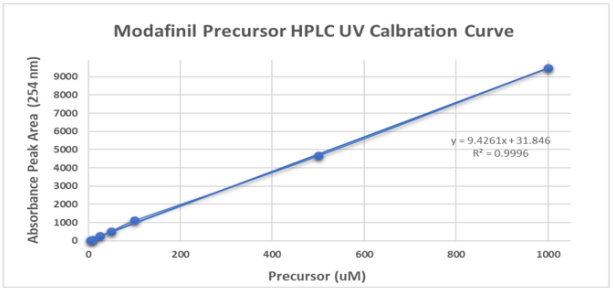

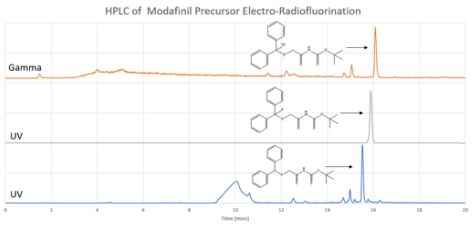

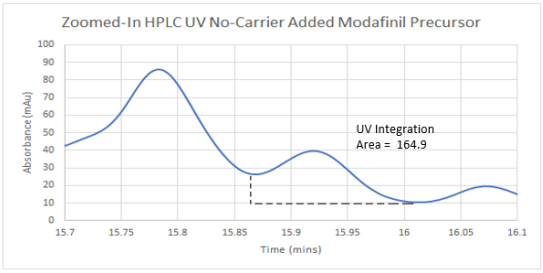

Precursor (uM)	254nm Absorbance
1000	9485.6
500	4662.1
100	1112.9
50	513.5
25	273.2
10	68.6
5	37.1

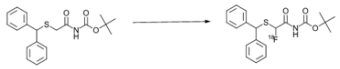

Decay Corrected Injected Activity and Volume into HPLC | TLC Conversion | HPLC Purity | Product Concentration from HPLC UV Calbration Curve

$$\frac{0.525\ \text{mCi}}{20\ \text{uL}} \times 16.6\% \times 57.8\% \times \frac{10^6\ \text{uL}}{1\ \text{L}} \times \frac{1\ \text{L}}{14.1\ \text{umol}} \times \frac{1\ \text{Ci}}{10^3\ \text{mCi}} = 0.179\ \text{Ci/umol}$$

Figure 95: Molar Activity Calculation for the Modafinil Precursor.

6.2.4 Data Summary of NCA-ECF of Modafinil Precursor

NCA-ECF Single Chamber with Single BOC protected Modafinil Precursor								
#	Other Additive (mM)	Solvent	Temp (°C)	Oxidation Voltage	Starting Activity (mCi)	RCC (%)	RCP (%)	RCFE (%)
Best 3	Ditertbutylpyrdine 50 mM	MeCN	RT	2.00	7.83±8.19	17.2±1.8	56.9±2.3%	9.7±0.6%
1	Ditertbutylpyrdine 50 mM	MeCN	RT	1.70	1.94	1.7%	84.3%	1.4%
2	Ditertbutylpyrdine 50 mM	MeCN	RT	1.90	2.83	10.3%	82.7%	8.5%
3	Ditertbutylpyrdine 50 mM	MeCN	RT	2.00	1.72	15.3%	59.2%	9.1%
4	Ditertbutylpyrdine 50 mM	MeCN	RT	2.00	2.37	19.7%	53.7%	10.6%
5	Ditertbutylpyrdine 50 mM	MeCN	RT	2.00	39.40	16.6%	57.8%	9.6%
6	Ditertbutylpyrdine 50 mM	MeCN	RT	2.10	1.65	25.0%	21.7%	5.4%
7	Ditertbutylpyrdine 50 mM	MeCN	RT	2.50	0.84	29.7%	7.4%	2.2%
8	Ditertbutylpyrdine 50 mM	MeCN	RT	3.00	0.63	10.1%	0.0%	0.0%
9	Ditertbutylpyrdine 25 mM	MeCN	RT	2.00	1.14	7.4%	62.7%	4.6%
10	Ditertbutylpyrdine 100 mM	MeCN	RT	2.00	2.38	17.7%	5.8%	1.0%
11	-	MeCN	RT	2.00	1.59	1.7%	Trace	Trace
12	Ditertbutylpyrdine 50 mM	TFE	RT	2.00	1.91	1.9%	0.0%	0.0%
13	Ditertbutylpyrdine 50 mM	TFE	RT	2.00	1.67	2.3%	0.0%	0.0%
14	-	TFE	70	2.00	1.72	1.4%	0.0%	0.0%
15	-	TFE	70	2.00	1.42	1.5%	0.0%	0.0%
16	-	TFE	RT	2.00	1.27	1.3%	0.0%	0.0%
17	-	TFE	RT	2.00	0.93	1.2%	0.0%	0.0%
All experiments used 1.5 ml solution, 50 mM Precursor, 50 mM TBAP, stirring at 600 RPM and electrolysis for 30 mins								

Figure 96: Data Summary of NCA-ECF of the Modafinil Precursor.

Chapter 7: No-Carrier-Added ^{18}F ECF of Naphthalene

7.1 Introduction to Electrochemical Fluorination of Aromatics

Aromatics are a common target in organic molecules for fluorination due to the availability of hydrogens on aromatic molecule that fluoride could easily replace. The benefit and desirability of fluorination on aromatic rings is that it has been proven to provide robust *in vivo* metabolic stability for a large majority of the potential aromatic PET probes [44], which is important since *in vivo* instability is one of the largest problems with experimental PET probes. Instable PET probes can degrade in the blood or in an organ, without ever having the ^{18}F reach its biological target and produce the signal necessary for an adequate PET image. Since fluorine is not a naturally occurring element in organic molecules, the body tends to metabolize molecules that contain it. By radiolabelling on an aromatic ring, the aromatic conjugation can help offset the large electronegativity of fluoride and the electron density of the aromatic ring can help camouflage fluoride to the *in vivo* metabolic process. Both of these effects help increase the metabolic stability of aromatically radiolabeled PET probes.

Currently, there are many different strategies to radiolabeled aromatics with [^{18}F]Fluoride [42, 44, 132]. Each of these methods has different limitations and advantages. Some potential limitations in established aromatic radiofluorination are in precursor synthesis, the need for directing groups, limitation in labeling position (ortho, meta, para), difficulty using some functional groups, or harsh conditions such as high temperature or pH. The late stage fluorination of aromatic compounds with [18F]fluoride, especially those that possess a high electron density, presents a challenge due to the disadvantaged interaction between a negatively charged fluoride and an electron rich reaction center. Various chemical methodologies have been reported to facilitate this dis-favored reaction including the use of organometallic intermediates, [38]

aryliodoinum as well as iodonium ylide leaving groups [39], catalysts [40] and strong oxidizing reagents [41]. An extensive overview of the field was recently published, reviewing emerging techniques for late stage 18F-fluorination of aromatic molecules [42]. Electrochemistry can also be used to radiofluorinate aromatics. The potential benefits are listed in section 1.6. A large scope of aromatic compounds with both electron withdrawing groups and electron donating groups has been electrochemically fluorinated under high concentrations of carrier added conditions [4, 52, 133].

7.1.1 Previous Electrochemical Radiofluorination (Reischl et al.)

A previous research group, Reischl et al, has performed electrochemical radiofluorination under carrier added conditions [2, 4, 5]. Their results will be summarized in this section. This group and their 3 publications are the only published group besides our own in this field to our knowledge. Their first paper fluorinated benzene using Et_3N*3HF in MeCN [2] where they identified the optimal conditions to be 33 mM of the fluoride source and 66 mM of Et_3N*HCl which resulted in 16$\pm$9% RCFE. Et_3N*HCl was used as an additional electrolyte. Using Et_3N*3HF as solvent produced poor RCFE due to the high concentration of [^{19}F]Fluoride. The ratio of unreacted ^{19}F to unreacted ^{18}F is the same as these isotopes behave the same chemically. Reducing the fluoride source concentration to 33 (mM) increased RCFE substantially (Figure 97).

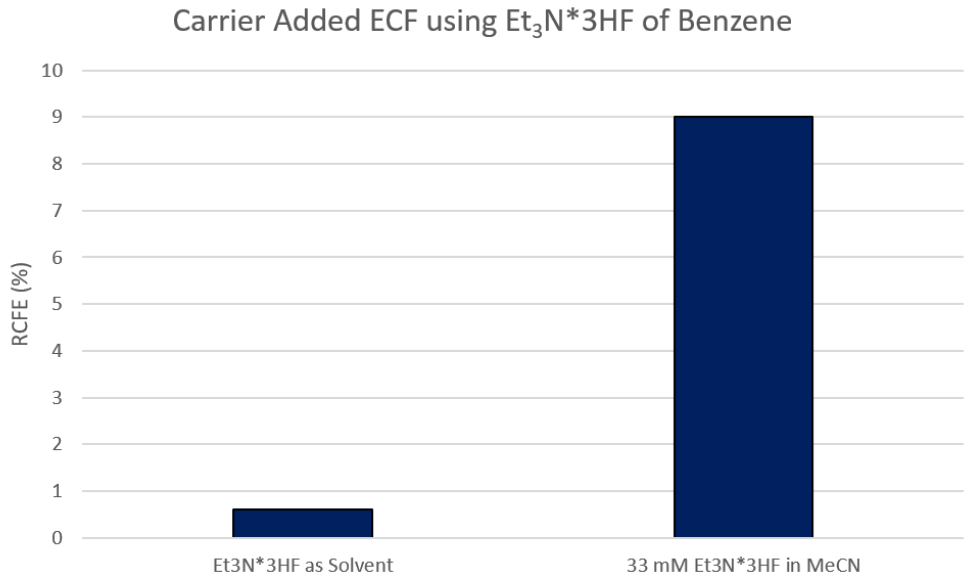

Figure 97: Carrier Added ECF using Et_3N*3HF of Benzene. The optimal fluoride source concentration was 33 (mM) [2].

Increasing the precursor concentration led to an increased RCFE (Figure 98) with the optimal precursor concentration to be 1.0 M. This is likely due to the side product formation during electrolysis from oxidation or reduction. This can break aromaticity and form side products that have lower oxidation potential than the precursor and are preferentially oxidized. The same is seen with dimer formation which tend to have lower oxidation potential than the monomer precursor [134, 135]. Thus, the high concentration of precursor led to a low ratio of side product concentrations compared to precursor concentration reducing the effect of preferential oxidation of the lower oxidation potential side products.

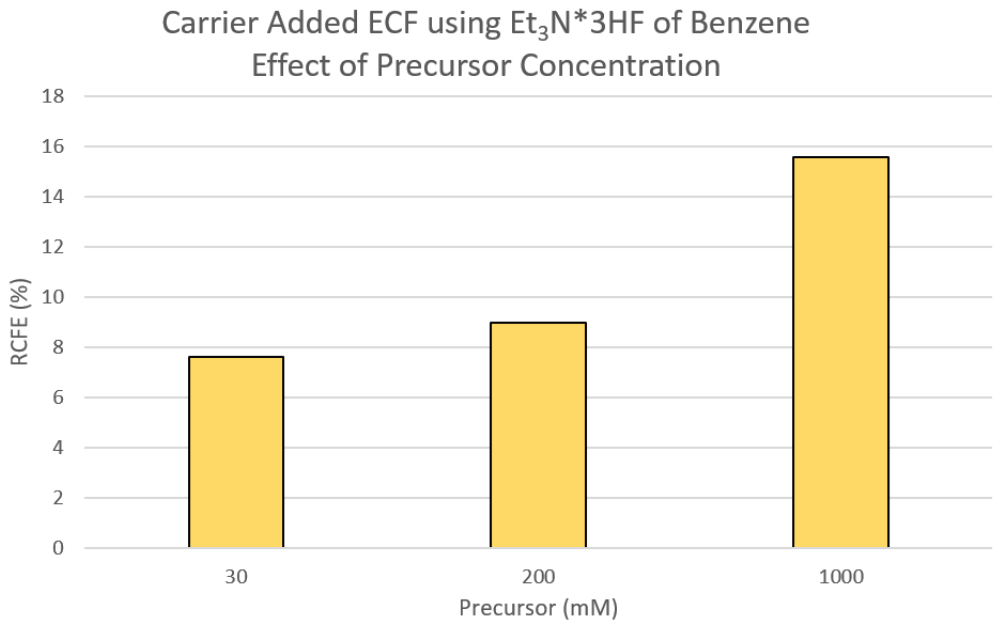

Figure 98: Carrier Added ECF using Et3N*3HF of Benzene. The optimal precursor concentration was 1.0M [2].

The second publication from the Reischl et al. group used monosubstituted benzene and monitored whether the fluorination occurred at the substituents or hydrogen on the benzene ring [5]. In all cases they reported fluoride was more likely to replace hydrogen (Figures 99-100). The monosubstituted t-butyl had slightly higher RCFE of 7.9% compared to when solely using benzene (7.4%) to replace the hydrogen atoms for fluoride (Figure 99) The order of RCFE for the added substituents on benzene after t-butyl was F>Cl>Br for fluoride replacing hydrogen.

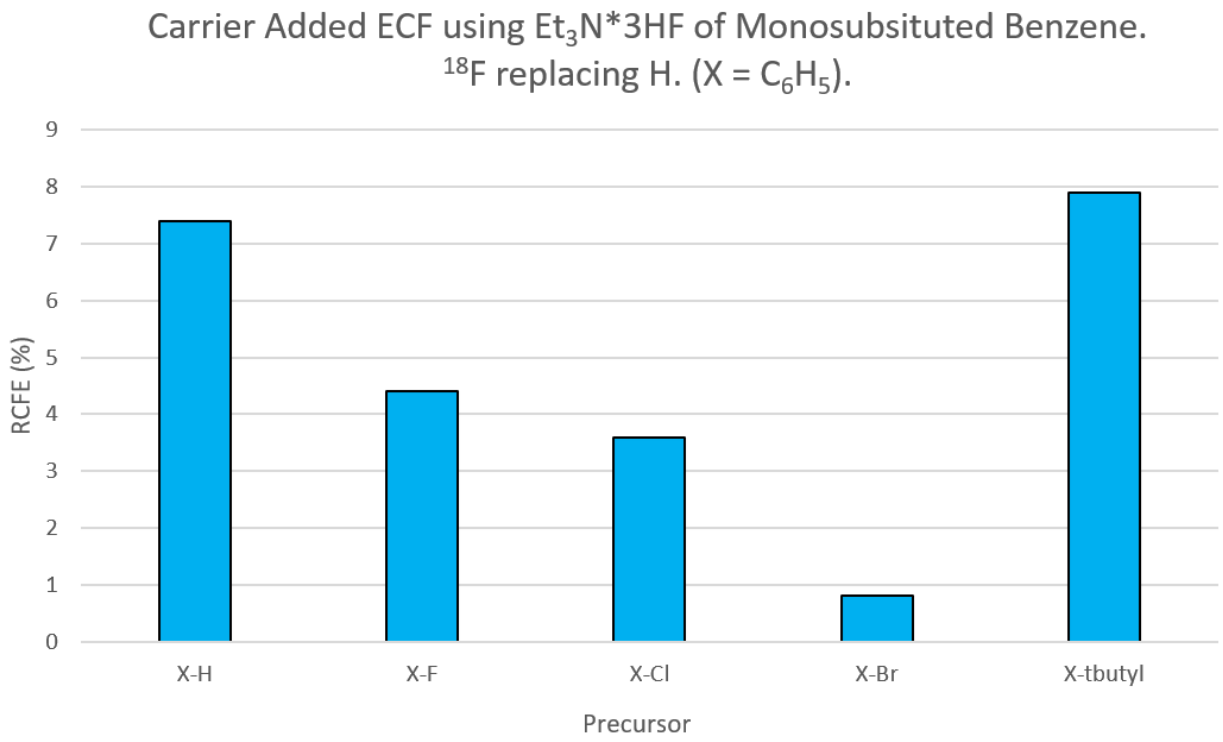

Figure 99: Carrier Added ECF using Et3NF*3HF of Monosubstituted Benzene. 18F replacing hydrogen [5].

The most effective substituent replaced by fluoride was the t-butyl group at 1.7% RCFE followed by Cl>F>Br for substituent replacement (Figure 100). These resulting RCFE values were lower than reactions that had hydrogen replacement instead (Figure 100). T-butyl groups are good leaving group due to the stability of the t-butyl carbocation. However, hydrogen is more favorable as a substitution for fluoride in ECF on benzene rings whereas t-butyl groups are only slightly more favored than the other halogens for substitution by fluoride in ECF.

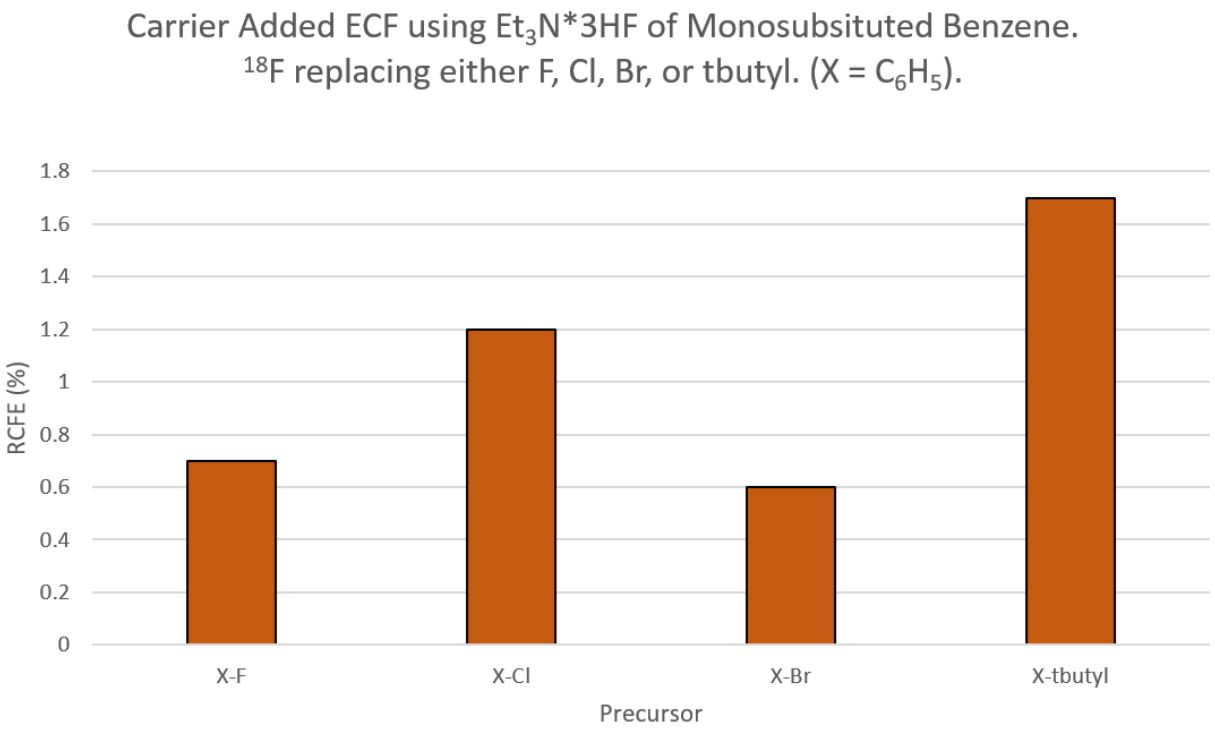

Figure 100: Carrier Added ECF using Et3N*3HF of Monosubstituted Benzene. Fluoride replacing either F, Cl, Br or t-butyl [5].

The third paper from the Reischl et al. group investigated using phenylalanine derivatives (Figure 101) [4] as intermediates to F-DOPA as discussed in section 8.1. The highest RCEF results were obtained for N-trifluoroacetylphenylalanine methyl ester with an RCFE of 10.5±2.5% where the relative isomeric distribution of product was reported to be 50.5% ortho isomer, 11.5% meta isomer, and 38.8% para isomer. Varying supporting electrolytes were used with 33 mM of Et_3N*3HF. They found a greater concentration of Et_3N*3HF performed most favorably, with Et_3N*HCl performing second best (Figure 102). From the chart, it appeared all the electrolytes had a detrimental effect on fluorination besides the fluoride source. For example, Br and I easily oxidized which interfered with benzene oxidation and product formation.

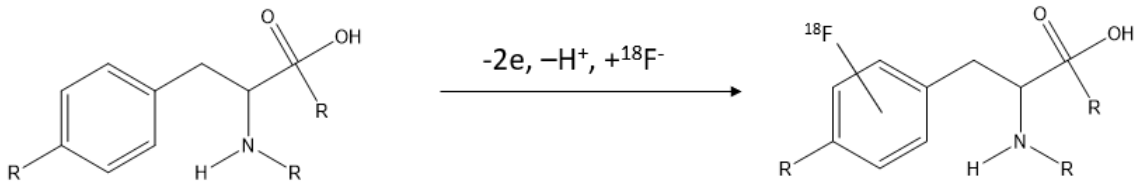

Figure 101: ECF Scheme of Phenylalanine derivatives [4].

.

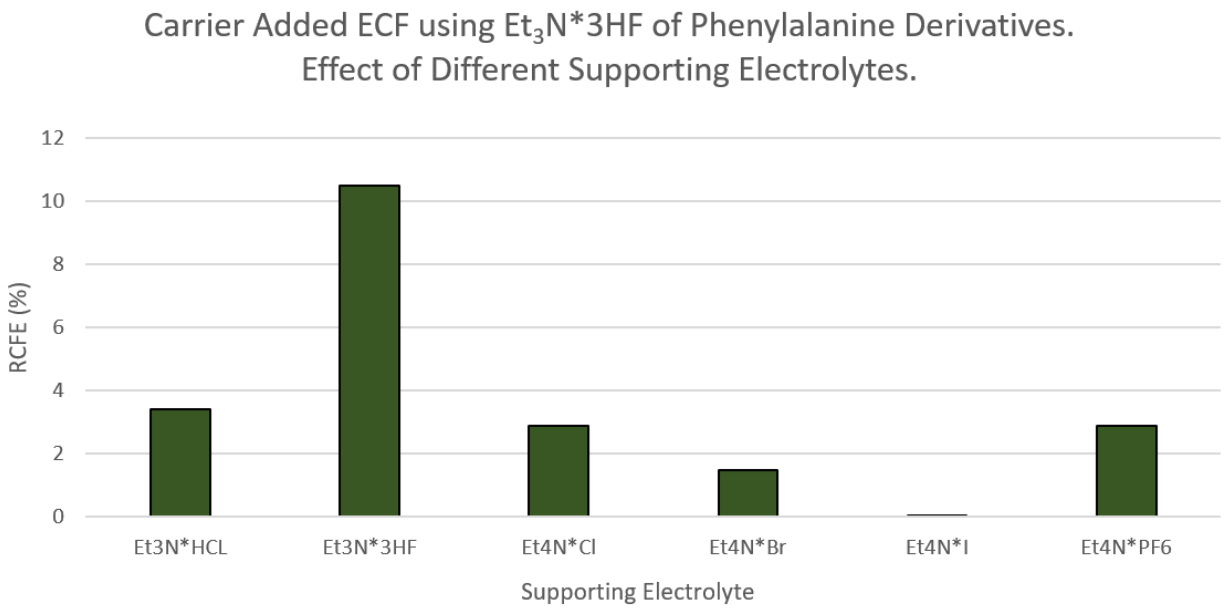

Figure 102: Carrier Added ECF using Et3N*3HF of Phenylalanine Derivatives. Effect of Different Supporting Electrolytes. Adding more of the Fluoride Source worked the best. HCl worked second best [4].

When investigating the optimal temperature, ECF of phenylalanine derivatives were found to have the optimal RCFE around 0 °C. Increasing or reducing temperature decreased RCFE (Figure 103) which was contrary to the thioether ECF findings that reported increasing temperature led to increased RCFE values. We reasoned this observation was a result from the fact that there is no fluoride stabilization of the FP mechanism in aromatics. Additionally, higher temperatures cause less stability of the cation intermediates.

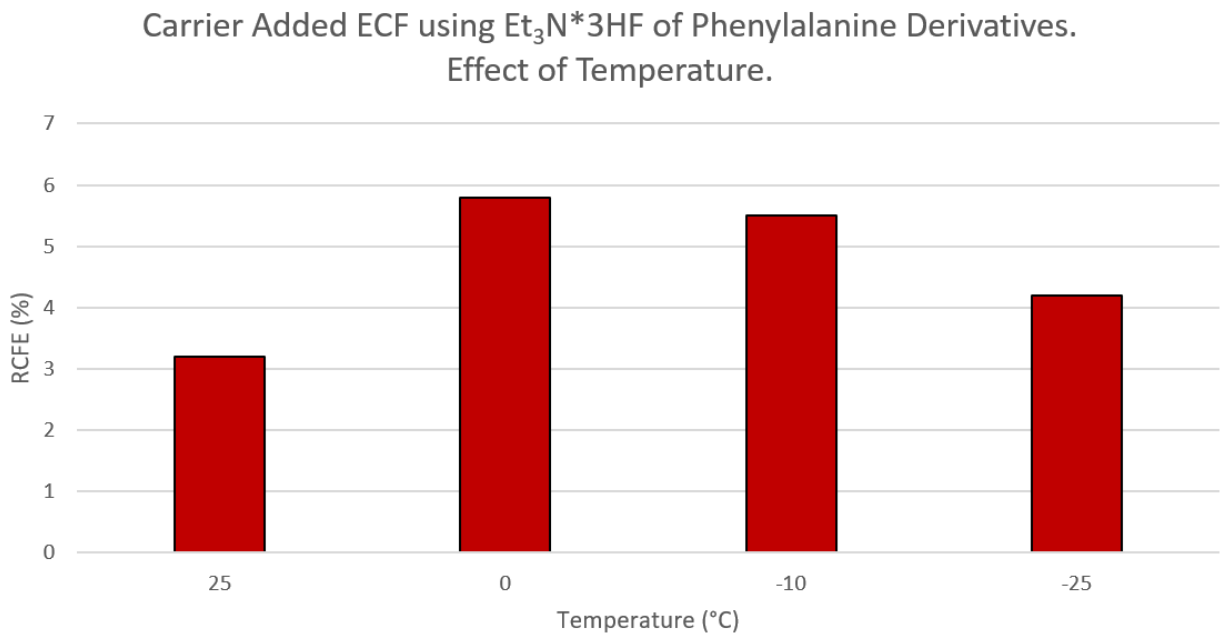

Figure 103: Carrier Added ECF using Et3N*3HF of Phenylalanine Derivatives. Effect of Temperature. The optimal temperature was at 0 °C [3].

The oxidation potential was also tested and they found 2.0V (Ag/Ag+) to performed better than 1.5V (Ag/Ag+) (Figure 104). Aromatic compounds begin to oxidize at higher potentials and to reach sufficient oxidation in shorter amount of time an even higher oxidation potential must be chosen.

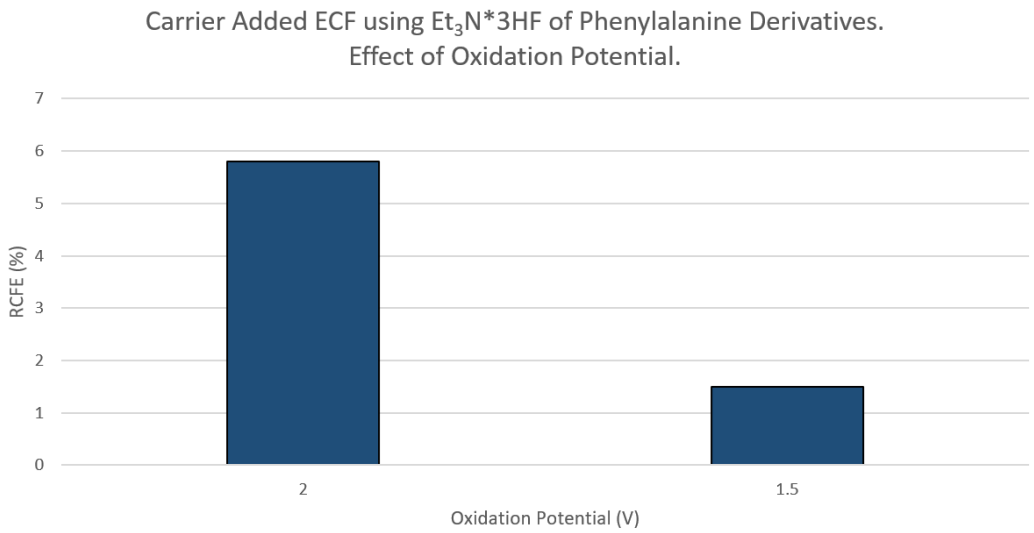

Figure 104: Carrier Added ECF using Et3N*3HF of Phenylalanine Derivatives. Effect of Oxidation Potential. The optimal oxidation potential was 2.0V [4].

Next, Reischl et al. investigated the effects of adding chloride in increasing concentration. They found this led to a decrease in RCFE as the chloride concentration increased (Figure 105). Chloride can cause HCl formation near the anode which increased the anodic acidity. Chloride can also compete with fluoride as a nucleophile. However, chloride reduces RCFE even when introducing much greater concentrations of fluoride in solution. This suggest the acidic role may play a more important role than competing nucleophile effect of chloride.

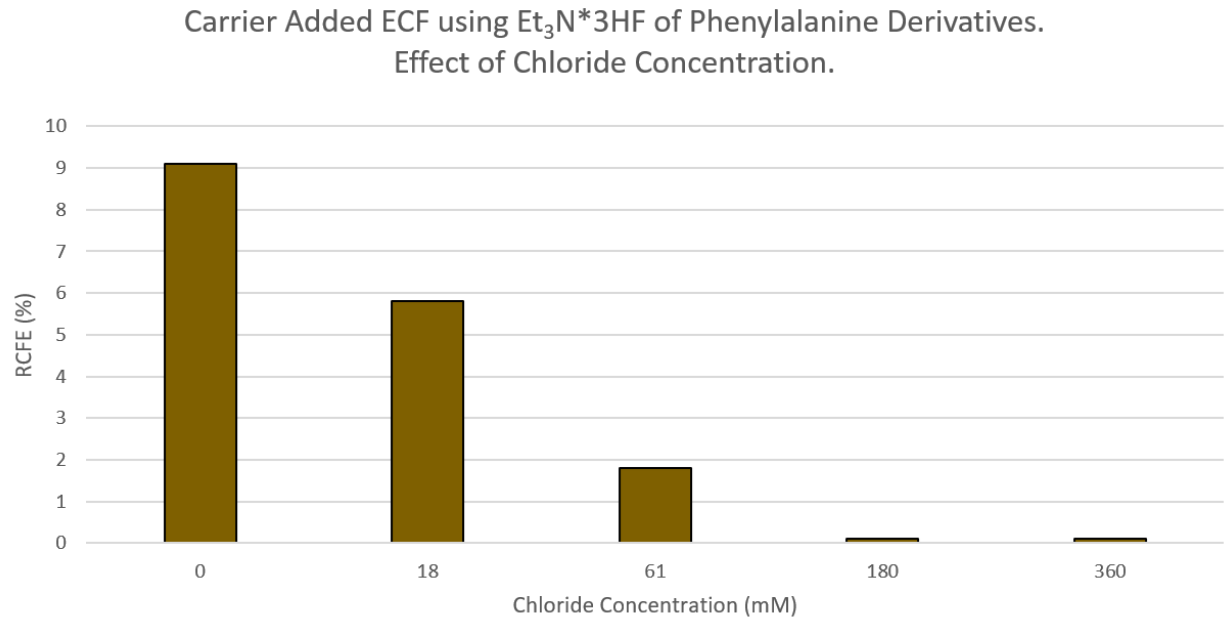

Figure 105: Carrier Added ECF using Et3N*3HF of Phenylalanine Derivatives. Effect of Chloride Concentration. Higher chloride concentration reduced fluorination [4].

7.2 Introduction to Electrochemical Fluorination of Naphthalene

Meurs et al. performed successful carrier added ECF using Et_3N*3HF of naphthalene in the single chamber electrochemical cell with MeCN. Single fluorinated naphthalene had a 6% product yield while difluorinated naphthalene had a 18% yield [68]. The addition of pyridine*3HF did not fluorinate naphthalene but pyridine added to naphthalene instead of fluoride. 1-Fluoronaphthalene was purchased as the product standard for HPLC for use in validating NCA-ECF of the ^{18}F labelled naphthalene product. This is in contrast to the other reference standards used here which were synthesized using electrochemistry and $Et_4NF*4HF$.

7.3 NCA ^{18}F Electrochemical Fluorination of Naphthalene

NCA-ECF of naphthalene was performed using MeCN, TFE and HFIP solvents. The reference standard, 1-Fluoronaphthalene, was purchased (Agros Organics). Using the solvent

MeCN produced 0 RCC even with the addition of DTBP. TFE produced an RCFE of 4.1±0.3% (n=2). Reactions performed with HFIP resulted in the most optimal RCFE value of 12.2±0.7% (n=3) at 70 °C (Figure 106) performing better at higher temperature. The cation intermediate of naphthalene and other highly conjugated aromatic cations have been previously shown to have very long lifetimes in HFIP which is discussed in the Laser Flash Photolysis section 12.10. Since naphthalene has a long cation lifetime in HFIP, it does not degrade as rapidly when exposed to increased temperature on cation stability. The added benefit of forming more cations at increased temperature likely cause higher RCFE (Figure 106).

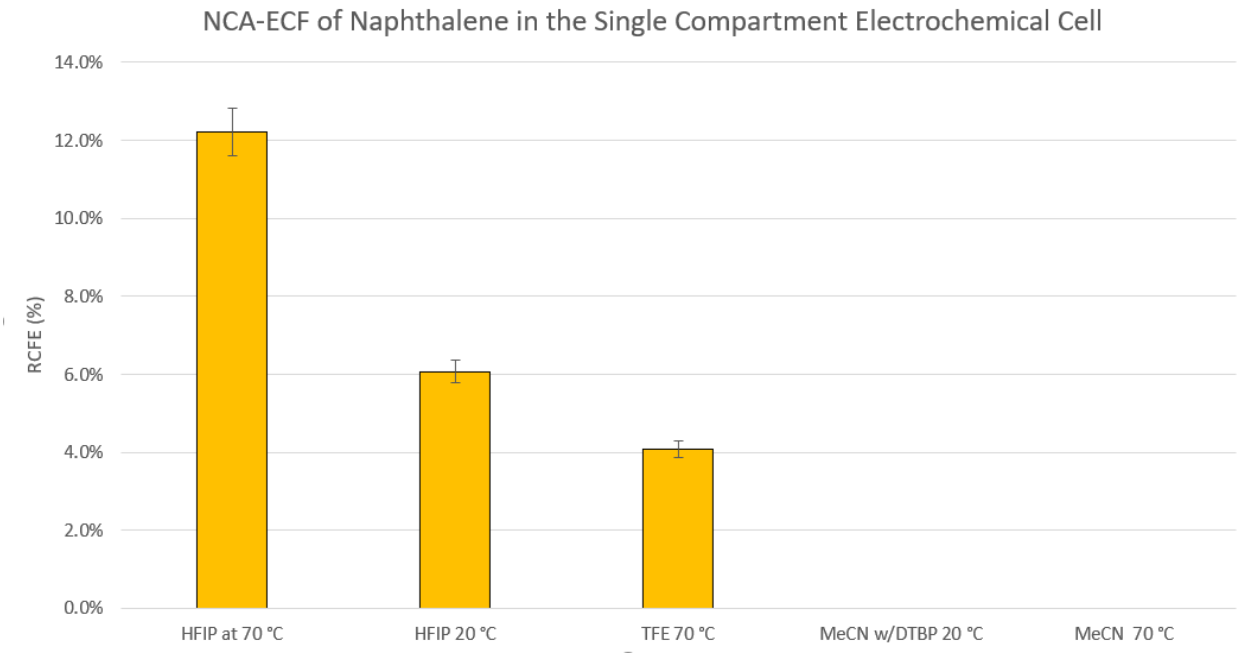

Figure 106: NCA-ECF of Naphthalene in the Single Chamber Electrochemical Cell. HFIP solvent at 70 °C performed the best.

7.3.1 HPLC and TLC of Naphthalene

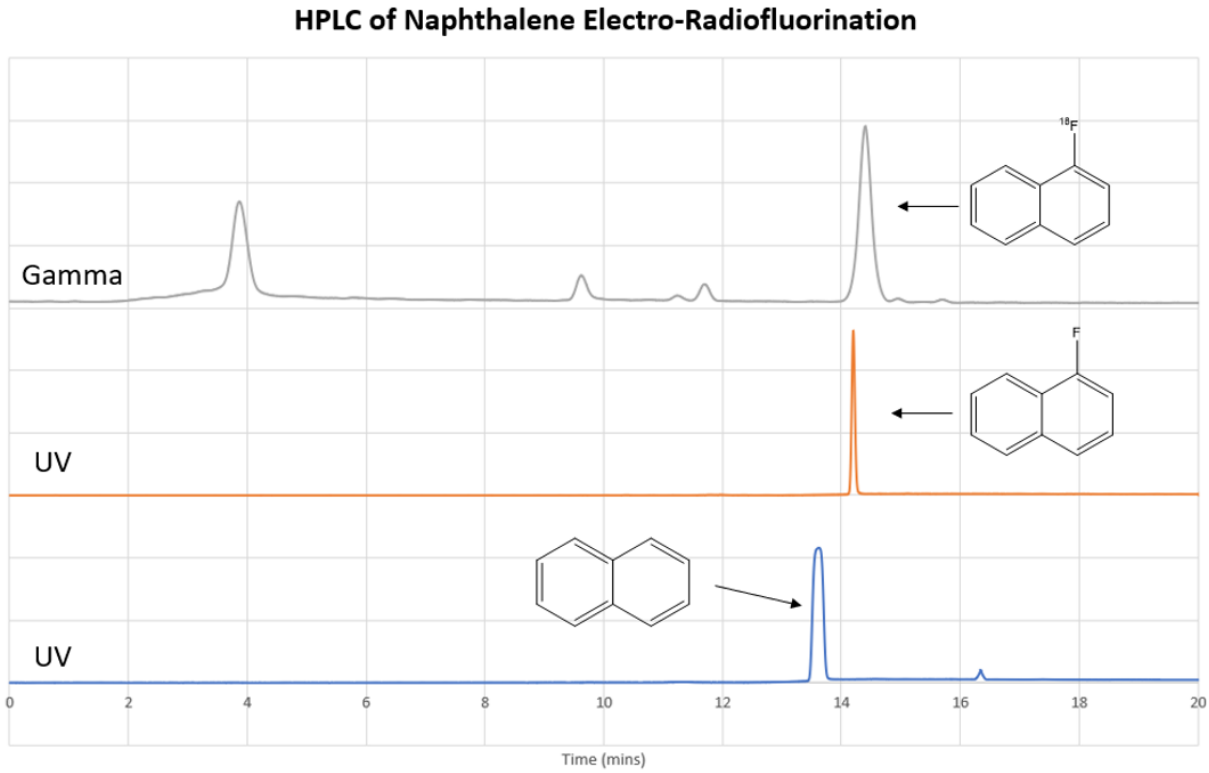

Figure 108: HPLC after NCA-ECF of Naphthalene. (Bottom) UV after electrolysis. (Middle) UV of isolated product. (Top) NCA-ECF Gamma signal of the product.

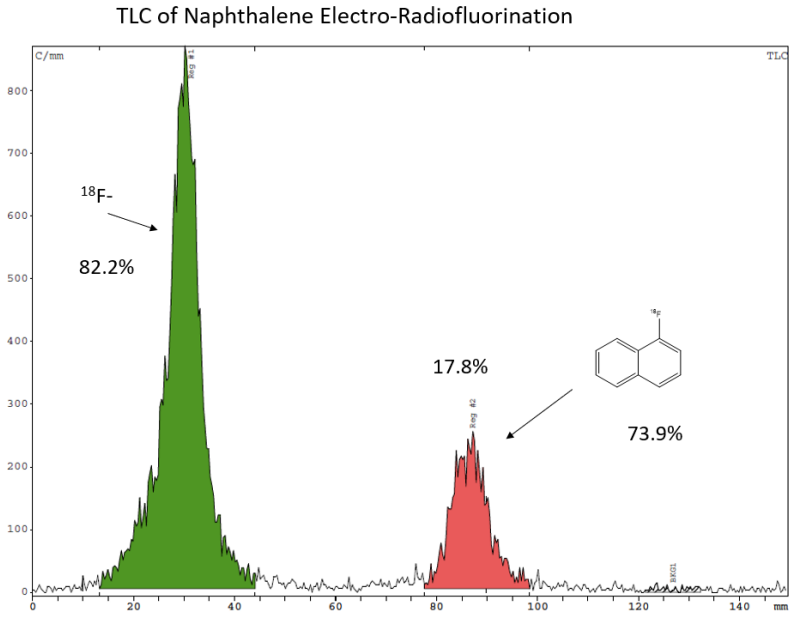

Figure 107: TLC after NCA-ECF of Naphthalene.

7.3.2 Data Summary of NCA-ECF of Naphthalene

NCA-ECF of Naphthalene in the Single Chamber 1.5 ml Electrochemical Cell							
#	Additive (mM)	Solvent	Temp (°C)	Starting Activity (mCi)	RCC (%)	RCP(%)	RCFE (%)
Best 3	-	HFIP	70	1.51±0.27	16.5±1.0	73.9±0.7	12.2±0.7
1	-	MeCN	70	1.32	0.0%	0.0%	0.0%
2	-	MeCN	70	0.94	0.0%	0.0%	0.0%
3	Ditertbutylpyridine 50 mM	MeCN	20	1.71	0.0%	0.0%	0.0%
4	Ditertbutylpyridine 50 mM	MeCN	20	1.48	0.0%	0.0%	0.0%
5	-	TFE	70	1.35	5.3%	82.9%	4.4%
6	-	TFE	70	0.86	4.5%	83.6%	3.8%
7	-	HFIP	20	2.33	8.1%	73.7%	6.0%
8	-	HFIP	20	2.02	8.6%	71.9%	6.2%
9	-	HFIP	70	1.83	15.3%	74.8%	11.4%
10	-	HFIP	70	1.54	17.8%	73.9%	13.2%
11	-	HFIP	70	1.17	16.3%	73.1%	11.9%
All experiments used 50 mM Precursor and TBAP, oxidation voltage of 2.0V and electrolysis for 30 mins							

Figure 109: Data Summary of NCA-ECF of Naphthalene

Chapter 8: NCA ^{18}F ECF of an Intermediary Molecule for F-DOPA

8.1 Introduction to F-DOPA

[^{18}F]F-DOPA is a useful clinical PET probe to assess dopaminergic function. This is particularly useful for patients affected by Parkinson's disease, which cause the degeneration of dopaminergic neurons in substantia nigra [136], as well as detecting brain and neuroendocrine tumors [14, 137]. F-DOPA is based on the precursor of dopamine, L-DOPA (L-dihydroxyphenylalanine). Dopamine is a neurotransmitter primarily found in the nigrostriatal region. L-DOPA is carried through the Blood Brain Barrier (BBB) via an amino acid transport system which also carries F-DOPA in the same mechanism. [^{18}F]F-DOPA PET imaging is used to clinical assess the dopaminergic system. F-DOPA synthesis is often used in radiochemistry as proof to validate a method to aromatically radiolabel fluoride.

8.2 Carrier-Added ^{18}F Electrochemical Fluorination of F-DOPA Intermediary Molecule

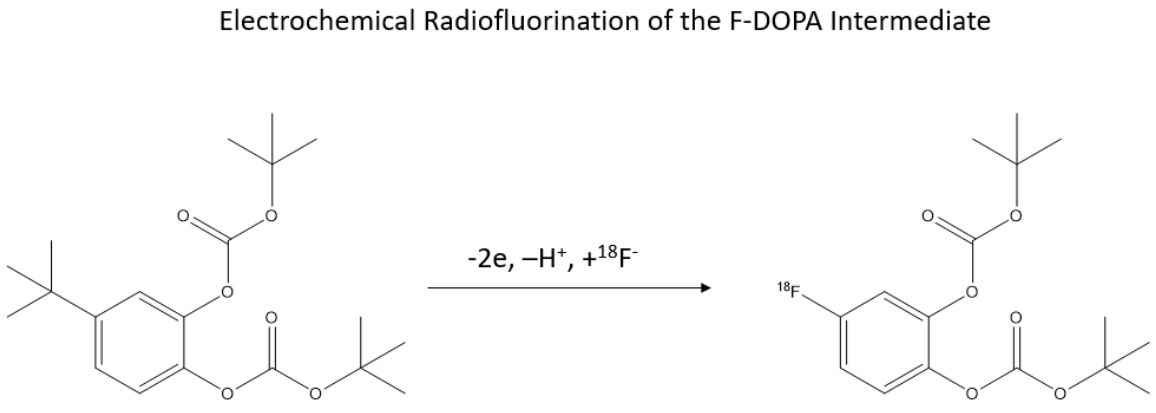

Figure 110: General Scheme of the ECF of the F-DOPA Intermediate Molecule.

A carrier added electrochemical radiofluorination method was performed using the aromatic molecule tert-butyloxycarbonyl (BOC) protected catechol based on our previous work

[73]. Kaneko et al., synthesized [^{18}F]F-DOPA from the 18-F labeled intermediary formed here. [138]. In the ECF mechanism (Figure 110), ^{18}F substitutes the t-butyl group instead of hydrogen. The carrier added ECF used Et_3NF*4HF with MeCN in a single chamber electrochemical cell. Without BOC protection, the hydroxyl group had a very low oxidation potential (~0.55V, Ag/Ag+) and prohibited product formation. The best result had an RCFE of 10.4 ± 0.6% (n = 4) after one-hour electrolysis at 0°C. This intermediate molecule has been previously reported to be potentially converted to [^{18}F]F-DOPA [138]. The tertbutyl group may reduce the oxidation potential of the aromatic and also be a good leaving group due the stability of the cation [139].

8.2.1 Optimization Parameter: Precursor Concentration

The RCFE of the F-DOPA intermediate with increasing precursor concentration increased up to 50 mM, which was identified to be the optimal precursor concentration, and then decreased at 80 mM (Figure 111). At higher precursor concentration, more side product formation was present which interfered with fluorination. These effects of increased current (cation formation) and interference from side production formation likely balance out at 50 (mM) concentration.

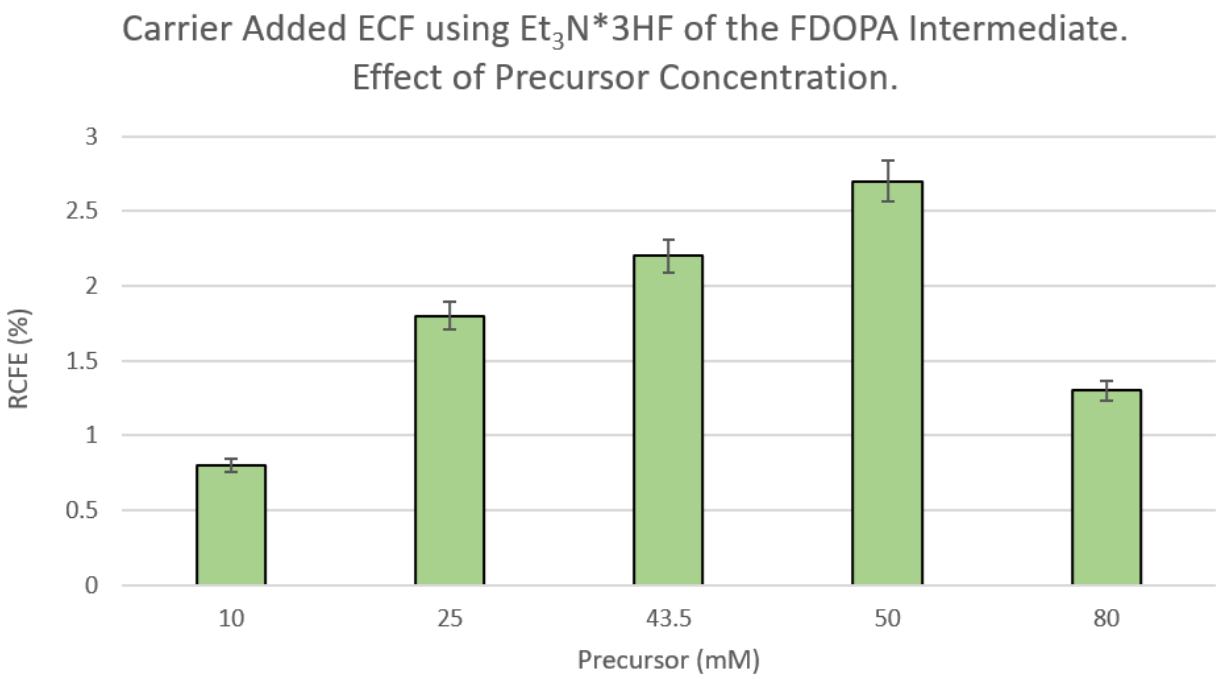

Figure 111: Carrier Added ECF using Et3N*3HF of the F-DOPA Intermediate Molecule. Effect of Precursor Concentration. The optimal precursor concentration was found to be 50 (mM).

8.2.2 Optimization Parameter: $Et_4NF*4HF$ Concentration

Two different fluoride source concentrations were tested where we found the optimal conditions to be 50 mM of $Et_4NF*4HF$ in contrast to 33 mM (Figure 112).

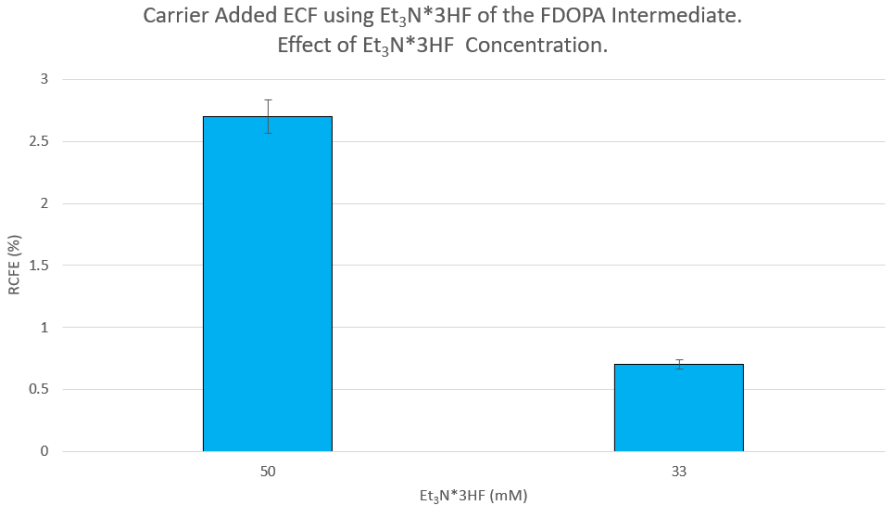

Figure 112: Carrier Added ECF using Et_3N*3HF of the F-DOPA Intermediate Molecule. Effect of Fluoride Source Concentration. The optimal fluoride source concentration was found to be 50 (mM).

8.2.3 Optimization Parameter: Electrolyte

Using Et_3N*3HF as the sole electrolyte resulted in the optimal RCFE measurement of 2.7 ± 0.6%. Two different supporting electrolytes were tested, TBAP and tetrabutyl hexafluorophosphate (TBAHFP). Both electrolytes significantly improved RCFE and product yields seen in Figure 113. TBAHFP was used in ECF instead of TBAP and increased RCFE.

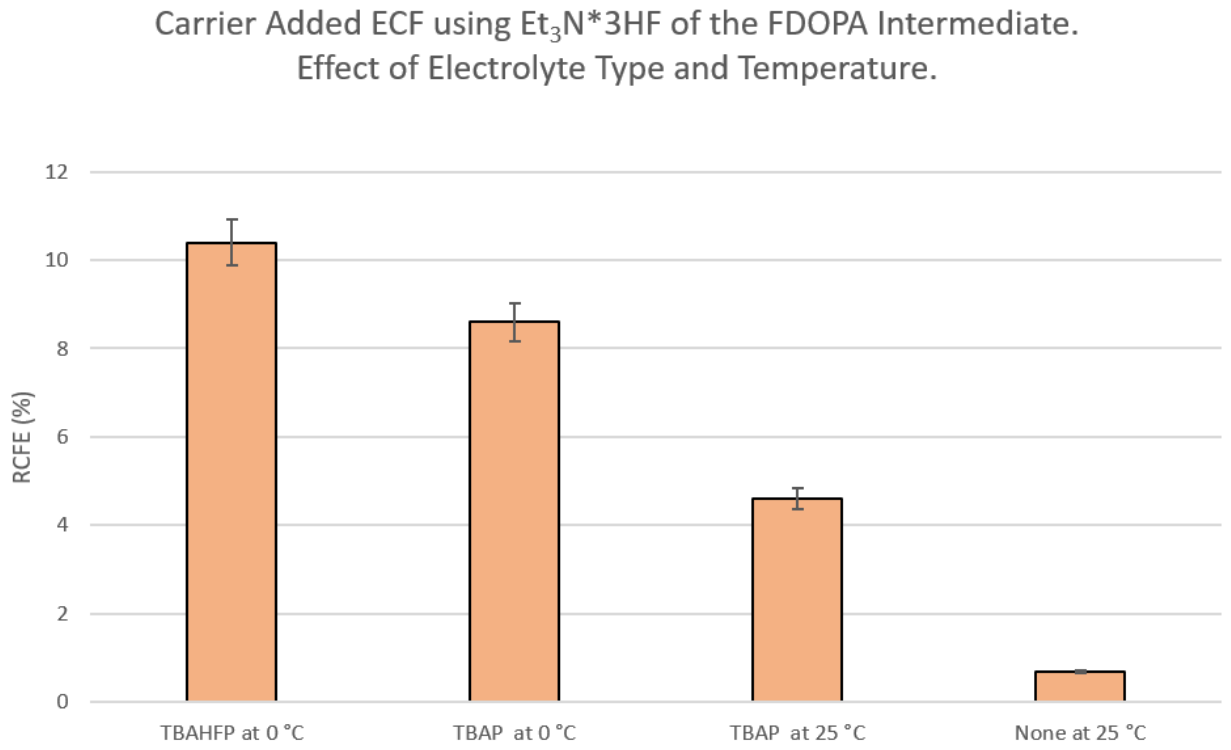

Figure 106: Carrier Added ECF using Et3N*3HF of the F-DOPA Intermediate Molecule. Effect of Electrolyte Type and Temperature. Both stable electrolytes of TBAP and TBAHFP increased RCFE. Decreasing temperature to 0 °C also increased RCFE.

8.2.4 Optimization Parameter: Temperature

Decreasing the temperature to 0 °C led to a two-times increase in the RCFE values (Figure 113). For instance, using TBAP at 25 °C had an RCFE of 4.6±0.4 (n=4) and at 0 °C had an RCFE of 8.6±1.1 (n=4). This observation was comparable to a similar finding with benzene where 0 °C

was the optimal temperature. This is likely due to increasing the short cation lifetime under cold temperatures.

8.2.5 Optimization Parameter: Oxidation Potential

The optimal oxidation potential was found to be 2.6V (Ag/Ag+) (Figure 114) since oxidation potential of higher or lower potential had less RCFE.

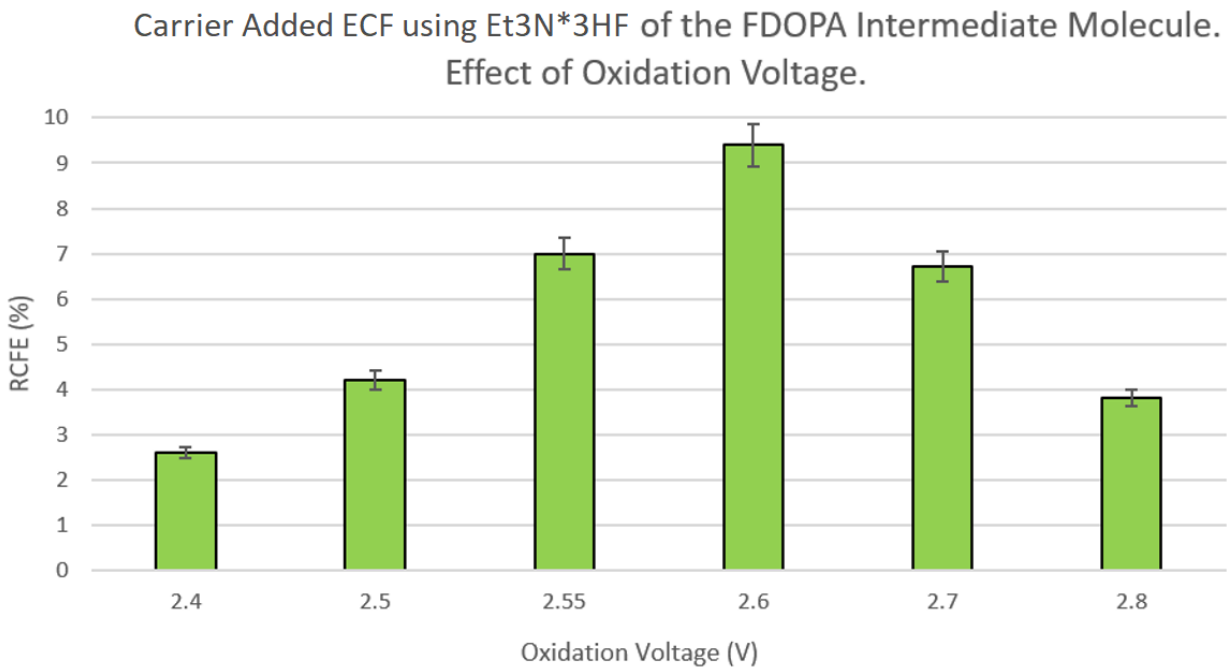

Figure 114: Carrier Added ECF using Et3N*3HF of the F-DOPA Intermediate Molecule. Effect of Oxidation Potential. The optimal oxidation potential was 2.6V.

8.2.6 Two Chamber Nafion

Many experiments were performed in the two-chamber cell separated with nafion CEM with $Et_4NF*4HF$ with no product yields. Several different solvents, such as MeCN, TFE and HFIP, were investigated, as well as varying the supporting electrolytes, such as TBAP and TBAHFP. It was determined that without additional methods to reduced acidity, NCA-ECF is unlikely in the two-chamber cell separated by CEM for this precursor.

8.3 No-Carrier-Added ^{18}F ECF of F-DOPA Intermediary Molecule

NCA-ECF of the F-DOPA Intermediate di-tertbutyl-(4-[18F]fluoro-1,2-phenylene)-dicarbonate was performed using 10 mM of triethylamine acetic acid (Et_3N*3HAc) and 100 mM TBAP in MeCN with electrolysis for 60 mins [74]. The RCFE was 6.8 ± 1.3 % (n=3) and specific activity of up to 13 GBq/umol. This was 300 times higher than the carrier added synthesis. The oxidation potential of acetic acid is 0.9V (Ag/Ag+) which was much lower than the precursor and did not interfere with fluorination. Using only 10 mM of acetic acid and passing it through a column with phosphorous pentoxide to remove trace water could potentially form acetic anhydride. It is difficult to determine the acidity in the electrochemical cell especially after electrolysis and the redox of acetic acid or anhydride. The lower concentration of acid may help the stability of the t-butyl leaving group increasing ECF. Another possible explanation could result from the t-butyl group leaving prior to the ECEC mechanism. The acidity may facilitate the t-butyl cation leaving prior to the BOC protected catechol to proceeding in the ECEC mechanism.

8.3.1 Single Chamber in MeCN

8.3.1.1 Optimization Parameter: Et_3N*3HAc Concentration

The optimal Et_3N*3HAc concentration was 10 mM since lower or higher concentrations, 5 and 15 mM of Et_3N*3HAc respectively, concentration performed worse (Figure 115). This reaction is very sensitive to pH and the results point to slight acidity necessary for the t-butyl cation to be a good leaving group.

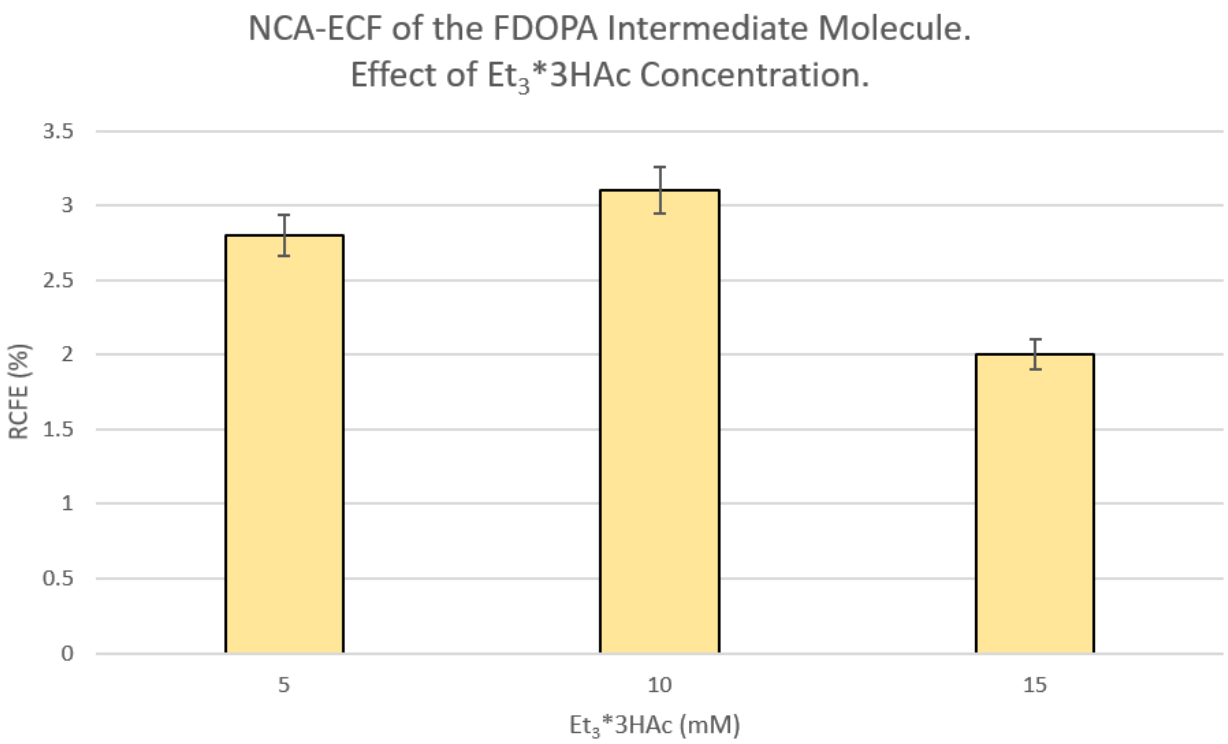

Figure 115: NCA-ECF of the F-DOPA Intermediate Molecule. The optimal Et3N*3HAc concentration was found to be 10 (mM).

8.3.2 Single Chamber in TFE and HFIP

Performing NCA-ECF for the F-DOPA intermediary in MeCN or MeCN with DTBP produced no RCFE in the single chamber cell when using 50 mM TBAP as electrolyte. The oxidation potential was of the precursor is greater than that of the DTBP base which led to poor results due to base oxidation. Switching solvents to TFE and then HFIP also did not produce fluorination yields in the single chamber electrochemical cell. TFE and HFIP are compatible solvents for electrochemistry but their electrochemical window limits these solvents from working well with precursor with higher onset oxidation potentials. Although both TFE and HFIP oxidized at similar onset potentials as the F-DOPA intermediary, many other aromatic molecules including most arenes and this precursor oxidize above this potential. Successful ECF can occur with solvent oxidation but this is mostly limited to when the solvent and precursor have quite similar onset

oxidation potentials. If the solvent has significantly less oxidation onset potential than the precursor, it usually inhibits fluorination.

8.3.3 Two Chamber Cation Exchange Membrane

The two-chamber electrochemical cell was explored using three different solvents and 50 mM TBAP with a cation exchange membrane in-between the chambers. MeCN and TFE did not produce appreciable product radioyields whereas HFIP produced low levels of RCP as measured via HPLC (Figure 116). In Figure 116, CEM refers to the use of the cation exchange membrane in the two-chamber cell where AEM refers the use of the anion exchange membrane.

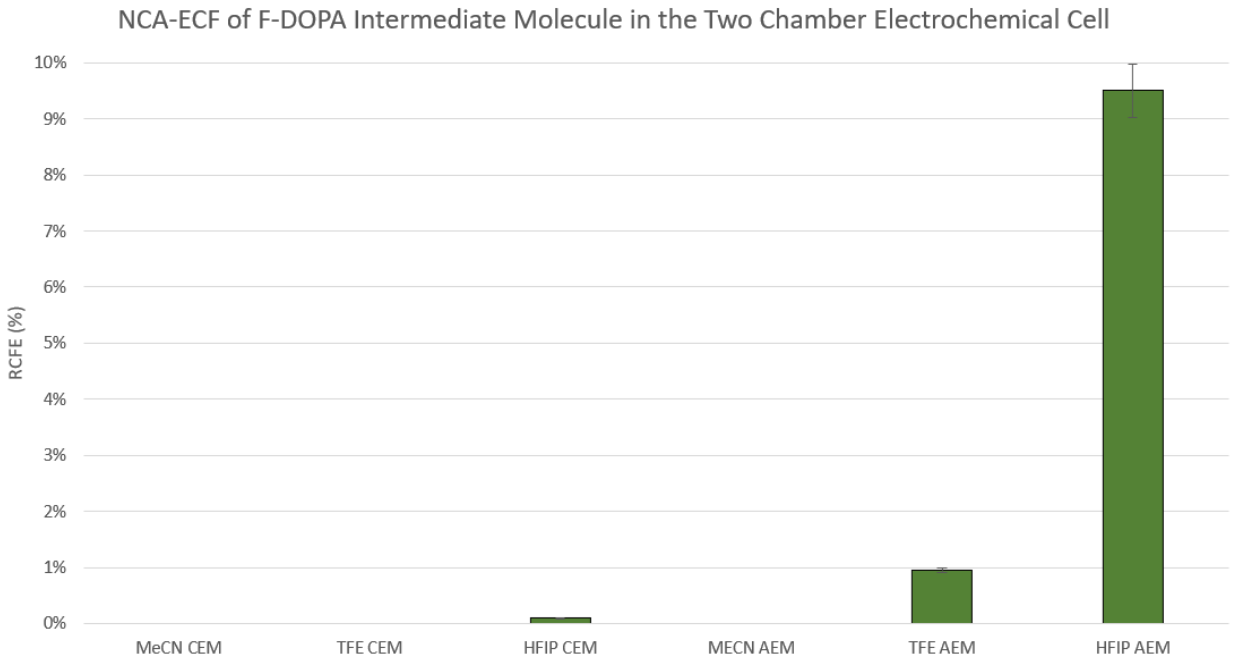

Figure 116: NCA-ECF of the F-DOPA Intermediate Molecule in the two-chamber electrochemical cell. Using the AEM and HFIP was optimal.

8.3.5 Two Chamber Anion Exchange Membrane

Using the anion exchange membrane (AEM) in the two-chamber cell produce higher RCFE than the CEM using 50 mM TBAP. This is likely due to the slower increase in acidity in the anodic

chamber using AEM compared to the CEM. MeCN still did not produce the fluorinated intermediary. TFE produced ~1% RCFE and HFIP resulted in an RCFE of 9.5±0.4% (n=3) (Figure 116). The slight acidity of HFIP may help to stabilize the t-butyl leaving group which has also observed when using low concentration of acetic acid in our previous experiments in the single chamber cell. The reduced acidity during electrolysis using AEM caused improved RCFE measurements in the two-chamber cell. There is a large UV peak on HPLC corresponding to BOC protected catechol, suggesting the removal of the t-butyl group prior to the ECEC mechanism. It may be the case that the t-butyl group hindered the ECF and was likely not a directing group under these conditions. However, this precursor was tested to confirm this.

8.3.6 HPLC and TLC of the F-DOPA Intermediate Molecule

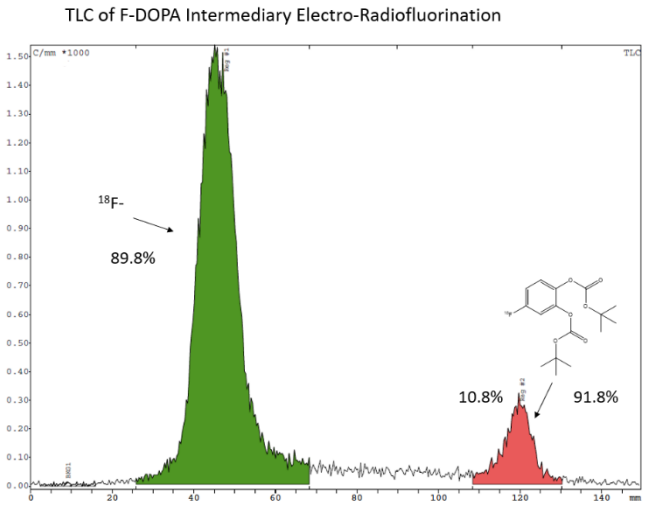

Figure 117: TLC after NCA-ECF of the F-DOPA Intermediary.

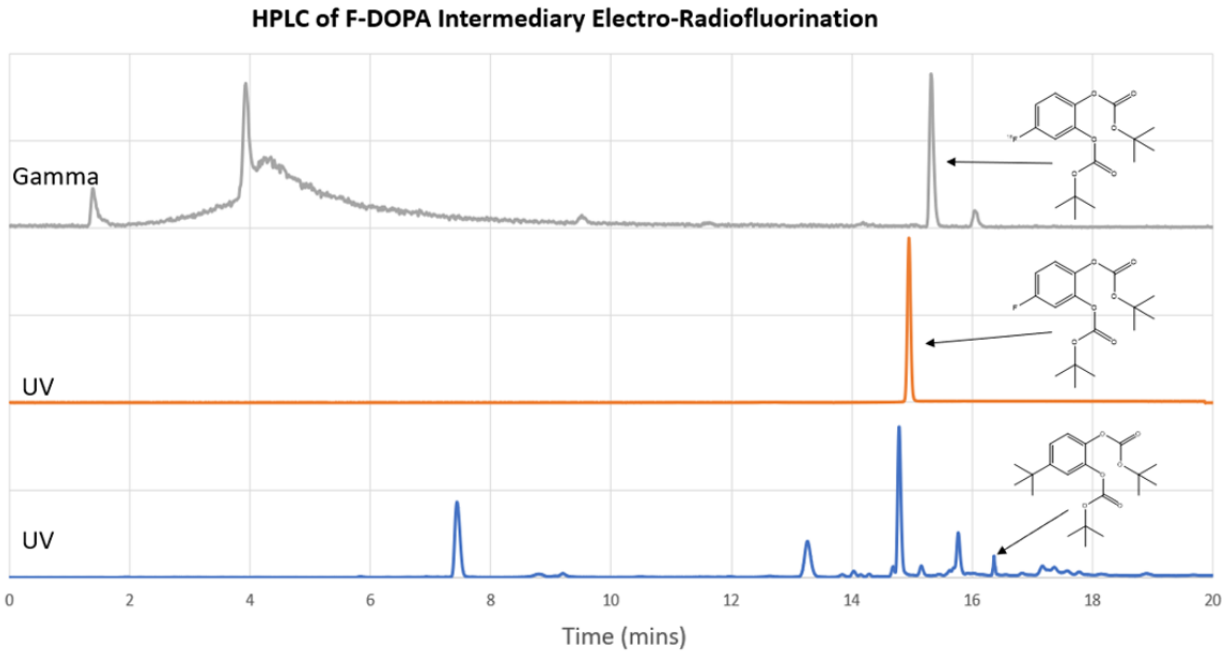

Figure 118: HPLC after NCA-ECF of the F-DOPA Intermediary. (Bottom) UV after electrolysis. (Middle) UV of isolated product. (Top) NCA-ECF Gamma signal of the product.

8.3.7 Data Summary of the F-DOPA Intermediate Molecule

NCA-ECF of the BOC Protected F-DOPA Intermediary Molecule										
#	Cell Type	Temp (°C)	Time	Additive (mM)	Solvent	Membrane	Starting Activity (mCi)	RCC (%)	RCP(%)	RCFE (%)
Best 3	Two Chamber	70	60	-	HFIP	Anion	25.8±3.4	10.4±0.4	90.6±0.9	9.5±0.4
1	Single Chamber	70	30	-	MeCN	-	1.83	0.0%	0.0%	0.0%
2	Single Chamber	70	30	-	MeCN	-	1.57	0.0%	0.0%	0.0%
3	Single Chamber	20	30	Ditertbutylpyridine 50 mM	MeCN	-	1.99	0.0%	0.0%	0.0%
4	Single Chamber	20	30	Ditertbutylpyridine 50 mM	MeCN	-	1.60	0.0%	0.0%	0.0%
5	Single Chamber	70	30	-	TFE	-	2.71	0.0%	0.0%	0.0%
6	Single Chamber	70	30	-	TFE	-	2.47	0.0%	0.0%	0.0%
7	Single Chamber	70	30	-	HFIP	-	1.55	0.0%	0.0%	0.0%
8	Single Chamber	70	30	-	HFIP	-	1.26	0.0%	0.0%	0.0%
9	Two Chamber	70	60	-	MeCN	Cation	19.1	0.0%	0.0%	0.0%
10	Two Chamber	70	60	-	MeCN	Cation	16.3	0.0%	0.0%	0.0%
11	Two Chamber	70	60	-	TFE	Cation	23.8	0.0%	0.0%	0.0%
12	Two Chamber	70	60	-	TFE	Cation	20.2	0.0%	0.0%	0.0%
13	Two Chamber	70	60	-	HFIP	Cation	18.7	0.7%	trace	trace
14	Two Chamber	70	60	-	HFIP	Cation	14.9	0.9%	trace	trace
15	Two Chamber	70	60	-	MeCN	Anion	26.0	0.0%	0.0%	0.0%
16	Two Chamber	70	60	-	MeCN	Anion	22.6	0.0%	0.0%	0.0%
17	Two Chamber	70	60	-	TFE	Anion	23.3	1.1%	77.3%	0.9%
18	Two Chamber	70	60	-	TFE	Anion	19.4	1.4%	74.8%	1.0%
19	Two Chamber	70	60	-	HFIP	Anion	29.8	10.8%	91.8%	9.9%
20	Two Chamber	70	60	-	HFIP	Anion	26.1	10.6%	89.6%	9.5%
21	Two Chamber	70	60	-	HFIP	Anion	21.5	9.9%	90.4%	8.9%
All experiments used 50 mM Precursor and TBAP, stirring at 600 RPM, oxidation voltage of 2.0V										

Figure 119: Data Summary of the NCA-ECF of the F-DOPA Intermediary Molecule.

Chapter 9: Carrier Added ECF of a COX-2 Inhibitor Probe

9.1 Introduction into Potential PET Inflammation Probes

Inflammation is common in many different types of medical conditions and diseases, such as injury, arthritis, viral or bacterial infection, asthma, Crohn's disease, and hepatitis [140]. Carcinogenesis and inflammation are closely linked with most tumors being associated with an increase in inflammation. Neuroinflammation is common in many neurodegenerative diseases such as Alzheimer's disease (AD), Parkinson's disease (PD), amyotrophic lateral sclerosis (ALS) and multiple sclerosis (MS) [141-144]. A PET inflammation probe could help diagnosis and provide additional information to help manage some of these inflammatory conditions.

There have been many attempts to make a successful PET inflammation probe but none have been useable for a wide scope and translated for routine use in the clinic. A recent review on inflammation PET probes [145],mentions only 3 types of probes can cross the Blood Brain barrier (BBB) with targets in the CNS. These experimental PET probes for neuroinflammation are translocator protein (TSPO), cannabinoid type 2 receptor (CB_2R) and Cyclooxygenase-2 (COX-2) Inhibitor [145]. TSPO PET probes have been tested for over a decade and are on the third generation. However, TSPO probes have different expression in for different human phenotypes of translocator proteins on microglia that generates strong, mixed and weak binding affinities based on heterogeneity of genes in the human population [146-148]. CB_2R is another activated microglia PT tracer that is currently being tested in small animal models [149-151]. COX-2 Inhibitor PET probes bind to COX-2, an enzyme, which regulates the conversion of arachidonic acid to various prostanoids and their downstream products initiating inflammation [152]. Several different COX-2 PET probes have been tested but had many problems such as low *in vivo* stability

or low binding affinity [153, 154]. Thus, developing a useable COX-2 inhibitor PET probe without these limitations will be valuable for medical and scientific applications.

9.2 Introduction into Potential COX-2 Inhibitor PET Probes

There are many types and variation on COX-2 inhibitors that have been developed for therapeutic applications [152] but a translatable PET tracer for COX-2 expression in clinical applications has not been developed. COX-2 inhibitor PET probes so far have suffered from low metabolic stability or have had low affinity to the enzyme [154, 155]. The possible applications for a successful COX-2 inhibitor PET probe could be vast. Many processes in carcinogenesis are correlated with COX-2 overexpression such as apoptosis, angiogenesis, cell proliferation, invasiveness and metastasis. Epigenetic and genetic studies have shown a correlation between COX-2 expression and carcinogenesis [152, 156]. COX-2 inhibitors have had anti-cancer effects [157] and is up-regulated in inflamed tissues, as well as most malignant brain tumors [158]. Several studies indicate that COX-2 overexpression may induce neuronal degeneration [159], providing evidence that COX-2 inhibitor probe would be an effective neuroinflammation marker.

9.3 Carrier Added Electrochemical Fluorination of a COX-2 Inhibitor Probe

We have designed a COX-2 inhibitor probe that is based off a celecoxib analog, a popular anti-inflammatory drug that inhibits COX-2, with fluoride attached to the pyrazole ring (Figure 113). This COX-2 inhibitor probe has low nanomolar affinity to the enzyme and a fluoride bond directly attached to the heteroaromatic moiety. This is important since our structural studies show that bulky substituents on COX-2 inhibitors are not well tolerated [160]. Additionally, PET probes with fluorine attached to aromatic rings have better *in vivo* stability [161, 162]. Using electrochemistry, a high affinity ^{18}F labelled COX-2 inhibitor was labeled on the heteroaromatic

ring with favorable biodistribution and metabolic stability in our previous works [75, 76]. Using the automated electrochemical platform up to 5 mCi of the probe was synthesized in 4 hours with up to 2% radiochemical yield. *In vitro* studies showed clear correlation of tracer uptake and COX-2 expression. Metabolism data from *in vivo* testing showed more than 95% of the injected activity remains in the form of the parent molecule after 1 hr., which was positive preliminary data with this tracer.

9.3.1 Carrier Added COX-2 Inhibitor Probe Synthesis

The electrofluorination method used carrier added $Et_4NF*4HF$ fluoride source to radiolabel the pyrazole moiety in the celecoxib analog (Figure 120). Electrolysis was performed at an oxidation potential of 2.7V (Ag/Ag+) for 4 seconds and 0.3V (Ag/Ag+) for 1 second to prevent surface fouling and passivation in the ERCP electrochemical cell. The radiochemical yield was determined to be between 0.8-2% making up to 5 mCi of the final purified PET probe.

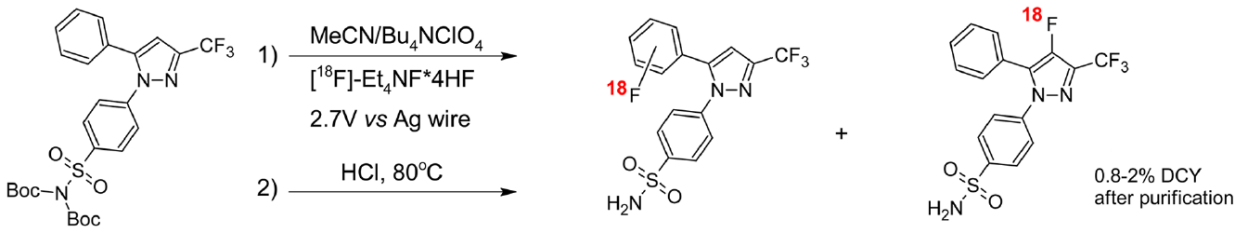

Figure 120: Scheme of the Carrier Added ECF of the COX-2 Inhibitor Probe.

The first step is the electrolysis of the BOC protected precursor which involves producing the fluorinated product with fluoride on the pyrazole ring and a side product with fluoride on the arene (Figure 111). HCl and heat are then added to remove the BOC protection. The unprotected precursor without the BOC groups was also tested as the initial precursor resulting in no product

formation. Then the product was isolated by HPLC separation with the ERCP subsystem. The ECF steps are seen in Figure 121 with the ECEC proposed mechanism.

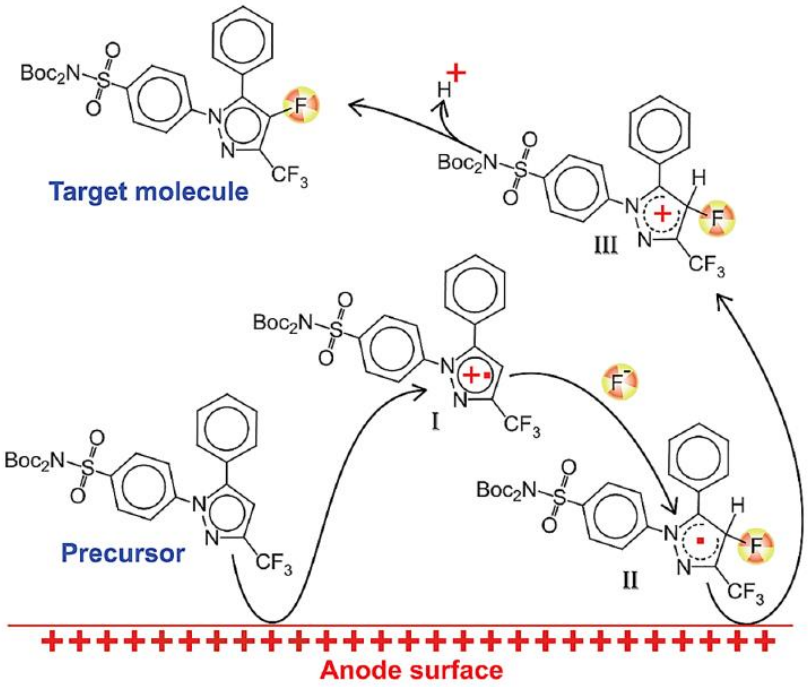

Figure 121: ECEC mechanism of ECF for the COX-2 Inhibitor Probe.

In the ECEC mechanism of the COX-2 inhibitor probe (Figure 121), the pyrazole ring is oxidized and anionic F- attacks the radical cation followed by oxidation again and proton abstraction. There are several potential problems with this mechanism. First, the neutral fluorinated radical is more likely to diffuse into the bulk solution than to travel back to the anode to be oxidize again. Second, the neutral fluorinated radical has a higher oxidation potential than the precursor so is less preferred thermodynamically than the precursor for oxidation. In the discussion section, alternatives will be proposed to this mechanism.

9.3.2 HPLC and ^{19}F-NMR of the COX-2 Inhibitor Probe

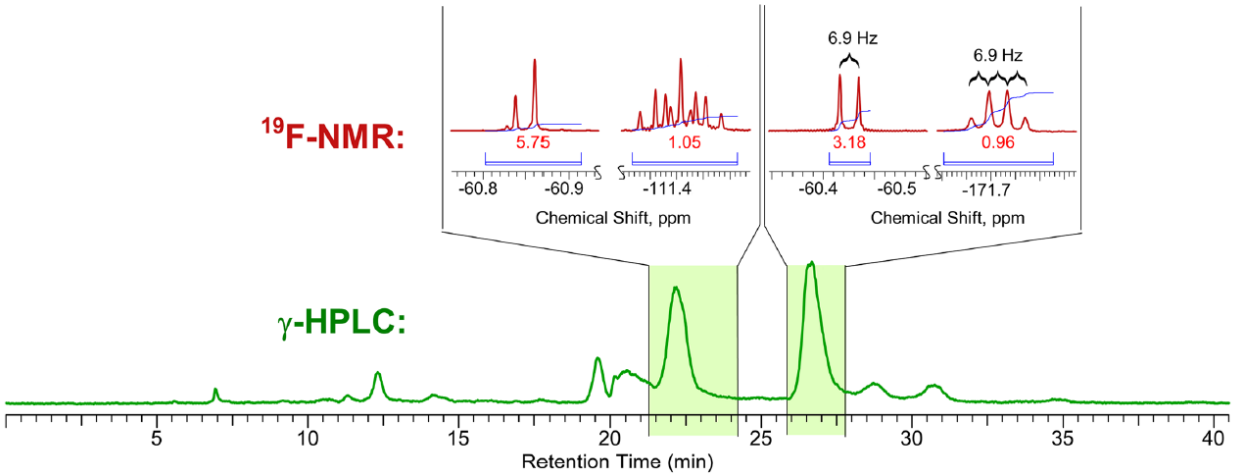

Figure 122: HPLC and ^{19}F-NMR of the COX-2 Inhibitor Probe. The Fluorinate Arene has a retention time around 22 mins. The product with the fluorination on the pyrazole ring has a retention time around 27 mins.

9.3.3 In Vitro Cell Uptake Studies

In vitro cell studies show uptake of COX-2 inhibitor probe with increasing lipopolysaccharides (LPS) concentration which activates the immune system and produces inflammation which was blocked by celecoxib (Figure 123). The COX-2 enzyme is a homodimer in the nuclear envelope of the endoplasmic reticulum [163, 164], which is bonded to the membrane surface by the intermembrane domain [165]. The COX-2 inhibitor probe needs to diffuse through two membranes to reach the COX-2 enzyme. Most celecoxib binding was found to be in the plasma. This may indicate the tracer is bound to cytostolic proteins [166]. There may be many intermediate steps to uptake but the probes dissociation from the COX-2 enzyme is the slowest step due to increased tracer uptake with inflammation.

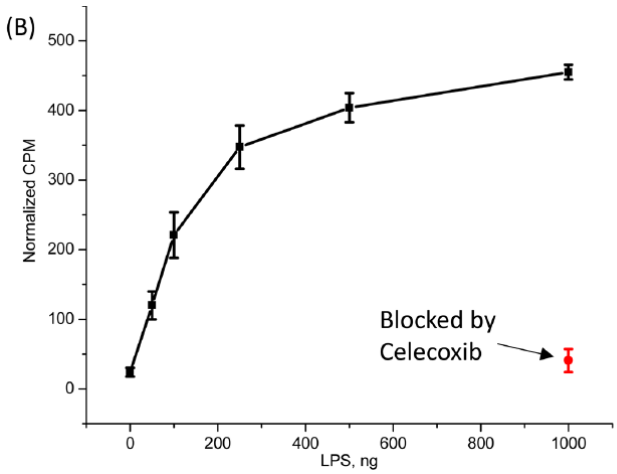

Figure 123: Increased COX-2 Inhibitor Probe with increased LPS Concentration which causes inflammation.

9.3.4 In Vivo Cell Metabolism Studies

The *in vivo* metabolism studies in mice showed that over 95% of the probe was intact from samples of the urine, kidney, brain, liver, small intestines and blood plasma (Figure 124). There was some degradation of products that accounted for less than 1% of the injected activity in the urine.

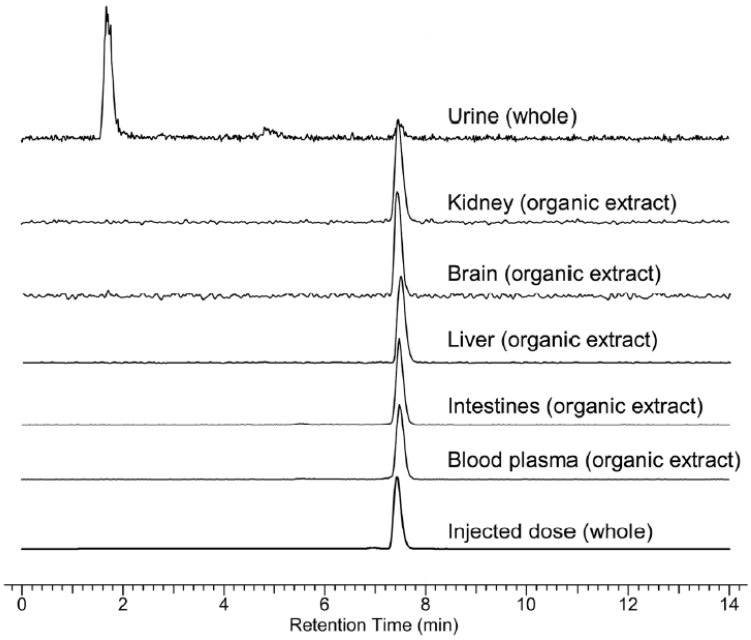

Figure 124: The in vivo cell metabolism studies showed that the probe remains intact in the organs.

9.3.5 Ex Vivo Biodistribution

The *ex vivo* biodistribution is shown in Figure 125. The brain has a significant amount of uptake suggesting the probe may be useful for neuroimaging.

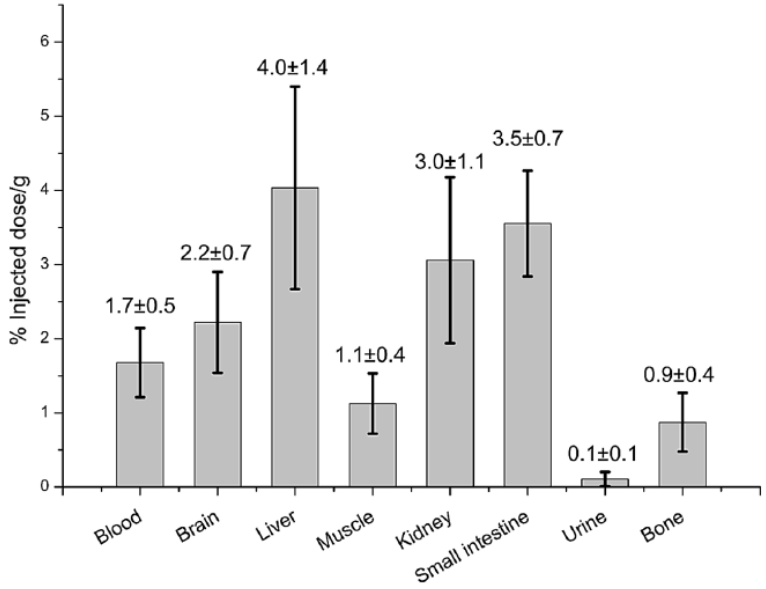

Figure 125: Ex Vivo Biodistribution of the COX-2 Inhibitor Probe.

9.3.6 PET Imaging

Static and dynamic PET imaging studies were performed with region of interest (ROI) analysis (Figure 119) which agreed to ex-vivo biodistribution data that supported the probe's high metabolic stability *in vivo*. There was no ^{18}F bone uptake or free ^{18}F in the blood, which would suggest defluorination. The PET image data showed the COX-2 Inhibitor probe crossed the blood brain barrier (BBB) with no major metabolites present in the major organs. The probe metabolic behavior is different to that of celecoxib because it lacks the methyl group responsible for oxidation and further breakdown [167]. Almost all major organs showed activity that stabilized at no more than twice that of the muscle, suggesting the probe has good image contrast. The brain radioactivity decreased and then stabilized at twice the uptake of muscle which indicates the tracer crosses the

BBB with good washout of unbound probe. This may indicate the possibly for using this probe for neuroinflammation. The time activity profile for the COX-2 inhibitor probe can be seen in Figure 126.

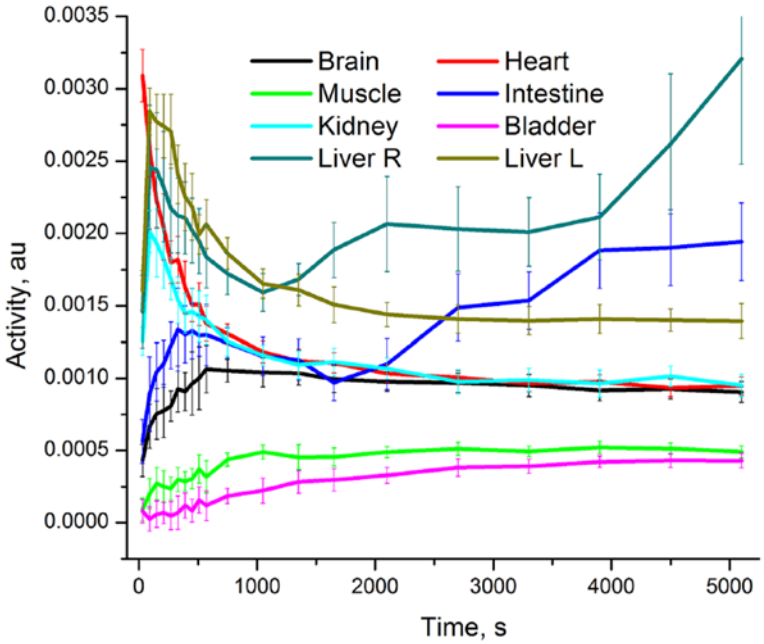

Figure 126: Time Activity Profile of the COX-2 Inhibitor Probe.

Chapter 10: No-Carrier-Added ^{18}F ECF of a COX-2 Inhibitor Probe

10.1 Single Chamber Electrochemical Cell

MeCN, DME, TFE, and HFIP were tested in the single chamber electrochemical cell with and without DTBP using TBAP as electrolyte. DME was the only solvent that produced trace results. The other solvents did not radioyields (Figure 132).

10.2 Two Chamber Electrochemical Cell

Studies using MeCN, DME, TFE, and HFIP were repeated in the two-chamber electrochemical cell with a cation exchange membrane between the two chambers. MeCN, TFE, and HFIP did not produce product radioyields whereas DME had above trace levels at 0.2% RCFE (Figure 120). The anion exchange membrane was also tested with the same solvents. DTBP had a lower oxidation potential and interfered with ECF at the oxidation potential of 2.7V (Ag/Ag+) so it was instead added to the cathodic chamber (CC). In this manner, the protons would diffuse more rapidly out of the anodic chamber leading less acidity. Without using DTBP in the CC, MeCN had 0% RCFE while experiments with 500 mM DTBP in the CC had RCFE of up to 1.3% when using the AEM. DME performed similarly using the AEM with 500 mM DTBP in the CC with RCFE of 1.2%. TFE and HFIP had no product formation as detected via HPLC (Figure 127). We reasoned this is likely due to the onset oxidation potential of the COX-2 inhibitor precursor being above the stable electrochemical window of TFE and HFIP.

10.3 Two Chamber with additional Proton Sink Chamber

An additional chamber was added to the anodic chamber with nafion CEM separating the chambers to further reduce the acidity in the anodic chamber. 500 mM of DTBP was added to this proton sink chamber which increased the RCFE using the DME solvent up to 2.1$\pm$0.2% (n=2), as

well as the RCFE using MeCN and AEM up to 6.8±0.7 (n=3) under NCA condition for the COX-2 inhibitor probe (Figure 127). The lower result in DME was likely caused by the decrease current from the lower conductivity of the solvent. This result is promising due to the poor image quality of the previous synthesized COX-2 inhibitor probe under carrier added conditions due to low molar activity. The increase molar activity using the NCA method may improve PET image quality.

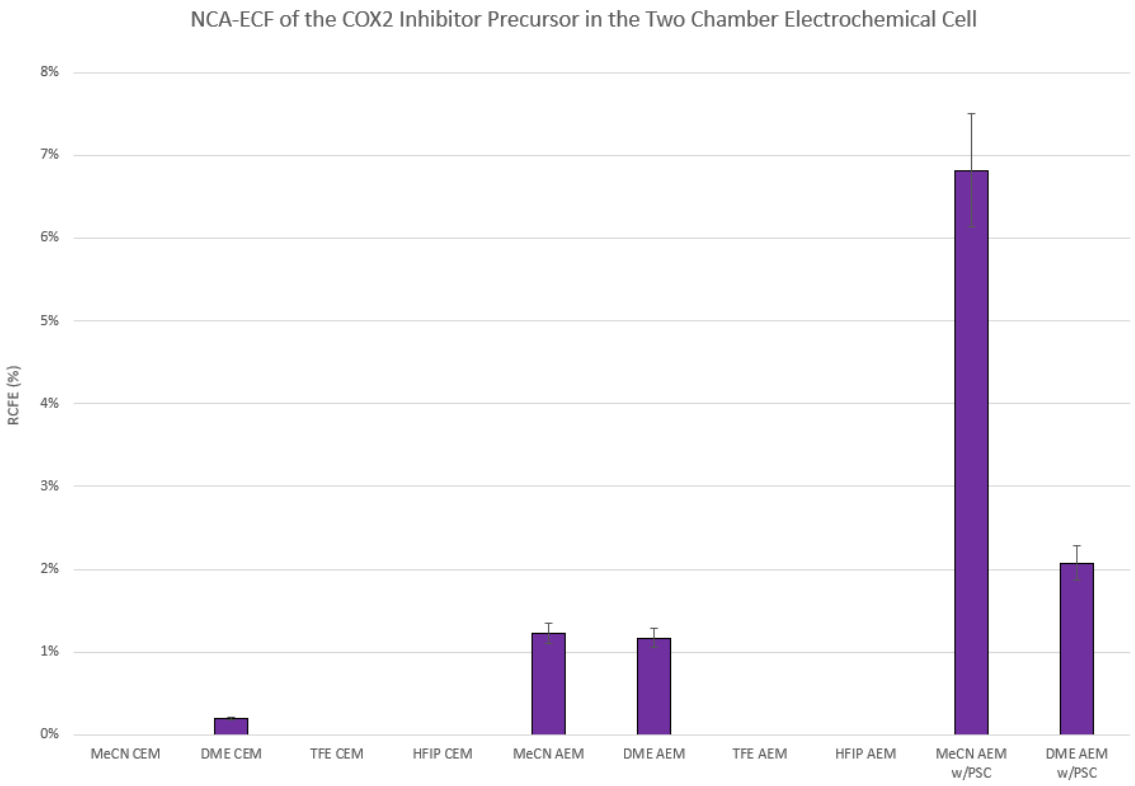

Figure 127: NCA-ECF of the COX-2 Inhibitor Probe in the Two-Chamber Electrochemical Cell.

10.4 HPLC and TLC of COX-2 Inhibitor Probe

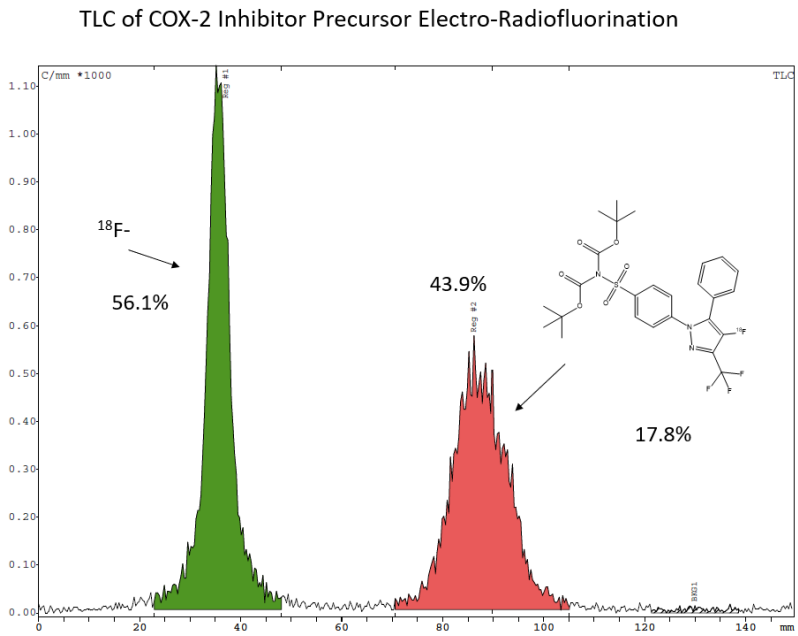

Figure 128: TLC after NCA-ECF of the COX-2 Inhibitor Probe.

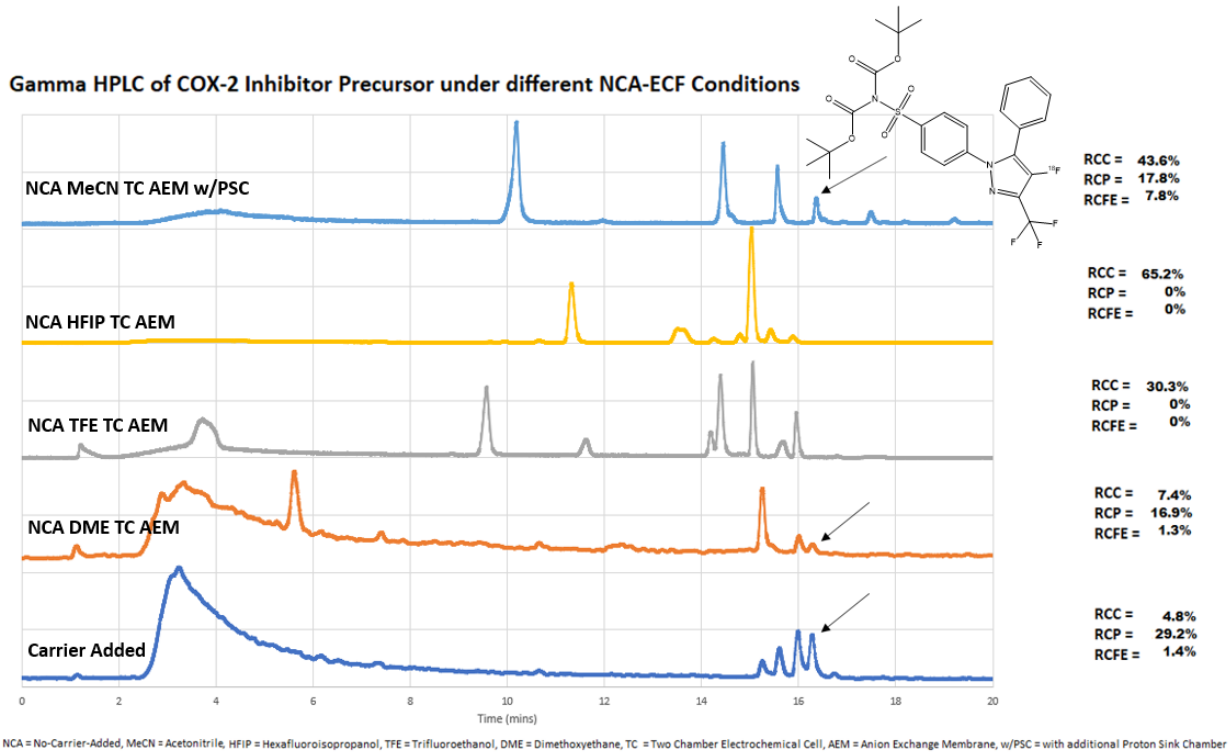

Figure 129: HPLC after NCA electrolysis of the COX-2 Inhibitor Probe using different solvents in the two-chamber cell with the anion exchange membrane (AEM) and top with additional proton sink chamber (PSC).

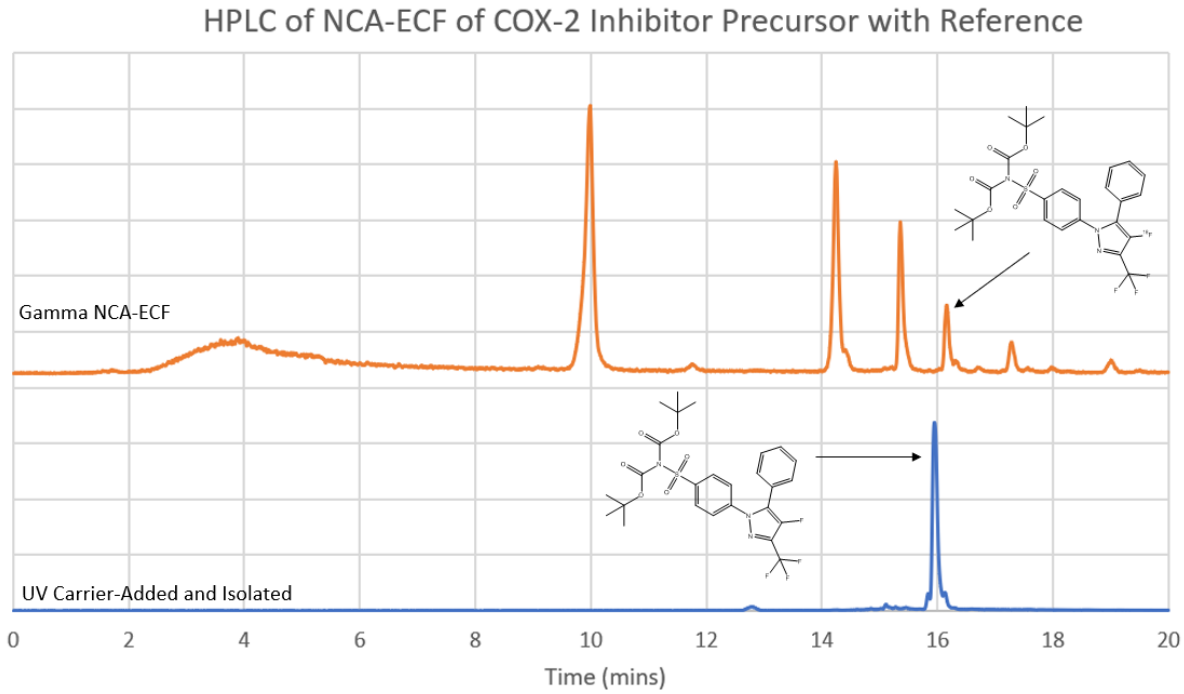

Figure 130: HPLC after NCA electrolysis of the COX-2 Inhibitor Probe. (Top) Gamma after electrolysis. (Bottom) Reference from synthesis with $Et_4NF*4HF$.

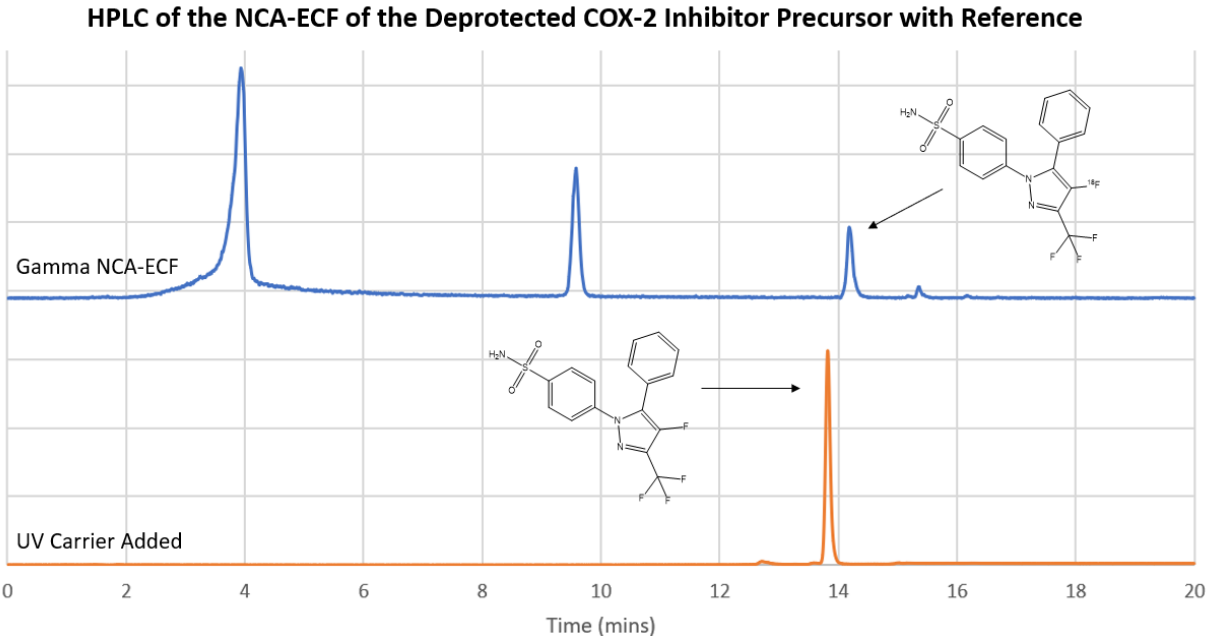

Figure 131: HPLC after NCA electrolysis and BOC deprotection in HCl of the COX-2 Inhibitor Probe. (Top) Gamma after electrolysis. (Bottom) Reference from synthesis with Et4NF*4HF.

Similar to Methyl (phenylthio) Acetate in NCA-ECF, the COX-2 inhibitor precursor formed many different radio side products in different solvents and electrochemical conditions (Figure 129). These fluorinations may have applications in a variety of fields. Again, changing the solvent had the largest effect on which radio side products were produced. Under carrier added condition, there are three main radio side products in the 15-16 min range on HPLC approximately at 1-2% RCFE. DME under NCA conditions had a larger side product peak at 15 mins at ~5% RCFE. Both TFE and HFIP did not form the fluorinated product under NCA conditions but did form many radio side products in the 1-15% RCFE range. Even under optimal conditions using the MeCN with AEM in the two-chamber cell with proton sink chamber resulted in three larger radio side products that were mostly inconsistent with the other solvents and even MeCN under carrier added conditions.

The COX-2 inhibitor precursor has multiple oxidation sites at the potential of 2.7V (Ag/Ag+) which was necessary to oxidize the pyrazole ring. The other two arene aromatic rings and the BOC protecting groups can be oxidized at this potential. One challenged we encountered was the ability to oxidize a large oxidation potential target found within the pyrazole ring. There will be radio side product formation from oxidation of untargeted sites in the organic molecule. Similar to side products formation using Methyl (phenylthio) Acetate, it was difficult to isolate and identify each side products since they may not form under carrier added conditions.

In Figure 130, the carrier added synthesis of the COX-2 inhibitor probes was successfully performed and the product was isolated and verified by NMR and GC. This standard was used on HPLC to verify the NCA-ECF of the COX-2 inhibitor probe product. The NCA product was also deprotected and validated against the deprotected product standard on HPLC (Figure 131). The

NCA protected or unprotected product both match up with the standard and unprotected standard for the fluorinated COX-2 inhibitor probe.

10.5 Data Summary of COX-2 Inhibitor Probe

NCA-ECF of the BOC Protected COX-2 Inhibitor Precursor

#	Cell Type	Temp (°C)	Time	Additive (mM)	Solvent	Membrane	CC Additive (mM)	Sink Membrane	Sink Chamber (mM)	Starting Activity (mCi)	RCC (%)	RCP(%)	RCFE (%)
Best 3	Two Chamber w Sink Chamber	20	120	-	MeCN	Anion	-	Nafion	Ditertbutylpyridine 500 mM	39.1+1.6	40.9+2.2	16.6+0.8	6.8+0.7
1	Single Chamber	70	30	-	MeCN	-	-	-	-	1.62	0.0%	0.0%	0.0%
2	Single Chamber	70	30	-	MeCN	-	-	-	-	1.43	0.0%	0.0%	0.0%
3	Single Chamber	20	30	Ditertbutylpyridine 50 mM	MeCN	-	-	-	-	1.98	10.3%	0.0%	0.0%
4	Single Chamber	20	30	Ditertbutylpyridine 50 mM	MeCN	-	-	-	-	1.62	12.5%	0.0%	0.0%
5	Single Chamber	70	30	-	DME	-	-	-	-	2.37	0.0%	0.0%	0.0%
6	Single Chamber	70	30	-	DME	-	-	-	-	2.08	0.0%	0.0%	0.0%
7	Single Chamber	70	30	Ditertbutylpyridine 50 mM	DME	-	-	-	-	2.11	0.9%	trace	trace
8	Single Chamber	70	30	Ditertbutylpyridine 50 mM	DME	-	-	-	-	1.84	0.7%	trace	trace
9	Single Chamber	70	30	-	TFE	-	-	-	-	1.86	0.0%	0.0%	0.0%
10	Single Chamber	70	30	-	TFE	-	-	-	-	1.42	0.0%	0.0%	0.0%
11	Single Chamber	70	30	Ditertbutylpyridine 50 mM	TFE	-	-	-	-	1.30	0.0%	0.0%	0.0%
12	Single Chamber	70	30	Ditertbutylpyridine 50 mM	TFE	-	-	-	-	1.19	0.0%	0.0%	0.0%
13	Single Chamber	70	30	-	HFIP	-	-	-	-	1.51	0.0%	0.0%	0.0%
14	Single Chamber	70	30	-	HFIP	-	-	-	-	1.15	0.0%	0.0%	0.0%
15	Single Chamber	70	30	Ditertbutylpyridine 50 mM	HFIP	-	-	-	-	2.19	0.0%	0.0%	0.0%
16	Single Chamber	70	30	Ditertbutylpyridine 50 mM	HFIP	-	-	-	-	1.92	0.0%	0.0%	0.0%
17	Two Chamber	20	30	-	MeCN	Cation	-	-	-	24.8	3.5%	0.0%	0.0%
18	Two Chamber	20	30	-	MeCN	Cation	-	-	-	20.3	2.7%	0.0%	0.0%
19	Two Chamber	20	60	-	MeCN	Cation	Triethylamine 100 mM	-	-	22.1	6.1%	0.0%	0.0%
20	Two Chamber	20	60	-	MeCN	Cation	Triethylamine 100 mM	-	-	18.6	6.6%	0.0%	0.0%
21	Two Chamber	20	60	-	MeCN	Cation	Ditertbutylpyridine 500 mM	-	-	27.7	51.2%	0.0%	0.0%
22	Two Chamber	20	60	-	MeCN	Cation	Ditertbutylpyridine 500 mM	-	-	24.1	38.7%	0.0%	0.0%
23	Two Chamber	20	60	-	TFE	Cation	-	-	-	25.4	0.0%	0.0%	0.0%
24	Two Chamber	20	60	-	TFE	Cation	-	-	-	23.7	0.0%	0.0%	0.0%
25	Two Chamber	20	60	-	HFIP	Cation	-	-	-	19.1	0.0%	0.0%	0.0%
26	Two Chamber	20	60	-	HFIP	Cation	-	-	-	16.9	0.0%	0.0%	0.0%
27	Two Chamber	20	60	-	DME	Cation	-	-	-	28.7	3.7%	5.1%	0.2%
28	Two Chamber	20	60	-	DME	Cation	-	-	-	23.0	4.2%	4.6%	0.2%
29	Two Chamber	20	60	-	MeCN	Anion	-	-	-	23.3	33.5%	0.0%	0.0%
30	Two Chamber	20	60	-	MeCN	Anion	-	-	-	19.3	29.9%	0.0%	0.0%
31	Two Chamber	20	60	-	MeCN	Anion	Ditertbutylpyridine 500 mM	-	-	25.7	38.4%	3.4%	1.3%
32	Two Chamber	20	60	-	MeCN	Anion	Ditertbutylpyridine 500 mM	-	-	20.8	41.3%	2.8%	1.2%
33	Two Chamber	20	60	-	TFE	Anion	Ditertbutylpyridine 500 mM	-	-	20.6	28.1%	0.0%	0.0%
34	Two Chamber	20	60	-	TFE	Anion	Ditertbutylpyridine 500 mM	-	-	16.4	30.3%	0.0%	0.0%
35	Two Chamber	20	60	-	HFIP	Anion	Ditertbutylpyridine 500 mM	-	-	23.5	65.2%	0.0%	0.0%
36	Two Chamber	20	60	-	HFIP	Anion	Ditertbutylpyridine 500 mM	-	-	18.3	57.9%	0.0%	0.0%
37	Two Chamber	20	60	-	DME	Anion	Ditertbutylpyridine 500 mM	-	-	22.6	6.7%	16.3%	1.1%
38	Two Chamber	20	60	-	DME	Anion	Ditertbutylpyridine 500 mM	-	-	17.7	7.4%	16.9%	1.3%
39	Two Chamber w Sink Chamber	20	60	-	DME	Anion	-	Nafion	Ditertbutylpyridine 500 mM	40.3	10.8%	17.1%	1.8%
40	Two Chamber w Sink Chamber	20	60	-	DME	Anion	-	Nafion	Ditertbutylpyridine 500 mM	44.9	12.4%	18.6%	2.3%
41	Two Chamber w Sink Chamber	20	120	-	MeCN	Anion	-	Nafion	Ditertbutylpyridine 500 mM	37.8	43.6%	17.8%	7.8%
42	Two Chamber w Sink Chamber	20	120	-	MeCN	Anion	-	Nafion	Ditertbutylpyridine 500 mM	38.2	38.2%	16.3%	6.2%
43	Two Chamber w Sink Chamber	20	120	-	MeCN	Anion	-	Nafion	Ditertbutylpyridine 500 mM	41.4	40.9%	15.8%	6.5%

All experiments used 50 mM Precursor and TBAP, stirring at 600 RPM and oxidation voltage of 2.7V. There were several high RCC and no RCP due to unidentified fluorinated side product that is not BOC protected.

Figure 132: Data Summary of the COX-2 Inhibitor Probe

Chapter 11: Cyclic Voltammetry

Cyclic Voltammetry (CV) is an analytical electrochemistry method that changes the working electrode potential linearly with time to produce a graph of current vs. potential due to the oxidation and reduction of the solution in the electrochemical cell. In a reversible reaction the reduction part of the graph will reflect the oxidation part of the graph. The oxidized species will become reduced and the reduced species will become oxidized making this process reversible. The electrochemical conditions of ECF produce mostly non-reversible transitions. The precursor after oxidation on the anode and forming a cation intermediate does not travel to the cathode and become reduced to return to its original form. This can be noted by the reduction peaks as they are minimal compared to the oxidation peaks. After oxidation it is possible for the precursor to return to its original form chemically even though this does not occur through electrical reduction. The is usually not the case for most organic molecules unless they are highly conjugated in stabilizing solvents. The addition of fluoride immediately changes these quick reversible CVs to irreversible due to the fluoride reactivity in the nanosec to microsec range which will be discussed in section 12.3.

The critical CV information in ECF is focused on the onset oxidation of the precursor and the amount of oxidation of the precursor at a given potential. The background is defined as the electrochemical solution without the precursor on the CV graphs. The CV of the precursor have all the constituents of the background. The background CV is much lower than the precursor and consist of solvent and/or electrolyte oxidation and reduction.

The onset oxidation potential is determined by subtracting the CV of the background from the CV containing the precursor. The oxidation of the precursor generates a potential that separates in an exponential manner due to the Nernst equation, which relates oxidation potential to current

in electrochemistry. Usually this exponential trend tappers off due to mass transfer limitations which is mostly due from precursor transfer to the anode surface. An oxidation potential for electrolysis in ECF is chosen to maintain a certain precursor oxidation current above background.

Most organic precursor molecules have several possible oxidation sites. It is important that the lowest or near lowest oxidation site is the fluorination site since oxidation preferentially occurs at lower oxidation sites and can exclude the higher oxidation sites. Protection groups can increase the oxidation potential for unwanted oxidation sites on the precursor molecule. CV is not always a sensitive method at determining much higher oxidation sites than the target site in the electrochemical cells and conditions used here due to the mass transfer limitation at higher oxidation potentials. Additionally, because fluorine is electron withdrawing, the fluorinated product tends to have a higher oxidation potential at the target site and is not as preferentially oxidized as the precursor. This allows the product concentration to buildup while the precursor is continually oxidized. As electrolysis is performed, many side products can result from this which affects the CV and ECF process due to their different oxidation and reduction potentials from the precursor or the original electrochemical solutions constituents. These side products often undergo further redox and chemical reaction with the precursor, solvent or other additives. This is even more evident under NCA conditions due to low concentration of fluoride leads to less than 0.1% formation of fluorinated organics by mass and greater than 99.9% side product formation by mass.

11.1 Thioether Cyclic Voltammetry

The CV of thioether precursors can be seen in Figure 133. The CVs of the thioether precursors before electrolysis are higher than after electrolysis. During electrolysis, the product and side products formed have a much higher oxidation potential which lowers the oxidation peak of the CV at the same potential. These reactions do not go to full completion due to the small concentration of precursor remaining at the end of electrolysis. The background is composed of TFE solvent and TBAP as electrolyte. Thioether compounds do not have significantly different CVs trends between different precursors when performing experiments in the 1.5 ml electrochemical cell.

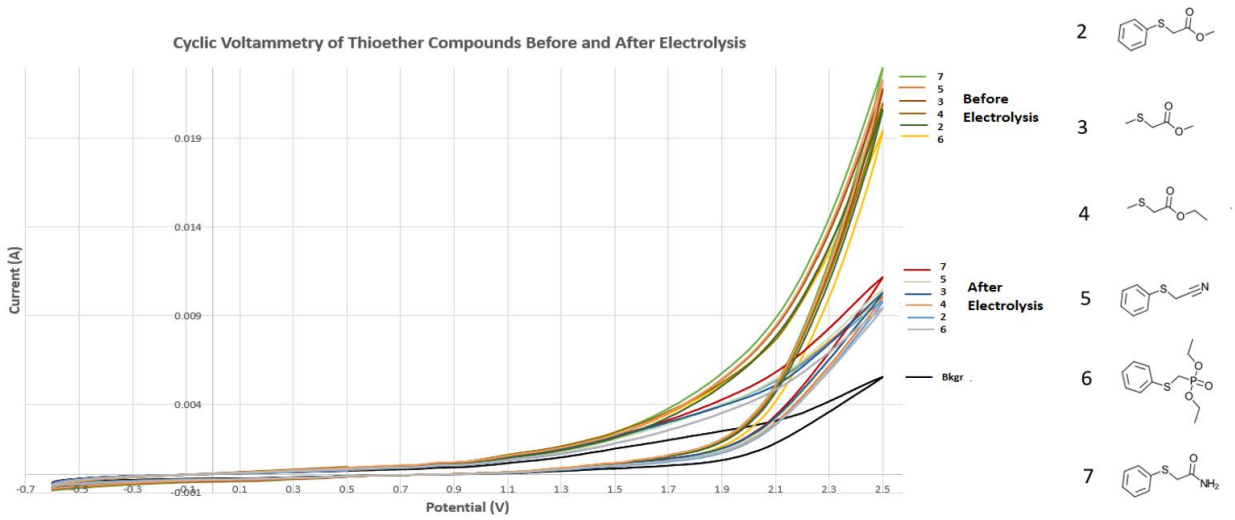

Figure 133: Cyclic Voltammetry of Thioether Compounds Before and After Electrolysis.

11.2 Modafinil Precursor Cyclic Voltammetry

The CV of the modafinil precursor can be seen in Figure 134. The fluorinated product formation required the addition of DTBP base to MeCN with TBAP. DTBP onset oxidation is approx. 2.1V (Ag/Ag+) much higher than the onset of the modafinil precursor at approx. 1.3V

(Ag/Ag+). Performing electrolysis at 2.0V (Ag/Ag+) will almost completely exclude the oxidation of the DTBP while maintaining a high oxidation current from the oxidation of the modafinil precursor. The nitrogen is single BOC protected to raise its oxidation potential and protect the amine group from oxidation. Without BOC protection very little fluorinated product was formed during electrolysis.

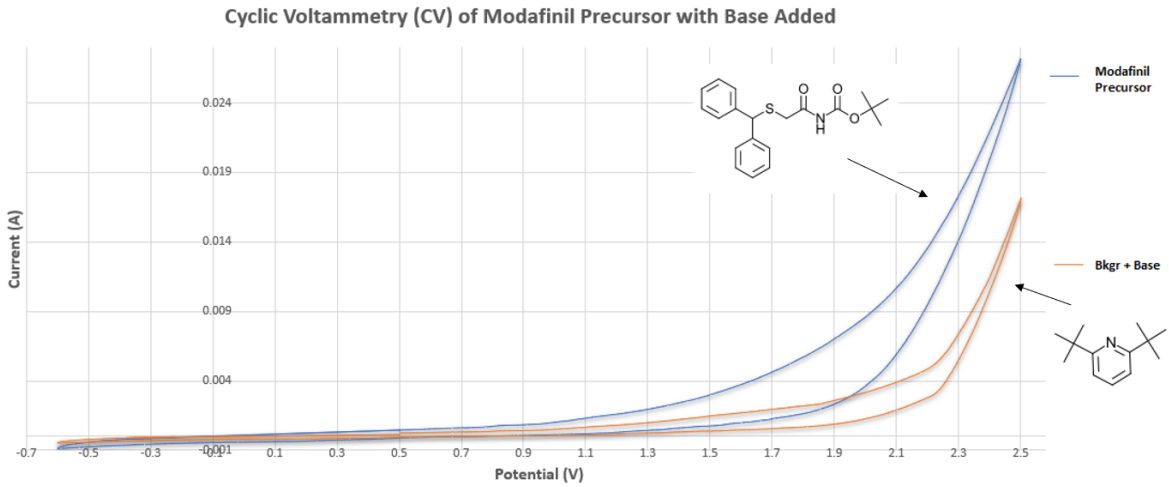

Figure 134: Cyclic Voltammetry of Modafinil Precuror with Base Added.

11.3 Naphthalene Cyclic Voltammetry

The CV of Naphthalene using HFIP solvent and TBAP as electrolyte can be seen in Figure 135. HFIP has a lower dielectric constant and less current at the same voltage as TFE or MeCN. This can be seen with the lower background. The onset oxidation of Naphthalene starts increasing around 1.5V (Ag/Ag+). Naphthalene also has a larger reduction current, this resulted in the CV is performed only to -0.2V instead to -0.6V. It is suspect that the reduction on the cathode of Naphthalene leads to side product formation that could interfere with oxidation and subsequent

fluorination. The optimal reactivity of NCA-ECF using Naphthalene was performed using HFIP as the solvent.

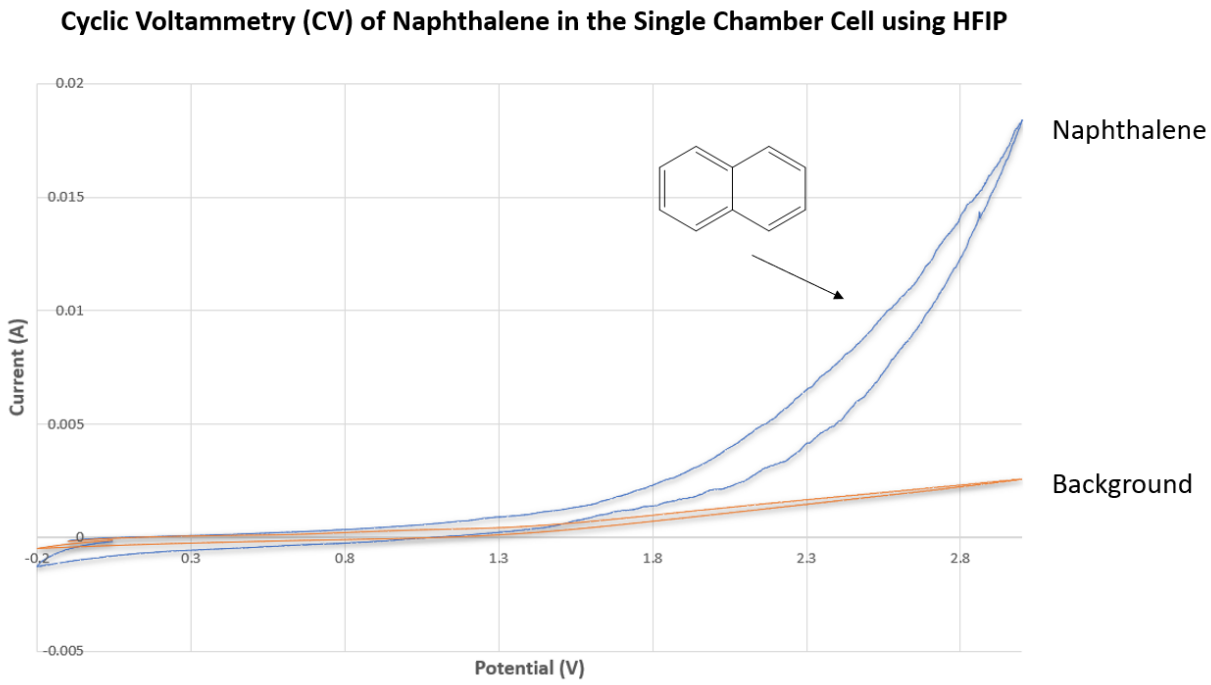

Figure 135: Cyclic Voltammetry of Naphthalene in the Single Chamber Cell using HFIP

11.4 Thioether with Cation Exchange Membrane (CEM)

The CV of Methyl (phenylthio) Acetate in the two-chamber cell is shown in Figure 136. At the higher oxidation potential, the current plateaus due to the nafion CEM membrane limiting the current based on the transport of protons or other small cations through it. The electrochemical conditions should be optimized to reach the desired potential due to this membrane limitation. Adding the precursor causes the current to reach the membrane limitation at lower oxidation potentials. In some conditions, it may reach this limitation before reaching 1.9V (Ag/Ag+). Electrolysis was performed at 1.9V. When using the two-chamber cell for these reactions. The reactions conditions will change with electrolysis and often shift the oxidation potential limitation

to lower oxidation potentials over time. Monitoring the potential during these changing conditions is critical to maintain the proper oxidation potential. Additionally, solvent conditions change during electrolysis such change in pH and side product formation. These changes can shift the membrane plateau to the left, causing a limit at lower oxidation potential often below the oxidation potential of choice for the experiment which will often lead to poor RCFE.

Using the cation membrane cause a quick buildup of acidity in the anodic chamber due to the slow diffusion of protons through the membrane and into the cathodic chamber. This acidity likely causes the poor yields when using the CEM for ECF in the two-chamber electrochemical cell.

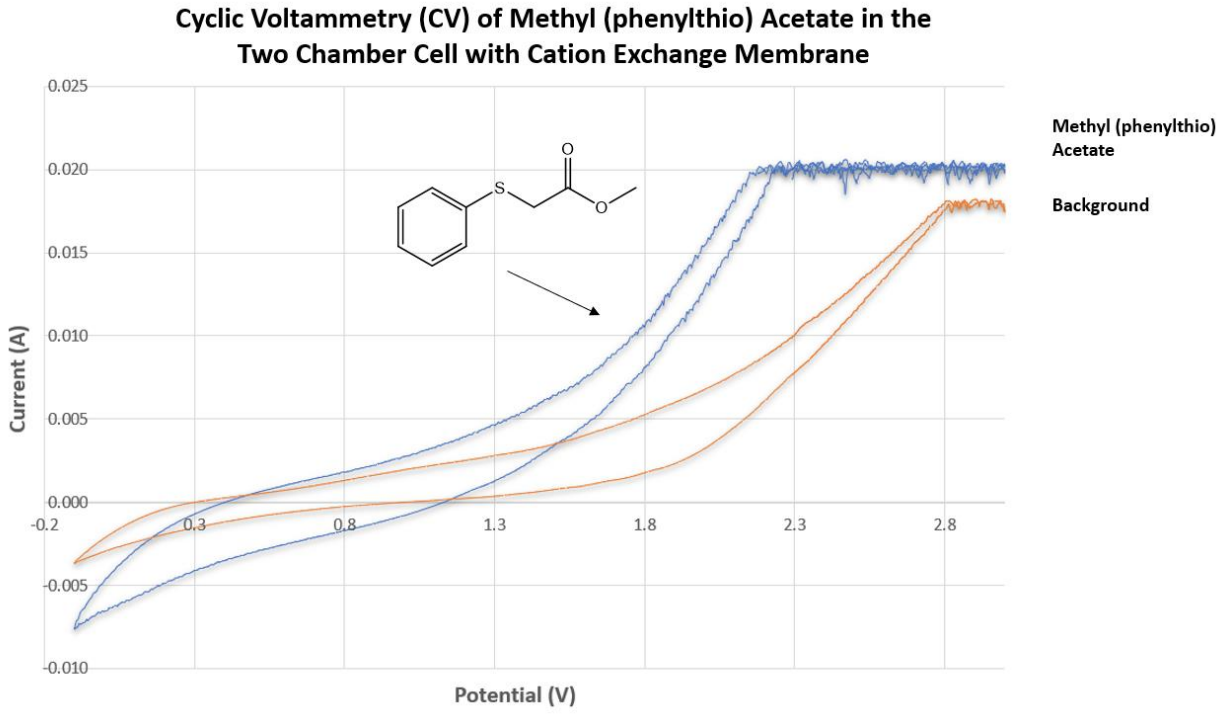

Figure 136: Cyclic Voltammetry of Methyl (phenylthio) Acetate in the Two Chamber Cell with Cation Exchange Membrane.

11.5 F-DOPA Intermediary with Anion Exchange Membrane (AEM)

The CV of F-DOPA Intermediary in the two-chamber electrochemical cell with AEM is noted in Figure 137. Similarly to CEM, the oxidation potential is limited due to the maximum rate ions, in this case anions, are allowed to pass through the membrane. The plateau peak is slightly higher at the beggining which reached the limited current compared to using the CEM which is more flat at the plateau. The onset oxidation potential is approx 1.9V (Ag/Ag+) for the F-DOPA Intermediary precursor. The limiting current is less for the AEM than the CEM but occurs at greater oxidation potential using the same conditions for both membranes. This makes usign the AEM benefical for organic precursor with higher oxidation potentials such as arenes and pyrazoles.

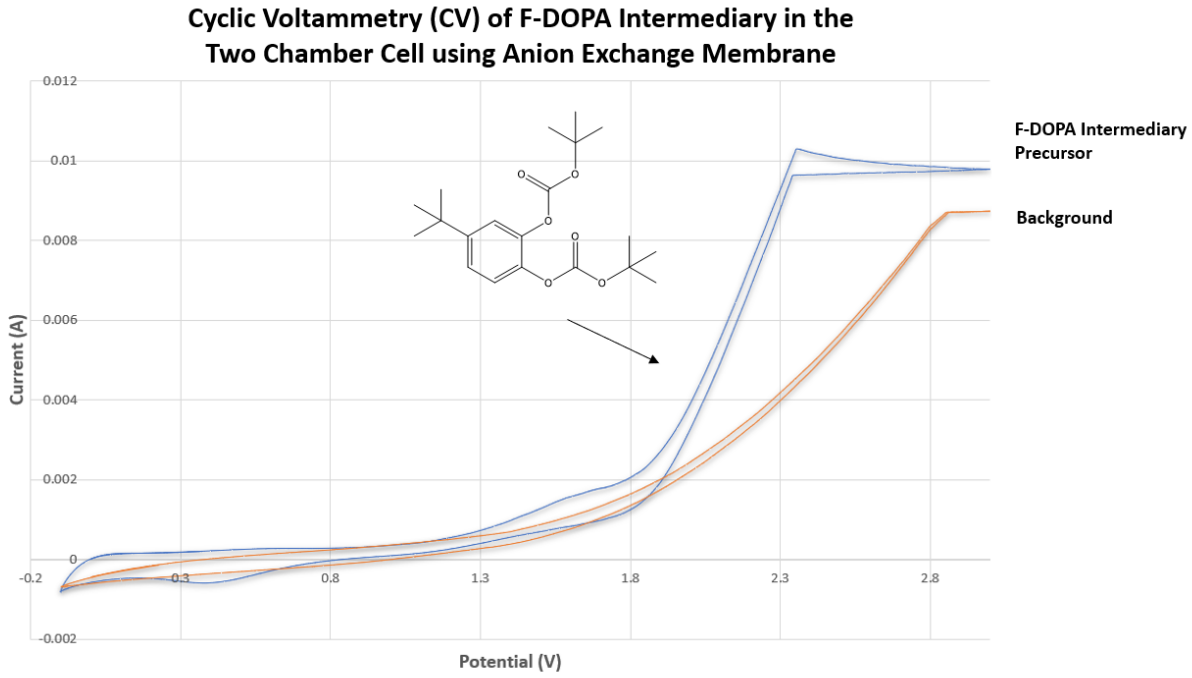

Figure 137: Cyclic Voltammetry of F-DOPA Intermediary in the Two Chamber Cell using Anion Exchange Membrane.

11.6 COX-2 Inhibitor Precursor with AEM and Proton Sink Chamber

The CV of the COX-2 inhibitor precursor in the two-chamber cell with the additional proton sink chamber is seen in Figure 138 with the onset oxidation potential at approx. 2.1V (Ag/Ag+) for the precursor. The current limitation due to the AEM is less stable likely due to the addition of the CEM and proton sink chamber. Since ions are moving between three different chambers in this setup, an oxidation potential of 2.7V (Ag/Ag+) or even 3.0V (Ag/Ag+) was easily achieved after some initial optimizing. As with any of these two chamber electrochemical setups, over time the current limitation or plateau often shifts to the left making higher oxidation potentials unreachable. This is very evident with the COX-2 Inhibitor probe synthesis. The reaction needs to be periodically monitored and changed to maintain the desired oxidization potential. To address this, we reduced the surface area on the anode to decreases current and shift the limiting oxidation potential back to above the chosen oxidation potential. Adjusting the surface area is most easily accomplished by designing the cell to raise the anode which reduces surface area gradually throughout the electrolysis.

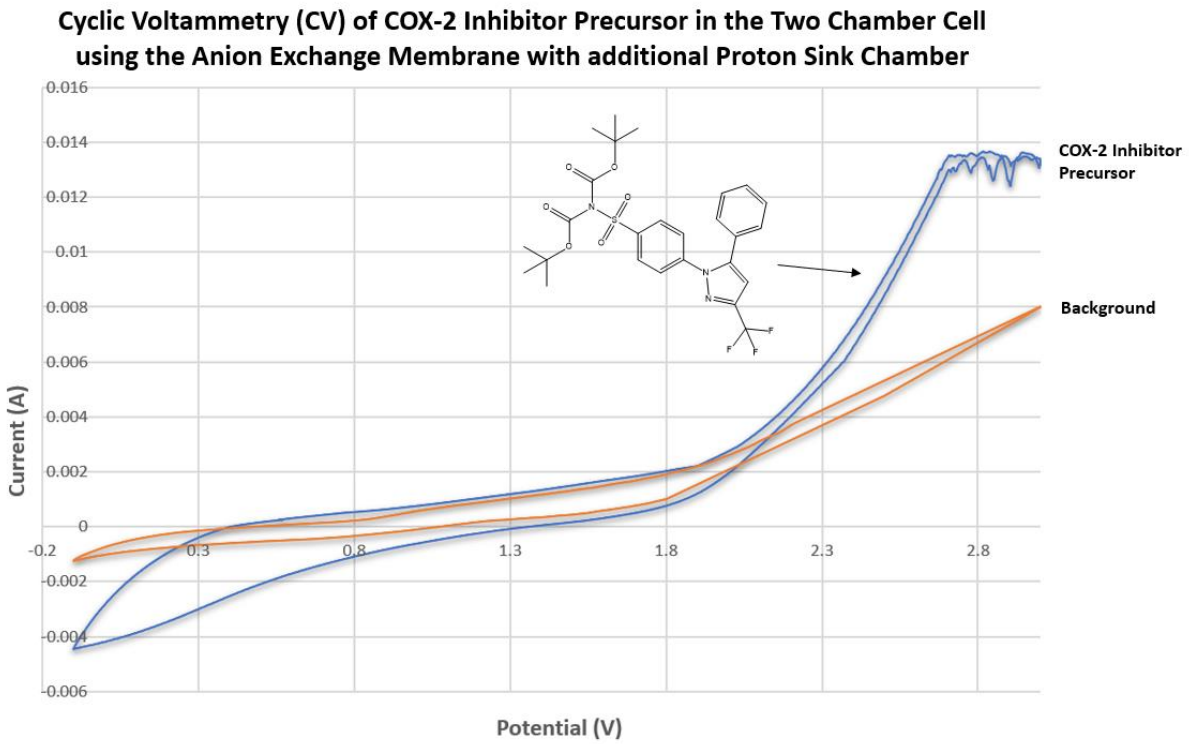

Figure 138: Cyclic Voltammetry of the COX-2 Inhibitor Precursor in the Two Chamber Cell using the Anion Exchange Membrane and additional Proton Sink Chamber.

Chapter 12: Discussions

12.1 Discussion

Electrochemical radiofluorination is a young research field with few published studies. More work must be done to continue developments to produce PET probes through the use of electrochemistry. This work herein will review previously published results, as well as our own data. Specifically, an overview, current theories, important tendencies and exceptions in the data is discussed. The focus is on information that is most essential to continue work to produce PET probes through the use of electrochemistry.

12.1.1 Fluoride and Electrochemistry

There are two intrinsic and fundamental properties of fluoride which makes the process of selective electrochemical fluorination feasible. First, the high oxidation potential of fluoride of 3.9V(SHE) is above the oxidation potentials used here for organic molecules. If fluoride would be oxidized it would be more difficult to control the selectivity of the neutral or positive fluoride radicals. Second, the high electronegativity of fluoride allows the product molecule to hold onto electrons strongly which increases the oxidation potential above the precursor. This is beneficial and protects product from further oxidation, reactions and side product formation.

In contrast to fluoride, other halogens have much lower oxidation potentials which can form neutral and even positive radicals after oxidation on the anode at the potentials used for organic molecules discussed further in section 12.1.14. These halogen radicals react electrophilically with organic molecules, often leading to low regio-selectivity of the added halogen, as well as many unwanted side products and reactions of the precursor. Halogen oxidation often form diatomic molecules (i.e., Cl_2, Br_2, IBr, and ICl) that can serve as an electrophilic source of halogenation. ECF has previously been performed with high oxidation potentials using the

Simons process which produces unselective fluorination and side reactions from the precursor. Under these conditions, organic carbons are oxidized at >3.5V (Ag/Ag+). Because of its high oxidation, using fluoride for these reactions allows for selective ECF to occur with high product yields and radiochemical yields. This can be achieved by preventing oxidation of fluoride for specific oxidation to occur on organic molecules with lower oxidation potentials instead.

The second advantage of fluoride is its ability to cause fluorinated product to have higher oxidation potential than the precursor. Here, the electronegativity of fluoride pulls the electron density away from neighboring nuclei causing them to tightly hold onto their electrons increasing oxidation potential. This ability encourages the buildup of the fluorinated product throughout the electrolysis process. The increase in oxidation potential of fluorinated aromatics compared to the precursors is smaller than thioethers. Molecules with lower oxidation potentials in the solutions will be preferably oxidized. This result in higher yields of the, fluorinated product and allows the reaction to go towards full completion with minimal precursor remaining after the oxidation reaction.

12.1.2 Reducing HF Concentration in Carrier Added ECF

When assessing fluorination yields, the ratio of (^{19}F in the product / total ^{19}F) is observed to be the same as (^{18}F in the product / total ^{18}F) which is expected since these fluorine isotopes are chemically identical. The ^{18}F ratio above is the radiochemical yield which needs to be reasonably high in a short duration in order to use the method to produce PET tracers for imaging. The ratio of (^{18}F in the product / ^{19}F+^{18}F in the product) is molar activity (A_m) usually measured in Ci/umol. For carrier added ECF, the added ^{19}F in poly HF fluoride sources will lower molar activity. In no-carrier-added conditions, about 1 uM of ^{19}F will remain in the solution from fluoride contamination

in solvents, chemicals and in other components of from the cyclotron production; a known entity in the field of radiochemical fluorination [168]. This results in low fluorination yields, radioyields, using poly HF salts as solvent or in high concentrations.

Decreasing the poly HF fluoride concentration also affects fluorination yields in ECF. From our results using Methyl (phenylthio) Acetate and MeCN, we observed a rise in fluorination yield to 10% at 25 mM poly HF fluoride source. From 1 M to 25 mM poly HF fluoride source the fluorination yield increase from approximately 0.1 to 10%. At lower fluoride concentrations less than 25 mM poly HF the fluorination yield drastically decreases. When decreasing from 25 mM poly HF fluoride source to 5 mM the fluorination yield drops from 10% down to ~1%. When decreasing Et_3N*3HF and $Et_4NF*4HF$ concentrations, the resulting reduction of fluorination yields was easily seen int eh results using Methyl (phenylthio) Acetate, F-DOPA Intermediary and Phenylalanine derivatives in Figures 36, 39, 49, 100, and 110. The rapid decrease seen in the product yields and RCFE when lowering fluoride concentration is likely due to multiple roles associated with poly HF in ECF which will be discussed in the next section.

12.1.3 Potential Roles of High Concentrations of HF

Poly HF fluoride sources in ECF can serve several simultaneous functions in the single chamber electrochemical cell (Figure 139). These different roles have not been investigated independently since previous ECF under high carrier concentration of poly HF fluoride sources worked well in single chamber cells. Identifying optimal conditions to explore each possible role of poly HF fluoride sources is not always feasible due to the interconnectedness of the multiple steps in the ECF mechanisms.

Potential Roles of Poly HF Salts in Traditional Electrochemical Fluorination	
1	Fluoride Source
2	Provide Conductivity
3	Form a more reactive H_nF_{n+1} Anodic Species of Fluoride
4	Proton Abstraction
5	Provide Fluoride to Stabilize sulfur in the fluoro-Pummerer Mechanism
6	Reduce on the Cathode instead of the Precursor or Product
7	Provide a Source of Hydrogen to form H_2 gas on the Cathode
8	Act as a pH buffer near both Electrodes

Figure 139: Potential Roles of Poly HF Salts in Traditional Electrochemical Fluorination

The primary role of poly HF fluoride sources is to provide fluoride and conductivity which is evident in all ECF reviews. There was much speculation of the poly HF forming anionic species of fluoride in the form H_nF_{n+1}. This negatively charge fluoride would more readily react with the cations produced from oxidation. Additionally, anionic forms of fluoride accumulates near the anode or onto the surface of the anode due to the attraction to the positively charge anode [169]. This accumulation near the anode surface where oxidation of the precursor occurs increases fluorination yields. H_nF_{n+1} complexes can distribute the negative charge increasing reactivity to cation intermediates with positive charge also distributed. All of the proposed cations in the ECF mechanisms are conjugated with the aromatics having the most conjugation likely increasing their reactivity to more distributed anionic forms of fluoride.

Proton abstraction is an important step in both ECEC and FP mechanisms. In some schemes, the proton is abstracted before fluoride addition whereas other schemes show the proton to be abstracted after fluoride addition. It is usually more favorable for the fluoride ion to bind after proton abstraction due to the reactivity of the proton to fluoride at the carbocation. When using poly HF sources, a common ECEC mechanism starts with anionic fluoride first abstracting a proton away after oxidation which is followed by the oxidation of the neutral radical on the anode. Next, the anionic fluoride is added to the carbo cation site with the hydrogen vacancy

(Figure 1). Removing poly HF source likely requires another anion or base for proton abstraction. This is seen in the results where the reduction on the cathode, such as the conjugate base of TFE in thioethers may assists with proton abstraction.

In the FP mechanism for thioethers, fluoride is necessary to stabilized the intermediate sulfur cation produced in the first oxidation (Figure 5). We proposed that the conjugate base of TFE could replace fluoride in the stabilizing role (Figure 47). It is unclear how many secondary roles TFE or the conjugate base of TFE need to perform to achieve successful NCA-ECF results (Figure 139). An important and sometimes overlooked effect of poly HF salts is their ability to be reduced easily on the cathode to shield the precursor and product from reduction in the single compartment cell. With removal of the poly HF sources in NCA-ECF, the solvent, precursor or product could be reduced, which can decrease RCFE yields depending on the reduced species and the chemical reactions after reduction. One benefit of having slightly acid solvents, such as TFE and HFIP, is their ability to be easily reduced shielding unwanted reduction of the precursor or fluorinated product. Aromatic reduction can be a significant problem in ECF often causing loss of aromaticity. . This is a significant problem due to the fact that once one of the aromatic rings bonds are broken, the molecule's alkene groups have lower oxidation potential and will be preferentially oxidized. Consequently, during electrolysis, this will rapidly increase the concentration of these less conjugated reduction side products and can block the oxidation of the precursor. This is likely one of the important roles of the poly HF sources in the ECF of aromatics which is to shield aromatics from reduction.

In the single chamber cell, the reduction of hydrogen in poly HF can immediately form H_2 gas because of the high concentration of HF providing additional hydrogen. Without this source of additional hydrogen, reduction on the cathode will have much more difficulty in producing H_2

gas and can produce more side products that could interfere with ECF. An additional benefit of the slightly acidic solvents of TFE and HFIP is their ability to provide hydrogen to form H_2 gas. Although, TFE forms a thick adsorption layer on the cathode surface during electrolysis with little bubbling, suggesting little H_2 gas formed from reduction in TFE. Gas formation does occur with no passivation in HFIP suggesting this solvent is better at shielding from reduction. Another important and often overlooked role of poly HF sources is to serve as a pH buffer. The anionic species of HF can eliminate protons produce on the anode. Similarly, the cationic species of HF can eliminate the anions produced on the cathode. This can help stabilize the pH at the electrodes during electrolysis even though the organic molecule concentrations are changing over time. An additional consideration for poly HF sources in the single chamber electrochemical cell is that ion species can travel quickly from one anode to the other due to the 600 (rpm) stirring rate. This can bring anions to the anode to reduce the anodic acidity, as well as cations to the cathode to reduce basicity. In this work, our experimental results include those without poly HF sources and also those that separate reductions into the cathodic chamber. This provides data that can help identify some of the critical roles of poly HF sources to be able to transition away from them in NCA-ECF.

12.1.4 Electrolysis Time

When using $Et_4NF*4HF$ or NCA-ECF with TFE solvent, methyl (phenylthio) acetate fluorinated with high yields, but degraded with further electrolysis (Figures 19 and 54). The addition of TBAF/triflic acid, which include THF and some water, prevented breakdown of the fluorinated product with further electrolysis time. This is likely due to the fact that these additives have an oxidation potential in-between the thioether precursor and the fluorinated product. Inserted

molecules whose oxidation potential is in-between the precursor and product may be useful to help limit oxidation and unwanted further reactions of the fluorinated products.

12.1.5 Temperature

Methyl (phenylthio) Acetate had increased product yields and RCFE under both carrier-added and NCA-ECF syntheses with increasing temperature (Figures 20, 43 and 55). Phenylamine and the F-DOPA intermediate using Et_3N*3HF had optimal product yields and RCFE at 0 °C. Naphthalene had increased NCA-ECF yields in HFIP at 70 °C compared to 0 °C. The effect of DTBP with increased temperature could not be tested due a particulate formation which interferes with ECF.

In summary, thioethers showed increases in product yields and RCFE under high temperature conditions, regardless of solvent. The carrier added ECF of aromatics in MeCN performed optimally around 0 °C except for Naphthalene which was an exception likely due to its exceptionally long cation lifetime in HFIP. We also consistently observed that when TFE or HFIP were successfully used in NCA fluorination the effect produced better yield at higher temperature.

In general, the increase in temperature should increase the kinetics of the ECF mechanism, leading to higher fluorination yield. The main drawback of performing experiments under high temperature conditions is the potential to decrease carbocation stability and lower the lifetime of cation intermediate reducing or inhibiting fluorination yields. This is especially unfavorable for cations which have short lifetimes. Thioethers are not significantly affected by this due to the stabilizing effect of fluoride binding to intermediate sulfur cation. We reasoned the shorter cation lifetime with increased temperatures is why the ECF with aromatic cations, such as benzene or the F-DOPA intermediary precursor with shorter lifetimes, had less fluorination yields. ECF of

aromatic cations with longer lifetimes such as naphthalene in HFIP are likely not affected drastically by increases in temperature.

12.1.6 Convection

Increasing the stirring rate improved product yields using Methyl (phenylthio) Acetate with Et_4N*4HF and without stirring only trace fluorinated product was formed (Figure 21). Sonication also led to similar observations with increased product yields but with lower optimal yields compared to that with stirring (Figures 22). The static screen-printed cell had no convection and no fluorination using long oxidation pulses. Short alternating oxidation and reduction pulses were necessary to produce reasonable product yields (Figure 31). The product yields using flow cells were much lower than in the single chamber cell. Laminar flow in flow cells causes little mixing of the solution off the surface of the electrodes (Figure 32). All of these results point to convection being one of the strongest effects on ECF. The lack of adequate mixing causes low yields which it was hypothesized is due to the formation of anodic acidity from oxidation near the anode, inhibiting fluorination discussed more thoroughly in section 12.2.

The single chamber electrochemical cell had much higher product yields than the other cell types when using Methyl (phenylthio) Acetate with Et_4N*4HF. This is likely due to the constant removal of anodic acidity. The fast convection rate of 600 RPM aided in the removal of acidity. The convection int eh single chamber cell greatly reduces the proton accumulation near the anode in two different ways. Directly by removing protons quickly from anode surface with high convection. Also, indirectly by quickly sending anions produced on the cathode to anode to help neutralize acidity.

12.1.7 Oxidation Potential

When performing carrier added ECF on Methyl (phenylthio) Acetate, the optimal oxidation potential was 2.2V using Et_4N*4HF and 1.4V with TBAF/triflic acid the 1.4 (Ag/Ag+) reference electrode. The lower oxidation potential using the TBAF/triflic acid combination is due to oxidation of TBAF and triflic acid which at higher potentials increases current likely disturbing the balance of the TBAF/triflic acid ratio. When switching to NCA and TFE solvent using the same thioether precursor, the optimal results were obtained using an oxidation potential of 3.5V. Here, the TFE solvent under NCA conditions is more abundant than 100 (mM) of the poly HF fluoride source used in carrier added conditions. This likely causes a higher concentration of the conjugate base of TFE to be formed at the higher oxidation potential which can stabilize the intermediate sulfur cation or abstract hydrogen in the FP mechanism.

Surprisingly, the modafinil precursor thioether was not successful for NCA-ECF in TFE or HFIP like the other thioether compounds. This is likely due to the instability of the benzylic position in TFE or HFIP. This modafinil precursor did work well in MeCN with the DTBP base. The results from TFE or HFIP with the modafinil precursor may be from increased acidity or reduction. Further experimentation is required in the two-chamber cell to investigate this hypothesis. The amine group thioether, (Phenylthio) Acetamide, had successful NCA-ECF in TFE without BOC protection of the amine group. The modafinil precursor required BOC protection of the amine group for successful NCA-ECF in MeCN with DTBP. In electrochemistry the amine group tends to acts as a nucleophile which may attacks the benzylic position in the modafinil precursor leading to poor results. The F-DOPA Intermediate and the COX-2 Inhibitor precursor both required BOC protection due to the low oxidation potentials of hydroxyl group (~0.5V

Ag/Ag+) which preferentially oxidizes instead of the aromatic ring due to the large difference in onset oxidation potential.

Most of the precursors' optimal oxidation potential is much higher than the onset potential. For instance, the F-DOPA Intermediary and the COX-2 Inhibitor Precursor had onset oxidation potentials of ~2.0V but optimal oxidation potentials of 2.58V and 2.7V, respectively. In both carrier added and NCA, higher currents and oxidation rates were required for optimal results even with very low concentration of NCA [^{18}F]Fluoride.

12.1.8 Reduction

There are several reductive effects which can influence ECF as mentioned in section 11.1.3. Removing the poly HF fluoride source to perform NCA-ECF can cause the precursor and product to undergo reduction and reduce yields. This is likely using aromatic precursors whose reduction can lead to less conjugated side products that have lower oxidation potentials. Benzene product yields increased in the presence of high precursor concentrations which may be due to less effect of side product at the higher precursor concentration (Figure 98)[2]. The two-chamber electrochemical cell can separate and remove reduction form the anodic chamber where ECF occurs. Fluoride adding to the precursor often lowers the reduction potential making it easier to be reduced. This can make the fluorinated product preferably reduced in the absence of poly HF, acids or other easily reduced molecules. Using the aromatic precursors, successful NCA-ECF required the use of either an easily reducible solvent or the two-chamber cell.

12.1.9 Stable Electrolyte

The use of stable electrolyte increased fluorination yields even when it was not needed for conductivity. There is an optimal concentration of TBAP which is different in NCA and carrier added synthesis. Tetrabutylammonium perchlorate (TBAP) performed better than tetrabutylammonium triflate (TBAOTf), Tetrabutylammonium tosylate (TBAOTs) in NCA-ECF of Methyl (phenylthio) Acetate (Figure 59). TBAP also outperformed hexafluorophosphate (HFP) and tetrafluoroborate (TFB) in experiments with Methyl (phenylthio) Acetate. TFB under electrolysis often incorporates ^{18}F into the electrolyte, even up to 99%, making TFB unusable for many ECF applications. HFP performed only slightly worse than TBAP for Methyl (phenylthio) Acetate and HFP, performed slightly more favorably for the F-DOPA intermediary (Figure 113).

TBAP electrolyte increased product yield even in presence of fluoride salt which did not noticeably increase conductivity. Similar observations were seen with and RCFE in carrier added and NCA-ECF (Figures 29 and 44). Other tetrabutylammonium electrolytes besides HFP did not have this effect, suggesting the anion is responsible for this activity. We reasoned this effect was due to the stable anion such as perchlorate positioned close to the anode may help to reduce acidity or help to form more reactive anionic species of fluoride.

12.1.10 Aqueous Conditions

Water can solvate fluoride ions making them unreactive. HF and H_2O form tight hydrogen bonding complexes, making HF very unreactive. In TFE, the NCA-ECF of Methyl (phenylthio) Acetate was only partially reduced by the addition of 1% water by volume (Figure 56). This limited effect suggest water in TFE likely does not have a similar solvation ability on fluoride. TFE has a strong hydrogen donating properties which could shield fluoride from water. Since [^{18}F]Fluoride

is produce in [^{18}O]water, the removal of water is necessary prior to performing nucleophilic radiochemistry reactions. The oxidation of water is similar to that of the thioether precursors. It is difficult to tell if the solvation of fluoride reduced RCFE in TFE or if it was the oxidation of water and subsequent reactions reduced RCFE.

12.1.11 Effect of Acids

This section will discuss the acidity of the solution and section 12.2 will discuss anodic acidity specifically. The addition of acids reduces fluorination and product yields in ECF. For example, 5 mM HCl decreased product yields of Methyl (phenylthio) Acetate by 90% when using Et_4N*4HF (Figure 27). The addition of Triflic or pToluenesulphonic acid significantly reduced NCA-ECF RCFE of Methyl (phenylthio) Acetate in TFE (Figure 58). Two-chamber ECF with CEM becomes incredibly acidic with pH (~2-3) in the first few minutes leading to no RCFE in NCA conditions and low product yields carrier added (Figures 33). TBAF and triflic acid noticeable react which neutralizes the acid. However, in these reactions when triflic acid concentration exceeds that of TBAF, it causes little to no product yields (Figure 41). Both sulfuric acid and acetic acid with TBAF produce poor product yields (Figure 42). The acidic thioether, (Phenylthio) Acetic acid had the worst RCFE of all the thioethers in NCA-ECF. However, this may be due to the low oxidation potential of the hydroxyl group on the thioether interfering with sulfur fluorination and not the acidity. There are many different sources of data here that suggest acidity negatively impacts ECF. This is likely due to three negative effects of acidity; (1) inhibiting hydrogen abstraction, (2) neutralizing anionic forms of fluoride which are less reactive (3) neutralizing anionic form of fluoride so it is not electrostatically attracted to the anode where the cation intermediates are produced. Acidity can also positively affect the cation intermediate lifetime although this does not seem to be as important as these other negative factors of acidity.

The slight acidity of TFE and HFIP may have a positive effect on cation lifetime but pH lower than these solvents seems to be detrimental to ECF.

The NCA-ECF of the F-DOPA Intermediary in the single compartment cell used triethylamine acetic acid 10 (mM) which was noted as an outlier in the data. The oxidation potential of 2.58 (Ag/Ag+) was significantly higher than that of triethyl amine or acetic acid which both oxidized below 1.5V (Ag/Ag+) in this electrochemical cell. The electrolysis time of 60 mins suggest that both triethyl amine and acetic acid are likely to go through a significant oxidation and reduction which may neutralize the pH of the solution during electrolysis. The slight acidity during electrolysis may be necessary to remove the t-butyl group. In the two-chamber cell NCA experiments with the F-DOPA intermediary precursor, it appears acidity is only necessary to remove the t-butyl group before the ECEC mechanism begins which will be discussed in section 12.9.

12.1.12 Effect of Bases

Bases in ECF are limited in the anodic chamber or single chamber electrochemical cell due to their low oxidation potential and nucleophilicity. 2,6-ditertbutylpyridine (DTBP) is a base that is sterically hindered so that it has a higher oxidation potential (onset ~2.1V (Ag/Ag+)) and low nucleophilicity. Using an oxidation potential above 2.1V (Ag/Ag+) oxidizes the base which reduced production yields (Figure 84). DTBP also adds fluoride above this potential. Bases can also be added to a separate chamber with a cation exchange membrane in such as the proton sink chamber. This affects the proton concentration in the anodic chamber as proton diffuse across the membrane mostly in one direction due to difference in pH levels. DTBP reduces acidity but could also fulfill many of the other potential roles of the poly HF sources in Figure 129 such as proton

abstraction or in forming a more reactive species of anionic fluoride leading to increased fluorination yields.

There were several experimental results where the addition of base affected product yields or RCFE. The modafinil precursor NCA-ECF in MeCN had on trace results and increased to 9.7±0.6% (n=3) RCFE with addition of DTBP. Methyl (phenylthio) Acetate had a low RCFE for NCA-ECF in MeCN of 0.5% and with the addition of DTBP had RCFE of up to 26.4% similar to that of using the TFE solvent. Pyridinium pToluenesulfonate (PpTS) also increase yields of NCA-ECF using Methyl (phenylthio) Acetate up from 0.5% to 5.1% RCFE which was likely due to the pyridinium base because the pToluenesulphonic acid decreased RCFE (Figure 59). Using the two-chamber cell, the CEM caused acidity to increase rapidly while using the AEM the acidity was much slower to increase and resulted in greater fluorination yields (Figure 61). Thus, creating an electrochemically stable pH environment that is not too acidic seems to be preferential for ECF. Yet, this is a challenging undertaking since the low oxidation of bases and the high nucleophilicity of bases causes problems for ECF. One solution that was used here is to use an additional chamber as a proton sink chamber and fill it with a high concentration of base connected to the anodic chamber by a nafion membrane. This causes protons to continually diffuse based on the concentration gradient keeping the anodic chamber from becoming too acidic.

12.1.13 t-butyl leaving Group

The F-DOPA Intermediary contained a t-butyl leaving group which was hypothesized to aid in the fluorination to a targeted site on the aromatic ring in the ECEC mechanism. This was proposed as being likely due to the good stability of the t-butyl cation leaving group. When fluorinating benzene, hydrogen was still favored by a factor of 4 to 1 over the t-butyl group for

replacement by fluoride [5]. When performing NCA-ECF in the single chamber cell with the F-DOPA Intermediate, triethylamine and acetic acid was necessary to produce RCFE. In the two-chamber cell with AEM, HFIP was necessary to produce appreciable RCFE while most of the precursor lost the t-butyl group after electrolysis. HFIP acidity is mild acid (pKa of 9.3) but slightly more acidic than TFE (pKa of 12.4), producing better RCFE values than TFE. One possibility is that slight acidity is necessary for the t-butyl leaving group to exchange with fluoride. Another explanation could be the primary role of the acidity is for the t-butyl group to leave under electrolysis and then the BOC protected catechol proceeds through the ECEC mechanism. If this is true, using the BOC protected catechol would produce higher fluorination yields due to the inefficient removal of the t-butyl leaving group. However, this was not tested.

12.1.14 Other Halogens

When discussing the application and scope of electrochemistry to fluorination it is also necessary to mention other electrochemical halogenations. Similarly, as in electrochemical fluorination, it was not worthwhile to perform electrochemistry with low halogen concentrations. For instance, the electrochemical halogenation using chlorine, bromine and iodine has been thoroughly explored and reported in the literature using a large excess concentration of the halogens[170]. Chlorination was reported to proceed through an ECEC mechanism, similar to fluorination, when the oxidation potential was less than that of chlorine, for instance in allyl groups [170]. Chlorination at higher potentials with benzene causes chlorine to form neutral radicals and Cl_2 which then can proceed to add to benzene via electrophilically attack on benzene. There have been reports of both dioxymethylbenzenes and naphthalene can be chlorinated by ECEC up to an oxidation potential around 1.7V (SHE) due to the low onset oxidation potential of these aromatics [170]. Bromine and iodine both have lower oxidization potentials than chlorine which leads to

forming neutral and positive radicals which react electrophilically. This does not always inhibit the electrochemical halogenation process from being highly regio-selective with high product yields.

The other non-fluoride halogens have a much lower oxidation potential than fluoride, which leads to the formation of neutral and positive halogen radicals that are highly reactive at the oxidation potentials of most organic molecules. For instance, chlorine has an oxidation potential around ~1.4V (SHE), bromine ~1.0V (SHE), and iodine ~0.5V (SHE). The oxidation of these non-fluoride halogens can interferes with the oxidation of the precursor (Figure 105) [4]. The non-fluoride halogens also interfere with fluoride by acting as a competing nucleophile. A primary reason that the other halogens cannot be used in a similar manner as fluoride is due to their low oxidation potential which creates halogen radicals that ionize and often added to the precursor in unwanted side reactions. In the case of high oxidation potential organic molecules this electrophilic halogenation is often indiscriminate and with low site specification, making these halogens difficult to be used as a halogen mediator in fluorination. Halogen mediation is a technique where the lower oxidation halogen such as bromide becomes a radical electrochemically which then proceeds to oxidize the precursor to form the cation intermediate for the higher oxidation halogen, such as fluoride, to be added. Although this can an effective approach to add fluoride, this method produces many different side reactions and side products. The feasibility of using other halogens to enhance fluorination in ECF, such as in halogen mediation, does not at this point seem plausible for using electrochemistry to produce PET probes. Additionally, using electrochemistry to produce halogen radioisotope probes such as ^{124}I similarly as the nucleophilic ECEC mechanism of fluoride will not work. Electrochemistry may be able to label this isotope by forming ^{124}I radicals which

electrophilically add to the organic precursor. However, this is a different electrochemical process and outside the scope of this work.

12.1.15 Solvents

The solvent effect on ECF was the was the most significant effect in determining the radiochemical products formed from electrolysis. Solvation of the precursor can influence: (1) the orientation of the molecule to the anode and direct oxidation to a wanted or unwanted oxidation site; (2) stabilize or destabilize the cation intermediate increasing or decreasing the lifetime; (3) block or make available the fluorination site of the cation; and also (4) help or hinder proton abstraction due to solvation of the cation and the abstracting molecule. Additionally, the solvent can serve additional roles including oxidized or reduced species of the solvent to control the ECF. The solvents should also possess low nucleophilicity to prevent immediately reactivity with the produced radical cation.

The solvent effects were the least noticeable in the carrier added ECF of thioethers where it was observed that different solvents produced varying product yields. For instance, mono fluorination of alkyl phenyl sulfide in high concentration of fluoride occur in a variety of different solvents [70]. The main characteristics of the organic solvents with successful ECF in thioethers were oxidation potentials equal to or higher than the thioethers, low polarizability, low nucleophilicity and dielectric constant large enough to oxidize most the precursor in the electrolysis time at the chosen potentials. The ability to fluorinate thioethers in a variety of different solvents is likely due to the large availability of fluoride in carrier added synthesis, as well as the quick stabilization of the sulfur cation in the FP mechanism.

In the carrier added experiments using aromatic precursors, ECF reactions were more sensitive depending on the solvent. There is no easy stabilization of the aromatic cation using

fluoride as in thioethers with the FP mechanism. The stability of aromatic cations is primarily due to solvent effects which is likely why aromatic ECF is more solvent specific. Aromatics with high oxidation values require compatible solvents to be able to tolerate these conditions, such as MeCN. Unfortunately, solvents with moderate conductivity, low polarizability, low nucleophilicity and good solubility for ECF that are suitable for these reactions are quite limited.

For effective NCA-ECF experiments, the solvent had a large effect on product yields and in preventing side product formation for both thioethers and aromatics. The lack of poly HF fluoride source causes more variability in radio side product formation under NCA conditions.

Both TFE and HFIP were the most suitable solvents under NCA conditions for precursor with onset oxidation potentials in their electrochemical window. Using TFE and HFIP as solvents for higher oxidation potential aromatics caused solvent oxidation and no fluorination yields. TFE and HFIP remarkable properties for electrochemistry. HFIP and TFE properties of low nucleophilicity, low hydrogen bond acceptor strength, and high hydrogen bond donor strength make it the ideal solvent for cations increasing their lifetime [117]. Dimers and trimers of TFE and HFIP form via hydrogen bonding which exert solvolysis and catalytic effects that are beneficial to ECF [171]. HFIP form discrete complexes due to hydrogen bonding [172] TFE and HFIP also likely form complexes with fluoride increasing its reactivity. HFIP has the highest hydrogen binding energy to F- compared to other organic solvents used in electrochemistry [117].

TFE and HFIP are also slightly acidic due to their CF_3 groups which enables the hydroxy group to be slightly acidic with pKa values of 9.3 and 12.4, respectively [172]. This is beneficial as the solvents will reduce instead of the product or precursor under NCA conditions without poly HF fluoride source. Slightly acidic environments of HFIP or TFE are not as detrimental as strong acidic environments where ECF is inhibited.

HFIP as a solvent was recently highlighted in a nature review article [173]. HFIP is a widely used solvent in different research areas, including electrochemistry, due to its unique characteristics. HFIP has been seen as a possible tool for electrochemistry since it can generate persistent radical cations [174]. For comparison, different naphthalene cations had lifetimes ~30-150 times longer in HFIP than in trifluoro acetic acid [117] whereas aryl cations have longer lifetime in TFE [120]. The anodic limit of HFIP is ~1.8V (Ag/Ag+) which is similar in TFE. This lower oxidation limit likely prevents fluorination yields in ECF reactions containing aromatics with higher oxidation potentials such as the COX-2 inhibitor which has an onset oxidation potential around ~2.1V (Ag/Ag+). Lower oxidation aromatics, such as naphthalene and the F-DOPA intermediate, resulted in reasonable NCA-ECF in HFIP where the F-DOPA intermediary has an onset oxidation potential comparable to that of HFIP. Unlike HFIP, buildup accumulates on the cathode of TFE during reduction conditions, causes adsorption and polymerization on the cathode. The buildup on the cathode does not seems to prevent or negatively affects fluorination. Both HFIP and TFE can vastly attenuate the reactivity of anions. It is likely the suppression factor for weaker competing anions in these solvents increases the chances for stronger anions such as fluoride. This effect can be seen from Laser Flash Photolysis (LFP) in section 12.3. Thus, HFIP and TFE are appropriate solvents that can be advantageous for NCA-ECF to synthesize many types of organic PET probes. However, the modafinil thioether did not work in TFE likely due to the instable benzylic positioning, as discussed in section 12.7.

Higher oxidation aromatics have work well in MeCN. We also identified other suitable solvents with high oxidation potential and stability suitable for ECF as previously discussed. For example, DME is a suitable solvent but has a low dielectric constant leading to low conductivity in the electrochemical solution and DME also has a lower oxidation potential than MeCN.

Dichloromethane was also explored but has an even lower dielectric constant than DME, making it difficult to generate enough oxidation in a short time for appreciable fluorination yields to produce PET probes due to the half-life of ^{18}F. We found adding DTBP base increased fluorination in oxidation potentials below 2.1V (Ag/Ag+). Above this potential, additional cell types and modification were necessary to achieve NCA fluorination discussed in the next section.

12.1.16 Electrochemical Cell Types

The single chamber, two-chamber, static and flow electrochemical cells were used. Carried add ECF using poly HF sources has been successful with many different types of cells. Cation permeable membranes are commonly used in two-chamber ECF experimental set-ups and has been used for ECF with pyridine HF fluoride sources [175]. Micro flow cells were also used in carrier added ECF. Ethyl(phenylthio) Acetate was fluorinated in a micro-flow cell in MeCN with high $Et_3NF*3HF$ concentrations with product yield of 60% using a specialized microfluidic mixer [176]. Flow cells and electrochemistry have been used to concentrate fluoride from the cyclotron to be transferred into organic phase for radiochemistry. A flow cell was used to concentrate [^{18}F]Fluoride for use in organic solvents and to produce several different PET radiotracers through conventional Kryptofix S_N2 reactions [177]. This trapping of fluoride by electrochemistry is beneficial for ECF since it allows a straightforward transfer of fluoride into organic phase in the same electrochemical cell as the synthesis, preserving resources and time.

There were several trends and correlations between fluorination yields and electrochemical cell types. For instance, both the single and two-compartment set-ups led to high product yields comparable to static and flow electrochemical cell. This was true for both the NCA and carrier added syntheses. Higher convection rate of 600 RPM stirring in the single and two-compartment

cells resulted in higher fluorination yields where as in static cells, fluorination only proceeded with fast cycling of negative and positive potentials. In the flow cell, laminar flow prevented mixing off the double layer of the anode reducing yields. Low fluorination yields from static and flow cell set-ups was likely due to increase anodic acidity produced from oxidation of the anode without adequate convection/neutralization to counter it which will be discussed in section 12.2.

Using the CEM in the two-compartment cell rapidly produced a high acidic environment and was only slightly improved by using an AEM as mentioned in section 12.1.11. Aromatic molecules likely require the two-chamber cell for high fluorination yields under NCA conditions in order to avoid reduction of the product and precursor. To maintain a more consistent less acidic pH environment a Proton Sink Chamber (PSC) was added to the anode chamber of the two-chamber cell with AEM. This limited acid formation and increased fluorination yields.

12.2 Anodic Acidity

One consistent factor throughout the experiments directly correlated to fluorination yields was the rapid removal of anodic acidity. Anodic acidity can build up due to the oxidation of molecules on the anode which produces protons resulting in anodic acidity.

Anodic Acidity Hypothesis: In electrochemical fluorination, oxidation on the anode generates protons which increases the acidity near the anode. The rapid removal of this anodic acidity is necessary to generate high fluorination yields. This is more critical in no-carrier-added electrochemical fluorination where poly HF fluoride sources do not help buffer pH near the anode.

There is strong evidence for the anodic acidity hypothesis within our ECF experimental data which suggest it as one of the most fundamental effects when preforming NCA-ECF. Low poly HF fluoride concentrations lead to more proton formation near the anode surface in result of oxidation, which increases the acidity near the anode hindering ECF. This is evident with the single chamber cell as the faster the convection rates the higher the fluorination yield. The faster the convection rates in the single chamber cell the quicker anodic acidity is removed. Initial static experiments without convection produced little to no product yields. Increasing convection in the single chamber cell in carrier added conditions caused fluorination yields to increase. Using the static chip cell, fluorination only occurred with rapid pulsing from positive to negative potentials in carrier added conditions, which generated product without applied convection. This suggested that the removal of the buildup of anodic acidity from the pulsing of the negative potential is necessary for ECF. In flow cells, even at high flow rates produced low product yields under carrier added conditions. Laminar flow inhibited diffusion off the anode surface even with continual flowing of solution over the cell. The layer adjacent to the anode remains acidic due to the difficulty of mass transfer against laminar flow. Experiments with increased acidity from adding acid in both NCA and carrier added conditions resulted in lower to zero product yields and lower to zero RCFE. To reduce acidity, a base was introduced into the reaction which was added either directly or indirectly in the single or two-chamber cell. In the two-chambers cell where the convection rate is the same as the single chambers cell, the fluorination yields are reduced due to increased acidity. The conjugate bases of TFE and HFIP also likely serve a similar role as poly HF sources in neutralizing proton formation at the anode surface whereas DTBP, does the same as well in MeCN.

Anodic acidity and proton formation neutralization is likely critical for a successful NCA-ECF. Anodic acidity inhibits the proton abstraction step and the ECF mechanism cannot go to completion. The excess protons also reduce the reactivity of fluoride, which prevents anionic species of fluoride from forming. With reduced anionic species of fluoride, there will less concentration of fluoride attracted to the anode to react with the produced cation. The presence of a high proton concentration may also highly destabilize or react with neutral radicals present in both ECEC and FP mechanisms.

During electrolysis, anionic species of fluoride concentrate near the anode surface due to electrostatic attraction. In carrier added conditions, high concentration of anionic fluoride is found near the anode no matter the convection rate. This was proven by varying the oxidation pulse length, which we noted that even 100 millisecond oxidation pulses produced similar product yields as using 60 second oxidation pulses. Anodic acidity reduces anionic fluoride species which negatively impacts ECF in two important ways. First, the acidity reduces anionic fluoride species, preventing the positive oxidation potential from attracting the anionic species of fluoride near the anode. Without the additional effect this will result in insufficient anionic fluoride present near the anode to be used in the ECF mechanism. Second, the anodic acidity reacts and decreases the concentration of most anions and bases from vicinity of the anode. In return, this removal results in the lack of available proton abstracting molecules in the ECF mechanisms. Without proton abstraction, ECF mechanisms cannot proceed resulting in minimal to no fluorinated products.

The anodic acidity can be neutralized in several ways. One strategy is to use an electrochemically stable non-nucleophilic base such as DTBP. Another is to use reduction reactions to produce anionic species that will counter anodic acidity, as well as perform the role of proton abstraction in the ECF mechanism. This is likely the role of TFE in the NCA-ECF of

thioethers. Another strategy involves designing gradients to reduce acidity in the two-chamber cell, such as using the proton sink chamber.

12.3 Laser Flash Photolysis and Radical Cation Lifetime

All ECF mechanisms are known to form radical cation intermediates. The lifetime of these cation intermediates is important to determine if the mechanism will proceed towards completion. Determining the intermediate cation lifetime is difficult in the electrochemical conditions and there are very few environments able to simulate the electrochemical conditions for cation production. Cations are formed as a sheet of ions dissociating from the anode repelled by a large electrostatic potential. When cations are repulsed from the anode due to the potential and are solvated, they are met with a higher concentration of anions in the double layer to counter the positive potential. In addition, the cations must overcome the destabilizing effects from the shear force between the double layer and the bulk solution. This exact environment is not captured in Laser Flash Photolysis (LFP). However, LFP is the only available experimental data on many of the cation lifetimes of organic molecules.

LFP uses pulses of lasers at the specific wavelength to excite and produce cation radicals. The lifetime of these cation radicals is detected and measured by UV absorption. LFP experiments are typically conducted using TFE and HFIP solvents due to their cation extending properties as mention in section 12.1.15. The rest of this section will discuss various LFP experiments and how they relate to ECF.

Using LFP, Benzyl, Cumyl and Phenethyl cations all had extended lifetimes in TFE and HFIP compared to MeCN [178]. TFE increased the cation lifetime by 2 to 3 orders of magnitude and HFIP by 4 to 6 orders of magnitude over MeCN. The cations lifetime in HFIP, TFE, and

MeCN were reported to last within the milliseconds range for HFIP, the microseconds range for TFE, and nanoseconds range for MeCN. The addition of a high concentration of a nucleophile, Br-, reduced the cation lifetime to nanoseconds for all solvents. This suggests in a high concentration of fluoride the solvent effect of extending the lifetimes of cations may not be critical in ECF as demonstrated in the carrier added experiment using MeCN. In NCA conditions, the solvent extending of the cation lifetime may be necessary due to the scarce availability of fluoride.

Carbocation lifetimes were tested with LFP in MeCN, TFE and HFIP [179]. Carbenium ions lifetime was extended by about 1 order of magnitude for TFE and 2 orders of magnitude for HFIP compared to MeCN. The general reactivity of benzylic cations with the solvent HFIP is in the millisec range, for aryl cations in the microsec range and non-conjugated carbocations in the nanosec range. Diarylmethyl cations lifetimes were measured in 1:4 ratio of MeCN:H_2O [180]. TFE extended the lifetime of diarylmethyl cations by 3 to 5 orders of magnitude compared to other solvents. Dibenzosuberenyl cations have longer lifetimes (>100 microsec) only in TFE [181], which was not observed in other organic solvents (HFIP was not tested). It was also noted this particular cation had a comparable lifetime with up to 5% water in TFE.

Mesitylene, hexamethylbenzene, and 1,3,5-trimethoxybenzene cations were produced using LFP in HFIP [182]. TFE increase the lifetime of these cations by 3 orders of magnitude and HFIP by more than 4 orders of magnitude which exceeded the instruments' limitations to measure these results accuracy. LFP produced 9-florenyl cations in HFIP which have a lifetime of 30 microsec, which was longer than in water or methanol which was reported to last less than 20 picosec [183]. Due to the weak nucleophilicity of HFIP, it enables the cations to undergo electrophilic substitution of benzene not seen in other solvents which could be a problem causing

dimerization using aromatic precursors in ECF. HFIP solvent performs well with even 0.5M water due to its hydrogen bonding properties [173].

Various quinones neutral radicals and radical cations were formed in HFIP with LFP [184]. HFIP, an acidic solvent, tends to form hydroquinones cations and radicals. Aryl radical formed in HFIP tend to dimerize instead of react with tetranitromethane which is typically occurs in other solvents exclusively [185]. This was attributed to the cation extending properties and anion solvation by hydrogen bonding of the solvent molecules.

Thirty two benzyl, phenethyl, cumyl and vinyl cation variants were investigated in HFIP and TFE [186]. It was observed the lifetimes of these cations in more nucleophilic solvents such as methanol, ethanol and water were less than 20 nanosecs. Using the solvents of TFE and HFIP expanded the lifetime by a factor of 1,000 to 10,000 times longer, respectively. The reactivity of Br- ions with the cations suggest that a lifetime of 100 microsecs should be sufficient for nucleophilic addition of bromide.

Phenyl cations were formed by LFP in HFIP with a lifetime in the micro-millisec range which was concluded upon the addition of the aromatic cations to the HFIP conjugate base [187]. The addition of nucleophiles greatly reduces that lifetime. For instance, halogens were shown to react in the nanosec range with the phenyl cations. These cations were 100,000 times more likely to react to halogens than HFIP. In LFP, if toluene is present with benzylic cations then biphenyls will likely to form via an electrophilic attack.

The mechanism of LFP produced aromatic cations in HFIP when reacting with halogens has been previously investigated [188]. Several of the radical cation half-lives were measured to last at around an hour without halogens. Different dimethoxybenzenes were also explored along with two possible radical cation pathways. The first was the oxidative substitution reaction with

halide ion whereas the second involved halogen atom transfer from a halogenating agent such as Br_2 or ICl. These halogen agents were determined to be 100 times faster than with the halide ion. This was thought to be due to the attenuation of reactivity experienced by nucleophiles in HFIP as the primary explanation. However, anion reactivity requires a two-photon process where as the halogenating agent does not.

LFP data can explain many phenomena of the ECF experiments. For instance, successful ECF in TFE and HFIP may partly result from using compatible solvents able to extend radical cation lifetimes as mentioned in section 12.1.15. Findings from experiments with the naphthalene and F-DOPA intermediate further supported this finding where HFIP greatly improved the radiochemical yields under NCA conditions which may be attributable to longer cation lifetimes in this solvent. Both TFE and HFIP can form hydrogen bonds with water to reduce its unfavorable impact on fluoride, which was observed by little reduction in cation lifetimes with small amounts of water added as confirmed in our own results. Benzylic cations tend to react in TFE and HFIP much faster than aryl cations, which could explain why the modafinil precursor did not work well in TFE due to reactivity with the solvent. TFE and HFIP suppresses some nucleophiles leading to dimerization or side product formation, which could explain some of the radio side products formed under NCA conditions.

12.4 The fluoro-Pummerer (FP) Mechanism

As well-reported in the history of electrochemistry, the electrochemical mechanism is postulated by the oxidation potential used to accomplish the product formation, side product formation in different conditions and the differences in yield between similar precursors. It is challenging to investigate each individual steps of the electrochemical process. Altering the

electrochemical conditions to probe the mechanism can often lead to other changes due to additional effects from one of the electrical or chemical steps that can occur at either electrode. The FP mechanism provides a good foundation for the ECF of thioethers under carrier added conditions. Further details are needed to understand the FP mechanism in its relation to the NCA-ECF of thioethers. The Auxiliary Facilitation Hypothesis and the Single Fluoride Atom Hypothesis are two proposed hypotheses that explains how the FP mechanism relates under very low fluoride concentration using TFE solvent.

In the fluoro-Pummerer (FP) mechanism with poly HF sources, fluoride plays multiples roles of stabilizing the sulfur cation, proton abstraction, and fluoride addition to the alpha carbon (Figure 46). However, when using TFE solvent under NCA conditions, the Auxiliary Facilitation Hypothesis suggests that the TFE conjugate base plays the roles of fluoride for the first two steps of the FP mechanism (Figure 47).

Auxiliary Facilitation Hypothesis: In the no-carrier added electrochemical fluorination of thioethers an auxiliary molecule (conjugate base of TFE) stabilizes the positive charge on sulfur in a similar manner as to fluoride in the fluoro-Pummerer mechanism after the first oxidation. The auxiliary molecule also performs the role of hydrogen abstraction in the fluoro-Pummerer rearrangement.

This Auxiliary Facilitation Hypothesis could explain the successful NCA-ECF in thioethers. This hypothesis does not adequately explain our observations of using DTBP in MeCN (Figure 57) or using the pyridinium salt both which led to high RCFE measurements (Figure 59). These bases seem very unlikely to participate in the FP mechanism in a similar manner as to

fluoride or the conjugate base of TFE. DTBP is sterically hindered and lacks the strong negative charge necessary to stabilize the positive charge on sulfur. However, it is likely that DTBP does participate in proton abstraction. In the proposed Single Fluoride Atom Hypothesis, only one [^{18}F]Fluoride is required due to the same fluoride being present next to the thioether for both stabilization of sulfur and addition of the alpha carbon (Figure 140).

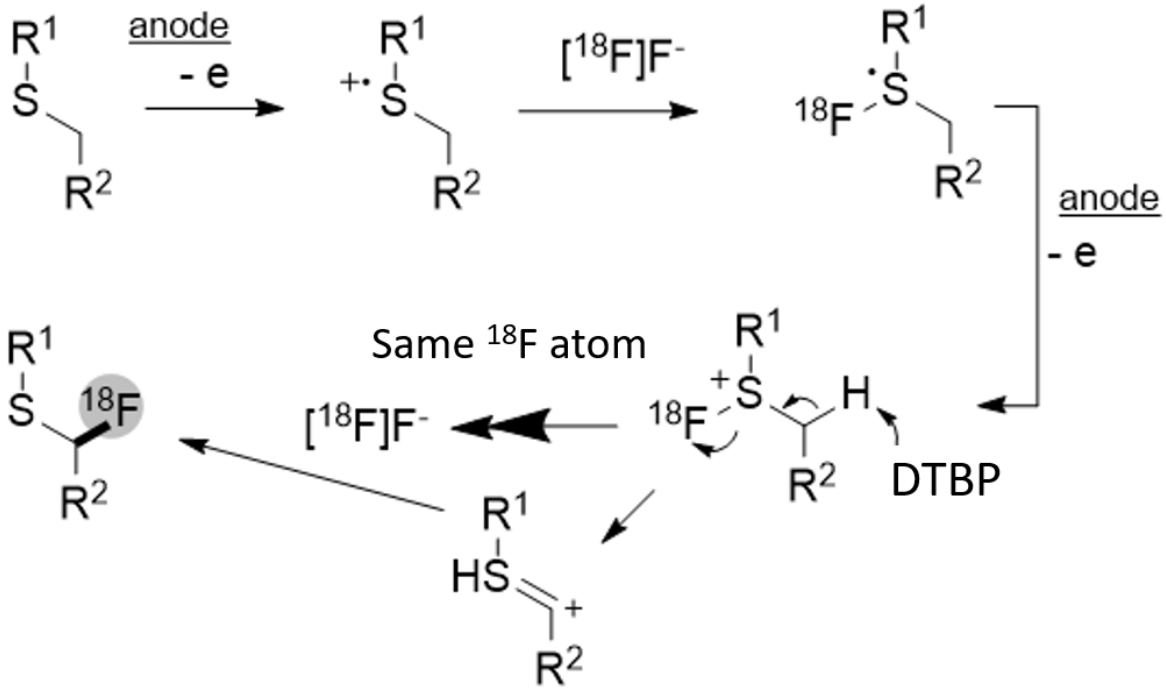

Figure 140: DTBP assisted FP mechanism of thioether in MeCN. In the single fluoride atom hypothesis, the same fluorine that is stabilizing the sulfur is the one that adds to the alpha carbon. In this way, only one fluoride is necessary for NCA-ECF.

Single Fluoride Atom Hypothesis: In the no-carrier added electrochemical fluorination of thioethers the same fluoride atom that is attached to the sulfur for stabilization is the fluorine atom that binds to the alpha carbon. This would mean the only role for the auxiliary molecule

(conjugate base of TFE) is proton abstraction in the fluoro-Pummerer mechanism which can also be filled using other bases such as DTBP.

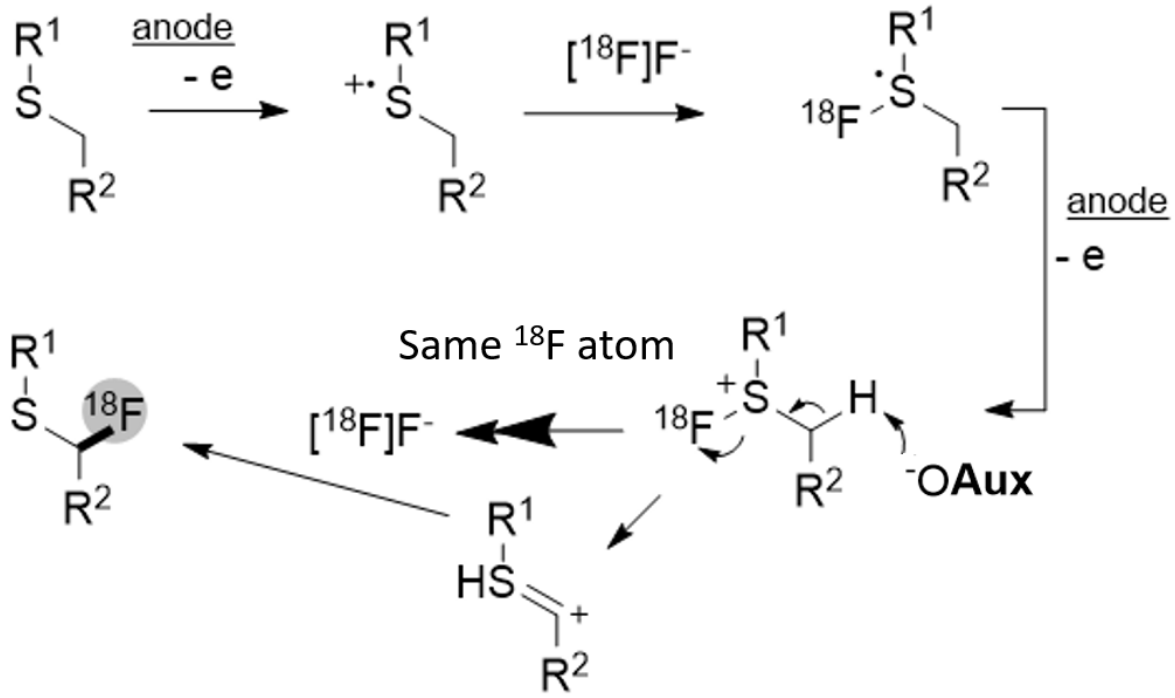

Figure 141: The single fluoride atom fluoro-Pummerer mechanism using TFE as solvent. The role of the conjugate base of TFE is proton abstraction.

The Single Fluoride Atom Hypothesis (Figure 141) fits the data more appropriately through its explanation of 3 successful results of the NCA synthesis in thioethers using TFE, DTBP and pyridinium salt. This FP mechanism using the same fluoride atoms means that neither cations produced in the mechanism needs to have a substantial lifetime. Fluoride near the anode immediately stabilizes the first cation after oxidation. Once the fluoride leaves after 2nd oxidation, the base (TFE conjugate base or DTBP) proton abstracts, which is then followed by the same fluoride atom that leaves the sulfur now binding to the newly formed carbocation. It could be likely that even in high concentrations of poly HF fluoride sources this single atom hypothesis may be responsible for improved thioethers fluorination yields when compared to other precursors. This

mechanism only requires one fluoride atom and one proton abstracting molecule, similarly to other ECEC mechanisms. If thioethers required more than 1 fluoride atom in the mechanism, product yields would decrease more rapidly as fluoride concentrations lowered than other precursors which only need one fluoride in the ECEC mechanism. This is not the case. Thioethers are one of the easiest and straightforward molecules to fluorinate. The Single Fluoride Atom Theory may prove to be a more likely explanation which is most plausible as the produced cation after the 2nd oxidation moves in the opposite direction as the fluoride that leaves sulfur due to the oxidation potential. The positive potential likely forces these opposites charged ions together and there is vacancy on the alpha carbon that fluoride can easily attack due to the abstracted proton.

12.5 The ECEC Mechanism and Concerted Proton Electron Transfer (CPET)

The steps within the ECEC mechanism are quite similar to that found in the FP mechanism in the order of events. Typically, the oxidation and proton abstraction occur before the oxidation and fluorination steps. However, this is not true for the accepted ECEC mechanism of aromatic rings since it has the oxidation and fluorination steps situated before the oxidation and proton abstracting steps. The aromatic ECEC mechanism was proposed during the Simons fluorination era of electrochemistry in which the oxidation potential was high enough to form fluoride nickel complexes. This high oxidation potential on nickel was also strong enough to adsorb most organic molecules, which can proceed through multiple oxidation without leaving the anode due to adsorption. This is not the case under the ECEC mechanism at lower oxidation potential using a platinum anode for instance. In this case, molecules are not adsorbed and the oxidation creates cations that are repulsed from the surface of the anode due to electrostatics since similar charges

repeal one another. This line of thinking where fluorination can occur easily before proton abstraction about the ECEC mechanism of aromatics has persisted even though the Simon process is not occurring.

There are several potential problems with this reverse of proton abstraction and fluoride addition in ECF. First, after fluorination there is no force on the neutral radical molecule to travel back to the anode to oxide. The molecule is more likely to travel into the bulk solution rather than back to the anode. Due to this, the neutral radical is much more likely to undergo a chemical reaction and form an unwanted radio side product leading to very low product yields even in carrier added synthesis. This is not what was observed in the data. Second, it is less likely for fluorination to occur before proton abstraction since the neutral radical after fluoride is added t will have a higher oxidation potential than the precursor. The precursor will be preferentially oxidized whereas the higher oxidation potential will not favor oxidization of the fluoride added neutral radical. Without the immediate second oxidation, the aromatic ECEC mechanism will not proceed. This second oxidization step is unlikely to occur with all the competing precursor molecules traveling to the surface of the anode that have lower oxidation potentials. Third, fluorination is much more favorable after proton abstraction since there is a carbon lacking a hydrogen bond. It is much easier for fluoride to attack the carbon without the hydrogen due to the fact that fluoride has a great propensity to abstract a proton and form HF.

The evidence of increasing acidity reducing ECF fluorination yields may suggests that in that protons may need to be abstracted first before fluorination even in the aromatics ECEC mechanism. The main problem is that the proton abstracted aromatic cation is not as stable as the benzylic cation to be able to follow the same benzylic ECEC mechanism (Figure 2). Recent advances in surface electrochemistry could expand the ECEC mechanism to be more compatible

with ECF. Concerted events can occur at the electrode where it is energetically favorable for redox and chemical reaction to occur at the same time. This could form radicals without forming cations intermediates.

In the field of C-H activation, the transfer of both H+ and e- is described via Proton Coupled Electron Transfer reactions (CPET) [189]. Photochemical CPET reactions have been studied for the last decade and we are only beginning to better understand their influence on surface electrochemistry. According to Dr. Koper, a leading theorist into CPET, CPET reactions are ubiquitous in redox electrochemistry and electrocatalysis [190]. He further states that in the surface electrochemistry literature, one practically always assumes CPET pathways [190]. The two most important features of whether CPET occurs is the sequential Electron Transfer (ET) or Proton Transfer (PT) states and the solvent cross coupling and coordinating of the proton and electron transfer. This dependence on a particular solvent feature could explain some of the effective data on NCA-ECF being very solvent specific. In contrast to Hydrogen Atom Transfer (HAT), CPET involves the proton and electron travelling from a single donor to a different recipients where the acceptors and donors can both be two distinct molecules [1]. The theory of CPET has been developed for some time [191] and has been applied to variety of organic synthetic approaches [189]. The thermodynamic benefits of CPET seen in Figure 142 where CPET requires less energy than either of the stepwise oxidation and proton transfer. Although a downside to the CPET process is due to their slower kinetics, [192].

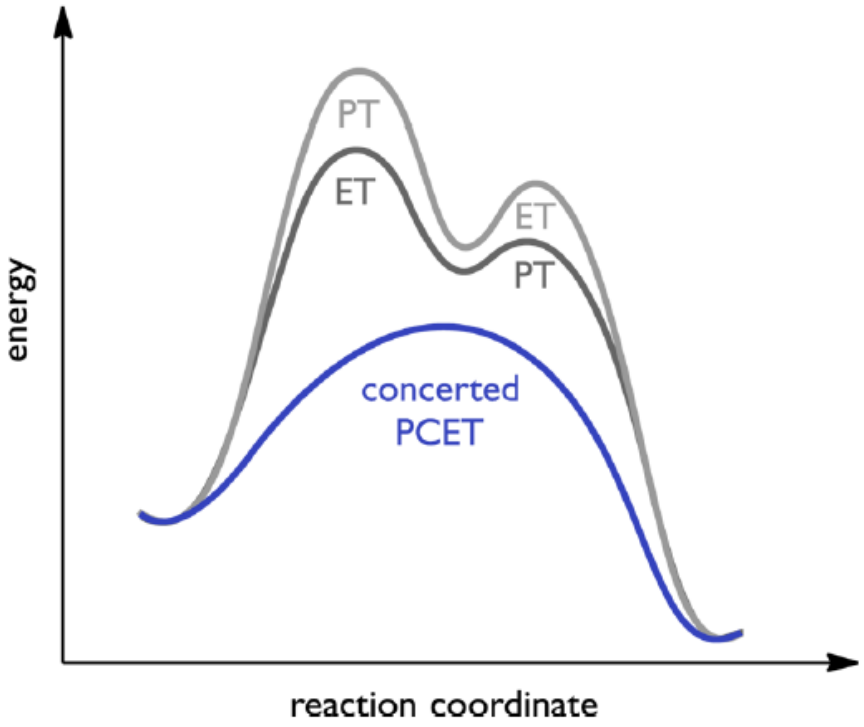

Figure 142: Concerted Proton Electron Transfer (CPET) is thermodynamically favorable to the step-wise Electron Transfers (ET) and Proton Transfer (PT) mechanisms in many electrochemical applications. Adapted from *Synthetic Applications of Proton-Coupled Electron Transfer [1]*.

There is a growing amount of literature in recent surface electrochemistry, suggesting t many electrochemical oxidations occur via a concerted proton electron transfer (CPET) [1, 189, 190, 192]. The concerted pathway lowers the oxidation potential of the molecule because the hydrogen is being abstracted simultaneously with oxidization. This concerted oxidation-abstraction is essentially the E and C steps happening in one step. CPET mechanism is more likely to occur in electrochemistry for conjugated systems, particularly for aromatics [193]. For instance, in the electrochemical ECEC mechanism of fluorination with 1,2,4,5-tetracyanobenzene and anthraquinone the data suggest that the reaction proceeds efficiently when H+ is abstracted in a CPET reaction at the anode [189]. Both CV data and Density Functional Theory (DFT) have shown carbamates to go through a concerted proton electron transfer (CPET) in an electrochemical ECEC

mechanism of alkoxylation [194]. The authors termed this a an (EC)EC mechanism due to the simultaneous nature of the first two steps. Although there are many CPET electrochemical models, the large number of parameters involved and the uncertainty of the quantum chemical calculations and experimental data makes it challenging to model each process accurately [192]. It was determined the photocatalyzed benzylic fluorination mechanism was likely proceed through CPET [193], which may extend to the ECF fluorination of benzylic groups with the first step likely to be CPET.

Laser Flash Photolysis (LFP) experiments of many aromatic molecule in TFE and HFIP have shown cation lifetimes in the second and minute ranges [120, 178, 186]. However, ECF of aromatic compounds has not been easy. This may suggest the stabilization of aromatic cations may not always be as critical a component for successful ECF by ECEC as previously thought. It may be that the intermediate cations never exist for long time periods in a CPET mechanism. In the (EC)EC mechanism, the first (EC) step creates a neutral radical, which is not repelled from the anode, becomes oxidized again on the anode (E) and reacts with fluoride (C). There may be several different possible routes to fluorination in the ECEC scheme. This mechanism is initiated by proton abstraction with oxidation step (CPET) seen in Figure 143. Crucially, each step of the (EC)EC mechanism proceeds without the need to leave the anode. If CPET occurs, this process would be inhibited by acidity which will neutralize proton abstracting molecules.

Concerted electrochemical phenomena offered more opportunities to expand electrochemistry into new applications. These finding warrant further investigation into each of the steps of ECF under NCA conditions.

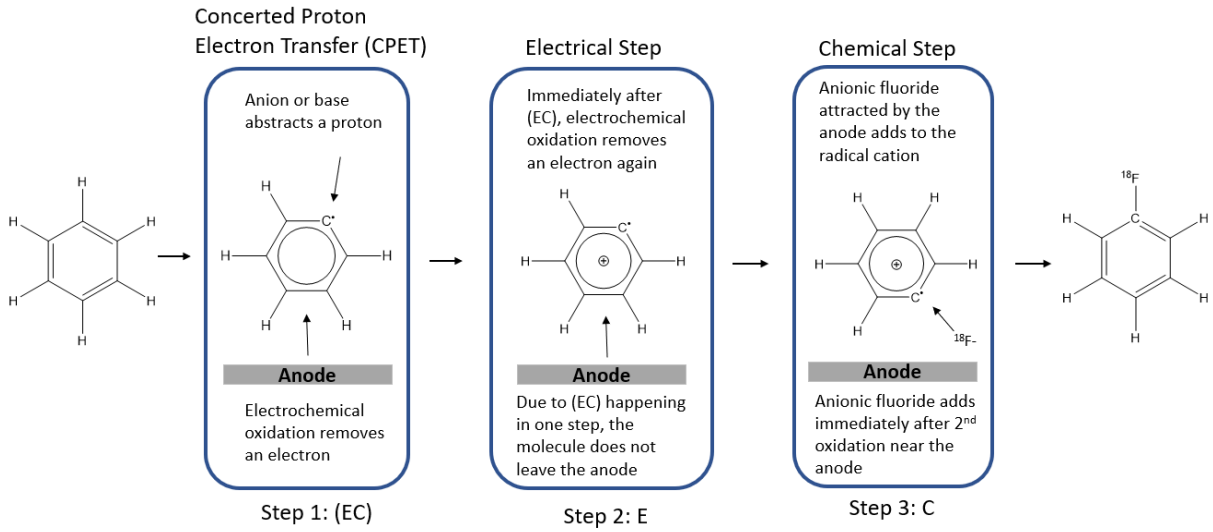

Figure 143: The propose alternative (EC)EC Mechanism of Electrochemical Fluorination (ECF) of aromatics which using a Concerted Proton Electron Transfer (CPET) as the first step.

12.6 Thioethers

There are some fundamental benefits to the FP mechanism in thioethers. Stabilizing the first sulfur cation with fluoride addition allows ECF to occur successfully in many different solvents using poly HF fluoride sources. Previous study found that thioether cations stability is due mostly to the polarizability of the solvent which was also consistent with the solvent experiments with poly HF using Methyl (phenylthio) Acetate [102, 195]. Under NCA conditions, the solvent had a large effect on the different radio side product formation, many of which did not form under the similar conditions when adding poly HF fluoride sources.

The oxidation on sulfur in thioethers is very kinetically and thermodynamically favored. In NCA-ECF using TFE, thioethers oxidize at sulfur preferably up to 4.0V (Ag/Ag+). Under these conditions, fluoride is added to the alpha position for fluorination although many other sites of the precursor could also oxidize at that potential. For instance, aromatic fluorination in thioethers was

seen only in trace amounts on GC when using an oxidation potential of 3.5V (Ag/Ag+) which is much higher than the onset oxidation potential of the aromatic ring.

The addition of different R groups on either side of the thioether greatly influenced fluorination yields. A previous thioether study found that both phosphate and cyanide groups next to the alpha carbon, resulted in reduced yields which was also consistent to the experimental results here [82]. The addition of an aromatic ring next to the alpha carbon in thioethers can also reduce fluorination yields. This is easily seen when using Methyl (methylthio) Acetate with a RCFE of 92.7%$\pm$2.2 (n=3) which had much higher fluorination yields than Methyl (phenylthio) Acetate with an RCFE of 49.8$\pm$0.5. This may suggest electron withdrawing group strength can destabilize the cation intermediates, leading to lower product yields. Amine groups did not inhibit product yields when next to the alpha carbon in thioethers even though they oxidize at these potentials. Both the phosphonate and nitrile groups next to the alpha carbon reduce fluorination yields. The amine had reduced fluorination but comparably less than the phosphonate or nitrile groups. The NCA RCFE and A_m were substantially higher than when using carrier for thioethers, which is beneficial for using this method for thioether PET probe synthesis.

The effect of anodic acidity reducing fluorination was found in all thioether precursors discussed in section 12.2. This anodic effect using thioethers was found in reducing convection in the single chamber cell, using microfluidic cells, quickly pulsing the electrode in the static chip cell, adding acid, having triflic acid concentration higher than TBAF, using the two-chamber cell, and, finally adding a base in MeCN to significantly increase NCA-ECF of fluorination yields. Additionally, the properties of successful NCA-ECF in TFE using thioethers can be attributed to the conjugate base of the solvent which can neutralize anodic acidity.

12.7 Modafinil Precursor

Unlike previous thioether or benzylic precursors, the Modafinil precursor possess potentially 2 alpha carbons to sulphur that can be fluorinated with one of them at the benzylic position. This combination of alpha carbon to sulfur and benzylic carbon is unusual and not reported in literature for ECF which was reasoned why NCA-ECF in TFE or HFIP did not work well with this precursor. A likely explanation is as result of solvent reactivity of TFE, HFIP or the conjugate bases to the benzylic radical cation. The fluorinated modafinil precursor was instable and NMR could not be completed to verify the fluorination site. It is likely that the fluorination site is at the benzylic position due to the instability of the fluorinated product, stability of the benzylic cation intermediate and the loss of fluoride due to instability. The non-benzylic alpha carbon if fluorinated was thought to likely show radiolabeled organics if instable on HPLC which was not the case. Defluorination occurred with instability.

There have been successful ECF in precursors which do contain both sulfur and benzylic positions, these oxidation sites often have similar oxidation potentials. Benzylic fluorination occurred preferentially in sulfides at low concentration of fluoride which was reversed to be alpha to sulfur at high concentrations of fluoride [81]. This is likely due to increased fluoride availability in the FP mechanism. In O-methyl S-phenethyl thiocarbonate, the alpha sulfur is favored whereas there was no benzylic fluorination [88]. Another study found that fluorination t is preferential on the alpha to sulfur position verses benzyl or aromatic positions [82]. Another potential problem is that benzylic precursors containing with the sulfur tend to dimerization which can occur from oxidation forming Ph-S-S-Ph [82].

The Modafinil precursor was successfully fluorinated in NCA conditions using MeCN as solvent with the addition of DTBP base. Without DTBP only trace fluorination occurs which

supports the anodic acidity hypothesis. Since fluorination was successful in MeCN, this s supports the evidence that TFE and HFIP may be reactive to benzylic position during electrolysis.

Without BOC protection the Modafinil precursor was unsuccessfully fluorinated in all solvents. The single BOC protected Modafinil precursor fluorinated under NCA-ECF in MeCN with DTBP. The unprotected amine group interfered in the ECF process either by oxidation of the amine or by acting as a competing nucleophile. This was not the case for (Phenylthio) Acetamide which resulted in a RCFE of 23.3±4.1%. The two-chamber cell was not investigated to determine if reduction had a negative or positive impact on the modafinil precursor in ECF.

12.8 Naphthalene

The consistent observations where different solvents greatly affect NCA fluorination outcomes was also observed with Naphthalene. MeCN with or without DTBP did not work for Naphthalene in the single chamber cell. The solvent TFE produced an RCFE of up to 4.4%whereas HFIP produced an RCFE of 12.2±0.7 (n=3). The improved fluorination is likely due to the highly conjugated Naphthalene cation which has a long lifetime in HFIP. HFIP also easily reduces on the cathode likely shielding aromatic reduction.

When using poly HF sources naphthalene has been observed to undergo difluorination in preference to monofluorination. Similar to naphthalene , quinolines underwent successful ECF in MeCN and Et_3N*3HF with high yields of double fluorination [54]. This could be due to the addition of fluoride to conjugated naphthalene cations only barely raising the oxidization potential of the molecule, making further oxidation likely. Difluorination is unlikely under NCA fluoride conditions as there is not enough fluoride in solution for multiple electrochemical fluorination reaction to proceed on the same molecule. However, this shows that multiple oxidations likely

occur with a significant impact on fluorination yields. The NCA-ECF in HFIP in the single chamber cell of several dimethoxybenzenes and trimethoxybenzenes was attempted. Gamma peaks were observed at the retention time near naphthalene, suggesting dimerization along with fluorination with these precursors. The two-chamber cell was not used to determine if reduction had a significant role in NCA-ECF using Naphthalene. This is an important factor for aromatics as the F-DOPA Intermediary and the COX-2 Inhibitor precursor NCA-ECF required use of the two-chamber cell.

12.9 F-DOPA Intermediary

In successful ECF of the F-DOPA Intermediary, it is evident that these reactions are pH sensitive. Our NCA-ECF results suggest the necessity to have slight acidity present for the t-butyl group to dissociate. The addition of acetic acid in the single chamber cell was required for successful NCA-ECF with RCFE of 6.8$\pm$1.3% (n=3). Slightly acidic condition was also used in the two-chamber cell using the AEM membrane in HFIP which also led to NCA-ECF RCFE of 9.5$\pm$0.4% (n=3). The AEM reduces the acidity build up in the anodic chamber during electrolysis compared to the CEM in the two-chamber cell. This evidence further supports the anodic acidity hypothesis. The slight acidity seems to be necessary to allow the t-butyl group to become a good leaving group in the ECEC mechanism. Although there is some evidence the t-butyl group could leave prior to ECEC. In the NCA-ECF two-chamber experiments in HFIP, the remaining precursor was identified to primarily be the BOC protected catechol with little precursor remaining with the t-butyl group. This may suggest that the t-butyl group leaves before proceeding towards the ECEC mechanism due to another electrochemical process.

Careful pH control is necessary to cause the t-butyl group to be a good leaving group. The ability to control the pH environment within electrochemistry is difficult since buffers are not electrochemically stable. Electrolysis can change the pH of the electrochemical solution causing a time variance to pH. More work needs to be performed to understand how to control pH more carefully during electrolysis for this reaction.

Hydrogen tends to be favored to the t-butyl group for substitution of fluoride in ECF. This is most noticeable in the studies with benzene where substitution of hydrogen was favored more than 3 to 1 over t-butyl. Based on our data, the detachment of the t-butyl group does not appear to be very beneficial for ECF over hydrogen in the same position.

The single chamber cell did not successfully fluorinate the F-DOPA Intermediary. It is difficult to observe whether this was a result of reduction, reductive side products, or the increase in pH caused by reduction. TFE also produced low RCFE yields, suggesting the increased acidity or cation stabilization effect of HFIP was responsible for successful NCA-ECF for the F-DOPA Intermediary. HFIP may also stabilize the t-butyl cation, making it a much stronger leaving group.

12.10 COX-2 Inhibitor Precursor

The carrier added synthesis of the COX-2 Inhibitor probe only resulted in fluorination yields of 2% in the single chamber cell. There were several radio-labeled side products but the RCC or total fluorination incorporation in organic molecules was also low (~5%). Increasing the duration of electrolysis or reducing poly HF concentration did not increase fluorination yields. This is most likely due to increased side product formation with more time or with less concentration of poly HF fluoride. Lowering the concentration of the easily reduced poly HF fluoride would increase the reductive side products.

The NCA-ECF experiments using the COX-2 Inhibitor Precursor did not have successful fluorination in the single chamber cell in any solvent, suggesting that reduction has a negative impact on fluorination. Performing single chamber cell experiments using MeCN, TFE, HFIP and DME solvents with and without DTBP base led to unsuccessful NCA-ECF. DTBP base oxidizes at this potential which was shown to decrease RCFE at higher potentials in the Modafinil precursor. TFE and HFIP both have oxidation potentials less than the COX-2 Inhibitor precursor, suggesting these solvents were incompatible with high oxidation potential precursors. DME also has a low oxidation potential and low dielectric constant. DME with DTBP did produce trace fluorination results in the single chamber cell, suggesting the solution should be more basic for fluorination to proceed NCA with the COX-2 Inhibitor precursor.

In the two-chamber cell, NCA fluorination greatly exceeded the RCC yields under carrier conditions. The solvent heavily influenced the species of radio side products formed in solution. Using the CEM in MeCN the addition of DTBP to the cathodic chamber (CC) increased fluorination of a radio side product from an RCC of 3.5% with no DTBP to 6.6% with DTBP in the CC. However, the fluorinated COX-2 Inhibitor was not formed in appreciable yields using the CEM. Only trace results were observed using DME and CEM. The DTBP in the cathodic chamber changes the reaction in the anodic chamber by reducing acidity due to increased diffusion of protons against the gradient caused by DTBP when using the CEM. Using the AEM with MeCN in the two-chamber cell with DTBP in the CC produced similar amounts of RCC. Changing the membranes produced >1% RCFE of the fluorinated product. AEM has been previously shown to reduce acidity in the anodic chamber leading to increased results in the F-DOPA intermediary synthesis. DME produced similar results as MeCN using the AEM with almost the exact same RCFE yields with much less radio side product formation. An additional chamber was added to

the anodic chamber to reduce acidity even further. The proton sink chamber (PSC) was added with a CEM and DTBP in the chamber to provide further proton removal from the anodic chamber decreasing anodic acidity. Using this two chamber AEM with PSC increased the RCFE in MeCN and DME to 6.8±0.7% (n=3) and 2.1±0.2% (n=3) respectively. The incorporation of fluoride into radio side products was high for MeCN with an RCC of 40.9±2.2% (n=3). This finding offers yet more strong support for the anodic acidity hypothesis, as well as evidence that reduction plays a role in decreasing fluorination yields in the single chamber cell. The next step is to image the COX-2 Inhibitor probe using this NCA-ECF synthesis method. There is one important caveat to consider. The NCA synthesis are identified by the HPLC retention time of the reference standard. In electrochemistry the number of possible reactions and side products can be large and difficult to predict. Although unlikely, this may lead to a radio side product with similar HPLC retention times as the reference standard.

12.11 Limitations of NCA-ECF

Although there are many advantages of ECF for PET probe synthesis, as described in section 1.6, there are also several limitations of using the ECF method that are important to discuss for the application of PET probe synthesis. The size of the precursor can have a negative impact on successful ECF. Small molecular weight precursors (~ <500 amu) which are comparable in size as many successful small molecule PET probes, are favored for NCA-ECF. The oxidation potential can be used to preferentially oxidize a targeted site and any other groups with lower oxidation potential are likely be easily protected. The smaller molecular size does not require the need to protect many groups and acid deprotection is a quick step frequently used after ^{18}F radiolabelling making this a straightforward process. The smaller size means that there is not likely many other

alternative sites to oxidize at the chosen oxidation potential which would lead to less radio side product formation. The smaller molecules are also likely to be kinetically and thermodynamically favored for ECEC and FP mechanisms as the they can travel faster with quicker orientation and less steric hinderance. These makes NCA-ECF a very favorable potential route to ^{18}F radiolabelling potential small molecule PET probes.

Larger precursors by molecular weight (>500 amu) do not have a large scope of successful ECF with poly HF fluoride sources like smaller molecular weight precursors. The use of the COX-2 Inhibitor precursor highlighted a few of the difficulties. There is likely to be several different competing oxidation sites under the chosen oxidation potential leading to radio side product formation. Additionally, these moderately sized molecules may have several lower oxidation groups that must be protected which may cause synthesis difficulties. This could often make traditional radiochemistry more appealing if it is possible. For the COX-2 Inhibitor tracer there is not a good route to fluorinate the pyrazole without using electrochemistry.

NCA-ECF of aromatics for PET probe synthesis could be an advantageous strategy to pursue due to their increased *in vivo* stability. The higher oxidation potentials of aromatics can lead to many different oxidation sites in organic molecules which have multiple aromatic rings with similar oxidation potentials. This can result in the formation of many different aromatically labelled side products.

Functional groups with low oxidation potential appear to be a limitation, particularity when they are hydroxyl, as well as the primary or secondary amines. A comprehensive review of oxidation potentials of different organic molecules can be found here [135]. BOC protection was used with good results to protect both hydroxyl and primary or secondary amines. Precursors with alkene groups are known to be easily fluorinated using ECF and may be the major site for

fluorination due to the lower oxidation potential causing lower fluorination yields at more desirable locations.

A current challenge in electrochemistry that is not found within in radiochemistry is the ability to control the large and varied concentration of side products that forms through electrolysis. This problem is not observed in carrier added ECF because the HPLC separation method can isolate the product in millimolar concentration with only a small overlap of contaminants in the micromolar concentration, which leads to ~99% product purity under carrier added conditions. When switching to NCA conditions, a vast amount of side product in the low micromolar range is formed, that is difficult and time consuming to purify via HPLC. This is an important downfall to consider when using this approach to synthesize PET probes in a very short timeframe since it may require extensive optimization efforts to isolate the ^{18}F labeled product in NCA conditions.

Lastly, there are differences between the ^{18}F labelled radio products formed under NCA conditions compared to carrier added conditions. This can make it difficult to identify the fluorinated species under NCA conditions since these radiochemical products may not form under carrier added conditions in sufficient amounts to perform MS or NMR identification. This makes the strategy of performing the ECF under carrier added conditions and moving to NCA not always an optimal or possible approach in some cases.

12.12 Concluding Remarks

Herein, we have shown electrochemical radiofluorination is demonstrated to have good potential to produce ^{18}F-labelled PET probes under no-carrier-added (NCA) conditions for both thioethers and aromatics throughout this work. Aromatics are an important target for fluorination

due to *in vivo* stability. Preliminary evidence suggests the electrochemical conditions beyond oxidation potential may be able to influence site selectivity in complex aromatic precursors. Since this research field is at the beginning stages of its development, further investigation is required in order to fully understand it's potential to radiolabel different types of precursors towards applications in radiotracer synthesis. Electrochemical fluorination (ECF) may simplify many nucleophilic radiolabelling processes. This methodology can quickly synthesize PET probes for testing with minimal time and investment. There is quite a large untapped design space for developing new PET tracers. Any technology that has the potential and scope to open up new design space in PET radiotracer synthesis should definitely be further explored with electrochemical radiofluorination as one such field to be seriously considered. The electrochemical approach should be further developed to be one of the tools in the toolkit of PET radiochemistry.

References

1. Gentry, E.C. and R.R. Knowles, *Synthetic applications of proton-coupled electron transfer.* Accounts of chemical research, 2016. **49**(8): p. 1546-1556.
2. Reischl, G., G. Kienzle, and H.-J. Machulla, *Electrochemical radiofluorination: Labeling of benzene with [18F]fluoride by nucleophilic substitution.* Journal of Radioanalytical and Nuclear Chemistry, 2002. **254**(2): p. 409-411.
3. Kienzle, G.J., G. Reischl, and H.J. Machulla, *Electrochemical radiofluorination. 3. Direct labeling of phenylalanine derivatives with [18F] fluoride after anodic oxidation.* Journal of Labelled Compounds and Radiopharmaceuticals: The Official Journal of the International Isotope Society, 2005. **48**(4): p. 259-273.
4. Kienzle, G.J., G. Reischl, and H.J. Machulla, *Electrochemical radiofluorination. 3. Direct labeling of phenylalanine derivatives with [18F]fluoride after anodic oxidation.* Journal of Labelled Compounds and Radiopharmaceuticals, 2005. **48**(4): p. 259-273.
5. Reischl, G., G.J. Kienzle, and H.J. Machulla, *Electrochemical radiofluorination. Part 21. Anodic monofluorination of substituted benzenes using [18F]fluoride.* Applied Radiation and Isotopes, 2003. **58**(6): p. 679-683.
6. Zhu, A., D. Lee, and H. Shim, *Metabolic PET Imaging in Cancer Detection and Therapy Response.* Seminars in oncology, 2011. **38**(1): p. 55-69.
7. Jiang, L., et al., *PET probes beyond (18)F-FDG.* Journal of Biomedical Research, 2014. **28**(6): p. 435-446.
8. Zhuang, H. and I. Codreanu, *Growing applications of FDG PET-CT imaging in non-oncologic conditions.* Journal of Biomedical Research, 2015. **29**(3): p. 189-202.
9. Ikotun, O., B. Clark, and J. Sunderland, *A snapshot of United States PET cyclotron and radiopharmaceutical production operations and locations.* J Nucl Med, 2012. **53**(Suppl 1): p. 1085.
10. S. Keppler, J. and P. Conti, *A Cost Analysis of Positron Emission Tomography*. Vol. 177. 2001. 31-40.
11. Pelc, N.J., P.E. Kinahan, and R.I. Pettigrew, *Special Section Guest Editorial: Positron Emission Tomography: History, Current Status, and Future Prospects.* Journal of Medical Imaging, 2017. **4**(1): p. 011001-011001.
12. Vallabhajosula, S., L. Solnes, and B. Vallabhajosula, *A broad overview of positron emission tomography radiopharmaceuticals and clinical applications: what is new?* Seminars in nuclear medicine, 2011. **41**(4): p. 246-264.
13. Phelps, M.E., *PET: molecular imaging and its biological applications*. 2004: Springer Science & Business Media.
14. Kubota, K., *From tumor biology to clinical PET: a review of positron emission tomography (PET) in oncology.* Annals of nuclear medicine, 2001. **15**(6): p. 471-486.
15. Schindler, T.H., et al., *Cardiac PET Imaging for the Detection and Monitoring of Coronary Artery Disease and Microvascular Health.* JACC: Cardiovascular Imaging, 2010. **3**(6): p. 623-640.
16. Gholami, S., et al., *Assessment of atherosclerosis in large vessel walls: A comprehensive review of FDG-PET/CT image acquisition protocols and methods for uptake quantification.* Journal of Nuclear Cardiology, 2015. **22**(3): p. 468-479.
17. Glaudemans, A.W.J.M., et al., *The Use of (18)F-FDG-PET/CT for Diagnosis and Treatment Monitoring of Inflammatory and Infectious Diseases.* Clinical and Developmental Immunology, 2013. **2013**: p. 623036.

18. Tarkin, J.M., F.R. Joshi, and J.H.F. Rudd, *PET imaging of inflammation in atherosclerosis.* Nat Rev Cardiol, 2014. **11**(8): p. 443-457.
19. Silverman, D.S., et al., *Positron emission tomography in evaluation of dementia: Regional brain metabolism and long-term outcome.* JAMA, 2001. **286**(17): p. 2120-2127.
20. Rice, L. and S. Bisdas, *The diagnostic value of FDG and amyloid PET in Alzheimer's disease—A systematic review.* European Journal of Radiology, 2017. **94**: p. 16-24.
21. Meles, S.K., et al., *Metabolic Imaging in Parkinson Disease.* Journal of Nuclear Medicine, 2017. **58**(1): p. 23-28.
22. Petrou, M., et al., *Amyloid deposition in Parkinson's disease and cognitive impairment: A systematic review.* Movement Disorders, 2015. **30**(7): p. 928-935.
23. Pagano, G., F. Niccolini, and M. Politis, *Current status of PET imaging in Huntington's disease.* European Journal of Nuclear Medicine and Molecular Imaging, 2016. **43**(6): p. 1171-1182.
24. Ahmad, R., et al., *PET imaging shows loss of striatal PDE10A in patients with Huntington disease.* Neurology, 2014. **82**(3): p. 279-281.
25. Scott, G., et al., *Microglial positron emission tomography (PET) imaging in epilepsy: Applications, opportunities and pitfalls.* Seizure, 2017. **44**: p. 42-47.
26. Bansal, L., et al., *PET hypermetabolism in medically resistant childhood epilepsy: Incidence, associations, and surgical outcome.* Epilepsia, 2016. **57**(3): p. 436-444.
27. Willmann, J.K., et al., *Molecular imaging in drug development.* Nature reviews. Drug discovery, 2008. **7**(7): p. 591.
28. Rudin, M. and R. Weissleder, *Molecular imaging in drug discovery and development.* Nature reviews. Drug discovery, 2003. **2**(2): p. 123.
29. Phelps, M.E., *Positron emission tomography provides molecular imaging of biological processes.* Proceedings of the National Academy of Sciences, 2000. **97**(16): p. 9226-9233.
30. Jadvar, H. and J.A. Parker, *Clinical PET and PET/CT*. 2006: Springer Science & Business Media.
31. Alauddin, M.M., *Positron emission tomography (PET) imaging with (18)F-based radiotracers.* American Journal of Nuclear Medicine and Molecular Imaging, 2012. **2**(1): p. 55-76.
32. Stenhagen, I.S., et al., *[18 F] Fluorination of an arylboronic ester using [18 F] selectfluor bis (triflate): application to 6-[18 F] fluoro-l-DOPA.* Chemical Communications, 2013. **49**(14): p. 1386-1388.
33. DiFilippo, F.P., et al., *Small Animal Imaging using a Clinical Positron Emission Tomography/Computed Tomography and Super-Resolution.* Molecular imaging, 2012. **11**(3): p. 210-219.
34. Böhm, H.-J., et al., *Fluorine in Medicinal Chemistry.* ChemBioChem, 2004. **5**(5): p. 637-643.
35. Kirk, K.L., *Fluorine in medicinal chemistry: Recent therapeutic applications of fluorinated small molecules.* Journal of Fluorine Chemistry, 2006. **127**(8): p. 1013-1029.
36. Gillis, E.P., et al., *Applications of Fluorine in Medicinal Chemistry.* J Med Chem, 2015. **58**(21): p. 8315-59.
37. Jacobson, O., D.O. Kiesewetter, and X. Chen, *Fluorine-18 Radiochemistry, Labeling Strategies and Synthetic Routes.* Bioconjugate Chemistry, 2015. **26**(1): p. 1-18.
38. Lee, E., J.M. Hooker, and T. Ritter, *Nickel-mediated oxidative fluorination for PET with aqueous [18F] fluoride.* Journal of the American Chemical Society, 2012. **134**(42): p. 17456-17458.
39. Rotstein, B.H., et al., *Spirocyclic hypervalent iodine (III)-mediated radiofluorination of non-activated and hindered aromatics.* Nature communications, 2014. **5**: p. 4365.
40. Sergeev, M.E., et al., *Titania-catalyzed radiofluorination of tosylated precursors in highly aqueous medium.* Journal of the American Chemical Society, 2015. **137**(17): p. 5686-5694.
41. Gao, Z., et al., *Metal-Free Oxidative Fluorination of Phenols with [18F]Fluoride.* Angewandte Chemie, 2012. **124**(27): p. 6837-6841.

42. Preshlock, S., M. Tredwell, and V. Gouverneur, *18F-Labeling of Arenes and Heteroarenes for Applications in Positron Emission Tomography.* Chemical Reviews, 2016. **116**(2): p. 719-766.
43. L. Cole, E., et al., *Radiosyntheses using Fluorine-18: The Art and Science of Late Stage Fluorination.* Current Topics in Medicinal Chemistry, 2014. **14**(7): p. 875-900.
44. Tredwell, M. and V. Gouverneur, *18F Labeling of Arenes.* Angewandte Chemie International Edition, 2012. **51**(46): p. 11426-11437.
45. Lee, E., et al., *A fluoride-derived electrophilic late-stage fluorination reagent for PET imaging.* Science, 2011. **334**(6056): p. 639-642.
46. Mosessian, S., et al., *INDs for PET Molecular Imaging Probes—Approach by an Academic Institution.* Molecular Imaging and Biology, 2014. **16**(4): p. 441-448.
47. Vallabhajosula, S., L. Solnes, and B. Vallabhajosula, *A broad overview of positron emission tomography radiopharmaceuticals and clinical applications: what is new?* Semin Nucl Med, 2011. **41**(4): p. 246-64.
48. Pacak, J., Z. Tocik, and M. Cerny, *Synthesis of 2-deoxy-2-fluoro-D-glucose.* Journal of the Chemical Society D: Chemical Communications, 1969(2): p. 77-77.
49. Ter-Pogossian, M.M., et al., *A Positron-Emission Transaxial Tomograph for Nuclear Imaging (PETT).* Radiology, 1975. **114**(1): p. 89-98.
50. Wagner, H.N., *A brief history of positron emission tomography (PET).* Seminars in Nuclear Medicine, 1998. **28**(3): p. 213-220.
51. Lopci, E., et al., *Imaging with non-FDG PET tracers: outlook for current clinical applications.* Insights into Imaging, 2010. **1**(5-6): p. 373-385.
52. Rozhkov, I.N., *Radical-cation mechanism of the anodic fluorination of organic compounds.* Russian Chemical Reviews, 1976. **45**(7): p. 615.
53. Noel, M. and V. Suryanarayanan, *Current approaches to the electrochemical synthesis of organo-fluorine compounds.* Journal of Applied Electrochemistry, 2004. **34**(4): p. 357-369.
54. Fuchigami, T. and T. Tajima, *Highly selective electrochemical fluorination of organic compounds in ionic liquids.* Journal of Fluorine Chemistry, 2005. **126**(2): p. 181-187.
55. Fuchigami, T. and S. Inagi, *Selective electrochemical fluorination of organic molecules and macromolecules in ionic liquids.* Chemical Communications, 2011. **47**(37): p. 10211-10223.
56. Khan, Z.U.H., et al., *Ionic liquids based fluorination of organic compounds using electrochemical method.* Journal of Industrial and Engineering Chemistry, 2015. **31**: p. 26-38.
57. Dawood, K.M., *Electrolytic fluorination of organic compounds.* Tetrahedron, 2004. **60**(7): p. 1435-1451.
58. Dinoiu, V., *Electrochemical fluorination of organic compounds.* Revue Romaine de Chimie, 2007. **52**(5): p. 453-466.
59. Momota, K., M. Morita, and Y. Matsuda, *Electrochemical fluorination of benzene in acetonitrile solutions.* Electrochimica Acta, 1993. **38**(4): p. 619-624.
60. Balandeh, M., et al., *Electrochemical Fluorination and Radiofluorination of Methyl(phenylthio)acetate Using Tetrabutylammonium Fluoride (TBAF).* Journal of The Electrochemical Society, 2017. **164**(9): p. G99-G103.
61. Waldmann, C.M., et al., *An automated synthesizer for electrochemical 18F-fluorination of organic compounds.* Applied Radiation and Isotopes, 2017. **127**: p. 245-252.
62. Reischl, G., G. Kienzle, and H.-J. Machulla, *Electrochemical radiofluorination: Labeling of benzene with [18F] fluoride by nucleophilic substitution.* Journal of Radioanalytical and Nuclear Chemistry, 2002. **254**(2): p. 409-411.
63. Gambaretto, G.P., et al., *The electrochemical fluorination of organic compounds: Further data in support of the ECbECn mechanism.* Journal of Fluorine Chemistry, 1985. **27**(2): p. 149-155.

64. Shreider, V. and I. Rozhkov, *Effect of anode material and solvent on ionic fluorination during anodic oxidation of aromatic compounds.* Russian Chemical Bulletin, 1979. **28**(3): p. 630-632.
65. Momota, K., M. Morita, and Y. Matsuda, *Electrochemical fluorination of aromatic compounds in liquid R4NF·mHF—part I. Basic properties of R4NF·mHF and the fluorination o.* Electrochimica Acta, 1993. **38**(8): p. 1123-1130.
66. Yoneda, N., *The combination of hydrogen fluoride with organic bases as fluorination agents.* Tetrahedron, 1991. **47**(29): p. 5329-5365.
67. LAURENT, E., B. MARQUET, and R. TARDIVEL, *Regioselectivity of the Anodic Fluorination of Benzyl Compounds.* ChemInform, 1991. **22**(36).
68. Meurs, J.H. and W. Eilenberg, *Oxidative fluorination in amine-hf mixturess.* Tetrahedron, 1991. **47**(4-5): p. 705-714.
69. Makino, K. and H. Yoshioka, *Selective fluorination of ethyl 1-methylpyrazole-4-carboxylates with poly(hydrogen fluoride)-amine complex under electrolytic anodic oxidation.* Journal of Fluorine Chemistry, 1988. **39**(3): p. 435-440.
70. Fuchigami, T., et al., *Electrolytic partial fluorination of organic compounds. 1. Regioselective anodic monofluorination of organosulfur compounds.* The Journal of Organic Chemistry, 1990. **55**(25): p. 6074-6075.
71. Yin, B., S. Inagi, and T. Fuchigami, *Highly selective electrochemical fluorination of dithioacetal derivatives bearing electron-withdrawing substituents at the position α to the sulfur atom using poly (HF) salts.* Beilstein journal of organic chemistry, 2015. **11**: p. 85.
72. Shiue, C.Y., et al., *Syntheses and specific activity determinations of no-carrier-added (NCA) F-18-labeled butyrophenone neuroleptics--benperidol, haloperidol, spiroperidol, and pipamperone.* Journal of nuclear medicine : official publication, Society of Nuclear Medicine, 1985. **26**(2): p. 181-186.
73. He, Q., et al., *Electrochemical nucleophilic synthesis of di-tert-butyl-(4-[18F]fluoro-1,2-phenylene)-dicarbonate.* Applied Radiation and Isotopes, 2014. **92**: p. 52-57.
74. He, Q., I. Alfeazi, and S. Sadeghi, *No-carrier-added electrochemical nucleophilic radiofluorination of aromatics.* Journal of Radioanalytical and Nuclear Chemistry, 2015. **303**(1): p. 1037-1040.
75. Lebedev, A., et al., *Electrochemical radiolabeling of COX-2 inhibitors: potential PET agents for imaging of inflammation.* Journal of Nuclear Medicine, 2015. **56**(supplement 3): p. 1045.
76. Lebedev, A., et al., *Radiochemistry on electrodes: Synthesis of an 18F-labelled and in vivo stable COX-2 inhibitor.* PLoS One, 2017. **12**(5): p. e0176606.
77. Campbell, M.G. and T. Ritter, *Late-Stage Fluorination: From Fundamentals to Application.* Organic Process Research & Development, 2014. **18**(4): p. 474-480.
78. Sartori, P. and N. Ignat'ev, *The actual state of our knowledge about mechanism of electrochemical fluorination in anhydrous hydrogen fluoride (Simons process).* Journal of fluorine chemistry, 1998. **87**(2): p. 157-162.
79. Conte, L. and G. Gambaretto, *Electrochemical fluorination: state of the art and future tendences.* Journal of Fluorine Chemistry, 2004. **125**(2): p. 139-144.
80. Momota, K., et al., *Electrochemical fluorination of aromatic compounds in liquid R4NF· MHF—Part II. Fluorination of di-and tri-fluorobenzenes.* Electrochimica acta, 1994. **39**(1): p. 41-49.
81. Fuchigami, T., et al., *Electrolytic partial fluorination of organic compounds. 12. Selective anodic monofluorination of fluoroalkyl and alkyl sulfides.* The Journal of Organic Chemistry, 1994. **59**(20): p. 5937-5941.
82. Fuchigami, T., M. Shimojo, and A. Konno, *Electrolytic Partial Fluorination of Organic Compounds. 17. Regiospecific Anodic Fluorination of Sulfides Bearing Electron-Withdrawing Substituents at the Position .alpha. to the Sulfur Atom.* The Journal of Organic Chemistry, 1995. **60**(11): p. 3459-3464.

83. Baroux, P., R. Tardivel, and J. Simonet, *Anodic Mono- and Difluorination of Aromatic Thioethers.* Journal of The Electrochemical Society, 1997. **144**(3): p. 841-847.
84. Shainyan, B., et al., *Selective aromatic electrochemical fluorination of methyl phenyl sulfone.* Russian journal of organic chemistry, 2002. **38**(10): p. 1462-1464.
85. Hou, Y., S. Higashiya, and T. Fuchigami, *Electrolytic Partial Fluorination of Organic Compounds. 24.1 Highly Regioselective Anodic Monofluorination of 2-Benzothiazolyl and 5-Chloro-2-benzothiazolyl Sulfides.* The Journal of Organic Chemistry, 1997. **62**(26): p. 9173-9176.
86. Shchepochkin, A.V., et al., *Direct nucleophilic functionalization of C(sp 2)–H-bonds in arenes and hetarenes by electrochemical methods.* Russian Chemical Reviews, 2013. **82**(8): p. 747.
87. Tajima, T., et al., *Electrolytic partial fluorination of organic compounds. 77. Reactivity of anodically generated benzylic cation intermediates toward fluoride ions in acetonitrile.* Journal of Electroanalytical Chemistry, 2005. **580**(1): p. 155-160.
88. Cao, Y. and T. Fuchigami, *Electrochemical partial fluorination of organic compounds: 81. Regioselective anodic fluorination of O-methyl S-aralkyl thiocarbonates.* Journal of Electroanalytical Chemistry, 2006. **587**(1): p. 25-30.
89. N, I. and M. Noel, *A comparative study of anodic fluorination of N-alkyl and N,N-dialkyl phenylacetamides in Et 3 N Á 4HF medium*. Vol. 632. 2009. 45–54.
90. Fukuhara, T., M. Sawaguchi, and N. Yoneda, *Anodic fluorination of phenols using Et3N-5HF electrolyte.* Electrochemistry communications, 2000. **2**(4): p. 259-261.
91. Baba, D. and T. Fuchigami, *Electrolytic partial fluorination of organic compounds. Part 61: The first example of direct α-fluorination of protected α-amino acids.* Tetrahedron letters, 2002. **43**(27): p. 4805-4808.
92. Tomilov, A.P. and M.Y. Fioshin, *Free radical reactions in the electrolysis of organic compounds.* Russian Chemical Reviews, 1963. **32**(1): p. 30-44.
93. von Rosenvinge, T., M. Parrinello, and M.L. Klein, *Ab initio molecular dynamics study of polyfluoride anions.* The Journal of chemical physics, 1997. **107**(19): p. 8012-8019.
94. Hagiwara, R., et al., *The Effect of the Anion Fraction on the Physicochemical Properties of EMIm (HF) n F (n= 1.0– 2.6).* The Journal of Physical Chemistry B, 2005. **109**(12): p. 5445-5449.
95. Prkić, A., et al., *Direct Potentiometric Determination of Fluoride Species by Using Ion-Selective Fluoride Electrode.* Int. J. Electrochem. Sci, 2012. **7**: p. 1170-1179.
96. Simon, C., T. Cartailler, and P. Turq, *Structure and speciation of liquid 2HF/KF: A molecular dynamics study.* The Journal of chemical physics, 2002. **117**(8): p. 3772-3779.
97. Dawood, K.M. and T. Fuchigami, *Electrolytic Partial Fluorination of Organic Compounds. 31.1 Regioselective Anodic Fluorination of 2-Quinolyl and 4-(7-Trifluoromethyl) quinolyl Sulfides and the Factors Affecting Its Optimization.* The Journal of organic chemistry, 1999. **64**(1): p. 138-143.
98. Higashiya, S., T. Sato, and T. Fuchigami, *Electrolytic partial fluorination of organic compounds Part 25. Regioselective anodic fluorination of naphthalene- and pyridine-acetate and -acetonitrile derivatives.* Journal of Fluorine Chemistry, 1998. **87**(2): p. 203-208.
99. Salanne, M., C. Simon, and P. Turq, *Molecular dynamics simulation of hydrogen fluoride mixtures with 1-ethyl-3-methylimidazolium fluoride: A simple model for the study of structural features.* The Journal of Physical Chemistry B, 2006. **110**(8): p. 3504-3510.
100. Shodai, Y., et al., *Anionic Species (FH)xF- in Room-Temperature Molten Fluorides (CH3)4NF·mHF.* The Journal of Physical Chemistry A, 2004. **108**(7): p. 1127-1132.
101. Sadeghi, N., et al., *Stereotactic Comparison among Cerebral Blood Volume, Methionine Uptake, and Histopathology in Brain Glioma.* American Journal of Neuroradiology, 2007. **28**(3): p. 455-461.

102. Yin, B., S. Inagi, and T. Fuchigami, *Highly selective electrochemical fluorination of dithioacetal derivatives bearing electron-withdrawing substituents at the position alpha to the sulfur atom using poly(HF) salts.* Beilstein J Org Chem, 2015. **11**: p. 85-91.
103. Inagi, S., T. Sawamura, and T. Fuchigami, *Effects of additives on anodic fluorination in ionic liquid hydrogen fluoride salts.* Electrochemistry Communications, 2008. **10**(8): p. 1158-1160.
104. Sawamura, T., S. Inagi, and T. Fuchigami, *Anodic Fluorination and Fluorodesulfurization in Ionic Liquid Hydrogen Fluoride Salts with Polyether Additives.* Journal of The Electrochemical Society, 2009. **156**(1): p. E26-E28.
105. Fuchigami, T. and S. Inagi, *Selective electrochemical fluorination of organic molecules and macromolecules in ionic liquids.* Chem Commun (Camb), 2011. **47**(37): p. 10211-23.
106. Khotavivattana, T., et al., *18F-Labeling of Aryl-SCF3,-OCF3 and-OCHF2 with [18F] Fluoride.* Angewandte Chemie International Edition, 2015. **54**(34): p. 9991-9995.
107. Welch, J.T., *Selective fluorination in organic and bioorganic chemistry*. 1991: ACS Publications.
108. Wilkinson, J.A., *Recent advances in the selective formation of the carbon-fluorine bond.* Chemical reviews, 1992. **92**(4): p. 505-519.
109. Fuchigami, T., K. Yamamoto, and Y. Nakagawa, *Electrolytic reactions of fluoro organic compounds. 7. Anodic methoxylation and acetoxylation of 2, 2, 2-trifluoroethyl sulfides. Preparation of highly useful trifluoromethylated building blocks.* The Journal of Organic Chemistry, 1991. **56**(1): p. 137-142.
110. Glaudemans, A.W., et al., *Value of 11C-methionine PET in imaging brain tumours and metastases.* Eur J Nucl Med Mol Imaging, 2013. **40**(4): p. 615-35.
111. Ilardi, E.A., E. Vitaku, and J.T. Njardarson, *Data-Mining for Sulfur and Fluorine: An Evaluation of Pharmaceuticals To Reveal Opportunities for Drug Design and Discovery.* Journal of Medicinal Chemistry, 2014. **57**(7): p. 2832-2842.
112. Hou, Y., S. Higashiya, and T. Fuchigami, *Electrolytic Partial Fluorination of Organic Compounds. 22.1 Highly Regioselective Anodic Monofluorination of Oxindole and 3-Oxo-1,2,3,4-tetrahydroisoquinoline Derivatives: Effects of Supporting Fluoride Salts and Anode Materials.* The Journal of Organic Chemistry, 1997. **62**(25): p. 8773-8776.
113. Drakesmith, F.G. and D.A. Hughes, *Electrochemical fluorination using porous nickel and foam nickel anodes.* Journal of Fluorine Chemistry, 1986. **32**(1): p. 103-134.
114. Bosque, R. and J. Sales, *Polarizabilities of solvents from the chemical composition.* Journal of chemical information and computer sciences, 2002. **42**(5): p. 1154-1163.
115. Suryanarayanan, V., S. Yoshihara, and T. Shirakashi, *Electrochemical behavior of carbon electrodes in organic liquid electrolytes containing tetrafluoroborate and hexafluorophosphate anionic species in different non-aqueous solvent systems.* Electrochimica Acta, 2005. **51**(5): p. 991-999.
116. Eberson, L., M.P. Hartshorn, and O. Persson, *1, 1, 1, 3, 3, 3-Hexafluoropropan-2-ol as a solvent for the generation of highly persistent radical cations.* Journal of the Chemical Society, Perkin Transactions 2, 1995(9): p. 1735-1744.
117. EBERSON, L., et al., *Making Radical Cations Live Longer.* ChemInform, 1997. **28**(8).
118. Shuklov, I.A., N.V. Dubrovina, and A. Boerner, *Fluorinated alcohols as solvents, cosolvents and additives in homogeneous catalysis.* Synthesis, 2007. **2007**(19): p. 2925-2943.
119. Hou, Y. and T. Fuchigami, *Electrolytic Partial Fluorination of Organic Compounds XL. Solvent Effects on Anodic Fluorination of Heterocyclic Sulfides.* Journal of The Electrochemical Society, 2000. **147**(12): p. 4567-4572.
120. Himeshima, Y., H. Kobayashi, and T. Sonoda, *A first example of generating aryl cations in the solvolysis of aryl triflates in trifluoroethanol.* Journal of the American Chemical Society, 1985. **107**(18): p. 5286-5288.

121. Wang, J.M., et al., *Thiodiketopiperazines produced by the endophytic fungus Epicoccum nigrum.* J Nat Prod, 2010. **73**(7): p. 1240-9.
122. McReynolds, M.D., J.M. Dougherty, and P.R. Hanson, *Synthesis of phosphorus and sulfur heterocycles via ring-closing olefin metathesis.* Chem Rev, 2004. **104**(5): p. 2239-58.
123. Clayden, J. and P. MacLellan, *Asymmetric synthesis of tertiary thiols and thioethers.* Beilstein Journal of Organic Chemistry, 2011. **7**: p. 582-595.
124. Haney, M., E. Rubin, and R. Foltin, *Modafinil reduces cocaine self-administration in humans: Effects vary as a function of cocaine 'priming'and cost.* Drug & Alcohol Dependence, 2017. **171**: p. e82.
125. Repantis, D., L. Maier, and I. Heuser, *Correspondence arising: Modafinil for cognitive neuroenhancement in health non-sleep-deprived-subjects.* European Neuropsychopharmacology, 2016. **26**(2): p. 392-393.
126. Kampman, K.M., et al., *A double blind, placebo controlled trial of modafinil for the treatment of cocaine dependence without co-morbid alcohol dependence.* Drug and alcohol dependence, 2015. **155**: p. 105-110.
127. Kaser, M., et al., *Modafinil Improves Episodic Memory and Working Memory Cognition in Patients with Remitted Depression: A Double-Blind, Randomized, Placebo Controlled Study.* Biological Psychiatry: Cognitive Neuroscience and Neuroimaging, 2016.
128. Zolkowska, D., et al., *Evidence for the Involvement of Dopamine Transporters in Behavioral Stimulant Effects of Modafinil.* Journal of Pharmacology and Experimental Therapeutics, 2009. **329**(2): p. 738-746.
129. Wisor, J., *Modafinil as a Catecholaminergic Agent: Empirical Evidence and Unanswered Questions.* Frontiers in Neurology, 2013. **4**(139).
130. Reith, M.E.A., et al., *Behavioral, biological, and chemical perspectives on atypical agents targeting the dopamine transporter.* Drug & Alcohol Dependence. **147**: p. 1-19.
131. Chatterjie, N., et al., *Anti-Narcoleptic Agent Modafinil and Its Sulfone: A Novel Facile Synthesis and Potential Anti-Epileptic Activity.* Neurochemical Research, 2004. **29**(8): p. 1481-1486.
132. Matthew, T. and G. Véronique, *18F Labeling of Arenes.* Angewandte Chemie International Edition, 2012. **51**(46): p. 11426-11437.
133. Noel, M., V. Suryanarayanan, and S. Chellammal, *A review of recent developments in the selective electrochemical fluorination of organic compounds.* Journal of Fluorine Chemistry, 1997. **83**(1): p. 31-40.
134. Weinberg, N. and H. Weinberg, *Electrochemical oxidation of organic compounds.* Chemical Reviews, 1968. **68**(4): p. 449-523.
135. Roth, H., N. Romero, and D. Nicewicz, *Experimental and calculated electrochemical potentials of common organic molecules for applications to single-electron redox chemistry.* Synlett, 2016. **27**(05).
136. Chaudhuri, K.R. and A.H. Schapira, *Non-motor symptoms of Parkinson's disease: dopaminergic pathophysiology and treatment.* The Lancet Neurology, 2009. **8**(5): p. 464-474.
137. Nanni, C., S. Fanti, and D. Rubello, *18F-DOPA PET and PET/CT.* Journal of Nuclear Medicine, 2007. **48**(10): p. 1577-1579.
138. Kaneko, S., et al., *Enzymatic synthesis of no-carrier-added 6-[18F] fluoro-l-dopa with β-tyrosinase.* Applied radiation and isotopes, 1999. **50**(6): p. 1025-1032.
139. Namavari, M., et al., *Regioselective radiofluorodestannylation with [18F] F2 and [18F] CH3COOF: a high yield synthesis of 6-[18F] Fluoro-L-dopa.* International journal of radiation applications and instrumentation. Part A. Applied radiation and isotopes, 1992. **43**(8): p. 989-996.
140. Ryan, G.B. and G. Majno, *Acute inflammation. A review.* The American Journal of Pathology, 1977. **86**(1): p. 183-276.

141. Hirsch, E.C. and S. Hunot, *Neuroinflammation in Parkinson's disease: a target for neuroprotection?* The Lancet Neurology, 2009. **8**(4): p. 382-397.
142. Lee, Y.J., et al., *Inflammation and Alzheimer's disease.* Arch Pharm Res, 2010. **33**(10): p. 1539-56.
143. Trapp, B.D., et al., *Axonal transection in the lesions of multiple sclerosis.* New England Journal of Medicine, 1998. **338**(5): p. 278-285.
144. Philips, T. and W. Robberecht, *Neuroinflammation in amyotrophic lateral sclerosis: role of glial activation in motor neuron disease.* The Lancet Neurology, 2011. **10**(3): p. 253-263.
145. Wu, C., et al., *PET Imaging of Inflammation Biomarkers.* Theranostics, 2013. **3**(7): p. 448-466.
146. Owen, D.R., et al., *Mixed-affinity binding in humans with 18-kDa translocator protein ligands.* J Nucl Med, 2011. **52**(1): p. 24-32.
147. Lavisse, S., et al., *Reactive Astrocytes Overexpress TSPO and Are Detected by TSPO Positron Emission Tomography Imaging.* The Journal of Neuroscience, 2012. **32**(32): p. 10809-10818.
148. Vivash, L. and T.J. O'Brien, *Imaging Microglial Activation with TSPO PET: Lighting Up Neurologic Diseases?* J Nucl Med, 2016. **57**(2): p. 165-8.
149. Horti, A.G., et al., *Synthesis and biodistribution of [11C]A-836339, a new potential radioligand for PET imaging of cannabinoid type 2 receptors (CB2).* Bioorganic & Medicinal Chemistry, 2010. **18**(14): p. 5202-5207.
150. Savonenko, A.V., et al., *Cannabinoid CB2 Receptors in a Mouse Model of Aβ Amyloidosis: Immunohistochemical Analysis and Suitability as a PET Biomarker of Neuroinflammation.* PLOS ONE, 2015. **10**(6): p. e0129618.
151. Haider, A., et al., *Synthesis and Biological Evaluation of Thiophene-Based Cannabinoid Receptor Type 2 Radiotracers for PET Imaging.* Frontiers in Neuroscience, 2016. **10**(350).
152. Harris, R.E., et al., *Aspirin, ibuprofen, and other non-steroidal anti-inflammatory drugs in cancer prevention: a critical review of non-selective COX-2 blockade (review).* Oncol Rep, 2005. **13**(4): p. 559-83.
153. Zarghi, A., et al., *Design, Synthesis and Biological Evaluation of New 5,5-Diarylhydantoin Derivatives as Selective Cyclooxygenase-2 Inhibitors.* Scientia Pharmaceutica, 2011. **79**(3): p. 449-460.
154. Uddin, M.J., et al., *Fluorinated COX-2 Inhibitors as Agents in PET Imaging of Inflammation and Cancer.* Cancer Prevention Research, 2011. **4**(10): p. 1536-1545.
155. Laube, M., T. Kniess, and J. Pietzsch, *Radiolabeled COX-2 inhibitors for non-invasive visualization of COX-2 expression and activity--a critical update.* Molecules, 2013. **18**(6): p. 6311-55.
156. Cherukuri, D.P., et al., *Targeted Cox2 gene deletion in intestinal epithelial cells decreases tumorigenesis in female, but not male, ApcMin/+ mice.* Mol Oncol, 2014. **8**(2): p. 169-77.
157. Liu, C.H., et al., *Overexpression of cyclooxygenase-2 is sufficient to induce tumorigenesis in transgenic mice.* J Biol Chem, 2001. **276**(21): p. 18563-9.
158. !!! INVALID CITATION !!! {Minghetti, 2004 #2405;Skutella, #3343}.
159. Yermakova, A. and M.K. O'Banion, *Cyclooxygenases in the central nervous system: implications for treatment of neurological disorders.* Curr Pharm Des, 2000. **6**(17): p. 1755-76.
160. Penning, T.D., et al., *Synthesis and biological evaluation of the 1,5-diarylpyrazole class of cyclooxygenase-2 inhibitors: identification of 4-[5-(4-methylphenyl)-3-(trifluoromethyl)-1H-pyrazol-1-yl]benze nesulfonamide (SC-58635, celecoxib).* J Med Chem, 1997. **40**(9): p. 1347-65.
161. Kharasch, E.D. and K.E. Thummel, *Identification of cytochrome P450 2E1 as the predominant enzyme catalyzing human liver microsomal defluorination of sevoflurane, isoflurane, and methoxyflurane.* Anesthesiology, 1993. **79**(4): p. 795-807.
162. Park, B.K., N.R. Kitteringham, and P.M. O'Neill, *Metabolism of fluorine-containing drugs.* Annu Rev Pharmacol Toxicol, 2001. **41**: p. 443-70.

163. Parfenova, H., et al., *Dynamics of nuclear localization sites for COX-2 in vascular endothelial cells.* Am J Physiol Cell Physiol, 2001. **281**(1): p. C166-78.
164. Liou, J.Y., et al., *Mitochondrial localization of cyclooxygenase-2 and calcium-independent phospholipase A2 in human cancer cells: implication in apoptosis resistance.* Exp Cell Res, 2005. **306**(1): p. 75-84.
165. Paulson, S.K., et al., *Plasma protein binding of celecoxib in mice, rat, rabbit, dog and human.* Biopharm Drug Dispos, 1999. **20**(6): p. 293-9.
166. Blobaum, A.L., et al., *Action at a distance: mutations of peripheral residues transform rapid reversible inhibitors to slow, tight binders of cyclooxygenase-2.* J Biol Chem, 2015. **290**(20): p. 12793-803.
167. Gong, L., et al., *Celecoxib pathways: pharmacokinetics and pharmacodynamics.* Pharmacogenet Genomics, 2012. **22**(4): p. 310-8.
168. Füchtner, F., et al., *Factors affecting the specific activity of [18F] fluoride from a [18O] water target.* Nuklearmedizin, 2008. **47**(03): p. 116-119.
169. Hamacher, K., T. Hirschfelder, and H.H. Coenen, *Electrochemical cell for separation of [18F]fluoride from irradiated 18O-water and subsequent no carrier added nucleophilic fluorination.* Applied Radiation and Isotopes, 2002. **56**(3): p. 519-523.
170. Lyalin, B.V. and V.A. Petrosyan, *Electrochemical halogenation of organic compounds.* Russian Journal of Electrochemistry, 2013. **49**(6): p. 497-529.
171. Berkessel, A., et al., *Unveiling the "Booster Effect" of Fluorinated Alcohol Solvents: Aggregation-Induced Conformational Changes and Cooperatively Enhanced H-Bonding.* Journal of the American Chemical Society, 2006. **128**(26): p. 8421-8426.
172. Bégué, J.-P., D. Bonnet-Delpon, and B. Crousse, *Fluorinated Alcohols: A New Medium for Selective and Clean Reaction.* Synlett, 2004. **2004**(01): p. 18-29.
173. Colomer, I., et al., *Hexafluoroisopropanol as a highly versatile solvent.* Nature Reviews Chemistry, 2017. **1**: p. 0088.
174. Eberson, L., et al., *for Electrochemistry'r.* Acta Chemica Scandinavica, 1998. **52**(102471028): p. 1024-1028.
175. Huba, F., E.B. Yeager, and G.A. Olah, *The formation and role of carbocations in electrolytic fluorination using hydrogen fluoride electrolytes in a nafion membrane-divided teflon cell.* Electrochimica Acta, 1979. **24**(5): p. 489-494.
176. Konno, A. and T. Fuchigami, *Electrolytic partial fluorination of organic compounds. Part X1 Regioselective anodic monofluorination of phenylsulfenylacetate using a flow-cell system.* Journal of Applied Electrochemistry, 1995. **25**(2): p. 173-175.
177. Wong, R., et al., *Reactivity of electrochemically concentrated anhydrous [18F]fluoride for microfluidic radiosynthesis of 18F-labeled compounds.* Applied radiation and isotopes : including data, instrumentation and methods for use in agriculture, industry and medicine, 2012. **70**(1): p. 193-199.
178. McClelland, R.A., et al., *Laser flash photolysis generation, spectra, and lifetimes of phenylcarbenium ions in trifluoroethanol and hexafluoroisopropyl alcohol. On the UV spectrum of the benzyl cation.* Angewandte Chemie International Edition in English, 1991. **30**(10): p. 1337-1339.
179. Pezacki, J.P., et al., *Lifetimes of Dialkylcarbocations Derived from Alkanediazonium Ions in Solution: Cyclohexadienyl Cations as Kinetic Probes for Cation Reactivity1.* Journal of the American Chemical Society, 1999. **121**(28): p. 6589-6598.
180. McClelland, R.A., V. Kanagasabapathy, and S. Steenken, *Nanosecond laser flash photolytic generation and lifetimes in solvolytic media of diarylmethyl and p-methoxyphenethyl cations.* Journal of the American Chemical Society, 1988. **110**(20): p. 6913-6914.

181. Johnston, L., J. Lobaugh, and V. Wintgens, *Laser flash photolysis studies of dibenzosuberenyl cations and radical cations.* The Journal of Physical Chemistry, 1989. **93**(21): p. 7370-7374.
182. Steenken, S. and R.A. McClelland, *248-nm Laser flash photoprotonation of mesitylene, hexamethylbenzene, and 1, 3, 5-trimethoxybenzene in 1, 1, 1, 3, 3, 3-hexafluoroisopropyl alcohol. Formation and electrophilic reactivities of the cyclohexadienyl cations.* Journal of the American Chemical Society, 1990. **112**(26): p. 9648-9649.
183. McClelland, R.A., N. Mathivanan, and S. Steenken, *Laser flash photolysis of 9-fluorenol. Production and reactivities of the 9-fluorenol radical cation and the 9-fluorenyl cation.* Journal of the American Chemical Society, 1990. **112**(12): p. 4857-4861.
184. Eberson, L. and M.P. Hartshorn, *On the existence of quinone radical cations. A study in 1,1,1,3,3,3-hexafluoropropan-2-ol.* Journal of the Chemical Society, Perkin Transactions 2, 1996(2): p. 151-154.
185. Lennart, E., P. Ola, and H.M. P., *Detection and Reactions of Radical Cations Generated by Photolysis of Aromatic Compounds with Tetranitromethane in 1,1,1,3,3,3-Hexafluoro-2-propanol at Room Temperature.* Angewandte Chemie International Edition in English, 1995. **34**(20): p. 2268-2269.
186. Cozens, F.L., et al., *Lifetimes and UV-visible absorption spectra of benzyl, phenethyl, and cumyl carbocations and corresponding vinyl cations. A laser flash photolysis study.* Canadian Journal of Chemistry, 1999. **77**(12): p. 2069-2082.
187. Steenken, S., et al., *Making Photochemically Generated Phenyl Cations Visible by Addition to Aromatics: Production of Phenylcyclohexadienyl Cations and Their Reactions with Bases/Nucleophiles.* Journal of the American Chemical Society, 1998. **120**(46): p. 11925-11931.
188. Eberson, L., et al., *Radical cation mechanism of aromatic halogenation by halogens or iodine chloride in 1,1,1,3,3,3-hexafluoropropan-2-ol.* Journal of the Chemical Society, Perkin Transactions 2, 1998(1): p. 59-70.
189. Field, M.J., S. Sinha, and J.J. Warren, *Photochemical proton-coupled C–H activation: an example using aliphatic fluorination.* Physical Chemistry Chemical Physics, 2016. **18**(45): p. 30907-30911.
190. Koper, M.T., *Theory of the transition from sequential to concerted electrochemical proton–electron transfer.* Physical Chemistry Chemical Physics, 2013. **15**(5): p. 1399-1407.
191. Hammes-Schiffer, S., *Theory of Proton-Coupled Electron Transfer.* 2009.
192. Costentin, C., M. Robert, and J.-M. Savéant, *Concerted Proton− Electron Transfers: Electrochemical and Related Approaches.* Accounts of chemical research, 2010. **43**(7): p. 1019-1029.
193. Bloom, S., M. McCann, and T. Lectka, *Photocatalyzed Benzylic Fluorination: Shedding "Light" on the Involvement of Electron Transfer.* Organic letters, 2014. **16**(24): p. 6338-6341.
194. Haya, L., et al., *Regioselectivity of Electrochemical CH Functionalization Via Iminium Ion.* Electrochimica Acta, 2014. **142**: p. 299-306.
195. Taras-Goslinska, K. and M. Jonsson, *Solvent Effects on the Redox Properties of Thioethers.* The Journal of Physical Chemistry A, 2006. **110**(30): p. 9513-9517.